Analysis of the role of Hsp90 in colon cancer and cancer stem-like cell biology *in vitro* using a genetically paired cell line model.

A thesis in fulfilment of the degree

of

DOCTOR OF PHILOSOPHY

in Biochemistry

RHODES UNIVERSITY

Faculty of Science

Department of Biochemistry and Microbiology

Cindy Slater

March 2015

Abstract

Colon cancers are commonly associated with mutations or changes in signaling in the Wnt/β-catenin pathway. Cancer treatments, such as chemotherapy and radiation, are challenged by the limited methods of disease detection and the insufficient elimination of contributing factors, such as cancer stem-like cells (CSC), to metastatic disease. CSC are characterised by their ability to survive anchorage-independently and attribute to therapeutic resistance. To examine the biological changes associated with the progression of human colon cancers and the role of Hsp90 in cancer and CSC biology, SW480 and SW620 genetically paired (isogenic) colon cancer cell lines from the same patient were characterised for populations of putative CSC, tumoursphere (TS) forming ability, cell growth, behaviour and response to anti-cancer therapeutics. The SW480 cell line was established from a primary colon adenocarcinoma and the SW620 was established from a lymph node metastasis of the primary cancer one year later. To address the role of Hsp90 in colon cancer, the sensitivity of cells and TS were analysed in response to geldanamycin and novobiocin, and an isoform-specific approach to the targeting of Hsp90α was developed. Flow cytometric analysis of putative CSC by phenotype revealed variable proportions of cells bearing the $CD44^{+}/CD133^{+}$ surface protein marker, widely used in the identification of colon CSC, in SW480 and SW620 cells. The paired cell lines maintained similar proportions of putative CSC, identified by the expression of the ABCG2 protein (side population; 1 %) and through high aldehyde dehydrogenase activity (ALDEFLUOR; 6 %). SW480 cells demonstrated greater TS forming efficiency than SW620 cells (49.9 and 35.5 %, respectively) and observations of wound-healing showed SW480 cells to be more migratory than SW620 cells. No difference in response to Hsp90 inhibition was observed between paired cell lines, however SW480 TS resisted treatment with geldanamycin. This the first study to report a dose-dependent increase in TS growth in response to novobiocin inhibition of Hsp90, and to demonstrate that that the sensitivity of SW480 and SW620 TS to oxaliplatin, a common drug for the treatment of metastatic colon cancers, was enhanced by novobiocin, providing promise for the elimination of CSC with combined chemotherapeutics. We analysed the Wnt/β-catenin pathway in response to expression of short hairpin RNA (shRNA) against Hsp90α or a control non-targeting shRNA, under the control of a tetracycline-responsive promoter. Hsp90α knockdown contributed to a deregulated stress response, presenting with reduced Hsp27 and β-catenin protein, but corresponded to an increase in the association between Hsp90, β-catenin and Hsp27 *in vitro*. The reduction of Hsp90α did not influence sensitivity of the colon cancer cells to activators or inhibitors of the Wnt pathway, but rather correlated to reduced TS formation, cell adhesion and spreading, identifying potential therapeutic benefit to the controlled reduction of Hsp90α for the deregulation of colon cancer characteristics. Given that Hsp27 and β-catenin are both

involved in cell adhesion, cytoskeletal dynamics and interact directly with each other, we propose a role for targeting Hsp90α in the regulation cell adherence indirectly via reductions in levels of β-catenin and Hsp27, rather than by modifying the transcriptional activity of β-catenin.

Declaration

I hereby declare that the work presented in this thesis for the degree of Doctor of Philosophy in Biochemistry (Rhodes University, Faculty of Science) is my own, unaided work, except where appropriately acknowledged. This research has not been submitted for examination at any other university.

……

Miss Cindy Slater

05 March 2015

Table of Contents

List of Figures

List of Tables

List of Abbreviations

17-AAG	17-N-allylamino-17-demethoxygeldanamycin
17-DMAG	17-dimethylaminoethylamino-17-demethoxygeldanamycin
5-FU	5-Fluorouracil
AGE	Agarose Gel Electrophoresis
ANOVA	Analysis of Variance
ALDH	Aldehyde Dehydrogenase
APC	Allophycocyanin
APC	Adenomatous Polyposis Coli gene
ATP	Adenosine Triphosphate
ATPase	Adenosine 5´-triphosphatase
bFGF	Basic Fibroblast Growth Factor
BSA	Bovine Serum albumin
C-terminal	Carboxyl terminal
CI	Cell Index
CK1	Casein Kinase 1
CSC	Cancer Stem-like Cells
CXCR/CCR	Chemokine receptor
DEAB	Diethylaminobenzaldehyde
DMEM	Dulbecco's s Modified Eagles Medium
DMSO	Dimethyl Sulphoxide
DNA	Deoxyribonucleic Acid
Dox	Doxycycline
EC_{50}	Effective Concentration to demonstrate a response, represented by 50 % change in viability
ECACC	European Collection of Cell Cultures
E-cadherin	Epithelial cadherin
ECM	Extracellular Matrix
E. coli	*Escherichia coli*
EDTA	Ethylenediaminetetraacetic Acid
EGF	Epidermal Growth Factor
EMT	Epithelial-Mesenchymal Transition
FAK	Focal Adhesion Kinase

FAP	Familial Adenomatous Polyposis
FBS	Foetal Bovine Serum
FCS	Foetal Calf Serum
FITC	Fluorescein-isothiocyanate
G418	Geneticin
GA	Geldanamycin
Grp	Glucose-regulated Protein
GSK3β	Glycogen Synthase Kinase 3β
H	Hour(s)
HEK	Human Embryonic Kidney
HNPCC	Hereditary Non-polyposis Colorectal Cancer
Hop	Hsp70/Hsp90 Organising Protein
HRP	Horseradish Peroxidise
Hsc70	Heat Shock Cognate Protein 70
HSF1	Heat Shock Transcription Factor 1
Hsp	Heat Shock Protein
HSP90AA1	Hsp90α gene
HSP90AB1	Hsp90β gene
IL8/CXCL8	Interleukin 8
JAK	Janus Kinases
LSM	Laser Scanning Microscope
LTR	Long Terminal Repeat
MET	Mesenchymal-Epithelial Transition
MMP	Matrix Metalloproteinase
MMR	Mismatch Repair gene
MTT	3-(4, 5-Dimethylthiazol-2-yl)-2, 5-diphenyltetrazolium bromide
N	Novobiocin
NEAA	Non-essential Amino Acids
NTshRNA	Non-targeting shRNA
N-terminal	Amino Terminal
Ox	Oxaliplatin
PBS	Phosphate-buffered Saline
PE	Phycoerythrin
PI3K	Phosphoinositide 3-kinase

PI	Propidium Iodide
PP2A	Protein Phosphatase 2A
PSA	Penicillin/Streptomycin/Amphotericin
PSTAT3	Phosphorylated Signal Transducer and Activator of Transcription 3
PTEN	Phosphatase and Tensin Homolog
PuroR	Puromycin Resistance gene
Q	Quercitin
RFP	Red Fluorescent Protein
RIPA	Radio-immunoprecipitation Assay
RNA	Ribonucleic Acid
RNAi	RNA interference
RNAse	Ribonuclease
SB	SB-216763 (GSK3β inhibitor)
SD	Standard Deviation
SDS	Sodium Dodecyl Sulphate
SDS-PAGE	Sodium Dodecyl Sulphate-Polyacrylamide Gel Electrophoresis
shRNA	Short Hairpin RNA
SIN	Self-inactivating
siRNA	Small Interfering RNA
SP	Side Population
STAT3	Signal Transducer and Activator of Transcription 3
TAE	Tris-acetate
TBS	Tris-buffered Saline
TBS-T	TBS-Tween
TCF	T-cell factor
TRAP1	Tumour Necrosis Factor Receptor-associated Protein 1
Tris	Tris-2-amino-2-hydroxymethyl-1, 3-propanol
TS	Tumoursphere(s)

List of symbols

α	Alpha
β	Beta
ɣ	Gamma
κ	Kappa
µ	Micro
°C	Degrees celsius
x g	Relative gravitational force
%	Percentage or g/100 ml
bp	Base pairs
CO_2	Carbon dioxide
g	Grams
l	Litre(s)
ml	Millilitre(s)
kDa	Kilodalton(s)
µg	Microgram(s)
µl	Microlitre(s)
µm	Micrometre(s)
µM	Micromolar
min	Minute(s)
mg	Milligram(s)
mM	Millimolar
M	Molar
mol	Mole(s)
ng	Nanogram(s)
nm	Nanometre(s)
nM	Nanomolar
pH	Hydrogen ion concentration
U	Unit(s)
V	Volt(s)
v/v	Volume to volume ratio
w/v	Weight to volume ratio

Acknowledgements

Cancer is a topic that hits close to home with many of us today. The more personal a struggle is, the more motivated we are. To the reviewers of this thesis, thank you for taking the time to consider this research thesis. I would also like to take this opportunity to show my sincere gratitude to all of the people in my life that have supported me in pursuit of my research goals and helped me dream big along the way.

To my supervisor, Dr Adrienne Edkins, I would like to convey my gratitude for her assistance, patience and leadership. Your passion for science is infectious and your guidance has set a benchmark with all of your students that is inspiring. I am grateful for the opportunities you have provided and assisted me with.

To my family, without whom I would have never had dared to dream or even achieve bigger goals than I had set for myself. Thank you for believing in me. I am forever indebted. Debbie, Allen, Vicky and Jonothan, thank you for your endless love and constant support throughout this research. Stefan, the kindness, love, positivity and faith you have shown me has opened my eyes. Thank you for accompanying me on this journey. Terry, Di, David and Katya, your encouragement and kind words spoke volumes to me. Thank you Jo, Kyle, Robyn, Jason, Tarryn, Lara, Tam, Stacey, friends, current and past members of the Biomedical Biotechnology Research Unit (BioBRU), the Young Royal Society, TED^{x}RhodesU and the Cancer Awareness Initiative at Rhodes (CAIR). Our shared enthusiasm, laughter and shenanigans are what keep us sane. Never let your passion fade. We are all capable of more than we set out to achieve. Thank you all for being a part of my life and sharing my goals with me.

To the survivors and sufferers, Munaf, Lynnette, Anne and Henry, though every day may be a battle anew, the depth and enormity of your impact has reached far beyond your disease. Finally, to those who have lost their fight, it was never your choice nor your fault, but in choosing to put your armour on in spite of your circumstances has lifted you up and given hope to so many others. Your light in the times of your strife will always resound with me.

And, lastly, I would like to acknowledge the invaluable contribution of financial assistance during this research by the National Research Foundation (NRF), the Department of Science and Technology (DST), the Medical Research Council of South Africa (MRC), Cancer Association of South Africa (CANSA) and the Henderson Prestigious Postgraduate Scholarship (Rhodes University). The financial assistance of the NRF towards this research is hereby acknowledged. Opinions expressed and conclusions arrived at, are those of the author and are not necessarily to be attributed to the NRF.

Chapter 1: Introduction

Cancer: definition and characteristics

Normal cellular processes are controlled by signaling molecules which ensures that cells behave in a controlled manner. These networks of signals are responsible for dictating whether a cell should die, divide or differentiate. “Cancer” is a term used to describe groups of cells, known as tumours, characterised by their autonomy from normal restricted cellular growth (Greene, 1951). Cancers are considered diseases of the cell cycle as they arise from the disruption of the delicate balance between cellular quiescence and growth.

A vast amount of literature is dedicated to understanding the risk factors involved in the causation of a cancer. It is widely accepted that these include both intrinsic and extrinsic factors, where intrinsic factors include influences from within the cell and extrinsic factors refer to influences from the environment. Intrinsic risk factors for the development of cancers in humans include aging and genetic predisposition through DNA mutations (Katoah, 2006). Cancers often arise from, or give rise to gain-of-function or loss-of-function mutations. Where proto-oncogenes undergo mutations, oncogenes that control cell proliferation are involved and deregulated to activate proteins in a gain-of-function mutation (Chow, 2010). Another characteristic example of cancer involves mutation of tumour suppressor genes, which normally control cell proliferation and growth. Loss of function mutations in a tumour suppressor often go undetected in individuals with heterozygous mutations, while individuals that contain the heterozygous mutations are more likely to develop cancer when expression is dominant for the mutated tumour suppressor (Collins *et al.,* 1997). Many therapeutics for the targeting of cancers, based on their evasion of regulatory signals, cause cell cycle arrest as a method to eliminate cancerous cells.

The majority of cancers have similar acquired characteristics, known as hallmarks of cancer. In their landmark paper, Hanahan and Weinberg characterised cancer by six vital functions, including insensitivity to anti-growth signals, self-sufficiency to growth signals, limitless proliferation, evasion of apoptosis, tissue invasion and metastasis, and sustained angiogenesis (Hanahan and Weinberg, 2000). Later, in 2011, Hanahan and Weinberg proposed four additions to this profile, including two emerging hallmarks, deregulation of cellular metabolism and evasion of immune system destruction, and two enabling characteristics, genome instability and mutation, and tumour-promoting inflammation (Hanahan and Weinberg, 2011). Understanding the characteristics of cancers has provided researchers with new insights by which to drive the development of novel therapeutics for the elimination of cancers.

Colorectal cancer remains the third most frequently diagnosed cancer, representing low survival rates estimated at 65 % for 5 years and 58 % for the survival after 10 years, post diagnosis (Jemal *et al.,* 2008; Cancer Facts & Figures, 2015). While the American Cancer Society report a decline of 2.5 % in the mortality rates for colorectal cancer from 2007 to 2011, an increased risk of individuals over the age of 50 is apparent, owing to 90 % of colorectal cancers diagnosed in 2011 (Cancer Facts & Figures, 2015). The implementation of routine screening by colonoscopy has seen a lowered incidence of colorectal cancers in the United States of America (Jemal *et al.,* 2010; Anderson *et al.,* 2011). Colon cancers follow a sequential progression from adenoma to carcinoma during tumour development. More than 95 % of colorectal cancers are classified as adenocarcinomas, originating from glandular tissues (Stewart *et al.,* 2006). As many as 5 – 10 % of colorectal cancer patients have been reported to have inherited genetic mutations, often in the Wnt pathway, attributing to the cause of their cancer (Lagerstedt Robinson *et al.,* 2007). An example of this is hereditary non-polyposis colorectal cancer (HNPCC or Lynch syndrome) which results from the mutation in a mismatch repair (MMR) gene (Vasen *et al.,* 2007). Familial adenomatous polyposis (FAP) is an autosomal dominant trait genetically passed on due to mutation in the gene encoding for adenomatous polyposis coli (APC), part of the Wnt destruction complex, which enables the development of benign polyps which may result in the progression of cancerous polyps capable of metastasis (Kotiligam *et al.,* 2008).

Origin of cancers

Tumours are defined by uncontrolled growth of cancerous cells. Defining the origin of the cancer is critical for the understanding of tumour progression. Tumours may be described as being monoclonal or polyclonal according to the origin of the cancer (Beck and Blanpain, 2013). Monoclonal tumours are cancers that arise following changes in cellular function, where uncontrolled proliferation has taken place and the cause of the cancer can be traced back to a single cell (Klco *et al.,* 2014; Kumar *et al.,* 2005). Tumours have also been described as polyclonal, when the origin of the cancer can be attributed to more than one cell. In a review of the evidence and implications of different tumour types, Parsons described polyclonal tumours as a cancer when more than one cell is involved in the generation of the cancerous population (Parsons, 2008). Like monoclonal tumours, polyclonal tumours are also subject to acquired genetic instability during proliferation, but unlike monoclonal tumours the origin of the cancer is not identifiable from single-cell lineage. Figure 1.1 described the basic process by which tumours progress to become heterogeneous from both monoclonal (Figure 1.1A) and polyclonal (Figure 1.1B) origin.

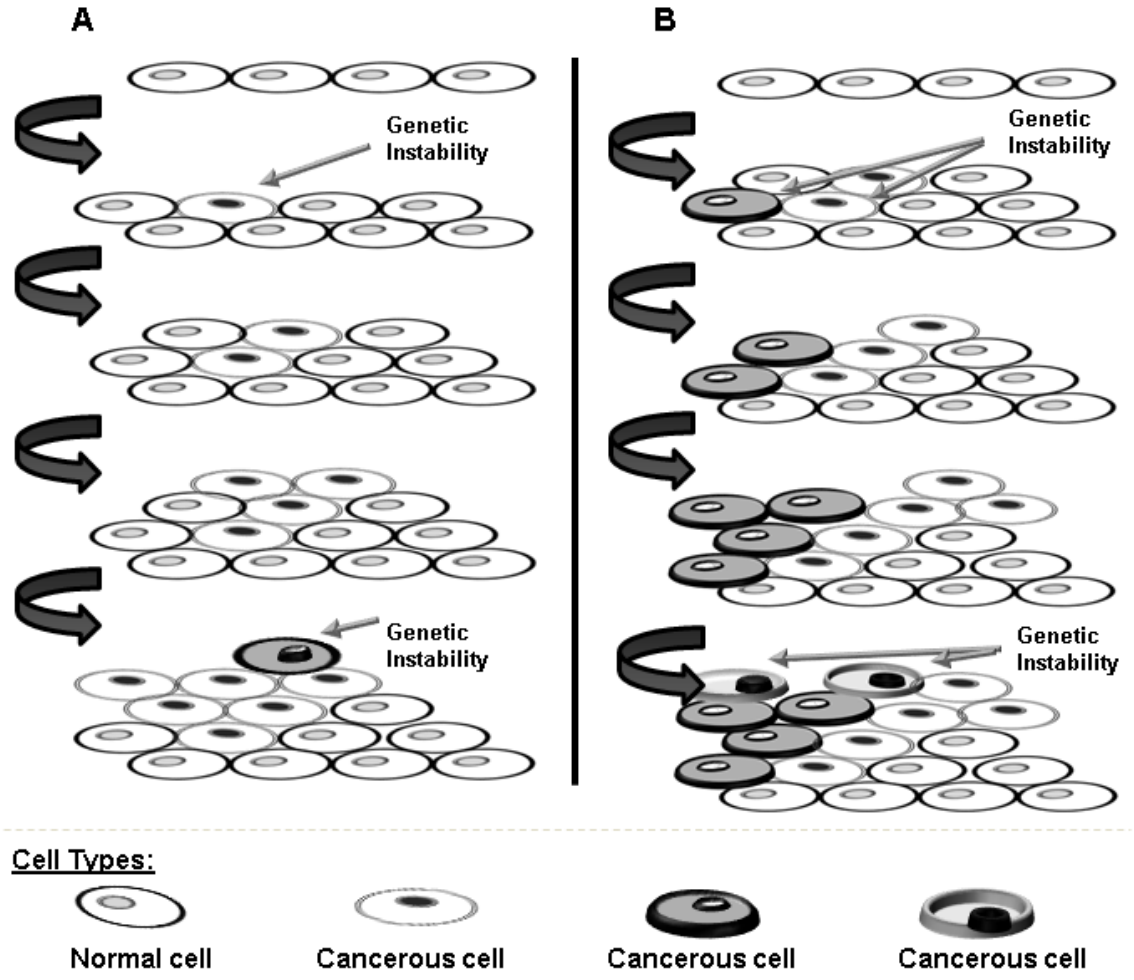

Figure 1.1. Genetic instabilities give rise to cancerous cells during tumour progression.

Examples of heterogeneous cell populations in tumour cells and their origin. A. Example of a monoclonal tumour, where the origin of the cancer can be traced back to one cell. B. Example of polyclonal tumour progression, where the cancer can be attributed to more than one cell of origin. Both types of tumours undergo uncontrolled proliferation and are subject to genetic instability.

Cancer Metastasis

Metastasis refers to the development and growth of malignant cells in a new environment (a secondary location) within the body. Metastasis incorporates cellular events of migration, invasion and tumourigenicity (Mehlen and Puisieux, 2006; Gupta and Massague, 2006). Increased cell motility is characteristic of metastatic cancer cells. In preparation for migration, a series of morphological changes take place that are reliant on the rearrangement of the cytoskeleton. The cytoskeleton consists of several structural proteins, including actin, cytokeratin, tubulin and vimentin. Actin forms complexes with focal adhesions. At the site of leading edge adhesion, the actin cytoskeleton provides the moving force for cell motility during depolarization and repolarisation of the actin cytoskeleton, while the detachment of the lagging edge by extracellular matrix (ECM) degradation by matrix metalloproteinases (MMP) enables cytosolic translocation (Yamazaki *et al.,* 2005). The remodelling of the ECM is critical to successful invasion of the cell into a new environment (Overall and Lopez-Otin, 2002).

The metastatic process that cells undergo is most often a characteristic of advanced malignant cancer (Calderwood *et al*., 2006). This, however, is a complex process that is highly inefficient, requiring millions of cells to attempt dissemination in order for a few to survive the metastatic cascade (Chambers *et al.,* 2002; Gupta and Massague, 2006; Klein, 2008). Metastatic cancer cells must survive cellular stresses such as hypoxia, nutrient depletion and loss of adhesion which would typically result in cell death (Mehlen and Puisieux, 2006). Anoikis typically results in cell death through apoptosis as cells lose adherence to the ECM (Streuli and Gilmore, 1999; Martin and Leder, 2001; Martin and Vuori, 2004). Cancer cells are described as growing anchorage-independently as they characteristically proliferate in the absence of adhesion to the ECM (Freedman and Shin, 1974). The anchorage independence of cancer cells is closely related to the ability of tumourigenic cells to survive and grow in secondary locations during metastasis. Intravasation, circulation and extravasation are selective processes that cancer cells must survive in order to metastasise. Tumour cells that enter by intravasation into circulation via the blood vessels and exit by extravasation to settle in a secondary tissue location either remain without contact with a matrix or are introduced to matrix components from a different source (Mehlen and Puisieux, 2006). Factors within the bloodstream, arrest within the capillary bed, relocation to the new site and the continuation of tumour growth and cell proliferation at the new tumour site must all be endured for successful metastasis (Chen *et al.,* 2009). Survival of metastatic cancer cells within the new tumour site is dependent on evasion of mechanical stresses and factors of the immune system, both of which would initiate cell destruction (Chambers *et al.,* 2002; Fidler, 2003; Mehlen and Puisieux, 2006).

The interaction between tumour cells and their microenvironment has been shown to be controlled through a number of pro-invasive proteins such as the MMP, epithelial (E-) cadherin

proteins and the integrin receptors (Wu *et al.,* 2005; Munshi and Stack, 2006; Hood and Cheresh, 2002). Guo and Giancotti (2004) discuss the mechanism whereby integrins promote cell survival through the activation of integrin-dependant signaling pathways. Integrins are a large family of cell-surface receptors that mediate adhesion to the ECM, and regulate the processes of proliferation, differentiation, migration, apoptosis and angiogenesis (Alpin *et al.,* 1999; Hynes, 2002; Nikolopoulos *et al.,* 2004; Naylor *et al.,* 2005; Reddig and Juliano, 2005). Structurally, integrins are made up of two subunits, each with its own cytoplasmic tail, membrane-bound domain and extracellular domain (Hynes, 2002). Regulatory proteins bind to the β-subunit short cytoplasmic domain of integrins and facilitate bidirectional signaling owing to a connection between the cytoskeleton using intermediate molecules, such as talin and vinculin, and signaling molecules such as the Heat shock protein 90 (Hsp90) chaperone protein and focal adhesion kinase (FAK) (Ramsay *et al.,* 2007). The modulation of FAK activity may still link integrin activity with metastatic tumour activity, as supported by studies that suggest integrins mediate metastasis (Bartish *et al.,* 2003; Vacca *et al.,* 2001).

Chemokines are small secreted proteins that interact with G-protein coupled receptors, chemokine receptors designated CXCR or CCR, to regulate the migration and development of cells (Zlotnil and Yoshie, 2000). The stromal cell-derived factor 1 (SDF-1) is a ligand of CXCR4 which is upregulated in a number of different cancers (Koshiba *et al.,* 2000; Uchida *et al.,* 2004). Cellular mechanisms of stem cell trafficking are not unique to stem cells, but may involve the utilization of the SDF-1α/CXCR4 chemotaxis pathway and links stem cell proliferation and movement, to molecular mechanisms common to developing and adult tissues (reviewed in Liard *et al.,* 2008). Marchesi and colleagues (2004) examined the upregulation of CXCR4 expression in pancreatic cancer corresponding to the increase in cell proliferation, survival, invasion, migration and metastasis. The SDF-1/CXCR4 interaction is suggested to regulate homing and adhesion of cancer cells to resident cells of a secondary location during metastasis (Crocker and Allan, 2008). Interleukin 8 (IL8 or CXCL8), which binds CXCR1 and CXCR2 chemokine receptors, was also shown to be upregulated in pancreatic cancer correlating to increased tumourigenic and metastatic potential in response to $TGF\beta_1$ signaling (Shi *et al.,* 1999; Wigmore *et al.,* 2002). As a majority of clinical studies report overexpression of chemokine IL8, much consideration has been given to the development of a treatment for metastatic cancers using CXC-chemokine suppression (Waugh and Wilson, 2008). IL8 expression and secretion has shown to be induced by chemotherapeutic treatments such as 5-fluorouracil, 5-FU (Collins *et al.,* 2000). Integrins and molecules associated with their trafficking by endocytosis are commonly found to be upregulated in carcinomas and the idea of integrin targeting, as an anti-cancer therapy using

molecules that specifically bind to integrins is being considered in therapeutic developments (Tucker, 2006; DiCara *et al.,* 2007).

Cancer stem-like cells and the cancer stem cell theory

In normal tissues, stem cells are responsible for producing progeny representative of all subtypes of cell populations needed for the organisation and functionality of the tissue (McCulloch and Jill, 2005). Stem cells are rare unspecialised cells within the body, representing a small subset of all cells. Stem cells are characteristically highly clonogenic, slow cycling and are able to self-renew (Write, 2000; Oshima *et al.,* 2001). Two distinct types of stem cells exist, namely embryonic and adult stem cells. Embryonic stem cells are unspecialized cells with the potential to give rise to somatic and germ line cells of an organism, while adult stem cells are produced by embryonic stem cells and can produce specialized progeny of a specific tissue or organ (Sylvester and Longaker, 2004). Thereby, stem cells not only divide symmetrically, but are capable of asymmetric division producing progeny that are more specialized, and have pluripotent capability to differentiate into cells representative of fully established tissues (Bjerknes and Cheng, 1999; Seaberg and Van Der Kooy, 2003). The early works of Virchow and Cohnheim, independently, led to the concept of cancer stem-like cells (CSC), comparing the resemblance between self-renewing capabilities of the cells responsible for foetal development and the cells of teratocarcinomas (Virchow, 1855; Cohnheim, 1867).

Similar to the structure of normal tissues, cancers display hierarchical organisation (Illmensee and Mintz, 1976; Reya *et al.,* 2001). The rapid rate of proliferation and subsequent genetic instabilities experienced by cancers supports this heterogeneity (Grady, 2006; Shackleton *et al.,* 2009). Understanding the heterogeneity of a tumour and defining the origin of a cancer has become important for the assessment of tumour evolution, and subsequently crucial in identifying therapeutic targets for treatment of the cancer (Buick and Pollak, 1984; Lawson *et al*., 2009). The discovery of tumour-initiating cells, also known as CSC, can account for tumour heterogeneity and are suspected to have the potential to initiate tumour progression (Kreso and Dick, 2014). Earlier, in 1993, Sell provided an alternative explanation for the presence of CSC, through the dedifferentiation of mature cells into CSC, but by 2004 Sell had concluded that cancers may develop from self-renewing tissue stem cells and progenitor cells (Sell, 1993; Sell, 2004). The CSC theory is still a controversial topic amongst the scientific community, as this theory is not supported by all tumours since committed progenitors may acquire the ability to self-renew and, by association, “stem-like” characteristics (Clarke *et al.,* 2006). Figure 1.2 illustrated the characteristics of CSC division. Like stem cells, CSC are thought to be able to

self-renew, divide symmetrically and asymmetrically, and are thereby capable of producing both CSC and differentiated progeny (Beck and Blanpain, 2013). Symmetric division results in the production of two stem daughter cells, while asymmetric division produces one stem daughter cell and one daughter cell that will undergo differentiation, a particularly important feature within tissues that require a high turnover (Molofsky *et al.,* 2004; Boman *et al.,* 2007). Differentiation results in the loss of stem cell potential, and the acquisition of different biological characteristics. Clarke and colleagues (2006) define a CSC as a cell capable of self-renewal, by asymmetric division, and creating a heterogeneous lineage of cancer cells within a tumour. Thereby, the number of CSC within a tumour is maintained by asymmetric stem cell division.

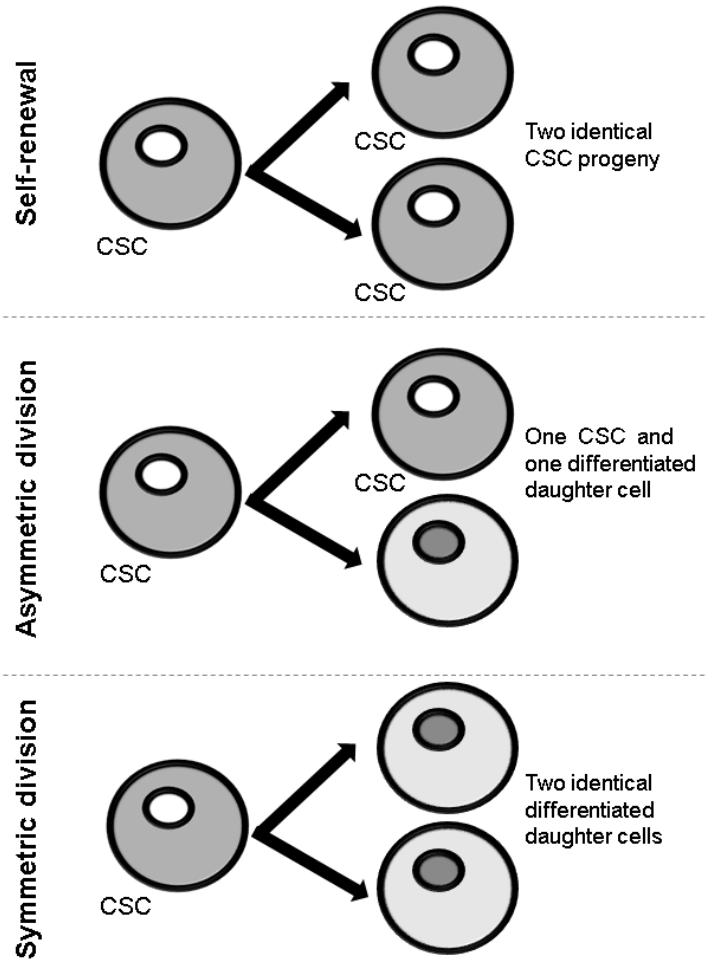

Figure 1.2. Cell division characteristics of cancer stem-like cells.

The proposed routes for producing progeny by CSC during cell division. Like stem cells, CSC have the ability to self-renew, producing identical CSC daughter progeny. By asymmetric division, CSC divide to produce two daughter cells, one with CSC characteristics and one differentiated cell type. Under symmetric division, the CSC divides to produce two differentiated daughter cells.

The implication of the hierarchical organisation of tumours and the discovery of CSC has led to the development of several CSC-targeted therapies. Traditional therapies, such as radiation and chemotherapy, target cells that are rapidly dividing, resulting in effective treatment against the bulk of the tumour (Reya *et al.,* 2001). Such methods have been thought to result in treatment failure, or cancer relapse, where the tumourigenic but slow cycling CSC evade therapy (Longley and Johnston, 2005). The mechanisms by which tumour cells evade treatment include the development of genetic mutations that confer resistance and the overexpression of proteins responsible for the flux of substances (such as drugs) in and out of the cell (Allikmets *et al.,* 1996). The discovery of CSC, and the apparent resistance of these cells to drug treatments, has initiated the search for new methods for CSC targeting, including the use of CSC characterisation and identification techniques, as well as new chemotherapeutic treatments or the combination of well characterised chemotherapeutics in synergy (Dalerba *et al.,* 2007; McNamara *et al.,* 2012).

CSC have been identified in B and T acute lymphoblastic leukaemia and several solid tumours including brain, breast, colon, lung, prostate, melanoma and glioblastoma (Al-Hajj *et al.*, 2003; Bonnet and Dick 1997; Collins *et al.*, 2005; Dou *et al.,* 2007; Ho *et al*., 2007; Qiang *et al.*, 2009; Singh *et al.,* 2003). A substantial amount of literature has begun to focus on methods to accurately identify CSC populations (Hermann *et al*., 2007; Vassilopoulos *et al.*, 2008; Wright *et al.,* 2008). Furthermore, CSC identified based on phenotype and unique functionality within human cancer cell lines have validated the use of cell lines to model tumour progression (Fillmore and Kuperwasser, 2008). The identification of unique CSC cell surface markers, such as CD44, CD133 (Table 1) and receptors like chemokines and integrins, would enable the identification of the CSC population in different cancers and serve as a possible mechanism of drug targeting. The ubiquitous expression of the CD133 marker across normal healthy colon eptheium cells, originally considered indicative of CSC tumour initiation has, however, potentially limits the usage of CD133 alone in the identification of intestinal stem or cancer-initiating cells (Shmelkov *et al.,* 2008). While there is great debate over the value of CD133 as a colon CSC marker, there is evidence to support the use of the CD133 marker in the identification of tumourigenic CSC in prostate cancers (Collins *et al.,* 2005). In addition to the identification of CSC by cell surface markers, pluripotency factors such as the Oct-4, Nanog and c-Myc oncogenes have been recognised in association with CSC (Chiou *et al*., 2008; Chiou *et al*., 2010; Gatti *et al*., 2009)

Table 1. Markers frequently used to identify CSC in solid tumours

Marker	Tissue	Characteristics	Reference
CD24	Breast	Cell surface protein	Ouhtit *et al.* (2007)
CD29	Breast	Cell surface protein	Shackelton *et al.* (2006)
CD44	Breast, prostate	Multistructural and multifunctional surface glycoprotein, implicated in inflammation; receptor for hyaluron	Patrawala *et al.* (2006), Brown *et al.* (2007)
CD133	Breast, brain, colon, pancreas, lung	5-transmembrane domain cell surface glycoprotein localized to protrusions	Wright *et al.* (2008), Singh *et al.* (2004), O'Brien *et al.* (2007), Hermann *et al.* (2007), Eramo *et al.* (2008)
EpCAM	Colon	Gastrointestinal carcinoma-associated antigen expressed in undifferentiated pluripotent cells	Dalerba *et al.* (2007)

In addition to the use of cell surface proteins in the identification of putative CSC populations, the culture of cells *in vitro* using simulated (non-adherent, serum-free, growth factor-supplemented) conditions mimicking that of the tumour environment has been proposed to enrich for cells bearing the CSC phenotype (Ricci-Vitiani *et al.,* 2007; Fang *et al.*, 2010). The culture of undifferentiated cells as tumourspheres (TS) is well characterised in literature. The TS are characterised by their rounded, three-dimensional shape with defined border, with cells largely expressing the same cell surface marker proteins (Todaro *et al.,* 2007) and in some cases enriched in putative CSC markers (de la Mare *et al*., 2013).

The unique functional characteristics of CSC have implicated them in chemotherapeutic resistance. The ATP-binding cassette (ABC) transporter proteins, located in the cell membrane, improve the tolerance to drugs by limiting the concentration of a drug within the cell through the use of an active protein-pump function. ABC transporter proteins prevent drug accumulation via drug efflux to mediate drug resistance (Zhou *et al.,* 2008). An ABC transporter enriched "side population (SP)" was first described for the identification of hematopoietic stem cells from mouse bone marrow (Goodell *et al*., 1996). This SP method has since been developed for identifying putative CSC and is based on high expression of the

ABCG2 transporter protein (Golebiewska *et al.,* 2011). Another unique marker for putative CSC identification is the expression of active aldehyde dehydrogenase (ALDH). The detoxifying effect of ALDH is thought to protect stem cells against oxidative damage and may modulate the cell proliferative capacity of stem cells (Yoshida *et al.,* 1998). ALDH1, initially discovered for breast cancers, has also been identified as a colon CSC enzyme marker, where an increased expression of ALDH1 corresponds to a higher probability of a population of cells containing CSC (Huang *et al.,* 2009). Recently, stage IV colon cancers with high ALDH1 (marker of "stemness") correlated with diminished patient survival, but the expression of ALDH1 did not increase along with colon cancer progression (Fitzgerald *et al.,* 2014).

Metastatic cancer cells typically display characteristics of tissue invasion, cancer initiation and tumour progression (through tumour maintenance and cell differentiation). Cancer cells that display invasiveness, tumorigenicity and "stemness" within malignant tumours are often capable of migrating (Hermann *et al.,* 2007). One feature of CSC, survival of anchorage independence, is vital for the formation of tumours at a secondary location and is characteristic of metastatic cancer cells. Following the CSC theory, tumorigenic and migratory CSC may be responsible for the development of metastasis through the initiation of tumour development and recurrence of tumours (Clarke and Fuller, 2006; Wicha *et al.*, 2006; Brabletz *et al*., 2005).

The receptor CD44 is a multifunctional cell surface adhesion molecule which acts as a signaling transmitter (Ponta *et al.,* 1998; Naor *et al.,* 2007). CD44 has been shown to play an important role in cancer invasion and metastasis in a variety of cancers, while strong evidence is provided for the involvement of CD44 in breast cancer metastasis to the liver (Ouhtit *et al.,* 2007). The relationship between CSC and metastasis has been studied and, for example, a distinct population of $CD133^{+}/CXCR4^{+}$ cells (see CSC markers in Table 1) in pancreatic carcinomas have shown to have strong migratory capability in vitro and displayed *in vivo* metastatic ability by migrating to and invading the liver to become tumorigenic (Herman *et al.,* 2007). These findings support the ability of metastases to arise from CSC, however our ability to assess tumourigenesis, initiation and CSC functionality is limited. The gold standard for analysing the CSC tumorigenicity involves the xenotransplantation of a cell population into model non-obese diabetic/severe combined immunodeficient (NOD/SCID) mice. NOD/SCID mouse models demonstrate CSC *in vivo* tumorigenicity, by characteristic features of CSC, such as the ability to re-establish the tumour and self-renew *in vivo* (Lapidot *et al.*, 1994; Bonnet and Dick, 1997). Putative colon CSC have been identified based on the expression of cell surface protein markers, CD44 and CD133, and by the expression of the ALDH enzyme and the ABCG2 transporter protein (Huang *et al.,* 2009; Ricci-Vitiani *et al*., 2007; Sussman *et al.,* 2007). $CD133^{+}$ colon cancer cells have successfully demonstrated the ability to survive anchorage-independently by serum-free sphere culture *in vitro* and engraftment *in vivo* (Ricci-

Vitiani *et al.,* 2007). This model supports the use of sphere formation as an indication of tumourigenicity and “stemness” based on the stem-like ability of CSC to survive anoikis.

Epithelial-mesenchymal transition

The characteristics of invasion and metastasis in tumour progression are associated with changes in adhesion at the cell-cell junctions (Behrens, 1999; Christofori, 2003). In epithelial malignancies, often cells develop a migratory phenotype, more representative of mesenchymal cancer cells (Thiery, 2002). This change is typically experienced by cells of the periphery of the tumour and is described by the epithelial-mesenchymal transition (EMT) of these cells. During EMT, epithelial cells gain a mesenchymal phenotype due to a loss of polarity as cells undergo remodelling of the cytoskeleton and reduced cell-cell adhesion (Moreno-Bueno *et al.,* 2008). EMT corresponds to increased motility and vimentin expression, but a loss of cytokeratins and E-cadherin (Menezes, 2014). In the metastatic cascade, cells leave the primary tumour through the acquisition of the mesenchymal phenotype as a result of EMP. Change in cell phenotype is considered essential to metastasis, and a relationship between EMT and CSC could be linked through the acquisition of stem cell properties (Mani *et al.,* 2007). The plasticity of stem cell may facilitate EMT events, abridging tumour initiation and survival in a foreign environment (Kand and Massague, 2004)

EMT is reversible, whereby cells gain an epithelial phenotype in a process known as mesenchymal-epithelial transition (MET). EMT and MET processes are regulated by Wnt, Notch and Hedgehog signaling (Yang and Weinberg, 2008). MET in cells corresponds to cell polarity and the increased expression of epithelial markers, such as E-cadherin, and decreased mesenchymal markers, such as vimentin (Liu *et al.,* 2014). Identifying the importance of EMT in cancer and CSC-related research has seen the development of novel inhibitors and modulators of Wnt/β-catenin signaling for the deregulation of EMT in cancer therapies (Yao *et al.,* 2013; Menezes, 2014). Investigation into the signaling pathways responsible for the regulation of cellular processes such as differentiation and stem cell self-renewal has revealed these systems may influence the development and progression of cancers (Reya and Clevers, 2005).

Signaling Pathways Associated with "Stemness"

The differentiation and self-renewal of cancer cells (see Figure 1.2) are largely under the control of the Wnt, phosphatase and tensin homolog (PTEN), Notch and Hedgehog signaling pathways. Together, the Hedgehog and Notch pathways create a feedback loop to control the development of the cell, where Hedgehog signaling is responsible for stimulating cellular self-renewal (Liu *et al.,* 2006) and Notch signaling actively prevents stem cell differentiation (Dontu *et al.,* 2004). The disruption of this feedback loop has been associated with carcinogenesis and the development or initiation of a cancer (Liu *et al.,* 2005). Although signaling pathways act independently of each other to regulate tissue self-renewal, differentiation and proliferation, it is known that the outcome of different pathways may influence others, and so become interlinked (Reya and Clevers, 2005). Examples of this can be found in the literature where there is proposed downstream Hedgehog signaling as a result of Notch signaling pathways (Liu *et al.,* 2006) and the suggestion that Sonic hedgehog acts upstream of the Notch signaling pathway (Morrow *et al.,* 2009).

The Wnt pathway acts downstream of both Notch and Hedgehog pathways, where transformation of the Notch signaling pathway activates the Wnt pathway (Liu *et al.,* 2005). Wnt, Notch and Hedgehog pathways are fundamentally important to tissue development, specifically during embryogenesis, which when deregulated may influence the development of a cancer (Han and Oh, 2013). Disruption of the Wnt pathway plays a crucial role in the majority of colon cancers where part of the destruction complex responsible for regulating β-catenin is deregulated (reviewed in Chapters 2 and 4). Furthermore, the development of colon polyps may lead to metastasis during cancer progression (Kotiligam *et al.,* 2008).

Molecular chaperones in cancer

Molecular chaperones are a large protein family that are essential to the functioning of a cell, as they maintain the folded state of proteins under physiological and stress conditions (Fink, 2004). Molecular chaperones help fold nascent polypeptides, assemble multimeric protein complexes and prevent the formation of unwanted protein aggregates, all of which are essential for maintaining cellular signal fidelity necessary to support tumours (reviewed in Trepel *et al*., 2010).

Heat shock proteins

Heat shock proteins (Hsp) are required for cellular survival and are synthesized in increasing amounts in response to elevated environmental temperature and cellular stress conditions. Many Hsp function as molecular chaperones (Kelly, 1999). Hsp were originally discovered in the larvae of Drosophila melanogaster exposed to elevated temperature (Ritossa, 1962;

Tissières *et al*., 1974). Hsp are found in both eukaryote and prokaryote cells and are localised within various compartments of the cell, including the cytosol, endoplasmic reticulum, nucleus and mitochondria (Kregel, 2002). Traditional Hsp nomenclature classifies proteins according to their respective molecular weights (Buchner, 1999). The major Hsp include Hsp90, Hsp70 and Hsp40, while Hsp27 is considered a small Hsp.

Certain Hsp mediate folding events, intracellular signaling (e.g. Hsp90) and protein processing events of refolding (e.g. Hsp70, Hsp60) or degradation (e.g. Hsp70), while others regulate chaperone activity and are named co-chaperones (Fink, 2004). Some Hsp, like some isoforms of the Hsp40 family, are involved in supression of aggregating proteins during protein synthesis, while others, such as Hsp90, specifically regulate the conformation of proteins (Fan *et al.,* 2003). In eukaryotes, the function of Hsp90 is regulated through association with numerous chaperones and co-chaperones (Pearl and Prodomou, 2006). Hsp tasked with *de novo* or stress-related protein folding and refolding include Hsp40, Hsp60 and Hsp70. Co-chaperones are responsible for selecting and presenting the substrate (client protein) to, and thereby facilitating an enhanced activity of, chaperones; such as in the relationship between the Hsp40 co-chaperone and Hsp70 chaperone (Wegele *et al.,* 2006).

Transcriptional regulation of Hsp

The transcription factor heat shock factor 1 (HSF-1) is the best characterised regulator responsible for the increased expression of Hsp during events of cellular stress. Heat shock protein 90, Hsp90, and HSF1 are found in the cytoplasm in a complex (Zou *et al.,* 1998). Normally, cellular HSF1 is inactive, in a monomeric state, stabilised by Hsp90. Increased temperatures and other cellular stresses facilitate the separation of HSF1 from Hsp90 to mediate the increase in Hsp expression (Zou *et al.,* 1998). Hsp90 dissociates from HSF1 facilitating the homotrimerisation and subsequent nuclear localisation of HSF1 (Jolly *et al.,* 1999; Zou *et al.,* 1998). The increased expression of Hsp induced by HSF-1 during cellular stress promotes cell survival by the modulation of other genes required for cellular recovery from stress. The upregulation of Hsp during cellular stress and in cancer cells reflects the significance of the study of Hsp and their roles in cancer progression (Bagatell and Whitesell, 2004).

Heat Shock Protein 90 (Hsp90)

Hsp90 is an evolutionarily conserved molecular chaperone that is ubiquitously expressed and plays an important role in regulating mitogenesis and cell-cycle progression. Under normal conditions, as much as 2 % of cellular proteome may comprise of Hsp90. In human cells, the Hsp90 family of proteins include the two cytoplasmic Hsp90 alpha (Hsp90α) and Hsp90 beta (Hsp90β) isoforms, encoded by the HSP90AA1 and HSP90AB1 genes respectively, and the

mitochondrial and endoplasmic reticulum Hsp90s, tumour necrosis factor receptor-associated protein 1 (TRAP1) and glucose-regulated protein 94 (Grp94), respectively.

Structurally, the Hsp90 dimer comprised of three domains per monomer, namely the N-terminal adenosine triphosphate (ATP) binding domain, regulating ATPase activity, a substrate-binding middle domain and a dimerisation domain at the C-terminus (Prodromou *et al.,* 2000; reviewed in Powers and Workman, 2006). Hsp90 is upregulated in response to environmental stress, including but not limited to elevated temperatures. Hsp90 displays cytoprotective properties through the conformational regulation of proteins and interacts with more than 300 client proteins (a comprehensive and regularly updated list of which can be found on the website of the Picard lab at www.picard.ch/downloads) (Richter and Buchner, 2001; Zhao and Houry, 2005). Hsp90 functions as a chaperone for numerous signaling proteins such as protein kinases (Table 2) and transcription factors, providing evidence for the importance of Hsp90 in cell growth, differentiation, apoptosis, signal transduction and the communication between cells (Pratt and Toft, 2003). Additional roles of Hsp90 under normal and stress conditions include its involvement in transcriptional regulation and chromatin remodelling (Zhao and Houry, 2005; Tariq *et al.,* 2009). The importance of Hsp90 during oncogenesis has been due to participation of Hsp90 chaperones in events typical of cancers via client proteins (Table 2), and subsequently inhibition of Hsp90 function has become the focus of many drug discovery programs.

Table 2. Some client proteins of Hsp90 and their link to the malignant phenotype

Client	Phenotype	Reference
HIFα	Angiogenesis	Isaacs *et al.,* (2002)
AKT	Impaired apoptosis	Basso *et al*., (2002)
Telomerase	Immortalization	Holt *et al*., (1999).
Serine and threonine kinases (e.g. CDK4, AKT), steroid hormone receptors (e.g. GR, AR, ER) and receptor tyrosine kinases (e.g. Her2)	Limitless proliferation	Beliakoff *et al.,* (1996), Munster *et al.,* (2002), Schulte *et al.,* (1996), Stepanova *et al.,* (1996).
MMP2	Invasion and metastasis	Eustace *et al.,* (2004)

Abbreviations in use: HIFα, hypoxia-inducible factor alpha; MMP2, matrix metalloproteinase 2; CDK4, cyclin dependent kinase 4; AKT, protein kinase B; GR, glucocorticoid receptor; ER, estrogen receptor; AR, androgen receptor; Her2, human epidermal growth factor receptor (HER/EGFR/ERBB).

Proteins of the Hsp90 chaperone cycle

In the cytosol, the Hsp90, Hsc70/Hsp70 (referred to henceforth as Hsp70), Hsp27 molecular chaperones and the Hsp40 co-chaperones perform cytoprotective tasks (Saibil, 2013). The chaperoning function of Hsp90 is assisted by Hsp70, dependent on the activity of their ATPase domains, and co-chaperones (e.g. Hsp40 and Hop) (Pratt and Toft, 2003). In the chaperone cycle, the co-chaperone Hsp40 mediates the selection of the misfolded client protein substrate and associates with Hsp70 in an early complex (Figure 1.3). The Hsp70/Hsp90 organising protein (Hop) co-chaperone, stabilises Hsp90 and facilitates the transfer of the misfolded client proteins from Hsp70 to Hsp90, forming an intermediate complex. As a dynamic protein, Hsp90 enables the binding of ATP at a specific site at its N-terminus and the binding of client proteins between the C-terminus and the M substrate-binding domain. The binding and hydrolysis of ATP by the Hsp90 drives a conformational cycle that is necessary for the functioning of the molecular chaperone (Li *et al*., 2012; Trepel *et al.,* 2010; see Figure 1.3 for illustration). The exact mechanism of client protein release from the chaperone machinery after folding events has yet to be discovered (Lu *et al*., 2014).

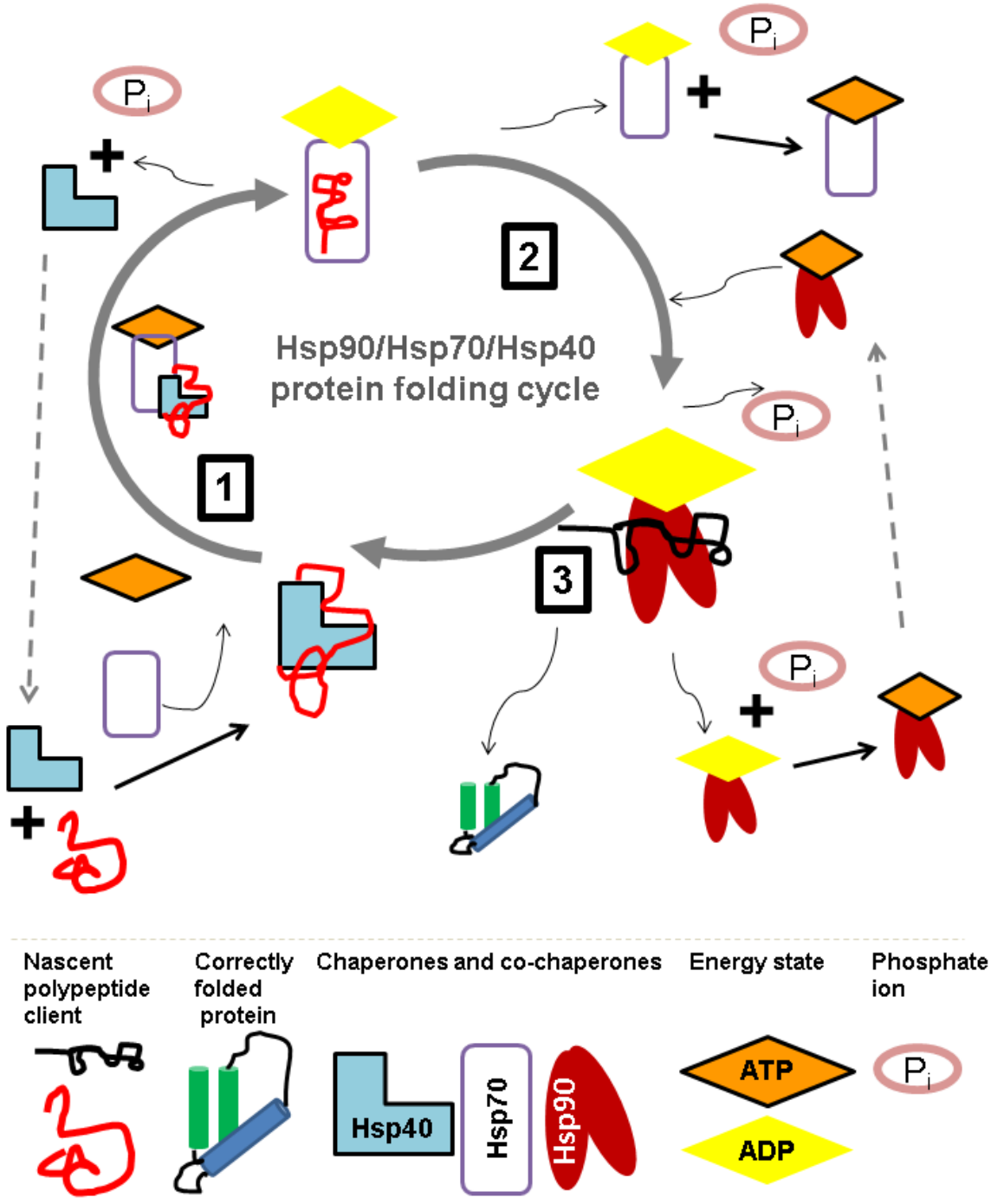

Figure 1.3. Folding of nascent polypeptides by molecular chaperones and co-chaperones.

The cyclical transfer of misfolded (or nascent polypeptides) clients by the Hsp70 and Hsp90 chaperones and the Hsp40 co-chaperone. 1. Early complex: misfolded client protein interacts with Hsp40 and Hsp70, in an ATP-dependent fashion. 2. Intermediate complex: the client is transferred from the Hsp70 to ATP-bound Hsp90, facilitated by the Hsp70/Hsp90 organising protein, Hop co-chaperone. 3. Release: the hydrolysis of ATP facilitates the release of the mature client protein from Hsp90. Adapted from (Zhang and Burrows, 2004; Li *et al*., 2012).

Hsp70 in humans has 13 isoforms, including both constitutive (Hsc70) and stress-inducible (Hsp72), and the mitochondrial and endoplasmic reticulum Hsp70s, Hsp75 (mortalin) and Grp78. Hsp70 proteins consist of three domains, the N-terminal ATPase domain, peptide-binding domain and C-terminal variable region for substrate binding (Flaherty *et al.,* 1990; Zhu *et al.,* 1996). Functionally, both Hsp27 and Hsp70 mediate protein folding. Hsp70 stabilises nascent (pre-mature) polypeptides before delivery to Hsp90 during protein folding. Importantly, Hsp27 and Hsp70 are also known to block programmed cell death, revealing an important anti-apoptotic nature of cancers with increased Hsp27 and Hsp70 (Calderwood *et al*., 2006). Hsp40s are encoded by 44 genes in humans and are characterised by an N-terminal J domain, a glycine/phenylalanine-rich domain, a cysteine-rich domain and a C-terminal dimerization domain (Venter *et al.,* 2001). Depending of the presence of these domains, the Hsp40 co-chaperones are denoted as either Type I, II or III; or DNAJ A, B or C (Ohtsuka and Hata, 2000). The J domain of Hsp40 proteins stimulates the ATPase domain of Hsp70s (Karzai and MaMacken, 1996). The Hsp40 co-chaperone assists in the folding of aggregated polypeptides by selecting and presenting the client substrate to Hsp70 and stimulating the basal ATPase activity of Hsp70 (see Figure 1.3 for illustration) (Hendrick *et al.,* 1993; Martin and Hartl, 1997).

Hsp90 in cancer and metastasis

During the development of a tumour, the expression of Hsp90 is thought to increase, thereby aiding the growth and survival of the cancerous cells (Ciocca and Calderwood, 2005). Hsp90, Hsp70, various co-chaperones and client proteins act together in a dynamic complex known as the Hsp90 chaperone machine (Pratt and Toft, 2003). Cancer cells make use of Hsp90 chaperone machinery to protect over-expressed oncogenes and other mutated proteins to ensure the survival of the cell and assist in cellular homeostasis (Dezwaan and Freeman, 2008). Growth signal self-sufficiency is largely mediated by Hsp90, which ensures signaling proteins are kept in easily activated conformations to enable a swift response to extracellular signals while facilitating in cellular development and renewal (Pratt *et al.,* 2004; Ciocca and Calderwood, 2005).

The expression of Hsp90 by a variety of cells has shown that Hsp90 is not confined intracellularly, but is also secreted into the extracellular space (Sidera and Patsavoudi, 2008). Eustace and colleagues described the role of extracellular Hsp90α in cancer cell motility and invasion, which are important features of metastasis (Eustace *et al.,* 2004). Metastatic cells have shown higher levels of Hsp90 on the cell surface, when compared to normal cells, and links Hsp90 with metastatic activity. Inhibiting or neutralizing secreted or extracellular Hsp90

inhibited *in vitro* cell motility and *in vivo* tumour metastatic activity, providing support for the role of Hsp90 in cancer progression (Becker *et al.,* 2004; Tsutsumi *et al.,* 2008). By interacting with CD91, a cell surface receptor, extracellular Hsp90 stimulated cell migration. While extracellular Hsp90's role currently appears to be restricted to cell migration, intracellularly, Hsp90 regulates the conformation of numerous client signaling proteins required for cell growth and differentiation, including signal transduction pathways (Cheng *et al.,* 2008; Tsutsumi *et al.,* 2008; reviewed in Trepel *et al.,* 2010). Furthermore, Hsp90β, but not Hsp90α has been found important during embryonic development in mammals, suggesting that the two isoforms are not functionally redundant and therefore may have different roles in cancer that are yet to be explored (Voss *et al.,* 2000). In support of this, the relationship between the level of chaperone expression and cellular senescence events in cancer are well established (Sherman *et al.,* 2007).

The link between chaperone function and longevity of stem cells has been defined in literature (reviewed by Soti and Csermely, 2002; Soti and Csermely, 2003). The shared upregulation of Hsp90 in embryonic stem cells and in cancer has posed several interesting questions into the role for molecular chaperones in the JAK/STAT3 pathway for self-renewal (Prinsloo *et al.,* 2009). The transcription factors Oct-4, Nanog and the signal transducer and activator of transcription (STAT3) are cruicial to the maintenance of self-renewal of murine embryonic stem cells. The Hsp70 and Hsp90 chaperone complex was implicated in the regulation of pluripotent signaling through support for the role of Hop in the nuclear translocation of STAT3 in murine embryonic stem cells (Longshaw *et al.,* 2009). The leukaemia inhibitory factor (LIF), required for pluripotency maintenance in the murine system, has been shown to promote the interaction between Hsp90 and STAT3 in mouse embryonic stem cells (Setati *et al.,* 2010). The expression of OCT-4, embryonic marker and a key regulator of self-renewal, is correlated with the tumour state of bladder cancers (Atlasi *et al.,* 2007). Through its regulation of Oct-4 and Nanog the importance of Hsp90 in murine embryonic stem cell pluripotency has been demonstrated (Bradley *et al.,* 2012). As the upregulation of Hsp90 is observed in both embryonic cells and cancer cells it may therefore be speculated that Hsp90 is upregulated in CSC, and poses further questions into the role of Hsp90 in cancer and CSC.

Targeting Hsp90 in therapeutics

Targeting Hsp90 is attractive because of the potential for therapeutics to simultaneously target multiple cellular pathways regulated by oncogenic client proteins of Hsp90 (Neckers, 2002). The involvement of Hsp90 in numerous cell activities, including protein folding, signal transduction, growth and apoptosis, and the 2 – 10 fold upregulation of Hsp90 in cancer cells,

has provided much support for the investigation of the role of Hsp90 in cancer biology (Pratt and Toft, 2003). Fundamental research on the function of Hsp90 in cancers has seen the development of several means by which to target Hsp90, in an attempt to produce novel therapeutics against cancers.

In 2003, Kamal and colleagues demonstrated that Hsp90 from tumour cells were approximately 100 times more sensitive to Hsp90 inhibition due to a high-affinity super-chaperone complex in tumour cells (Kamal *et al.,* 2003). There are 13 Hsp90 inhibitors involved in clinical trials in cancer patients, 3 of which are currently in use by clinics (Kim *et al.,* 2009), however, targeting Hsp90 as an anti-cancer therapeutic is not without concern for the potential for cytotoxic effects from the inhibition of Hsp90 in normal cells too. Geldanamycin is an ansamycin antibiotic (see Figure 1.4A), originally discovered as a benzoquinone microbial product, that directly competes with ATP for binding to the N-terminus of Hsp90 (Wehrli, 1977). The progress of geldanamycin in clinical trials was halted during preclinical studies where *in vivo* studies revealed the instability and hepatotoxicity of the inhibitor (Supko *et al*., 1995). The subsequent generation of analogues of geldanamycin have provided more success under clinical evaluation. Hsp90 inhibitor 17-N-allylamino-17-demethoxygeldanamycin (17-AAG; Figure 1.4B) is a derivative of the naturally occurring geldanamycin, and also binds the N-terminal domain of Hsp90, effectively inhibiting ATP binding and Hsp90 chaperone activity (Prodromou *et al.,* 1997; Stebbins et al., 1997; Panaretou *et al.,* 1998). The Hsp90 inhibitor, 17-AAG (drug name Tanespimycin™), entered clinical trials in 1999. The administration of 17-AAG was shown to produce anti-tumour activity in clinical trials (Blagosklonny, 2002).

Since then, improvements to aspects of the inhibitors have improved the solubility of the drug. Hsp90 inhibitor, 17-dimethylaminoethylamino-17-demethoxygeldanamycin (17-DMAG; drug name: Alvespimycin™), is a water-soluble analogue of geldanamycin that entered into clinical trials in 2004. While 17-DMAG showed improvements to solubility, little to no difference was seen in the activity of 17-DMAG in comparison to that of 17-AAG (Hollingshead *et al.,* 2005). Targeting Hsp90 in cancer, using geldanamycin or 17-DMAG, has resulted in an induction in the expression of other Hsp, including Hsp27 and Hsp70 (Lee *et al.,* 2012), in response to the inhibition of Hsp90 and may prove influential in determining the sensitivity of tumours to Hsp90 inhibitors. More recently, phase II clinical trials have begun using Ganetespib, 5-[2,4-dihydroxy-5-(1methylethyl)phenyl]-2,4dihydro-4-(1-methyl-1indol-5yl)-3H-1,2,4triazole-3-one. Ganetespib is a second generation novel triazolone heterocyclic N-terminal inhibitor of Hsp90 (Socinski *et al.,* 2013). Ganetespbib has shown to be a potent across a range of cancers, with manageable side effects, providing renewed interest in Hsp90 inhibition as a cancer therapy (Proia *et al.,* 2011).

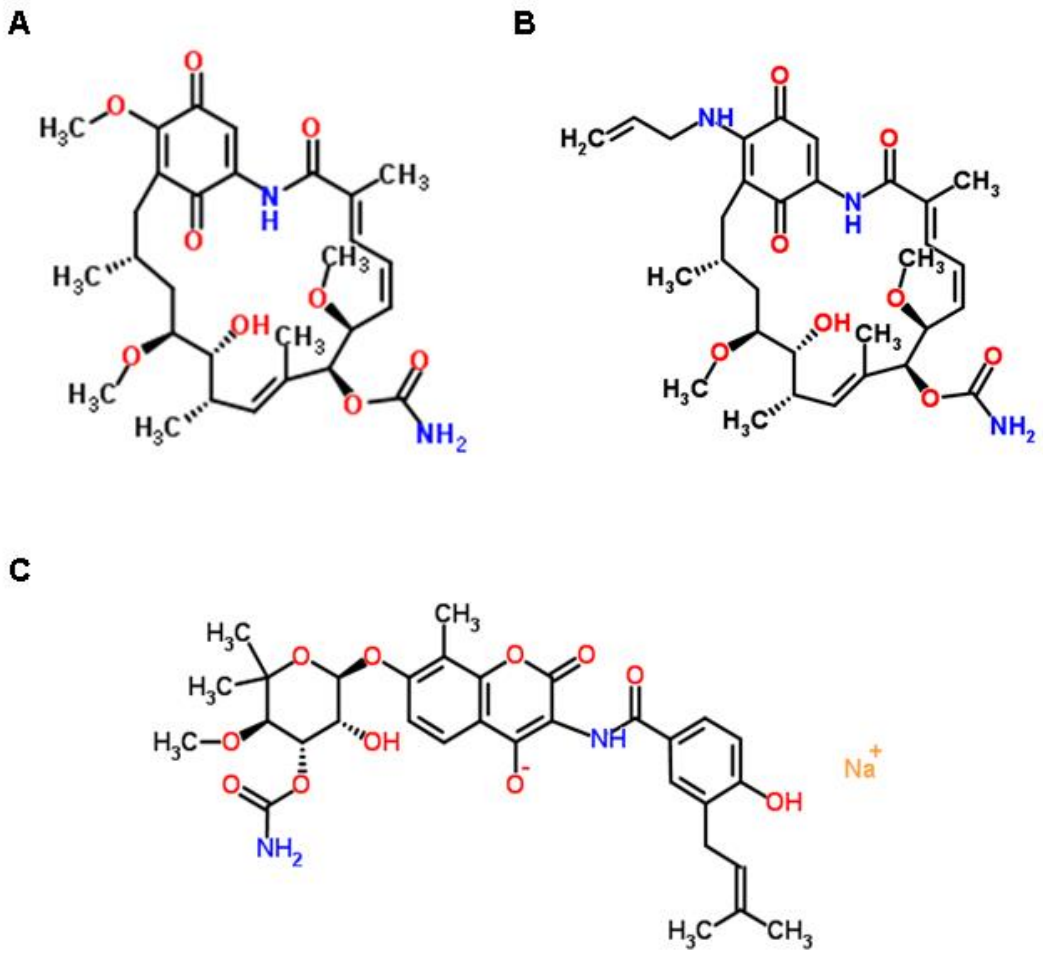

Figure 1.4. The chemical structure of selected Hsp90 inhibitors.

A. The structure of geldanamycin an N-terminal Hsp90 inhibitor. B. The structure of 17-AAG an N-terminal Hsp90 inhibitor. C.The structure of novobiocin, a C-terminal Hsp90 inhibitor. Adapted from (Patel *et al.,* 2004; Gava and Ramos, 2009; illustrations Royal Society of Chemistry, 2015).

A second means by which Hsp90 is inhibited, targets the C-terminal of Hsp90 to diminishe ATPase activity and dimerisation (Marcu *et al*., 2000). Novobiocin, a coumarin antibiotic, is one such Hsp90 inhibitor (Figure 1.4C). Novobiocin blocks the synthesis of DNA in bacteria by targeting DNA gyrase (reviewed by Zhang and Burrows, 2004; Trepel *et al*., 2010). Unlike the N-terminal inhibition by geldanamycin, inhibition of the C-terminus of Hsp90 by novobiocin was not shown to elicit the heat shock response (Mathews *et al.,* 2010). Successfully, C-terminal Hsp90 inhibition improved the response of cellular toxicity in comparison to the administration of benzoquinone ansamycin inhibitors. The downfall of C-terminal inhibition by novobiocin is evident where lower affinity for Hsp90 requires compensatory high dosages to achieve similar inhibition (Mathews *et al.,* 2010; Burlison *et al.,* 2008). Through side chain substitutions of the novobiocin coumarin ring second generation analogues have been derived with higher affinity for Hsp90. More recently, a more potent analogue of novobiocin, KU174, has demonstrated anti-cancer effects in prostate cancer cells without eliciting the heat shock response (Eskew *et al*., 2011). While recent advances have improved the toxicity and side effects of developing Hsp90 inhibitors, known inhibitors of Hsp90 do not specifically identify any one isoform of Hsp90; Hsp90α, Hsp90β, TRAP or Grp94.

Motivation for the current study

The discovery of tumours demonstrting tumour heterogeneity and putative CSC has implicated 'stemness' in the recurrence and aggression of cancers (Longley and Johnston, 2005; Reya *et al.,* 2011). Although the EMT has been associated with CSC, and CSC tumourigenicity is defined as being able to induce cancer formation at a secondary location, as in metastases, there is currently no definitive link between CSC and metastasis. Whether or not the presence of CSC defines the metastatic potential of the tumour has yet to be elucidated. CSC identified from cancer cell lines have demonstrated beneficial to the study of tumour progression (Fillmore and Kuperwasser, 2008).

Migrating CSC have been used to model the progression of cancers through tumour initiation and metastasis (Brablatz *et al.,* 2005). The SW480 and SW620 are isogenic (genetically paired) colon cancer cell lines, sharing a genetic background. The SW480 and SW620 cell lines were derived from the different stages (primary tumour and metastasis, respectively) of colon cancer in the same patient, sampled a year apart. The selection of the genetically paired SW480 and SW620 cell lines facilitated our investigations into the changes associated with the acquisition of a metastatic phenotype (Hewitt *et al.,* 2000). The CSC theory challenges the stochastic theory of cancer development and has implications for metastases. If CSC are

responsible for tumour initiation, they may also be responsible for cancer relapse, through the resistance to anti-cancer therapeutics, and thereby, metastasis.

The upregulation of Hsp90 in cancer has been associated to the growth, survival and spread of cancerous cells (Ciocca and Calderwood, 2005). Furthermore, an increased expression of Hsp90α, identified in breast CSC (Lee *et al.,* 2012), is correlated with a decreased chance of breast cancer survival (Jemeel *et al.,* 1992). The association of Hsp90 with cell surface receptors, such as MMP2 and CD91 (Eustace *et al.,* 2004; Cheng *et al.,* 2008), has strengthened evidence supporting a role of extracellular Hsp90 in cancer cell motility and invasion, features necessary for the metastatic spread of cancer. The importance of investigating Hsp90 as a potential therapeutic target against cancer is highlighted by the influence of Hsp90 on cell signaling, cell migration and cell-cycle progression (Zhang and Burrows, 2004). The identification of a role for extracellular Hsp90 in cell migration and invasion has seen the development of cell-impermeable Hsp90 agonists (inhibitors and antibodies), which have proven successful in blocking tumour cell motility and invasion (Tsutsumi *et al.,* 2008; Snigireva *et al.,* 2014). While inhibitors for the specific targeting of Hsp90 by isoform (Hsp90α, Hsp90β, TRAP1 or Grp94) have yet to be developed, some advancement in the field or RNA interference (RNAi) has facillitated the transient analysis of Hsp90α or Hsp90β knockdown (Azoitei *et al*., 2012). Since Hsp90 is considered a master regulator of cancer cell biology, invastion, metastasis, and Hsp90 is upregulated during embryonic development we speculated that Hsp90 may play a role in CSC biology.

Hypothesis

Hsp90 regulates proteins and signaling molecules that influence characteristics of cancer and CSC biology.

Aim and Objectives

We used a genetically paired cell line model derived from a single patient, representative of pre-metastatic and metastatic colon adenocarcinomas as an *in vitro* model to study the role of Hsp90 and CSC in colon cancer progression *in vitro*. As the SW480 and SW620 cell lines are genetically paired, they provide an *in vitro* model to study the cellular changes during development of a metastatic phenotype.

The following objectives were established in order to address the role of Hsp90 in colon cancer and CSC biology:

1. Comparison of SW480 and SW620 cell lines for distinguishable biological traits.
2. Comparison of SW480 and SW620 cell lines in response to Hsp90 inhibition.
3. Analysis of the effect of Hsp90α knockdown on the Wnt pathway in the SW480 cell line.

Chapter 2: Comparison of SW480 and SW620 cell lines for distinguishable biological traits.

Introduction

The CSC theory challenges the stochastic theory of cancer development and implicates a small proportion of cells within a cancer with stem-like properties in the development of tumours (Sell, 2004; Whicha *et al.,* 2006). In this model, CSC retain their differentiation potential and their ability to self-renew by undergoing symmetric or asymmetric division (see Figure 1.2). The CSC theory has been used to describe the propagation of leukaemic (blood) and solid (tissue) tumours from CSC of primary cancer tissues and cancer cell lines of the brain, breast, colon, lung, prostate, melanoma and glioblastoma (Bonnet and Dick, 1997; Singh *et al*., 2003; Al-Hajj *et al.,* 2003; Ho *et al*., 2007; Collins *et al*., 2005; Dou *et al*., 2007; Qiang *et al*., 2009).

Colon cancer-related deaths are often as a result of the failure of anti-cancer treatments to target the colorectal cancer cells (Jemal *et al.,* 2006). Periostin overexpression has been observed in many colon cancers, with highest levels of expression potentially correlating to the formation of metastatic tumours in the liver as a result of enhanced survival through modulation of the αvβ3 integrin Akt pathway (Bao *et al.,* 2004). Metastases are the main cause of death in cancer patients (Weigeit *et al.,* 2005). Brabletz and colleagues argue the use of a colorectal cancer cell model for the study of the migrating CSC as the driving force behind malignancy. This model accounts for the importance of Wnt/β-catenin signaling in both stem cell formation and EMT, thereby incorporating many aspects of tumour progression including tumour initiation and metastasis (Brabletz *et al.*, 2005). Primary colon cancer cells have been shown to form three-dimensional spheres (tumourspheres; TS) under serum-free conditions *in vitro* (Fang *et al.,* 2010). Spheres derived from the anchorage-independent growth of colon cancer cell lines has highlighted the importance of putative CSC in drug resistance and cancer relapse (Collura *et al*., 2013). While CSC from cell lines are poorly characterised, cell lines represent tumours without any influence of surrounding stromal tissue, and therefore can serve as a useful tool in cancer research to model tumour progression, describe and characterise putative CSC, and to best identify novel drugs for clinical use (Lajkó *et al*., 2012; Collura *et al*., 2013). To model breast cancer paired malignant and benign epithelial immortalised cell lines, such as the Hs578T and Hs578Bst pair and the MCF-7 and MCF-10A pair, and metastatic MDA-MB-231 cell lines have been used (Eckert *et al.*, 2004; Hughes *et al*., 2008; de la Mare *et al*., 2013).

Investigations into the early phase of colon cancer progression using two cell lines, SW480 and SW620, has validated the usage of paired cell lines to model the progression of colon cancers (Hewitt *et al*., 2000). The derivation of the SW480 and SW620 cell lines was established by Leibovitz and colleagues who classified both cell lines as Group 2 colon cancer

cell lines, displaying dedifferentiated morphologies with hyperdiploid chromosomal numbers. The SW620 metastatic cell line was derived from the lymph of the same patient from which the SW480 (primary) pre-metastatic adenocarcinoma was sampled (Leibovitz *et al.,* 1976). Several oncogenes, such as TERT, MAF, ERBB3 and SAP2, are upregulated in SW620 cells, but not SW480 cells, suggesting a role of these oncogenes in the metastatic spread of the SW620 cells (Melcher *et al.,* 2000).

Genetic and phenotypic differences and similarities between the SW480 and SW620 paired cell lines provided a model for the study of early and late colon cancer cells. The objective of this chapter was to assess the SW480 and SW620 cell lines as a model for cancer progression by comparing a range of biological activities linked to cancer development.

Materials and Methods

Materials

All general reagents mentioned were purchased from Sigma-Aldrich (Germany) or Saarchem (Merck, South Africa), unless otherwise stated. Please refer to Table 3, Table 4 and Table 5 for a detailed list of antibodies and their individual specifications used. Specialised reagents, plasticware and kits purchased are reflected in the appropriate methodology.

Methods

Adherent cell lines and culture conditions

Genetically paired human colon adenocarcinoma cell lines SW480 (primary/pre-metastatic tumour; cat no.: 87092801) and SW620 (lymph node metastasis; cat no.: 87051203) were purchased from the European Collection of Cell Cultures (ECACC). SW480 and SW620 cells were maintained in Leibovitz's L-15 medium (Invitrogen, UK) with GlutaMAX™-I, 10 % (v/v) foetal bovine serum (FBS; Biowest, France) and 100 U/ml antibiotic/antimycotic (Penicillin/Streptomycin/Amphotericin, PSA; Gibco, Invitrogen, UK) at 37°C.

Light and phase contrast microscopy

Cells and tumourspheres were analysed by light microscopy using an Olympus CKX41 microscope, or by phase contrast microscopy using a DSZ5000X inverted microscope. Both light and phase microscopes were capable of 40 x, 100 x and 400 x magnification. All images were analysed using ImageJ software (NIH).

Fluorescent microscopy

Cells seeded on coverslips coated with 5 µg/ml fibronectin (Sigma-Aldrich) were fixed in methanol and blocked in 1 % (w/v) bovine serum albumin (BSA) in phosphate-buffered saline (PBS, pH 7.4, 16 mM Na_2HPO_4, 2 mM KH_2PO_4, 137 mM NaCl, 3 mM KCl; 1 % (w/v) BSA/PBS) for 45 minutes prior to incubation in primary antibody (Table 3) in 0.1 % (w/v) BSA/PBS overnight at 4°C. Coverslips were incubated in secondary antibodies (Table 4) in 0.1 % (w/v) BSA/PBS for 1 hour (H) at room temperature after two washes in 0.1 % (w/v) BSA/PBS. Cells were washed twice in 0.1 % (w/v) BSA/PBS prior to nuclear staining with 1 µg/ml Hoechst 33342 in distilled water. Coverslips were mounted with DAKO mounting media and sealed. Microscopy was carried out using Zeiss AxioVert.A1 Fluorescence LED Inverted Microscope with a High Resolution AxioCam MRm Rev 3. Images were analysed using ZEN Lite 2012 1.1.2.0 (Zeiss).

Table 3. Primary and secondary antibodies for Western blotting and Immunofluorescence

Antibody	Company (Vendor)	Cat No.:	Clone	Species	Western Blot Dilution	Microscopy Dilution
Anti-α tubulin	Abcam	ab7291	DM1A	Mouse	1:5000	1:100
Anti-actin	Sigma-Aldrich	A2103	Polyclonal	Rabbit	1:2000	1:50
Anti-Axin	Santa Cruz Biotechnologies	sc-14029	Polyclonal	Rabbit	1:500	1:50
Anti-β1 integrin	Santa Cruz Biotechnologies	sc-59829	JB1B	Mouse	1:1000	1:50
Anti-β-catenin [H102]	Santa Cruz Biotechnologies	sc-7199	Polyclonal	Rabbit	1:1000	1:50
Anti-c-Myc	Santa Cruz Biotechnologies	sc-40	9E10	Mouse	1:500	1:50
Anti-DNAJB6	Abnova	H00010049-M01	2C11-C1	Mouse	1:1000	1:50
Anti-DNAJC6	Abcam	ab103321	Polyclonal	Rabbit	1:250	1:50
Anti-E-cadherin	Cell Signaling Technology	3195	Polyclonal	Rabbit	1:500	1:50
Anti-fibronectin	Sigma-Aldrich	F0916	IST-4	Mouse	1:1000	1:50
Anti-GSK3β [H-76]	Santa Cruz Biotechnologies	sc-9166	Polyclonal	Rabbit	1:1000	1:50
Anti-histone H3	Cell Signaling Technology	9715	Polyclonal	Rabbit	1:2500	1:100
Anti-HSF-1	Santa Cruz Biotechnologies	sc-13516	10H8	Rat	1:1000	1:50
Anti-Hsp27	StressMarq Biosciences Inc	SMC-161B	5D12-A12	Mouse	1:2500	1:100
Anti-Hsp40	Abcam	ab69402	Polyclonal	Rabbit	1:5000	1:100
Anti-Hsp70/Hsc70	Santa Cruz Biotechnologies	sc-24	W27	Mouse	1:1000	1:50
Anti-Hsp90α/β	Santa Cruz Biotechnologies	sc-1055	N-17	Goat	1:1000	1:50
Anti-Hsp90α	Enzo Life Sciences	ADI-SPA-840	9D2	Rat	1:1000	1:50
Anti-Hsp90α/β	Santa Cruz Biotechnologies	sc-13119	F-8	Mouse	1:1000	1:50
Anti-Hsp90β	StressMarq Biosciences Inc.	SPC-177 C/D	Polyclonal	Rabbit	1:1000	1:50
Anti-pan Akt	Cell Signaling Technology	2920	40D4	Mouse	1:2000	1:50
Anti-pan cytokeratin	Abcam	ab6401	PCK-26	Mouse	1:1000	1:50
Anti-phospho β-catenin [Ser33/37/Thr41]	Cell Signaling Technology	9561	Polyclonal	Rabbit	1:1000	1:50
Anti-phospho STAT3	Santa Cruz Biotechnologies	sc-7993	Polyclonal	Rabbit	1:1000	1:50
Anti-RFP	Thermo Scientific	MA5-15257	RF5R	Mouse	1:1000	1:50
Anti-vimentin	Cell Signaling Technology	5741	Polyclonal	Rabbit	1:1000	1:50

Table 4. Secondary antibodies used for Western blotting and immunofluorescence

Antibody	Company (Vendor)	Catalogue Number	Species	Isotype	Dilution
Anti-rat	Santa Cruz Biotechnologies	sc-2032	Goat	IgG	1:5000
Anti-mouse	Santa Cruz Biotechnologies	sc-2314	Donkey	IgG	1:5000
Anti-rabbit	Abcam	ab6802	Donkey	IgG	1:5000
Alexa Fluor-488 (green) anti-mouse	Life Technologies	A21202	Donkey	IgG	1:500
Alexa Fluor-633 (purple) anti-goat	Life Technologies	A21082	Donkey	IgG	1:500
Alexa Fluor-555 (red) anti-rabbit	Life Technologies	A10040	Donkey	IgG	1:500
DyLight-488 (green) anti-rabbit	Abcam	ab96891	Donkey	IgG	1:500

Cell proliferation WST-1 assay

Cells were seeded in 100 µl of medium at densities of 1000 - 5000 in 96-well plates at 37°C overnight. After the addition of 10 µl/well WST-1 proliferation reagent (Roche Applied Sciences, Germany; cat no.: 05 015 944 001) and incubation for 3 H, the absorbance at 440 nm was analysed on the PowereWave spectrophotometer (Bio-Tek Instruments, USA). Briefly, tetrazolium salts in the WST-1 reagent are cleaved into soluble formazan, which is quantitated by spectrophotometry, and indicative of metabolically active (viable or intact) cells.

Real-time analysis of cell growth

Real-time analysis of SW480 and SW620 cell lines was performed using the xCELLigence™ System (Roche Applied Sciences) for the electronic detection of the gold sensor electrode impedance by cells in culture. The 96-well E-plate was washed and equilibrated in PBS prior to the seeding of 3000 cells in 100 µl medium. SW480 and SW620 cells were analysed in the E-plate for 96 H at 37°C, in triplicate and in real time. The dimensionless Cell Index (CI) parameter was used to assess the biology of the cells by adhesion and growth *in vitro* using xCELLigence™ and RTCA 1.2.1 software. Cell Index (CI) output is calculated from the difference in impedance at an individual point of time (Z_i) from the impedance at the beginning of the experiment (Z_0), where $CI = \frac{Zi-Z0}{15}$. xCELLigence data were graciously provided by Dr de la Mare (Rhodes University, Faculty of Science).

Wound healing (scratch) assay

SW480 and SW620 cells were seeded into untreated 96-well plates (at a density of 1 x 10^6 cells/ml) or plates pre-treated with 0.01 % (w/v) type I collagen or 5 µg/ml fibronectin and allowed to adhere overnight at 37°C. Wounds to each well were created by the removal of a section of the confluent cell monolayer using a sterile toothpick and changes in the wound size analysed over 24 H. Images were taken at 0, 4, 8, 12 and 24 H after scratching away the wound monolayer of cells using a DSZ5000X inverted microscope. The change in wound area was analysed using ImageJ (NIH) software.

Live/Dead cell discrimination

Cells harvested by lifting in 1 % (w/v) trypsin solution made up in 0.3 % (w/v) ethylenediaminetetraacetic acid (EDTA) were washed, pelleted (500 *x g*, 5 minutes) stained with 2 µg/ml propidium iodide (PI; Sigma-Aldrich, Germany) for live/dead discrimination. A FACSAria II (BD Biosciences, Belgium) was used for the processing of cells by flow cytometry. Using the FACSDiva software, the fluorescent intensity of the signal detected using the blue (488 nm) laser to excite the PI fluorophore and emissions were recorded in the 585/42 filter channel. A gate was used to detect the threshold for high fluorescent intensities detected, and used to eliminate positively (PI) stained cells, to enable the capture of data specific to that of live cells.

ALDEFLUOR® assay

Cell populations with high ALDH enzyme activity were identified by flow cytometry using the ALDEFLUOR kit (Stem Cell Technologies, France) as per the manufacturer's instructions. Cells were lifted with 1 % (w/v) trypsin solution made up in 0.3 % (w/v) EDTA and resuspended at a density of 1 x 10^6 cells/ml in ALDEFLUOR assay buffer. Activated ALDEFLUOR reagent (150 µM per 1 x 10^6 cells) was added to the test sample. A total of 5 x 10^5 cells was removed from the test sample and 150 µM ALDH inhibitor, diethylaminobenzaldehyde (DEAB), was added to create the inhibited control. Both samples were incubated at 37°C for 45 minutes before washing twice in phosphate buffered saline (PBS; 16 mM Na_2HPO_4, 2 mM KH_2PO_4, 137 mM NaCl, 3 mM KCl [pH 7.4]) and resuspension in ALDEFLUOR assay buffer. Samples were analysed by flow cytometry using the FACSAria II and FACSDiva software (BD Biosciences, Belgium). Nucleated cells were identified based on side and forward scatter, and control (DEAB or uninhibited/unstained) cells were used to identify the $ALDH^{high}$ population of SW480 and SW620 cells. ALDEFLUOR fluorescence was measured by excitation using the 488 nm blue laser with emission detection within the fluorescein-isothiocyanate (FITC) 530/30

nm filter channel. Data were analysed using FlowJo software (Tree Star Inc, USA). The results are representative of the average of three technical experimental replicate analyses.

Hoechst efflux assay

The experimental procedure used by Goodell and colleagues was used for the development of the optimised Hoechst 33342 dye exclusion assay (Goodell *et al.,* 1996). Adherent cells were treated in T75 flasks (± 80 % confluency) following a 20 minute equilibration in fresh Leibovitz's L-15 medium (Invitrogen, UK) with GlutaMAX™-I, 10 % (v/v) foetal calf serum (FCS) and 100 U/ml PSA (Gibco, Invitrogen, UK) at 37°C. One flask was treated with the ABCG2 inhibitor, verapamil (50 µM), for 10 minutes before all media was replaced with pre-warmed medium alone, medium supplemented with 5 µg/ml Hoechst 33342 (Invitrogen, UK) or 5 µg/ml Hoechst 33342 and 50 µM verapamil for 60 minutes at 37°C. Cells were washed in PBS before lifting with 1 % (w/v) trypsin solution made up in 0.3 % (w/v) EDTA, quenching in ice cold medium and centrifugation at 300 *x g* for 8 minutes at 4°C. Cells were resuspended in PBS at a density of 1 x 10^6 cells/ml with 2 µg/ml PI for live/dead discrimination (as described above). The side population (SP) was analysed by flow cytometry using the FACSAria II and FACSDiva software (BD Biosciences, Belgium). The Hoechst 33342 dye was excited using the UV laser at 350 nm and the dual emission of Hoechst blue and Hoechst red analysed at 405/30 nm and 670/40 nm, respectively. Data were analysed with FlowJo software (Tree Star Inc, USA).

Staining cells for surface markers

Cells were harvested using 1 % (w/v) EDTA, washed twice with PBS and viable cells resuspended at a density of 5 x 10^6 cells/ml in PBS. A total of 5 x 10^5 cells were placed into tubes containing either 0.25 µg of the relevant directly conjugated antibodies or isotype controls (Table 5), or remained as unstained controls, and incubated at 4°C for 1 H. Following antibody incubation, samples were washed and collected by centrifugation in PBS (centrifugation at 800 x g for 2 minutes). The red (633 nm) laser was used to excite the allophycocyanin (APC) fluorophore and emissions were recorded in the 620/20 filter channel. The blue (488 nm) laser was used to excite the FITC and the PE fluorophore and emissions were recorded in the 530/30 or 585/42 filter channels, respectively. Considering the spectral overlap in the detection of FITC and PE, careful consideration was dedicated to the assignment and usage of conjugated antibodies. To prevent the detection of false results, FITC and PE conjugated antibodies were not used in combination, and BD™ CompBeads (Cat no.:552843/5) were used to compensate (correct for) spectral overlap. Compensation

controls established reference values for channel fluorescent overlap, providing a basis for background, negative and positive populations. Unstained (no antibody) control SW480 and SW620 cells were used to eliminate false positive results by implementing a gating strategy to account for cells presenting any artificial interference to the detection of positively-stained cells. Isotype-matched controls account for any non-specific binding that might influence any true result detected. The isotype controls are matched to complement the species, isotype and conjugated fluorophore of the antibodies used for the detection of surface markers (see corresponding group numbers between the antibodies and isotype controls in Table 5). Using the FACSAria II (BD Biosciences, Belgium) 50 000 events were recorded for each sample and data were analysed on FlowJo software (Tree Star Inc, USA). The experimental data represent the average (mean ± SD) of three independent experiments.

Table 5. Directly conjugated antibodies and isotype controls for flow cytometry

	Identity	Group*	Clone	Company (Vendor)	Catalogue Number	Isotype	Fluorophore
Antibody	**Anti- CD133/1 (AC133)**	1	AC133	Miltenyi Biotech	130-080-801	IgG1, κ	PE
	Anti-CD44	1 and 2	IM7	eBiosciences	17-0441	IgG2b, κ	APC
	Anti-CD24	2	SN3 A5-2H10	eBiosciences	17-0247	IgG1, κ	FITC
	Anti-CD49f (α6 Integrin)	3	GoH3	eBiosciences	17-0495	IgG2a, κ	APC
	Anti-CD338 (ABCG2)	3	5D3	eBiosciences	12-8888	IgG2b, κ	PE
Isotype Control	**Mouse IgG1**	1	P3.6.2.8.1	eBiosciences	12-4714	IgG1, κ	PE
	Rat IgG2b	1 and 2	eB149	eBiosciences	17-4031	IgG2b, κ	APC
	Mouse IgG1	2	P3.6.2.8.1	eBiosciences	11-4714	IgG1, κ	FITC
	Mouse IgG2b	3	eBMG2b	eBiosciences	12-4732	IgG2b, κ	PE
	Rat IgG2a	3	eBR2a	eBiosciences	17-4321	IgG2a, κ	APC

***** The group number assigned matches antibodies and isotype controls used in comparison during the establishment of the gating strategy for the analysis of cell surface markers by flow cytometry (e.g. Group 1 antibodies and Group 1 isotype controls were used in the detection and identification of $CD133^+$ and $CD44^+$ cells).

Anchorage-independent culture of tumourspheres (TS)

The ability of colon cancer cells to form tumourspheres (TS) under anchorage-independent conditions was analysed for 14 days using a protocol optimised after reviewing and adapting work by Kreso and O'Brien (Dontu *et al.,* 2003; Kreso and O'Brien, 2008). Cells were harvested with 1 % (w/v) trypsin solution made up in 0.3 % (w/v) EDTA and resuspended, in single-cell suspension, in conditioned medium to a density of 20 000 cells/ml. TS were maintained in conditioned medium (DMEM) lacking serum but supplemented with 1x B27 supplement (Gibco, Invitrogen, UK), 20 ng/ml basic fibroblast growth factor (bFGF, Thermo Fischer Scientific), 20 ng/ml epidermal growth factor (EGF, Sigma-Aldrich, Germany), 5 µg/ml insulin, 10 mg/ml heparin (Sigma-Aldrich, Germany) and 100 U/ml PSA in ultra-low attachment culture flasks and plates (Corning Incorporated, USA).

Tumoursphere (TS) self-renewal assay

SW480 and SW620 TS were cultured under anchorage-independent conditions from 2000 cells. After 7 days of growth, TS were pelleted by centrifugation at 1000 *x g* (5 minutes) and resuspended in accutase for the dissociation of TS into single-cell suspension and passaging. Cells were counted using a haemocytometer and stained by trypan blue (Sigma-Aldrich, Germany) for the discrimination of live cells. Following enumeration, 2000 cells were re-seeded into anchorage-independent conditions for the subsequent regeneration of tumourspheres of a later passage. The repeated lifting and re-seeding of cells for the generation of TS, known as self-renewal, were analysed by light microscopy for changes to morphological attributes of TS. In addition, cells sampled from each generation of passaged TS were stained for the CD44/CD133 surface marker phenotype and ALDH activity by flow cytometry.

Sodium dodecyl sulphate-polyacrylamide gel electrophoresis (SDS-PAGE) and Western blotting

Mammalian cells were lysed in SDS lysis (sample) buffer or RIPA buffer (50 mM Tris-HCl [pH 7.5], 150 mM NaCl, 0.5 % (v/v) NP-40, 1 mM phenylmethylsulfonyl fluoride, 1 mM EDTA, 1 mM sodium deoxycholate, 1 mM Na_3VO_4 and 2 µg/ml protease inhibitor cocktail). Equal amounts of quantified protein lysates were resolved by Sodium Dodecyl Sulphate-Polyacrylamide Gel Electrophoresis (SDS-PAGE). Gels were electrophoresed according to protocols described by Laemmli (1970). Proteins resolved by SDS-PAGE gels were transferred onto Hybond Supported Nitrocellulose membrane in Transfer buffer (25 mM Tris [pH 7.5], 192 mM Glycine, 20 % (v/v) Methanol) according to the protocol described by Towbin

and colleagues (Towbin and Gordon, 1979). Membranes were blocked in 5 % (w/v) non-fat dry milk in Tris-buffered saline (50 mM Tris [pH 7.5], 150 mM NaCl) buffer ahead of incubation in primary antibody (see Table 3 for details). Bound primary antibody was detected by chemiluminescence following membrane incubation in horseradish peroxidise-conjugated species-specific secondary antibody (see Table 4) on the Chemidoc™ EQ and Chemidoc™ XRS+ systems (Biorad; UK). Images were analysed for densitometry using ImageJ (NIH) software.

Results

The objective of this chapter was to assess the SW480 and SW620 cell lines as a model for early and late colon cancer progression, respectively. To understand colon cancer progression, we investigated biological characteristics and activities linked to cancer development.

Morphological comparison of SW480 and SW620 cells

SW480 and SW620 cell lines were analysed by phase contrast microscopy. Their adherent morphology revealed two distinct cell types (Figure 2.1A). The SW480 cell line showed small groupings of irregular-shaped cells, in comparison to the small spindle-like nature of the SW620 cells. These morphologies are similar to those reported by literature (Leibovitz *et al.,* 1976).

We next analysed the SW480 and SW620 for the expression of a range of proteins important in processes regulating tumour progression by fluorescence microscopy (Figure 2.1B). The control which lacked primary antibody demonstrated that there was no background staining from non-specific secondary antibody binding. E-cadherin, axin, GSK3β and β-catenin proteins were analysed due to their importance to the Wnt/β-catenin pathway in the development and spread of colorectal cancers, and the importance of the Wnt/β-catenin pathway in the self-renewal of normal stem cells and CSC (see Table 6 for summary of details). While the distribution of axin was similar between SW480 and SW620 cells, SW480 cells showed a wider distribution in E-cadherin (including in the vicinity of the nucleus) and in cytoplasmic GSK3β in comparison to SW620 cells (Figure 2.1B). No visible differences in β-catenin were evident between the SW480 and SW620 cell lines. E-cadherin, β-catenin, β1 integrin, cytokeratin and vimentin proteins were studied for their role in epithelial and mesenchymal morphology (see Table 6 for summary of details). Both the SW480 and SW620 cell lines stained positively for β1 integrin, cytokeratin and vimentin, but no substantial differences were observed in the distribution of the proteins. Akt and phosphorylated STAT3 (PSTAT3) were analysed for their importance to the PI3K and JAK/STAT pathways, which also exhibit crosstalk to the Wnt pathway (see Table 6 for summary of details). No differences in Akt distribution were detected between SW480 and SW620 cells, while phosphorylated STAT3 (PSTAT3) staining of SW620 cells showed an increased accumulation in close proximity of the nucleus (Figure 2.1B).

Table 6. Comparison of colon cancer cell by analysis of signaling intermediates

Antibody	Biologically-relevant Association	Protein Marker	Qualitative Observation for SW480 and SW620 cell lines
Cytokeratin (pan)	MET	Fundamental markers of epithelial differentiation	Cytoplasmic
Vimentin	EMT	Mesenchymal. Cytoskeletal intermediate filament. Remodelled in response to external stimuli and important in cell migration through endothelium	Predominantly perinuclear localisation
β1 integrin	EMT	Mesenchymal	Dominates both nuclear and cytoplasmic compartments
β-catenin	Wnt Pathway, EMT	Mesenchymal	Nuclear and cytoplasmic
Axin	Wnt Pathway	Scaffold protein for binding of β-catenin, APC and GSK3β	Predominantly cytoplasmic with nuclear staining
E-cadherin	Wnt Pathway	Epithelial	Punctate cytoplasmic structures
GSK3β	Wnt Pathway	Responsible for β-catenin phosphorylation	Dominantly within the cytoplasm
Akt (pan)	PI3K Pathway	Modulator of Cancer Cell Survival, Migration and Angiogenesis	Cytoplasmic and nuclear
STAT3 (phospho)	JAK/STAT Pathway	Mediates transduction of information between cells are essential for development, cellular differentiation and homeostasis	Predominantly nuclear within punctate structures
c-Myc	Wnt Pathway	Proto-oncogene downstream of Wnt Pathway activation	Predominantly nuclear

The oncogene, c-myc, and cytoskeletal protein, actin, were analysed by confocal microscopy for differences and similarities in the protein subcellular localisation. A closer examination of c-myc showed increased nuclear staining in SW620 cells in comparison to the SW480 cells (Figure 2.1C). The actin staining detected membrane ruffles and an accumulation of protein at the edges of the cells. The SW620 cells showed a more uniform distribution of actin throughout the cells, and the SW480 cells demonstrated increased staining at the cell membrane and membrane ruffles, suggesting a migratory phenotype of SW480 cells. Results from this analysis suggested both SW480 and SW620 cells were similar in the expression and distribution of a number of cancer related signaling proteins, with the exception of c-myc and actin.

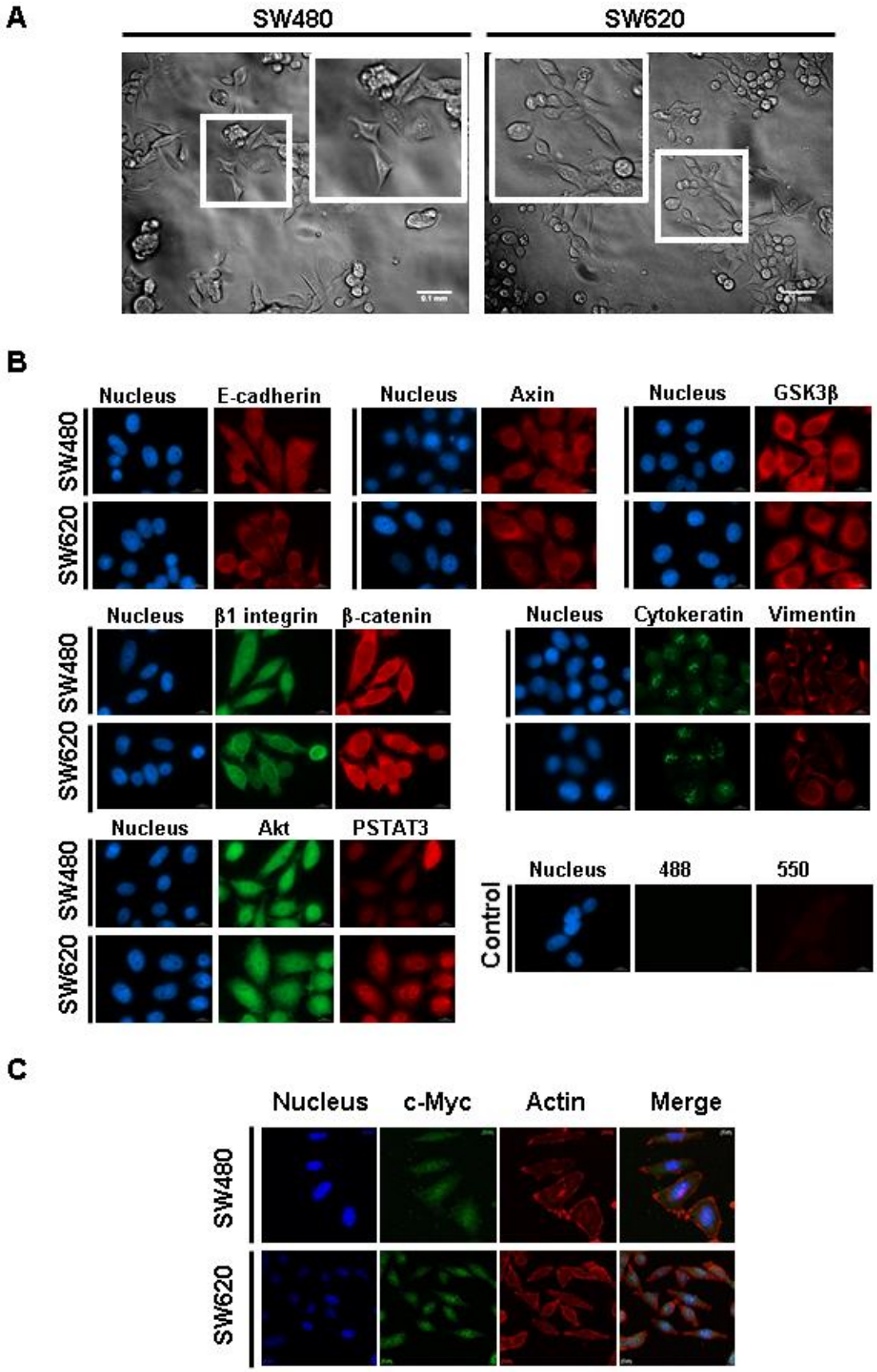

Figure 2.1. Comparison of morphology and expression of cancer related signaling intermediates in SW480 and SW620 cell lines (condinued over page).

Figure 2.1. Comparison of morphology and expression of cancer related signaling intermediates in SW480 and SW620 cell lines.

A. Adherent SW480 and SW620 cells were analysed by phase contrast microscopy 24 H after seeding. Images were taken using a DSZ5000X inverted microscope and analysed using ImageJ software. Scale bar: 0.1 mm; 200 x magnification. B. Protein markers characteristic of mesenchymal or epithelial morphology, Wnt/β-catenin, JAK/STAT or PI3K pathways were compared across SW480 and SW630 colon cancer cells. Epithelial marker: pan-cytokeratin, E-cadherin; Mesenchymal marker: Vimentin, β-1 integrin, β-catenin; Wnt pathway: β-catenin, Axin, E-cadherin, GSK3β; PI3K pathway: pan-Akt; JAK/STAT pathway: Phosphorylated STAT3. Images represent one of three replicated experimental results, taken using Zeiss AxioVert A1 Fluorescence LED Inverted Microscope with a High Resolution AxioCam MRm Rev 3. Data were analysed using ZEN Lite 2012 software. Scale bars: 200 µm, 200 x magnification. C. Immunofluorescent staining of SW480 and SW620 cells seeded on fibronectin (5 µg/ml) overnight at 37°C. Fixed cells were incubated with mouse anti-c-myc, rabbit anti-actin antibodies. Images were captured using the x40 objective on the Zeiss LSM 510 Meta confocal microscope and analysed on AxioVision LE 4.8.2 (Zeiss). Images are examples of triplicate images captured. Scale bars represent 10 µm, 400 x magnification. Nuclei were stained with Hoechst 33342 (blue). Alexa Fluor 488 conjugated donkey anti-mouse IgG (green) and Alexa Fluor 555 conjugated donkey anti-rabbit IgG (red) secondary antibodies were used.

Comparison of SW480 and SW620 growth phenotypes

SW480 and SW620 cells were next compared in cell density and growth. To assess differences in growth between the paired cell lines, the growth of equivalent numbers of cells (1000 – 5000) were analysed, in triplicate, after 72 H of adherence using the WST-1 assay for cell proliferation. Only minimal differences in growth were evident between the two paired cell lines (Figure 2.2A). At lower cell density, SW620 cells showed enhanced growth in the over the SW480, a difference which became less noticeable with cell density greater than 3000. The analysis of cell growth *in vitro* using the xCELLigence™ to assess the growth of 3000 SW480 and SW620 cells over 96 H in real time. Cell index (CI) output was used to compare the adhesion and growth of the two cell lines over time. The CI values reported for the SW620 cells were higher than that of the SW480 cells, which perhaps reflected the different morphologies of the cells observed earlier (Figure 2.2B). Both cell lines demonstrated similar growth trends, indicated by the similarity in the shapes of the respective curves. The trend of the graph demonstrated that SW480 and SW620 cells both required approximately 35 H to adhere as indicated by the lack of change in CI over this time frame. Between 35 and 90 H of growth the CI values for both cell lines steadily increased, showing similar proliferation, prior to a plateau at 96 H. These findings indicated the similarity in growth between both paired cell lines *in vitro*.

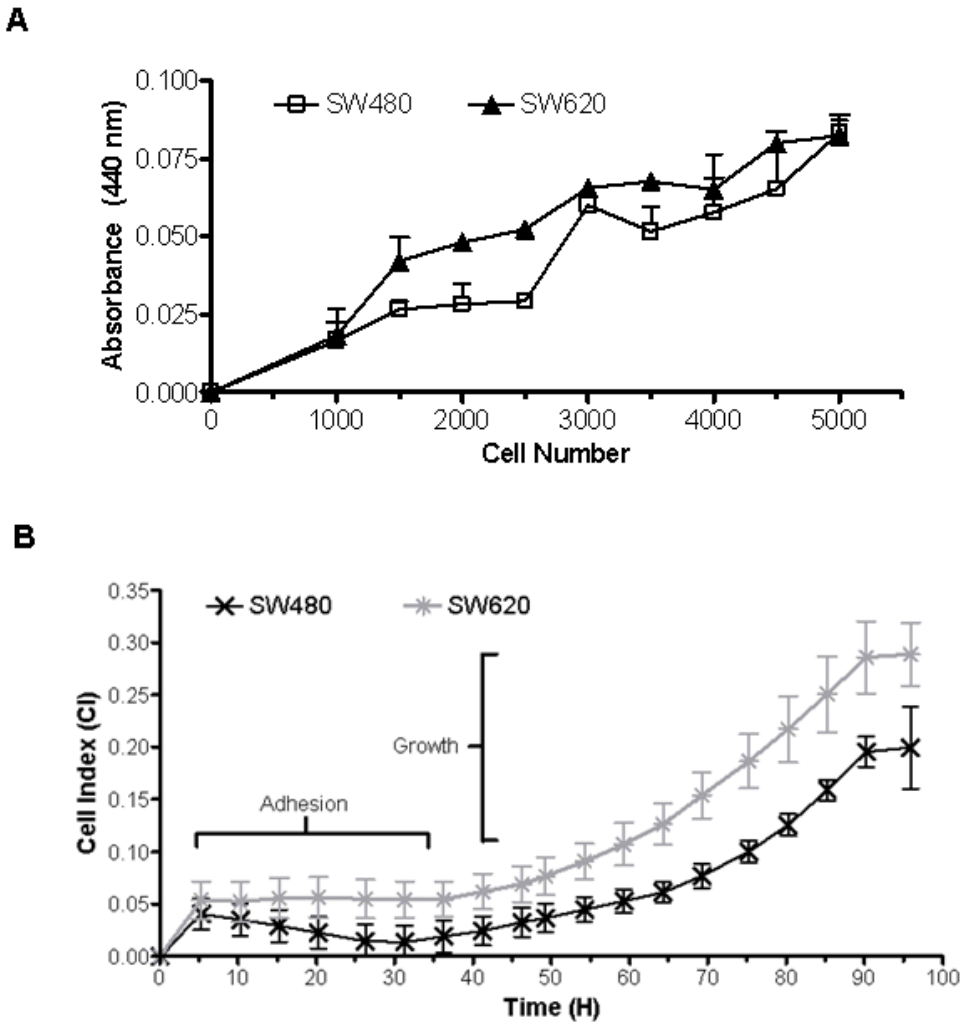

Figure 2.2. Comparison of the growth of the SW480 and SW620 cancer cell lines.

Comparitive differences in SW480 and SW620 cell growth. A. Equivalent numbers of SW480 and SW620 cells were incubated f or 72 H at 37°C to allow for adherence. The viability of 1000 – 5000 cells was comparatively assessed across the SW480 and SW620 cell lines by WST-1 assay. Results represent the mean ± SD of three replicates. Absorbance values were normalised to account for background detection of medium. B. The SW480 and SW620 cell lines (3000 cells/well) were assessed by growth at 5 H intervals for 96 H, by xCELLigence (RTCA 1.2.1). Cell Index (CI) denoted a dimensionless and relative value. CI was calculated from the difference in impedance at an individual point of time (Z_i) from the impedance at the beginning of the experiment (Z_0), where CI $= \frac{Zi-Z0}{15}$. xCELLigence data represented was graciously provided by Dr de la Mare.

Comparison of the migration of SW480 and SW620 cell lines

To characterise the migration of the SW480 and SW620 cell lines, a wound healing (scratch) assay was used. Extracellular matrix (ECM) proteins, collagen and fibronectin, were used to investigate the effect of different matrices on the ability of cells to migrate. The change in wound area over 24 H was monitored to define the migratory potential of the SW480 and SW620 cells *in vitro* (Figure 2.3). The least stimulation of movement across both cell lines (wound closure) was seen when cells were plated on tissue culture plastic in the absence of additional extracellular matrix proteins (Untreated; Figure 2.3A). Although neither cell line achieved total wound closure within 24 H, SW480 cells showed a greater migratory capacity, illustrating greater wound area closure over SW620 cells in the same amount of time (Figure 2.3A). Collagen produced the most statistically significant difference in migration in both SW480 and SW620 cells (> 35 and > 10 % difference, respectively), providing the most effective surface for attachment, while fibronectin only stimulated wound closure in the SW480 cells (Figure 2.3B). Data from this migration potential analysis was supported by statistical analyses of two-way ANOVA, comparing between cell lines. A one-way ANOVA comparison of migration across collagen after 24 H, between the two cells lines, supported the significance in this difference ($p < 0.05$). These data indicated that SW480 cells have a higher migratory potential over that of SW620 cells.

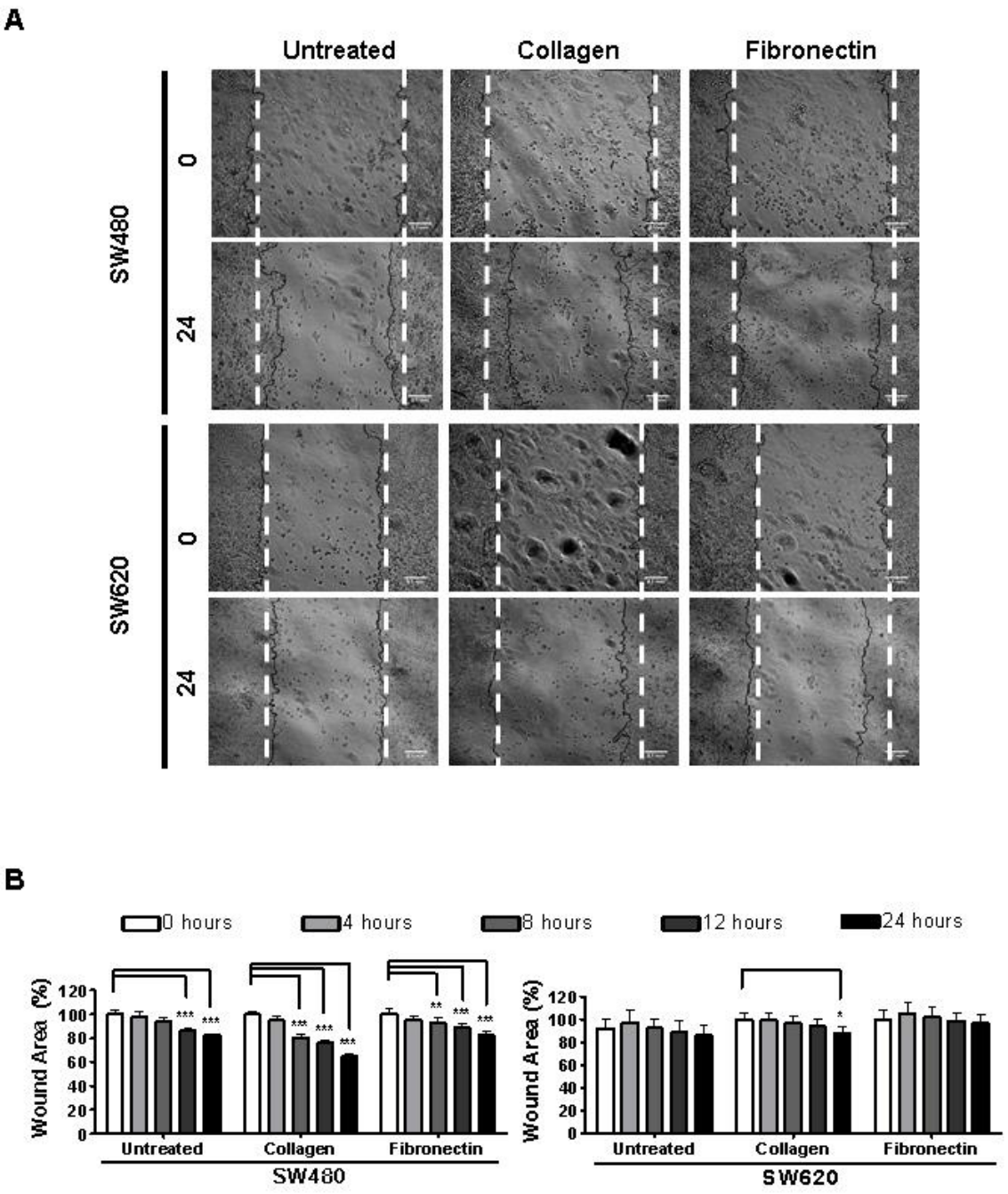

Figure 2.3. Comparison of migration of SW480 and SW620 cell lines.

The migration of SW480 and SW620 cells was analysed over 24 H for wound closure, with adhesion across an extracellular matrix protein coated surface. A. Comparative migration of cells on collagen or fibronectin matrices. Cells were seeded to confluency on 0.01 % (w/v) collagen type I or 5 µg/ml fibronectin in comparison to uncoated TC plate samples in a 96-well plate and allowed to adhere overnight. Wounds were made by scraping the cell monolayer using a sterile toothpick and images were taken of the movement of cells as closure of the wound at time 0, 4, 8, 12 and 24 H of incubation. Scale bars represent 0.1 mm (40 x magnification). B. Wound area represents the percentage of the area of the wound which remains open, relative to 0 H, as a result of cell migration. Results are representative of six experimental replicates (mean ± SD) and statistical significance was analysed by two-way ANOVA (* = $p < 0.05$; ** = $p < 0.01$; *** = $p < 0.001$) using GraphPad Prism software.

Identification of putative stem-like cell populations in SW480 and SW620 cells

CSC represent the rare subpopulation of cancer cells that display the functional and behavioural characteristics of stem cells (Reya *et al.,* 2001). Recent studies have suggested that the CSC subpopulations not only regulate the development of a tumour through self-renewal and differentiation capabilities, but may also regulate the progression of a tumour (Carpentino *et al*., 2009; Collura *et al*., 2013). Given that the SW620 cell line is a metastasis of the primary SW480 cell line, we hypothesised that the SW620 cells may be enriched in CSC-like cells. Several strategies based on functional and phenotypic assays have been proposed for the identification of putative CSC; these assays were applied to the SW480 and SW620 cell lines. Flow cytometry was used to identify putative CSC populations based on the functional characteristics, through the analysis of the side population (SP) based on cellular efflux of Hoechst 33342 (Goodell *et al*., 1996), expression of active aldehyde dehydrogenase (ALDH) and based on the expression of surface protein markers of model CSC (Dalerba *et al*., 2007; Carpentino *et al*., 2009; Fitzgerald *et al*., 2014). Anchorage-independent growth of colon cancer cells as tumourspheres (TS) was utilised to model CSC based on their stem-like behavioural characteristics (Collura *et al*., 2013; de la Mare *et al*., 2013).

Side population (Hoechst efflux) assay

The over expression of membrane transporter proteins, such as ABCG2, responsible for the transport of metabolic products, peptides, lipids and drugs in and out of the cell has been associated with the development of chemotherapeutic drug resistance and cells possessing stem-like characteristics (Allikmets *et al.,* 1996; Abdullah and Chow, 2013). To investigate putative populations of CSC, the ability of cells to actively pump dye (Hoechst 33342) out of the cells, based on the activity of the ABCG2 transporter protein was utilised to identify what is referred to as the side population (SP) by flow cytometry. Based on the side and forward scatter (granularity and size) of cells, illustrated by the dots, cell debris (high granularity and low size) was eliminated by the gating of the major population (Figure 2.4A). Propidium iodide (PI) is a cell impermeable dye which is unable to penetrate the membrane of intact cells, and was thereby used as a stain for the identification of live cells. From the major population identified, we defined the live cell population using live/dead discrimination (PI staining) to identify positively stained cells that lacked membrane integrity and could thereby be eliminated from the analysis (Figure 2.4B). A two dimensional dot plot showing fluorescence intensity of Hoechst blue and Hoechst red channels was generated from the live population (Figure 2.4C). The SP is characterised by being negative for both Hoechst blue (H^{blue-}) and Hoechst red (H^{red-}) staining. This H^{blue-}/H^{red-} SP was identified by comparing the signals obtained with or without treatment with verapamil, an inhibitor of the ABCG2 transporter protein that prevents the efflux

of Hoechst 33342. Hoechst 33342 stained cells treated with or without verapamil were compared with unstained uninhibited (control) cells and the difference in the two percentages determined as the proportion of SP cells. The average results obtained from three independent analyses, in Figure 2.4D, suggested little difference between the sizes of SP detected within SW480 and SW620 cell lines. In the SW480 cell line, 2.97 % of cells were Hblue-/Hred- and this decreased to 1.17 % of H^{blue-}/H^{red-} cells in the presence of verapamil, indicating a SP of approximately 1.8 %. In the SW620 cell line 2.16 % of cells were H^{blue-}/H^{red-}, while 0.82 % of cells were H^{blue-}/H^{red-} in the presence of verapamil, indicating a SP of 1.34 %. Together, this indicated similar SP between SW480 and SW620 cell lines.

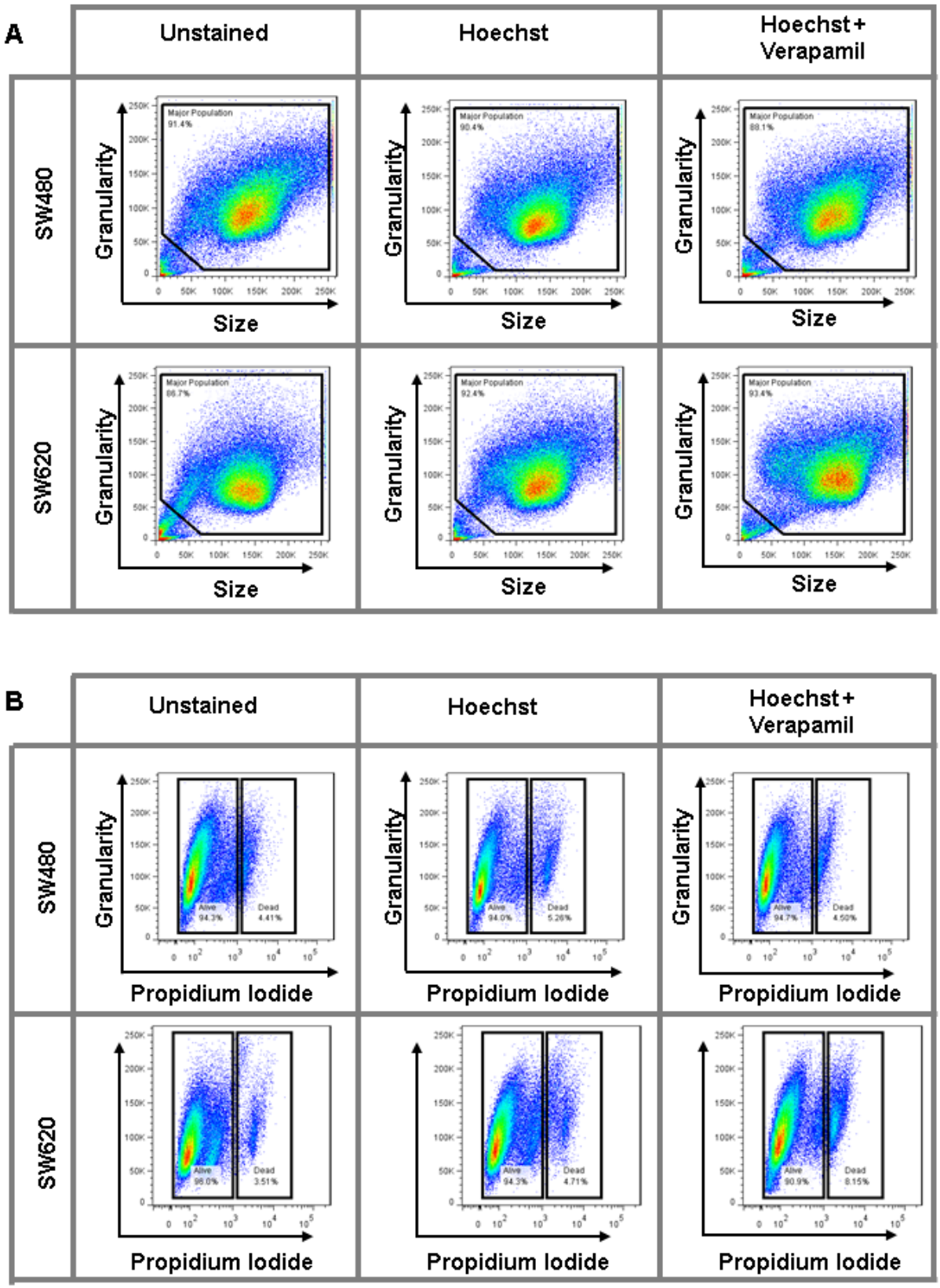

Figure 2.4. Fluorescence-based exclusion of Hoechst dye for the identification of cancer stem cell populations in SW480 and SW620 cells (condinued over page).

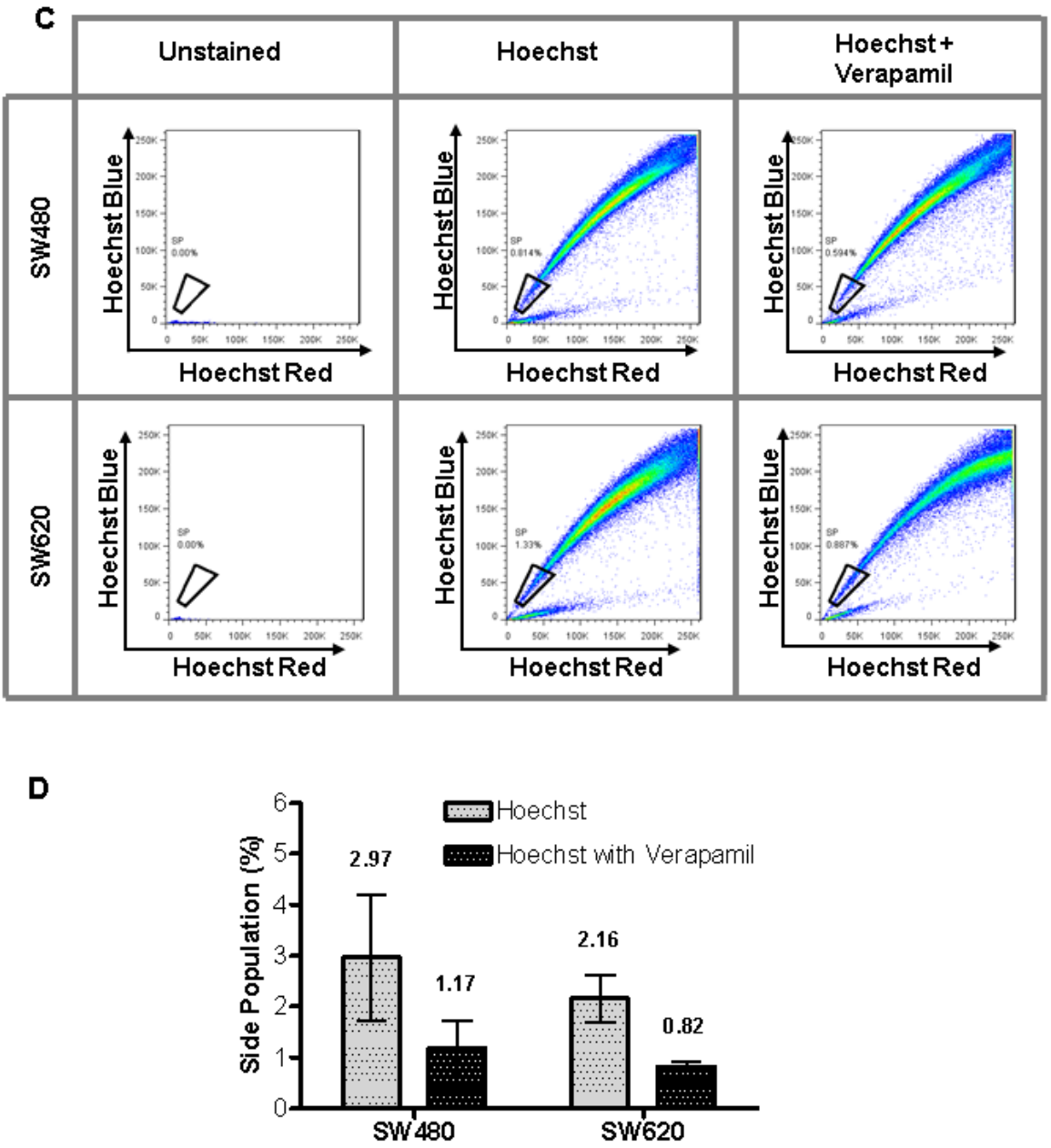

Figure 2.4. Fluorescence-based exclusion of Hoechst dye for the identification of cancer stem cell populations in SW480 and SW620 cells.

Identification of the Side Population (SP) by Hoechst 33342 efflux assay. A. Gating strategy for viable SW480 and SW620 cell identification by flow cytometry. To eliminate cell debris, a gate was constructed to identify the major population of cells and eliminate cellular debris. B. Non-viable (dead) cells were eliminated using propidium iodide (2 µg/ml) staining for the discrimination of dead and live cells based on fluorescent intensity and identification of putative cancer stem cell (side) populations by Hoechst 33342 exclusion. C. Live SW480 and SW620 cells were analysed for putative cancer stem cells within the SP using Hoechst 33342 and gating for SP cells based on Hoechst Blue/Red (H^{blue-}/H^{red-}) fluorescence. The SP was detected by the loss in the SP fluorescent population in the presence of the ABCG2 inhibitor, verapamil (50 µM). D. Putative cancer stem cell populations representative of the average percentage SP observed (mean ± SD) from triplicate independent experimentsas (SP = [% cells H^{blue-}/H^{red-} without verpamil] – [% cells H^{blue-}/H^{red-} with verapamil]). No significant differences were identified on comparing SW480 and SW620 cell lines (t-test with Welch's correction; $p < 0.05$).

Aldehyde dehydrogenase activity assay

A second strategy for the identification of putative cancer stem-like cells analysed cellular levels of active aldehyde dehydrogenase (ALDH), using the ALDEFLUOR® assay. High aldehyde dehydrogenase ($ALDH^{high}$) levels are a functional characteristic of CSC (Huang *et al*., 2009). SW480 and SW620 cells were treated with a fluorescent substrate of aldehyde dehydrogenase, ALDEFLUOR. The ALDEFLUOR is cleaved intracellularly by active ALDH, with the fluorescent product being detected in the green (FITC) channel by flow cytometry. Diethylaminobenzaldehyde (DEAB) is an inhibitor of ALDH that can be used to identify the presence of the $ALDH^{high}$ population. Using DEAB, the percentage of $ALDH^{high}$ cells was calculated based on the loss of a $FITC^{high}$ population from the ALDEFLUOR stained cells in the presence of DEAB (see Figure 2.5A for gating strategy). The difference in the level of $FITC^{high}$ population upon comparison with DEAB-treated cells facilitated the identification of the $ALDH^{high}$ population (% cells $ALDH^{high}$ = [% $FITC^{high}$ cells without DEAB] – [% $FITC^{high}$ cells with DEAB]). The average $ALDH^{high}$ population (mean ± SD) within SW480 and SW620 cells was determined to be 6.49 and 6.06 % of cells, respectively, (Figure 2.5B). There it was determined that there was no significant difference between the $ALDH^{high}$ population in the SW480 or SW620 cell line.

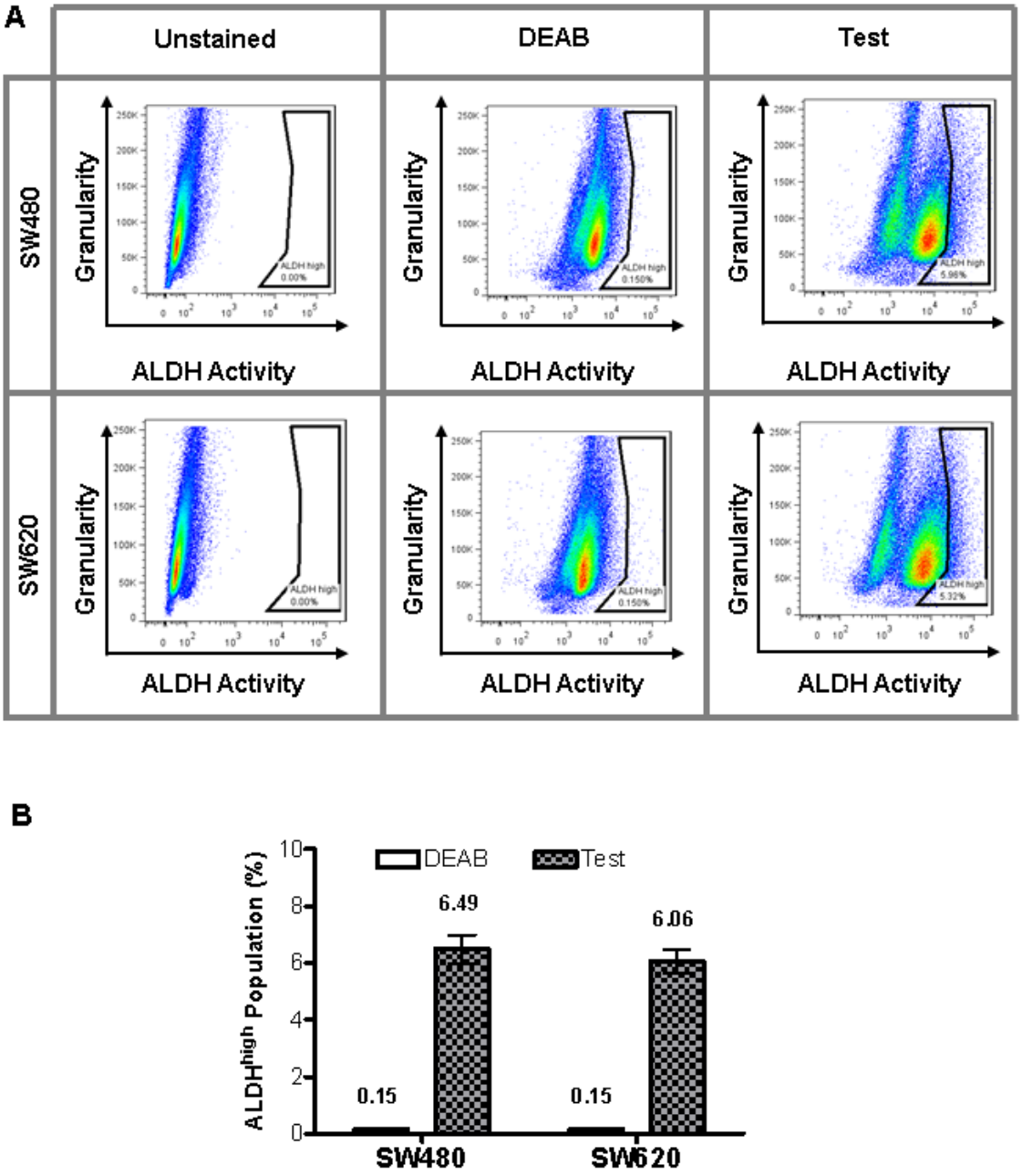

Figure 2.5. Comparison of putative colon cancer stem cells in SW480 and SW620 cell lines identified by aldehyde dehydrogenase activity.

A. Gating strategies to identify the ALDH^{high} population using the ALDH inhibitor, diethylamino-benzaldehyde (DEAB), from SW480 and SW620 cell lines. The ALDH^{high} population was calculated based on the formula % cells ALDH^{high} = [% FITC^{high} cells without DEAB] – [% FITC^{high} cells with DEAB]). B. Average percentage of populations (mean ± SD) observed from triplicate independent experiments are represented. No significant differences were identified on comparing SW480 and SW620 cell lines (t-test with Welch's correction; $p < 0.05$) using GraphPad Prism software.

Cell-surface antigen expression

A third strategy used proteins specific to the cell surface as markers to identify cancer stem-like cells by flow cytometry. SW480 and SW620 cells were analysed for CSC-associated markers, including ABCG2, CD44 and CD133, CD24 and α6 integrin (Collins *et al.,* 2001; Richardson *et al.,* 2004; Bisson and Prowse, 2009). The $CD44^{+}/CD24^{-}$, $CD133^{+}$ and α6 integrin subpopulations have been shown to identify breast CSC (Al-Hajj *et al.,* 2003; Wright *et al*., 2008; Stingl *et al.*, 2006). Additionally, CD133, CD24 and CD44 have been reported to represent putative colorectal cancer stem cell populations (Langan *et al.,* 2013). Side and forward scatter were used to establish the granularity and size of cells, from which the major population was gated for the identification of live cells which were used in the collection and representation of data for analysis (as illustrated for Figure 2.4A). To prevent false-positive results, isotype controls were used to account for any non-specific antibody binding to live cells by establishing a gating threshold according to fluorescence intensity and calculated compensation. Application of the gating threshold to test samples enabled the detection of multiple simultaneous surface antigens by fluorescent intensity (Figure 2.6A). SW480 and SW620 cells were stained for the detection of $CD44^{+}/CD133^{+}$, $CD44^{+}/CD24^{-}$ and α6 $integrin^{+}/ABCG2^{+}$ populations. The $CD44^{+}/CD133^{+}$ population was more than 20 % larger in SW620 cells in comparison with SW480 cells (50.57 % and 28.61 %, respectively). $CD44^{+}/CD24^{-}$ populations represented 62.73 and 75.33 % of SW480 and SW620 cells, and α6 $integrin^{+}/ABCG2^{+}$ staining revealed 0.29 and 0.59 % populations within SW480 and SW620 cells, respectively (Figure 2.6B). These phenotypic analyses showed no significant differences between the SW480 and SW620 cell lines in the putative CSC-like marker profiles assessed.

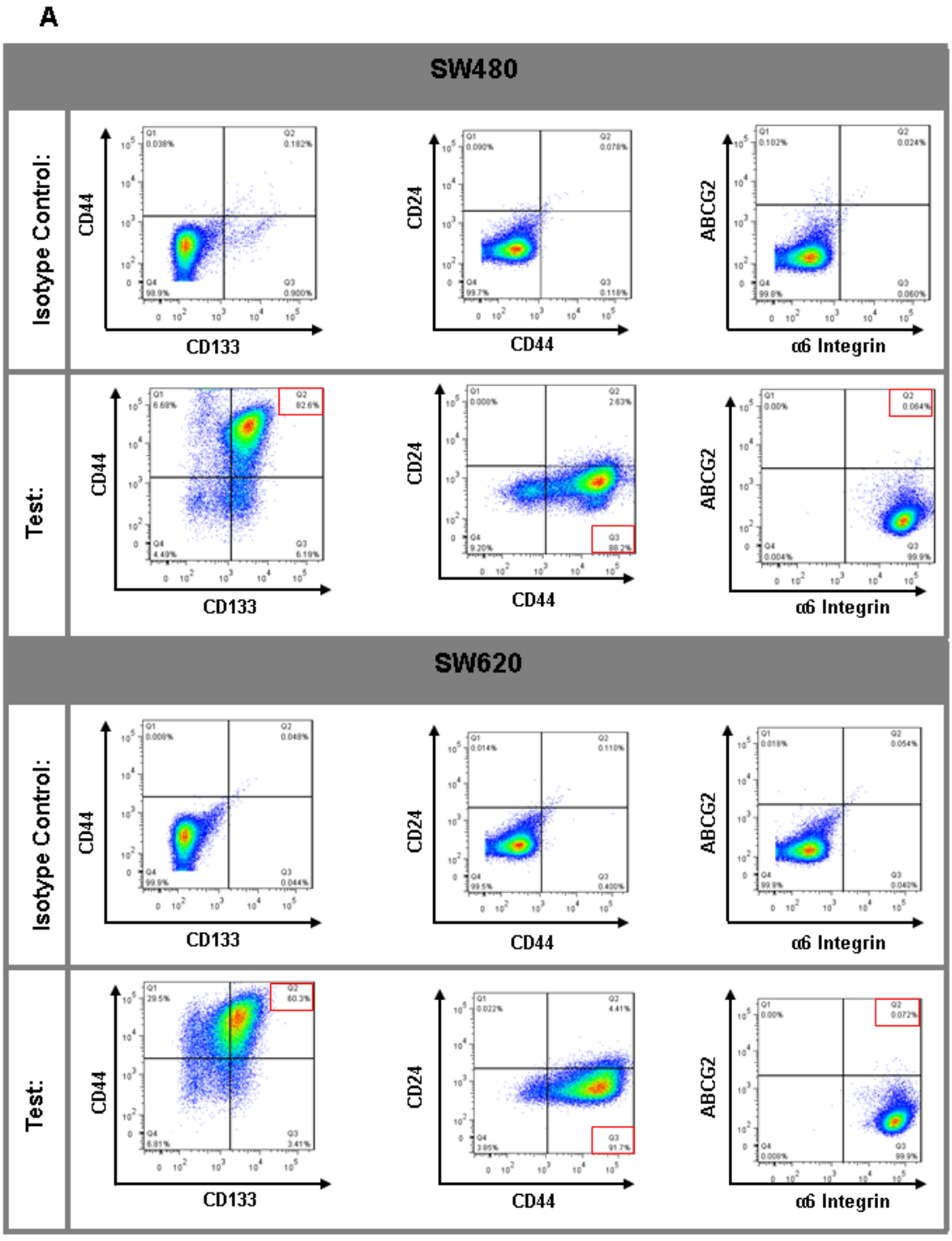

Figure 2.6. Comparison of cancer stem cell surface marker expression in SW480 and SW620 cell lines (continued over page).

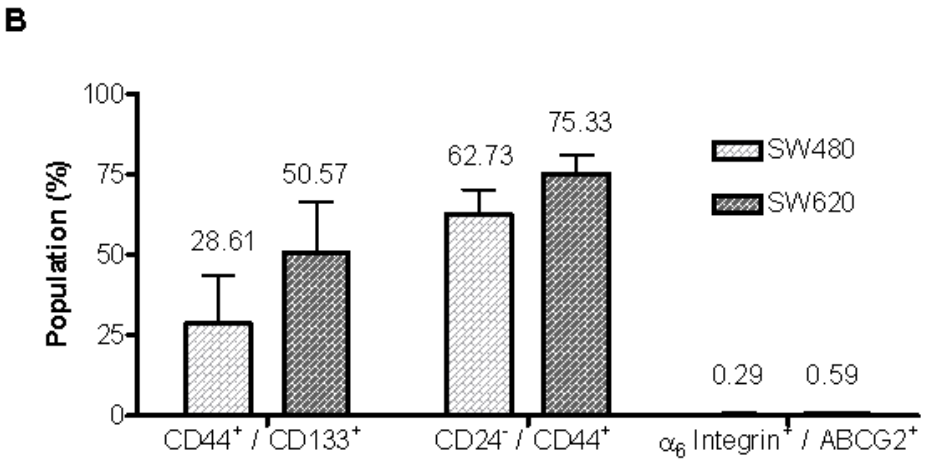

Figure 2.6. Comparison of cancer stem cell surface marker expression in SW480 and SW620 cell lines.

SW480 and SW620 were analysed for phenotypic subpopulations of $CD44^+/CD133^+$, $CD24^-/CD44^+$, and α_6 $Integrin^+/ ABCG2^+$ for cancer stem cell detection. A. Example of gating strategy used to identify different populations after elimination of cell debris and non-viable cells. Isotype-stained control cells were used in the development of the gating strategy for the elimination of non-specific binding events. Using dual antibody staining, putative cancer stem cell populations were characterised using an XY gating strategy applied first to the isotype control to identify Q4 (the double negative stain position on both x and y axes) used to set a limit of ≤ 0.5 % per positive quadrant. This gating was then applied to the corresponding antibody test, so as to account for false-positive results. Red boxes highlight the phenotypic subpopulations of interest; $CD44^+/CD133^+$, $CD24^-/CD44^+$, or α_6 $Integrin^+/ ABCG2^+$ for SW480 and SW620 cell lines. B. Average percentage of populations observed from triplicate results are represented (mean ± SD). No significant differences were identified on comparing SW480 and SW620 cell lines (t-test with Welch's correction; $p < 0.05$). Three independent analyses from individual experiments were utilised, gating on 50 000 events using the FACS Aria II with FACSDiva software (BD Biosciences, Belgium) and analysed using FlowJo software (Tree Star Inc, USA).

Comparison of SW480 and SW620 tumoursphere formation under anchorage-independent conditions

While the culture of cells in a monolayer (adherent conditions) is a useful tool for the study of the biochemistry of a cancer, monolayer cells typically lack aspects of a bulk tumour such as environmental conditions and structure. The nature of bulk tumours often affects the outcome of patient treatment, with low oxygen diffusion leading to a hypoxic environment and contributing to treatment resistance for therapeutics that require oxygen to achieve effective cytotoxicity (Lin *et al*., 2012). Anchorage-independence is a feature of tumourspheres (TS) that facilitates the growth and expansion of putative CSC *in vitro,* based on the stem-like

nature of tumour-initiating cells (Vermeulen *et al.,* 2009; López *et al*., 2012). To demonstrate the presence of putative cancer stem-like cells in the SW480 and SW620 cell lines, we investigated their ability to form TS under anchorage-independent conditions. Using medium supplemented with growth factors but without serum, similar to the culture methods used in literature, we established an assay for the generation of TS *in vitro* for our cell lines (Dontu *et al.*, 2003; Kreso and O'Brien, 2008; Ricci-Vitiani *et al.*, 2007). Figure 2.7A illustrated that after seeding as single cell suspensions, both SW480 and SW620 cell lines were capable of anchorage-independent growth, forming TS within 14 days of culture. Here we defined the appearance of tumourspheres as non-adherent three-dimensional suspended spherical colonies with distinct borders. SW480 and SW620 TS sizes were approximately 120 µm in diameter after 14 days of culture, which correlates with size reported in literature for other primary cancers and cell lines (Cao *et al*., 2011; López *et al*., 2012; Many and Brown, 2014). An assessment of the comparative ability of the SW480 and SW620 cell lines to form TS was conducted. The sphere formation efficiency was calculated by the number of spheres formed following 7 days of anchorage-independent culture from 100 cells seeded. Figure 2.7B indicated that 49.9 and 35.5 %, of SW480 and SW620 cells, respectively, were capable of TS formation. The difference between the two cell lines was deemed to be statistically significant ($p<0.05$).

To evaluate the viability of tumourspheres and their ability to return to adherent culture conditions, we assessed whether cells capable of TS formation under anchorage-independent conditions were still capable of surface attachment by adherence (Figure 2.8). The TS-derived cells from both cell lines were able to adhere; however, attachment to the plastic took substantially longer than cells cultured under adherent conditions. Three days after TS dissociation and placement of TS cells in complete medium, there was no sign of cell attachment, as indicated by the small circular SW480 and SW620 cells in suspension. Within 10 days under adherent conditions cells had begun to produce protrusions and within 14 days of adherent cell culture the majority of cells displayed evidence of adherence. Interestingly, SW620 cells seeded from disrupted TS displayed a change in morphology, appearing more epithelial-like than typically spindle-shaped.

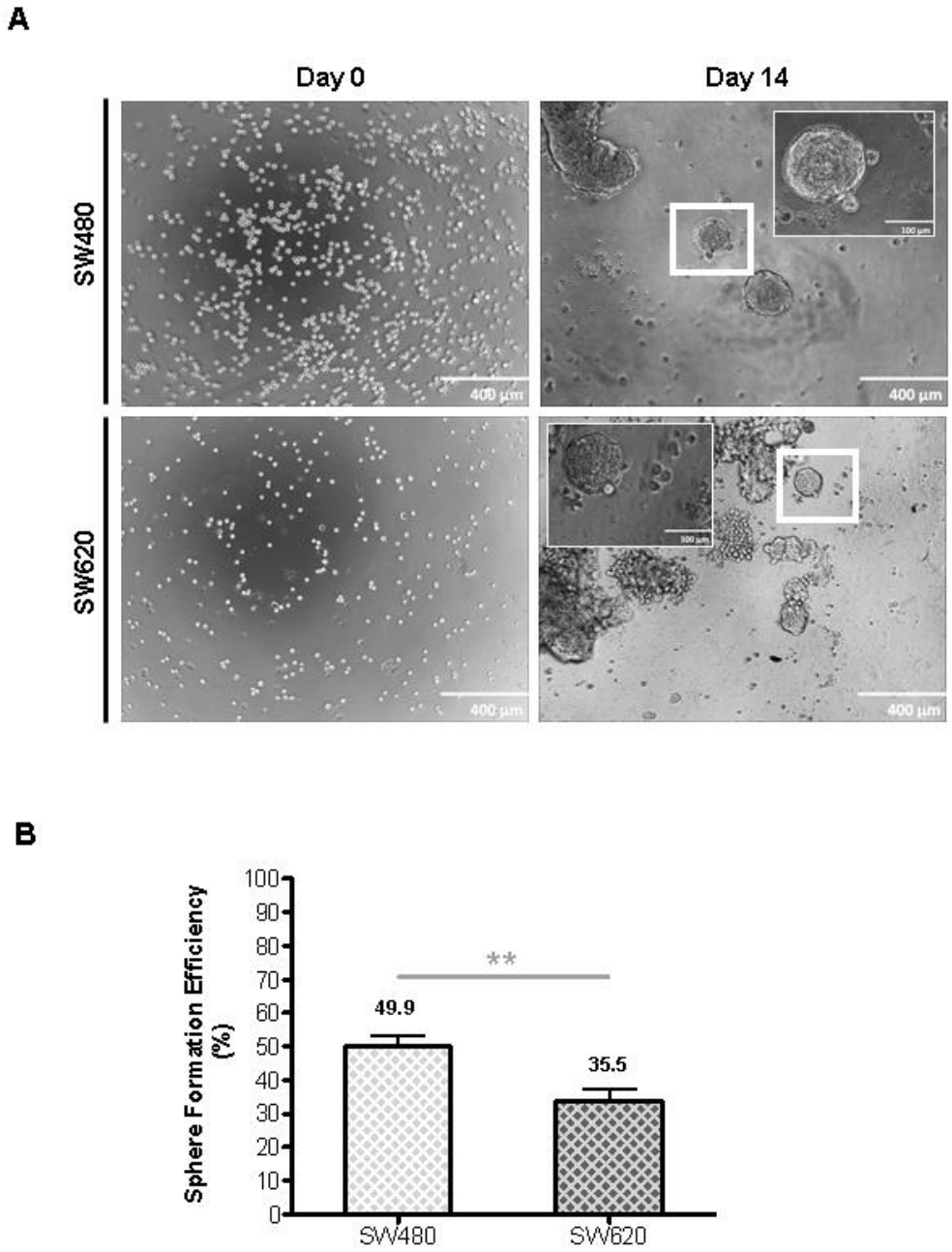

Figure 2.7. Morphological comparison of SW480 and SW620 colon cancer cells under anchorage independent growth conditions.

SW480 and SW620 cells were analysed for their ability to survive anchorage-independence and form tumourspheres *in vitro*. A. Tumoursphere development of 20 000 cells/ml under anchorage independent conditions from single suspension (Day 0) over 14 days. Pictures taken on an Olympus CKX41 light microscope (200 x and 400 x magnification) and analysed using ImageJ software. Scale bar: 400 and 100 µm. B. The sphere formation efficiency was calculated as the sum of spheres formed per 100 cells seeded and represented as a percentage. TS of 9 replicates (100 cells seeded) were counted following 7 days of anchorage-independent growth. Data represent mean ± SD of triplicate experiments and statistical significance using unpaired t-tests ($p < 0.05$) analysed by GraphPad Prism software.

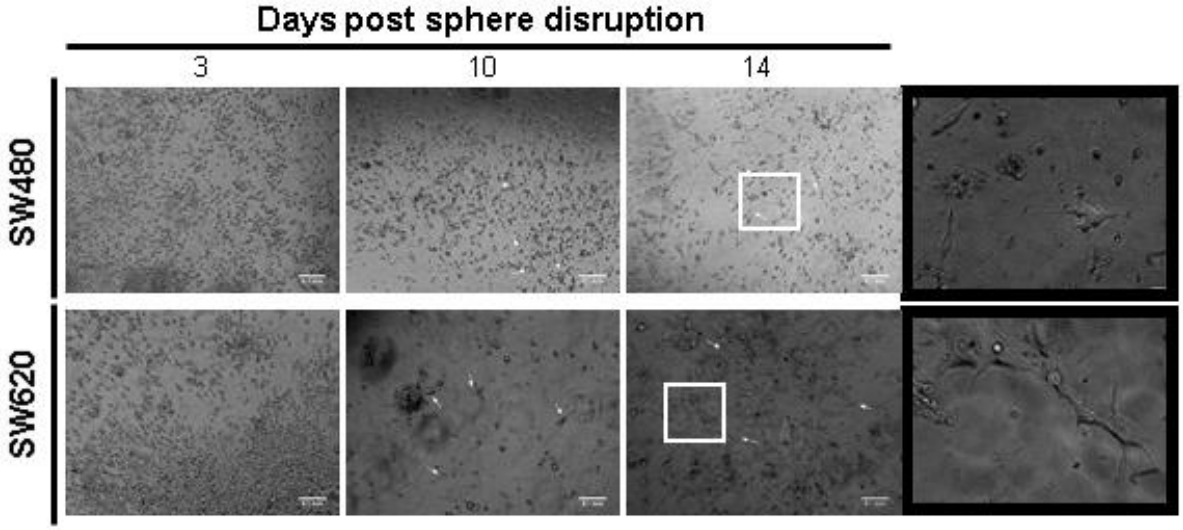

Figure 2.8. Assessment of the ability of SW480 and SW620 tumoursphere derived cells to return to adherent culture.

SW480 and SW620 tumourspheres were dissociated into single-cells after 7 days of growth under anchorage-independent conditions and 2 500 cells re-seeded under anchorage-dependent conditions. Images were taken over 14 days to analyse adherence using a phase contrast DSZ5000X inverted microscope (40 x and 400 x magnification) and analysed using ImageJ software. Scale bar: 100 µm. Arrows illustrated adherent cells.

We next wanted to test an ability for self-renewal through TS disruption and reseeding in limiting dilutions for the reformation of TS of a second (passage 1) or third (passage 2) generation. Preliminary data illustrated the ability of SW480 and SW620 tumoursphere cells to be passaged after 7 days of anchorage-independent growth (Figure 2.9A), demonstrated by triplicate images of TS after 7 day of culture. Passaged SW480 and SW620 TS continued to produce TS for three consecutive generations. Comparing the SW480 and SW620 TS across the passages showed the passage-dependent decrease in size of the average TS. The number of cells generated by the growth of TS after 7 days of culture, accounting for the 2000 cells seeded per generation, showed a dramatic increase at passage 1 and subsequent passages (Figure 2.9B), indicating that the cells are proliferating to form TS under these conditions, not just aggregating. There was a decline in cell number between passage 1 and 2, although between passage 2 and 4 the number of cells per passage showed evidence of recovery, with an increasing number of cells recovered per passage. These data indicated that the SW620 TS contained slightly greater cell numbers compared to the SW480 cells between the later passages, suggesting a greater self renewal capacity.

The population of $CD44^{+}/CD133^{+}$ cells did not differ significantly within both SW480 and SW620 passaged tumourspheres, but an increase in $CD44^{+}/CD133^{+}$ cells was noticed from the third TS passage (Figure 2.9C). SW480 and SW620 tumourspheres also showed a similar response to passaging upon analysis of ALDH (Figure 2.9D). Interestingly, the SW480 and SW620 tumoursphere passaging represented a substantial increase (greater than 5-fold; passage 1) in the proportion of $ALDH^{high}$ cells relative to that which was previously observed for adherent SW480 and SW620 cells (~ 6 %; Figure 2.5). The preliminary data following the self-renewing ability of the passaged SW480 and SW620 TS initially demonstrated an enrichment of cells with putative CSC characteristics, reporting $ALDH^{high}$ populations of 60 and 45 %, respectively in the second generation (passage 1) TS (Figure 2.9D). The second passage of TS revealed a reduction in the proportion of $ALDH^{high}$ TS cells and was followed by recovery of $ALDH^{high}$ cells after third passage. The $ALDH^{high}$ populations of the third generation of TS (passage 2) represented approximately half the $ALDH^{high}$ populations seen from passage 1 TS. Altogether, these findings demonstrated the ability of SW480 and SW620 TS to self-renew. These data further demonstrate that SW480 and SW620 TS are enriched in $ALDH^{high}$ cells compared to the cell lines grown under anchorage dependent conditions.

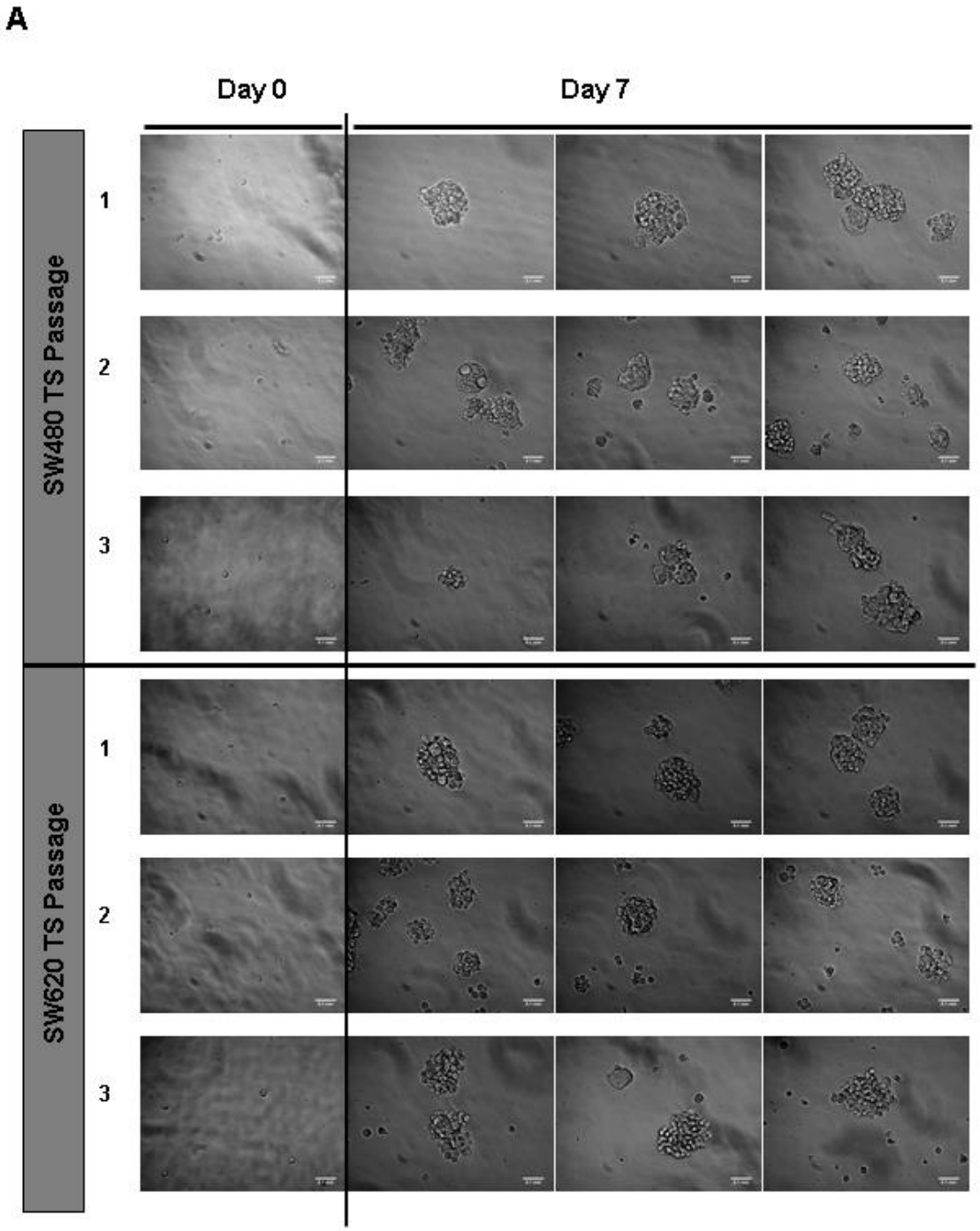

Figure 2.9. Analysis of self-renewal capabilities of SW480 and SW620 cell lines (continued over page)

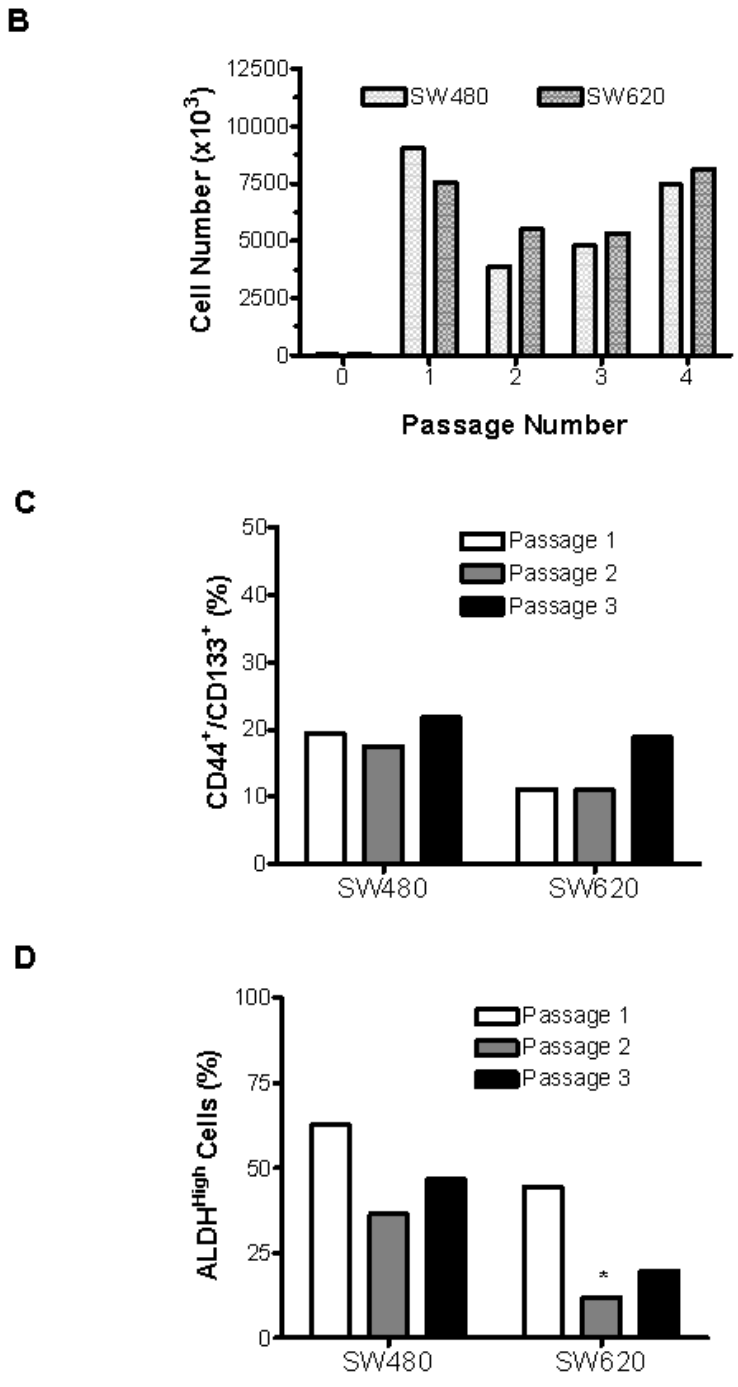

Figure 2.9. Analysis of self-renewal capabilities of SW480 and SW620 cell lines.

SW480 and SW620 tumourspheres were grown for 7 days prior to their passaging (dissociation into single-cells) and analysed (CD44/CD133 expression and ALDH activity) or re-seeded for self-renewal analysis under anchorage-dependent conditions. A. TS images were taken 7 days after seeding/passaging using a phase contrast DSZ5000X inverted microscope (100 x magnification) and analysed using ImageJ software. Images represent the total number of TS cells counted from each tumoursphere assay after each passage, from passage 0 - 4. Scale bar represents 100 µm. B. After the TS were dissociated, the cells were counted using a haemocytometer and Trypan Blue prior to the seeding of the next generation of TS. Passaged TS were analysed for $CD44^+$ and $CD133^+$ co-expression (C) and ALDH activity (D) by flow cytometry. Data were analysed using GraphPad Prism software for two-way ANOVA statistical significance (* = $p < 0.05$; ** = $p < 0.01$; *** = $p < 0.001$).

Comparison of protein expression in SW480 and SW620 cells cultured under adherent and anchorage-independent conditions

Molecular chaperones and co-chaperones, and proteins marking epithelial or mesenchymal phenotypes were analysed within the SW480 and SW620 cell lines when grown under adherent or anchorage-independent TS conditions. Two isoforms of cytokeratin, an epithelial marker, were detected in SW480 adherent cells: a lower isoform, also present in SW620 cells, and a larger (higher molecular weight) isoform (Figure 2.10). This higher molecular weight form was lost in the SW480 cells when cultured under TS conditions. No differences in cytoskeletal protein actin expression were observed when comparing SW480 and SW620 cells or TS. The TS of SW480 and SW620 cells showed slight increases in the protein levels of the mesenchymal marker fibronectin, relative to the adherent whole cell lysates (WCL). Both SW480 TS and SW620 TS showed slightly reduced Hsp90α levels and decreased levels of β-catenin in comparison to SW480 and SW620 cells cultured under adherent conditions, respectively. Interestingly, the oncogene c-myc, which is directly influenced by alterations to the Wnt/β-catenin pathway, was expressed in the whole cell lysates but substantially reduced in the TS lysates of SW480 and SW620 cell lines to below detectable levels. No differences in the expression of Hsp90β were detected across the whole cell lysates and TS lysates of SW480 and SW620 cells. Minor reductions in the level of co-chaperone Hsp40 were evident on comparing TS and whole cell lysates of SW480 and SW620 cell lines. While little difference was in the expression of Hsp90α and Hsp90β, and co-chaperone Hsp40 were discovered, the difference in physiology of cell and TS have revealed a decrease in β-catenin and lack of c-myc expression upon the anchorage-independent growth of TS. These differences in protein expression achieved between the SW480 and SW620 cells and TS suggested changes in the biology of the cells when grown under anchorage independent conditions *in vitro*.

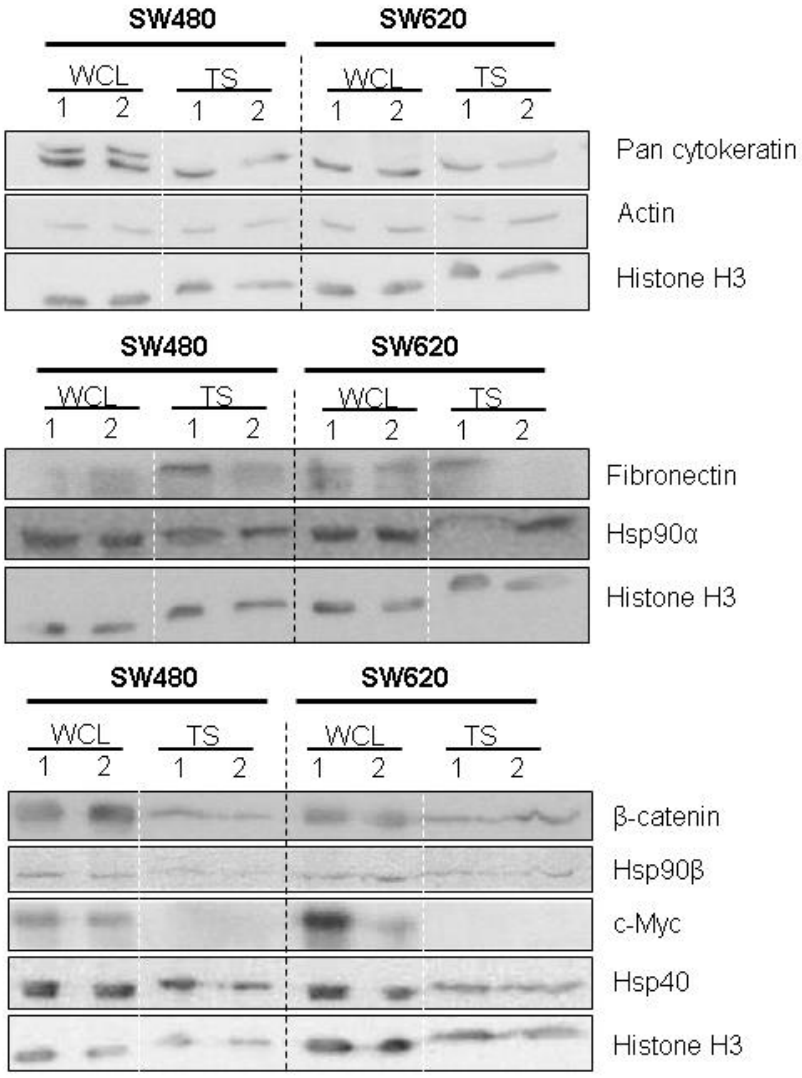

Figure 2.10. Comparison of protein expression in SW480 and SW620 adherent cells and tumourspheres.

Adherent SW480 and SW620 cells and tumourspheres (7 days after growth) were lysed and subjected to SDS-PAGE and Western Blotting. Western blot analysis of the expression of pan-cytokeratin, actin, fibronectin, Hsp90α, Hsp90β, β-catenin, c-myc, Hsp40 and histone H3 (loading control) from duplicate whole cell lysates (WCL) and tumourspheres (TS), with equal protein loading of 50 µg per well. Chemiluminescent detection of proteins using antibody-antigen detection using the Chemidoc EQ system (Biorad, UK).

Discussion

Comparison of the biological characteristics of SW480 and SW620 cell lines

In this study, we used a genetically paired cell line model to further understand the progression of colon cancers *in vitro*. The SW480 and SW620 cells were compared in terms of growth, migration potential and cell morphology. The SW480 and SW620 cell lines displayed similar growth profiles *in vitro* (Figure 2.2). From an assessment of linear wound closure, the SW480 cell line showed an enhanced migratory potential over the SW620 cell line and demonstrated a greater capacity for migration in the presence of ECM proteins collagen or fibronectin (Figure 2.3). Based on the presence or absence of morphological markers (such as vimentin, E-cadherin, β1 integrin and β-catenin) no distinguishable differnces were discovered between the paired cell lines (Figure 2.1). This indicated that both cell lines displayed overlap in the expression of such markers. Closer analysis of cell morphology by phase-contrast, however, revealed the small spindle-like morphology of the SW620 cells and confirmed the epithelial-like morphology of SW480 cells. Staining these cells for actin further demonstrated the different morphologies represented by SW480 and SW620 cell lines, supporting our use of the paired cell lines as a model of tumour progression.

The SW480 and SW620 genetically paired cell lines have previously been validated as a model for the changes associated with the progression of a colon cancer for the understanding of potential genetic influences in late stage colon cancers (Hewitt *et al*., 2000). Comparisons of different cell appearances of SW480 and SW620 cell lines confirmed the epithelial and mesenchymal-like morpnology of the paired cell lines (Leibovitz *et al.,* 1976). Analysis of the growth profile of SW480 and SW620 cells, by cell number and the sulforhodamine B protein stain (measured by spectroscopy), have shown the similarities between the growth of the paired cell lines *in vitro* (Duranton *et al.,* 2003). Studies have illustrated the enhanced adhesion and transwell migration across nucleopore membrane of SW480 cells over SW620 cells *in vitro,* on ECM proteins collagen I, collagen IV, lamanin and fibronectin (Hewitt *et al*., 2000). These findings support our experimental observations, demonstrating similar growth between the paired cell lines, and also the different morphology and enhanced migratory capacity of the SW480 cells over the SW620 cells.

Epithelial and mesenchymal phenotypes have been directly linked to Wnt/β-catenin signaling (Hay *et al.,* 1995). Cell motility or migratory capacity is largely governed by the cell adhesion molecules, including integrin and cadherin proteins, through the regulation of extracellular matrix adhesion (Brakebusch and Frassler, 2003). In the cytoplasm, β-catenin is associated

with E-caderin at the cell junctions. E-cadherin provides cell to cell adherence through adherens junctions, which influence traction by regulating actin organisation at cell-to-cell adherence sites (Danjo and Gipson, 1998). We observed a lower concentration of E-cadherin in SW620 cells (Figure 2.1), further supported the mesenchymal-like phenotype of the SW620 cells observed. The lower levels of E-cadherin however did not correlate with the lower migratory potential in the SW620 compared to the SW480 cell line. The karyotyping of SW480 and SW620 cell lines has revealed several upregulated oncogenes in metastatic SW620 cells (Melcher *et al.,* 2000). To further identify differences in the paired colon cancer cell lines Ghosh and colleagues identified several proteins shown to influence the migratory capacity of SW480 and SW620 cells, including decreased β-catenin in the SW620 metastasis (Ghosh *et al.,* 2011). However, we report that no difference in the concentration, localisation or distribution in β-catenin between SW480 and SW620 cells was detected. However, the presence of β-catenin in the nucleus of both SW480 and SW620 cell lines (Figure 2.1) suggested that the Wnt pathway was constitutively active in both cell lines.

We speculate that the similarities in the observed β-catenin levels were as a result of constitutively active Wnt pathway destruction complex, from an amino acid deletion of the APC protein in the paired cell lines (Brocardo *et al.,* 2005; Yang *et al.,* 2006). However, to confirm the the activation status of the Wnt pathway in our hands, reporter assays would be required to demonstrate the transcriptional activity of β-catenin. However, the SW480 and SW620 paired cell lines demonstrated low transfection efficiencies and a high sensitivity to plasmid transfection reagents such as Lipofectamine (see Supplementary Figure S3B) and Dharmafect (data not shown). To address this limitation in future, we plan to useviral delivery systems to deliver a TCF/LEF reporter construct into the cell lines. Alternatively, co-culture of the SW480 cells with a stable transduced TCF/LEF-luciferase reporter cell line has demonstrated success in the quantifying the activation of the Wnt pathway (Voloshanenko *et al.,* 2013).

Comparison of the putative CSC from SW480 and SW620 cell lines

In order to determine any correlation between metastasis and stemness, we compared the SW480 and SW620 cell lines in terms of putative CSC populations. Similar populations of putative CSC were identified in the paired cell lines based on functional and phenotype identification techniques, and self-renewal capabilities. This was unexpected as the SW620 had been previously shown to be more tumorigenic than the SW480 cell line (Hewitt *et al.,* 2000) and the proportion of CSC-like cell is thought to be correlated with tumourigenic potential. The SP identified were approximately 1 %, and the percentage of $ALDH^{high}$ cells

were approximately 6 % in both SW480 and SW620 cell lines. However, the $CD44^+/CD133^+$ populations was variable between the SW480 and SW620 cell lines, averageing 50.57 % and 28.61 % of the population, respectively. While both cell lines were capable of TS formation and expressed both epithelial and mesenchymal markers; the SW480 cells showed a significantly greater TS formation efficiency (49.9 and 35.5 % for SW480 and SW620 cells, respectively) and consistently maintained greater populations of $ALDH^{high}$ and $CD44^+/CD133^+$ populations after three consecutive TS passages in comparison to SW620 TS. Interestingly, here we reported both that the TS of the paired cell lines showed decreased levels of β-catenin and slightly reduced Hsp90α levels in comparison to adherent SW480 and SW620 cells.

Previous studies have reported a SP for SW480 cells of 4 %, SP for HCT15 cells of 5.5 % and an SP of 0.8 % in HT29 cells (Morita *et al*., 2014). Our analysis of the proportion of cells within the SP for the SW480 and SW620 cells (~ 1 %, Figure 2.4) was similar to that which has represented in literature for other colon lines and gastrointestinal tumours (Sussman *et al*. 2007; Haraguchi *et al*., 2006). We observed variation in the expression of the cell surface protein markers $CD44^+/CD133^+$ between the paired cell lines (Figure 2.6). Analysing both CD44 and CD133 expression in SW480 cells has demonstrated ~ 25 % of cells express both $CD44^+/CD133^+$ by immunofluorescent staining (Li *et al.,* 2010), which is approximately half of that identified in our study. In their analysis of the CD133 expression from SW480 and SW620 populations, Sheng-Dong Huang and colleagues confirmed that the SW480 line contained more $CD133^+$ cells than the SW620 cell line (~ 80 and ~ 50 %, respectively), in support of our findings (Huang *et al.,* 2013).

In colon cancer the CD133, CD24 and CD44 surface proteins have been reported to represent putative colorectal cancer stem cell populations (Langan *et al.,* 2013). However, the use of CD44 and CD133 markers for the detection of colon CSC remains controversial (Botchkina *et al*., 2009; Calvet *et al.,* 2014). But while there is evidence to suggest the $CD133^+$ marker has been used to identify drug-resistant CSC populations in colon cancer, there is some indication that both $CD133^+$ and $CD133^-$ populations in colorectal cancer can regenerate the growth of a tumour with *in vitro* serum-free culture (Fang *et al*., 2010; Hsu *et al*., 2013). The propagation of colon spheres *in vitro* has successfully demonstrated the expansion of colon CSC (Carpentino *et al*., 2009). Here, we reported that SW480 cells had a greater sphere-formation efficiency over the SW620 cells (Figure 2.7). Interestingly,TS generated from colon cancer cell lines have demonstrated similar expression of CSC markers as their adherent parent cells, including CD44, CD133, CD166, CD24,CD29 and ALDH, in genomic arrays (Collura *et al*., 2013) supporting our observed similarities between the paired adherent cell lines and their TS, even after 3 passages of TS (Figure 2.6 and 2.9). ALDH was initially used for the detection

of putative CSC in breast cancers, but has also shown promise in the detection of colon CSC (Huang *et al*., 2009; Carpentino *et al*., 2009). Studies have shown that enriching the proportion of $ALDH^{high}$ cells with additional $CD44^{+}$ and $CD133^{+}$ markers has improved the tumour-initiating capacity of colon cancers (Vermeulen *et al*., 2009).

The CSC theory implicates tumorigenic and migratory CSC in the development of metastasis through the initiation of tumour development and recurrence of tumours (Clarke and Fuller, 2006; Wicha *et al.*, 2006; Brabletz *et al*., 2005). However, our investigation demonstrated no significant differences in the putative CSC populations between the SW480 and SW620 cell lines, except that the SW480 showed enhanced TS formation. This contradicted our original hypothesis that if CSC were involved in metastasis, the SW620 cell line should show enrichment in cells bearing the CSC phenotype. Nevertheless, if you consider the definition of a CSC as a cell that is able to recapitulate the phenotype of the original tumour from which it arose (Fang *et al.,* 2010), then the similarity in the CSC populations of the two lines can be explained. Therefore, the similarity between the CSC profiles may still be consistent with a migratory-CSC derived from the SW480 giving rise to the SW620 metastasis. However, while we have used a range of accepted and published assays known to identify putative CSC-populations, we have not demonstrated that these putative CSC are in fact more tumourigenic than the non-CSC counterparts. In order to address whether or not the marker and functional assays are correlated with tumour-forming ability, further *in vivo* studies would be required to examine the links between tumourigenicity of cells identified as putative CSC and metastases.

To the best of our knowledge, this is the first study to report an extensive comparison of CSC between the SW480 and SW620 paired cell lines and to demonstrate similar levels of putative CSC populations. Here we used several techniques in an attempt to identify putative CSC. The only difference identified between the two cell lines was in anchorage-independence (serum-free tumoursphere culture). We subsequently went on to evaluate the effect of Hsp90 inhibition on the paired cell lines, and including the tumoursphere assay as a way to assess putative CSC-like characteristics that may be associated with cancer progression.

Chapter 3: Comparison of SW480 and SW620 cell lines in response Hsp90 inhibition.

Introduction

The “chaperome” is a term used to refer to all of the molecular chaperones and co-chaperones that are involved in protein homeostasis. Proteins of the chaperome are crucial for the correct maintenance of proteome (Albanese *et al.,* 2006). Research into the human chaperome has identified 332 genes based on biochemical properties and genomic profiling (Brehme *et al*., 2014). Functionally, 88 genes were classified as chaperones, 50 genes of which defined ATP-dependent chaperones and 38 genes corresponded to ATP-independent chaperones; while 244 were designated as co-chaperones. Hsp90-client interaction and subsequent folding are dependent on ATP hydrolysis (see Figure 1.3).

The balance between cellular death, proliferation and differentiation is carefully regulated within the body. Cancers arise from disturbances of this balance. Tumours consist of cells that have acquired the ability to proliferate endlessly, evade apoptosis, growth signaling self-sufficiency, insensitivity to anti-growth signals and sustained angiogenesis (Hanahan and Weinberg, 2000; Hanahan and Weinberg, 2011). Hsp90 is often upregulated in cancers (Neckers, 2002), and participates in the development and spread of cancers via the regulation of client protein stability. Extracellular Hsp90 (Hsp90 found in the extracellular space), through its interaction with cell surface receptors, such as MMP2, stimulates cell migration (Eustace *et al*., 2004; Sidera and Patsavoudi, 2008; Trepel *et al.,* 2010). The role of Hsp90 in cancer motility and invasion shows the importance of Hsp90 in the development of the epithelial-mesenchymal transition (EMT) phenotype for metastatic cancers (Thiery, 2002). The involvement of Hsp90 in oncogenesis has led to the identification of Hsp90 as a drug target, with several Hsp90 inhibitors being currently in use in clinical trials following the discovery of their anti-tumour activity (Kim *et al.,* 2009; Blagosklonny, 2002). Targeting Hsp90 by inhibition results in client protein degradation, which depleted downstream signaling intermediate proteins and oncoproteins (Connell *et al.,* 2001; Powers and Workman, 2006). Understanding the genetic control and regulation of Hsp90 has seen the development and improvement of novel cancer therapeutics. The success of using 17-AAG to target Hsp90 in colon cancer cells demonstrated the disruption of multiple downstream signal transduction pathways and alteration to the cell cycle by induction of apoptosis and necrosis, supporting Hsp90 as a target in colon cancer therapies (Hostein *et al.,* 2001).

Colon cancer is the third most frequent cancer in the Western world and is also known to be associated with cancer-related deaths through the failure of anti-cancer treatments to target the colorectal cancer cells (Jemal *et al.,* 2006). Metastases cause death in approximately 90 % of colon cancer patients (Weigeit *et al.*, 2005). The traditional method of metastatic colon

cancer treatment includes adjuvant chemotherapeutics. Phase 3 clinical trials have been successfully conducted using the platinum derivative, oxaliplatin, and 5-fluorouracil to determine the effect on mortality rate (Giacchetti *et al.,* 2000). Despite the progress made in colon cancer therapies, the disease remains a major cause of death worldwide, highlighting the importance and urgency of new more focused therapeutics (Anderson *et al*., 2011).

In this study, we used the genetically paired SW480/SW620 cell lines to compare the function of Hsp90 with respect to Hsp90 location, distribution, sensitivity to inhibition and the effects on tumoursphere formation and morphology.

Materials and Methods

Materials

General reagents mentioned were purchased from Sigma-Aldrich (Germany) or Saarchem (Merck, South Africa). Specialised reagents, plasticware and kits purchased were reflected in the appropriate methodology.

Methods

SW480 and SW620 cell lines were cultured under adherent conditions and anchorage-independently as tumourspheres (TS) as previously mentioned in Chapter 2. To analyse protein expression, SDS-PAGE and Western blotting techniques were performed (see Chapter 2 methodology). Table 3, Table 4 and Table 5 provide a detailed list of antibodies and their individual specifications used.

Confocal microscopy

Cells seeded on coverslips coated with 5 µg/ml fibronectin (Sigma-Aldrich) were fixed in methanol and blocked in 1 % (w/v) BSA/PBS [pH 7.0] for 45 minutes prior to incubation in primary antibody (Table 4) in 0.1 % (w/v) BSA/PBS overnight at 4°C. Coverslips were incubated in secondary antibodies (Table 5) in 0.1 % (w/v) BSA/PBS for 1 H at room temperature after two washes in 0.1 % (w/v) BSA/PBS. Cells were washed twice in 0.1 % (w/v) BSA/PBS prior to nuclear staining with 1 µg/ml Hoechst 33342 in distilled water.

Coverslips were mounted with DAKO mounting media and sealed. Confocal microscopy was carried out using the Zeiss LSM 510 Meta confocal microscope (40 x objective). Images were analysed using AxioVision LE 4.8.2.0 and ZEN Lite 2012 1.1.2.0 (Zeiss).

Cell proliferation WST-1 assay for cytotoxicity

Cells were seeded at 3 x 10^3 cells/well in 96-well plates at 37°C overnight, prior to treatment with geldanamycin, novobiocin, 5-fluorouracil (5-FU) or oxaliplatin at a variety of concentrations for 72 H, with untreated or dimethyl sulphoxide (DMSO) treated cells used as negative controls. After the addition of 10 µl/well WST-1 proliferation reagent (Roche Applied Sciences, Germany; cat no.: 05 015 944 001) and incubation for 3 H, the absorbance at 440 nm was analysed on the PowerWave spectrophotometer (Bio-Tek Instruments, USA).The percentage cell viability was calculated by dividing the absorbance of the sample by that of the untreated control, multiplied by 100. The concentration at which a chemotherapeutic agent effectively altered cell viability by 50 % (EC_{50}) for each cell line was calculated in GraphPad Prism using non-linear regression for geldanamycin, novobiocin, 5-FU and oxaliplatin cytotoxicity.

Cell cycle analysis using propidium iodide

Flow cytometry was used to determine the effect of geldanamycin and novobiocin on the cell cycle. To culture tumourspheres, cells were seeded (2 x 10^4 density) and cultured under anchorage-independent conditions for 5 days. For the analysis of adherent cells, 2 x 10^4 cells were allowed to adhere overnight, prior to treatment with either DMSO vehicle control, 65 nM geldanamycin or 150 µM novobiocin at 37°C for 48 H. Following treatment, cells were lifted or separated into single-cell suspension with accutase (Sigma-Aldrich), washed in PBS and pelleted at 1600 *x g.* Cells were resuspended in PBS and fixed with 70 % (v/v) ethanol. After washing, cells were again pelleted and stained for 40 min at 37°C in a propidium iodide solution (50 µg/ml PI, 100 µg/ml RNAse A, 0.05 % (v/v) Triton X-100; Sigma-Aldrich). Following centrifugation, cells were resuspended in PBS prior to analysis. Fluorescence was detected using the blue (488 nm) laser to excite the PI fluorophore and emissions were recorded in the 585/42 filter channel. Forward and side scatter were used to eliminate false positive results, and doublets were discriminated based on signals for PE area and width. Using FACSDiva and FlowJo software, gating was utilised to define the G1 (representative of G0 and G1 phases), S and G2M phases of the cell cycle.

Results

Using the SW480 and SW620 colon cancer cell lines as a model for pre-metastatic and metastatic cancers, we investigated the role of Hsp90 in cancer and cancer stem-like cell biology. Here we sought to understand the influence of stress and Hsp90 targeting on the development of a metastatic phenotype. The following studies characterise the SW480 and SW620 cell lines by their expression and location of molecular chaperones and co-chaperones. These findings were utilised to facilitate a comparison of the paired cell lines by their sensitivity to anti-cancer therapeutic agents, including the Hsp90 inhibitors, geldanamycin or novobiocin.

Characterisation of SW480 and SW620 cell lines by Hsp90 expression, location and in response to stress

SW480 and SW620 cell lines were analysed for the expression of Hsp90 and Hsp70 proteins by Western blotting. The proteins detected (Hsp90, Hsp70, actin and histone H3) revealed consistent levels of intensity, suggesting overall equivalent expression of Hsp90 and Hsp70 between the SW480 and SW620 cell lines (Figure 3.1A). To identify the expression and subcellular localisation of Hsp90α and Hsp90β isoforms within different compartments of cells, SW480 and SW620 cells were stained and analysed by confocal microscopy (Figure 3.1B). Hoechst 33342 was used to identify nuclei. While Hsp90α and Hsp90β were detected in both the nuclei and the cytoplasm, Hsp90α staining showed the highest level of protein within the cytoplasm of the cell, while Hsp90β staining showed an accumulation of protein within the nucleus, revealing a few punctuate nuclear structures, together with staining in the cytoplasm. Overall, Hsp90α and Hsp90β staining did not reveal any significant differences in localisation between SW480 and SW620 cell lines.

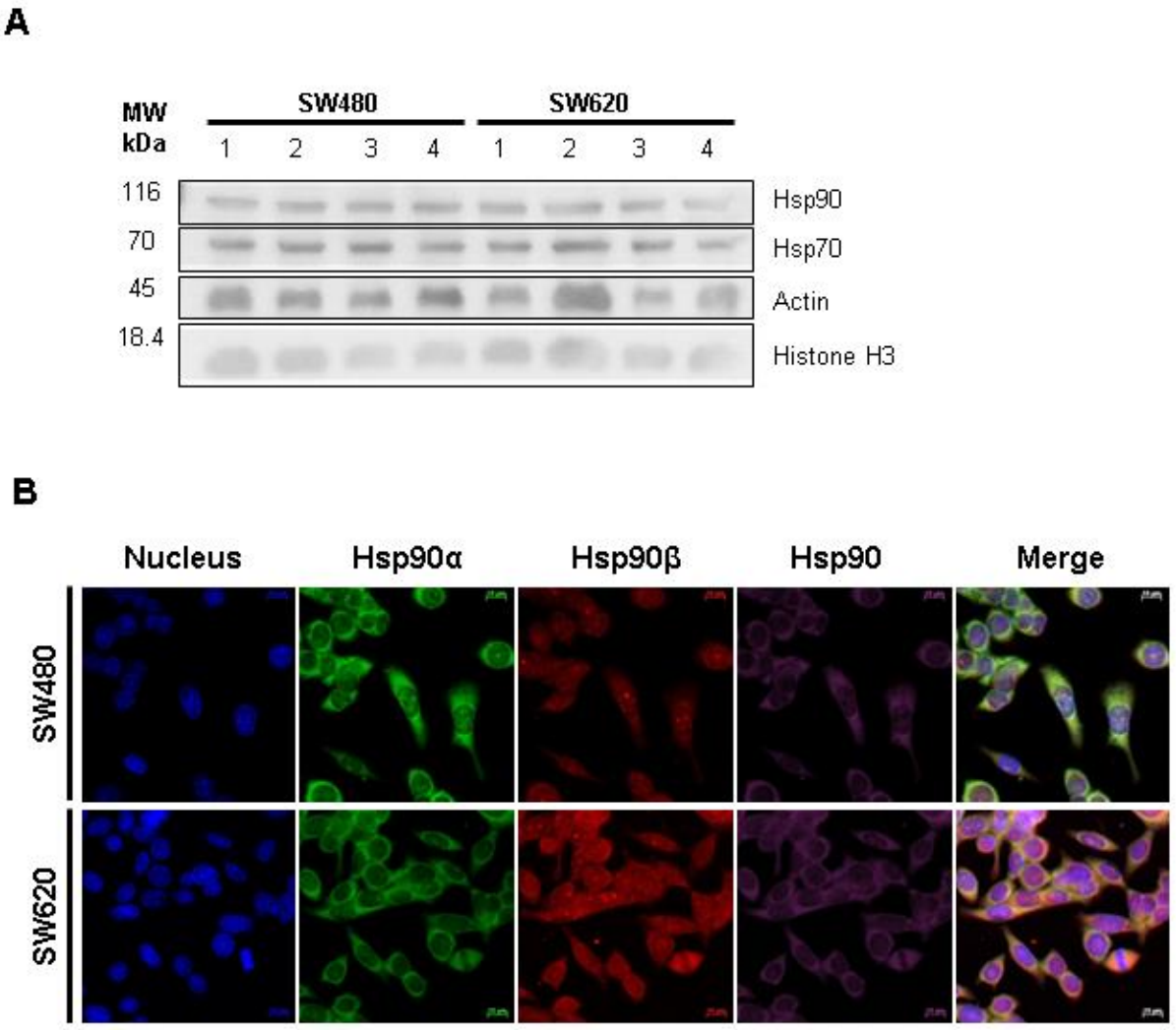

Figure 3.1. Expression and localisation of Hsp90 in SW480 and SW620 cells.

A. Western blot analysis of the expression of Hsp90, Hsp70, actin and histone H3 (loading control) from four replicate cell lysates (100 µg protein loaded per well). Chemiluminescent detection of proteins using antibody-antigen detection using the Chemidoc EQ system (Biorad, UK). B. Localisation of cytosolic Hsp90 isoforms (alpha and beta) in SW480 and SW620 cell lines. Cells were seeded on fibronectin (5 µg/ml) overnight at 37°C. Following fixation, cells were incubated with mouse anti-Hsp90α, rabbit anti-Hsp90β and goat anti-Hsp90α/β antibodies, followed by donkey anti-mouse IgG (green), donkey anti-rabbit IgG (red) and donkey anti-goat IgG (purple) antibodies. Nuclei were stained using 1 µg/ml Hoechst 33342 (blue). Images were captured using the Zeiss LSM 510 Meta confocal microscope and analysed by AxioVision (Zeiss) software. Images were representative of triplicate images captured at 400 x magnification. Scale bars: 100 µm.

Table 7. Proteins of the Hsp90 chaperome in SW480 and SW620 cells by immunofluorescent microscopy

Protein	Biologically-relevant Association	Qualitative Observation in SW480 and SW620 cell lines
HSF-1	Transcriptional regulator of chaperone expression	Predominantly perinuclear. Nuclear and cytoplasmic
Hsp90	Molecular Chaperone	Cytoplasmic
Hsp70	Molecular Chaperone	Cytoplasmic and nuclear
DNAJB6	Co-chaperone; part of the Wnt complex	Largely nuclear, some within the cytoplasm

The distribution of HSF-1, Hsp90, DNAJB6 and Hsp70 proteins were assessed in the SW480 and SW620 cell lines by immunofluorescent microscopy (see Table 7 for a summary of biological relevance). The fluorescence antibody-stained control demonstrated undetectable non-specific secondary antibody binding (Figure 3.2A). HSF-1 showed nuclear and cytoplasmic localisation within the SW480 and SW620 cell lines, while Hsp90 staining revealed a dominant cytoplasmic presence. Staining for DNAJB6 revealed a collection of the co-chaperone in the nucleus and lower concentration in the cytoplasmic localisation and Hsp70 showed an even distribution of protein between the cytoplasmic and nuclear compartments of the SW480 and SW620 cells. Figure 3.2A illustrated similar distributions of HSF-1, Hsp90, Hsp70 and DNAJB6 between SW480 and SW620 cell lines (see Table 7 for overview).

The response of SW480 and SW620 cells to stress was evaluated through an assessment of the known stress inducible proteins Hsp90α and Hsp27 proteins levels by western blot analyses (Figure 3.2.B and C). Hypoxic conditions were simulated with the addition of 500 µM $CoCl_2$ for 24 H, while cells under heat shock were incubated for 90 minutes at 42°C, followed by 16 H under normal conditions for analysis of protein recovery. Qualitative analysis of the level of Hsp90α across the paired cell lines showed that in the absence of hypoxic stress (indicated by the "-" sign; i.e. normal conditions), the SW620 cells expressed higher levels of Hsp90α and Hsp27 than the SW480 cells, relative to the α-tubulin loading control for the individual cell line (Figure 3.2B). Hypoxic stress conditions resulted in an increased expression of Hsp90α in both SW480 an SW620 cell lines, with negligible increases in Hsp27 (Figure 3.2B). Exposing the paired cell lines to heat shock and allowing for 16 H of recovery provided sufficient time for Hsp90α levels to normalise, illustrated by similar levels of protein with ("+") and without ("-") heat shock (Figure 3.2C). Interestingly, heat shock induced an increased expression of Hsp27 in the SW480 cell line, but not within the SW620 cell line. Surprisingly the level of Hsp70 was unaffected by heat and hypoxic stress conditions (data not shown).

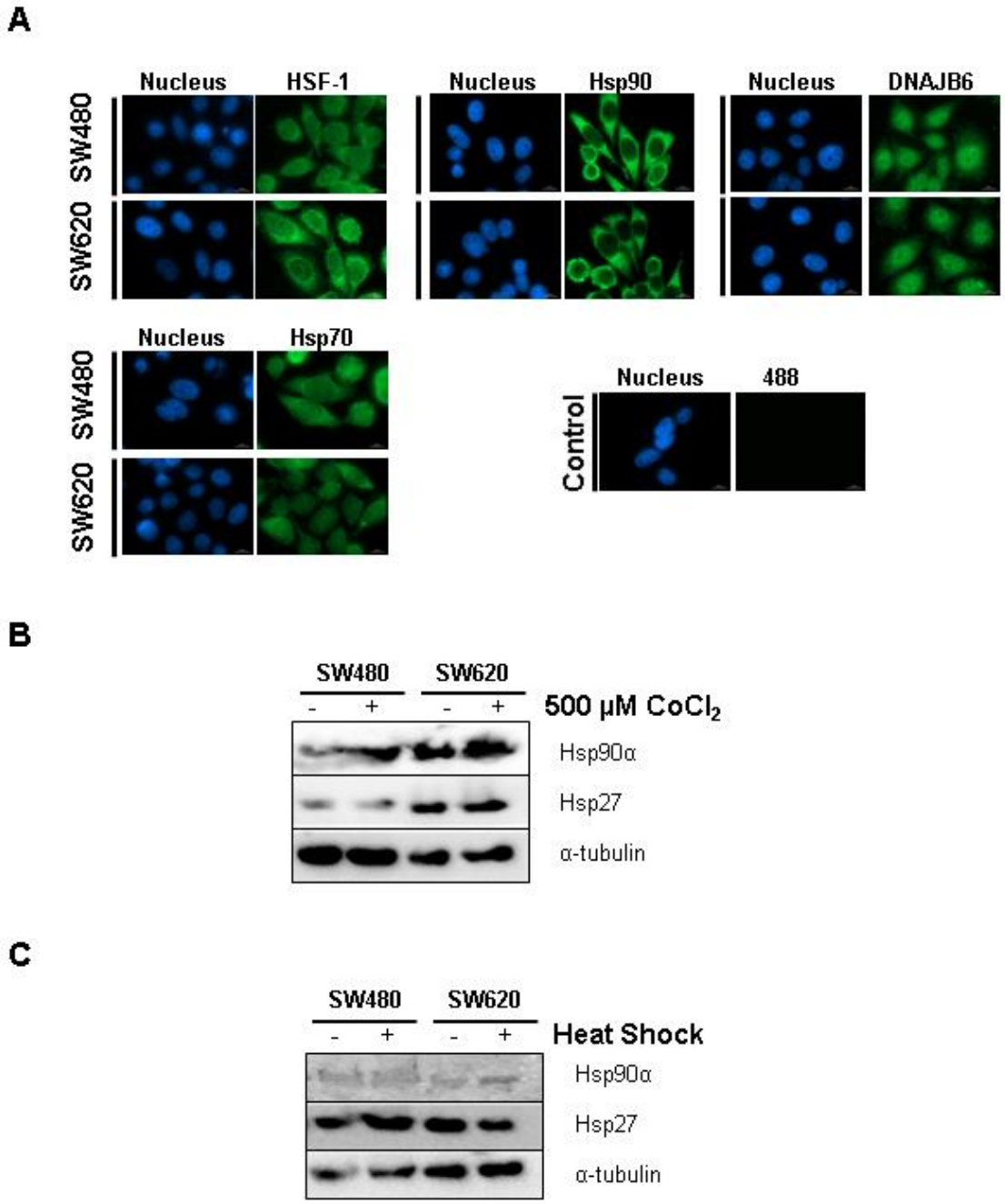

Figure 3.2. Comparing proteins of the chaperome in SW480 and SW620 cells and evaluation of the Hsp90α and Hsp27 response to stress.

A. Analysis of the regulator of transcriptional activity: Heat Shock Factor 1 (HSF-1); molecular chaperones: Hsp90 and Hsp70 and Wnt associated co-chaperone: DNAJB6 by fluorescent microscopy. Images depicted are representative of triplicate analyses, taken using Zeiss AxioVert.A1 Fluorescence LED Inverted Microscope with a High Resolution AxioCam MRm Rev 3 (400 x magnification). Data were analysed using ZEN Lite 2012 1.1.2.0 software. Scale bars: 200 µm. B Western blot analysis of SW480 and SW620 cells treated with 500 µM $CoCl_2$ for 24 H (hypoxic conditions). Western blot analysis for SW480 and SW620 cells heat-shocked (42°C for 90 min followed by 16 H recovery at 37°C). Western blots were analysed for Hsp90α, Hsp27and α-tubulin (loading control) proteins under hypoxic and heat stress using antibody-antigen detection.

Effect of extracellular Hsp90 on tumourspheres

Extracellular Hsp90 has been proposed to play a role in cancer metastasis, we assessed the effects of Hsp90 on TS. TS of the paired cell lines were cultured with a range of concentrations up to 100 ng/ml Hsp90β. Hsp90β was used because an endotoxin free source of the protein is commercially available. The growth of SW480 and SW620 TS for 7 days under supplementation with Hsp90β failed to produce any distinct changes in the size or morphology of SW480 and SW620 TS, relative to the untreated control TS (Figure 3.3A). WST-1 cell proliferation assay results supported our initial findings, by demonstrating little to no change in TS viability as an indication of cell survival or TS number in the presence of Hsp90β supplementation (Figure 3.3B). Interestingly, supplementation of the SW620 TS with Hsp90β showed minor but not statistically significant effect on cell survival, showing improved TS viability in the presence of concentrations as low as 5 ng/ml Hsp90β. This study suggested that extracellular Hsp90β had no statistically significant effect on TS formation in either cell line.

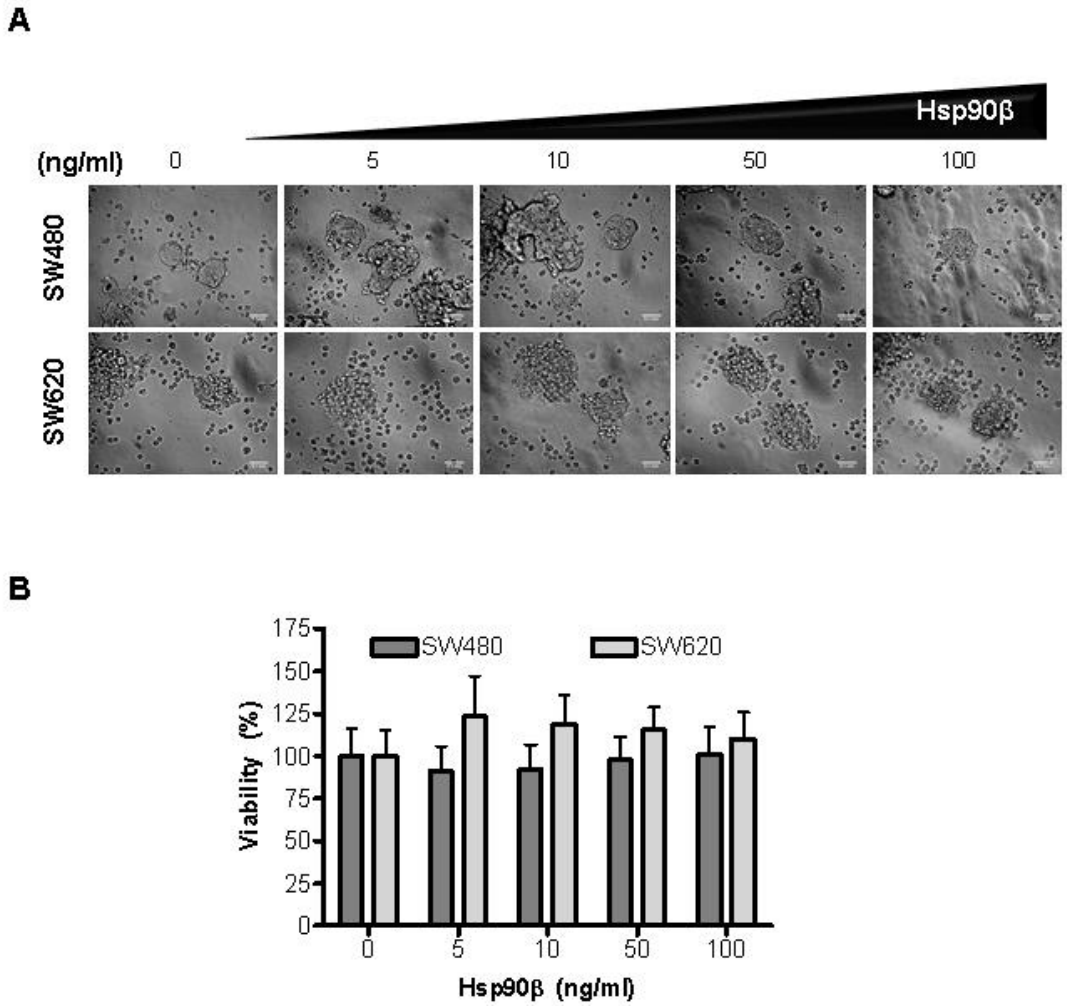

Figure 3.3. Analysis of tumoursphere growth with addition of Hsp90β.

The effects tumourspheres morphology and viability were assessed following the addition of Hsp90β. SW480 and SW620 tumourspheres were cultured for 7 days from 1000 cells with Hsp90β (0 – 100 ng/ml). A. Images were taken following 7 days of TS growth using a phase contrast DSZ5000X inverted microscope (200 x magnification). Scale bars represent 0.1 mm. B. WST-1 assay for cell proliferation was assessed for TS grown with/without Hsp90β. Percentage viability was determined using untreated controls as a reference of 100 % cell viability per cell line. Images were analysed using ImageJ software and results shown represent the average of 5 replicates. Data are representative of mean ± SD of 5 replicates, analysed by GraphPad Prism software.

Sensitivity of SW480 and SW620 cell lines to Hsp90 inhibition *in vitro*

Surgery, drug and radiation-based therapeutic strategies are common practice in oncology (Abdullah and Chow, 2013). Treating metastases has seen 90 % of treatment failures resulting from chemotherapeutic resistance (Longley and Johnston, 2005). Using the paired cell lines, the different sensitivities of the cell lines to Hsp90 inhibition using geldanamycin and novobiocin was compared to treatments with the known chemotherapeutic drugs 5-fluorouracil (5-FU) and oxaliplatin, which are used in the treatment of colon cancer (Figure 3.4). The chemosensitivity of SW480 and SW620 cells treated with anti-cancer therapeutics was assessed based on cell survival. Cell survival, represented as percentage viability, was determined from a non-linear regression of a WST-1 dose response curve to determine the effective concentration at which 50 % of the cell population remains viable (half the maximal effective concentration), known as the EC_{50}. Cytotoxicity results indicated that SW480 cells were more sensitive to oxaliplatin (Figure 3.4; EC_{50}: SW480: 35.13 µM, SW620: 107.4 µM), while SW620 cells equally sensitive to 5-FU treatment (Figure 4.3; EC_{50}: SW480: 627.1 µM, SW620: 468 µM). Inhibition of Hsp90 using geldanamycin and novobiocin was used to determine whether or not the paired cell lines represented differential chemosensitivities to Hsp90 inhibition. The SW480 and SW620 cells showed similar sensitivities to geldanamycin and novobiocin (Figure 3.4; geldanamycin EC_{50}: 45.6 and 59 nM, respectively and novobiocin EC_{50}: 139.2 and 155.1 µM, respectively). These data suggest that the SW480 and SW620 are similarly sensitive to Hsp90 inhibitors, despite showing differential sensitivity to other anti-cancer compounds.

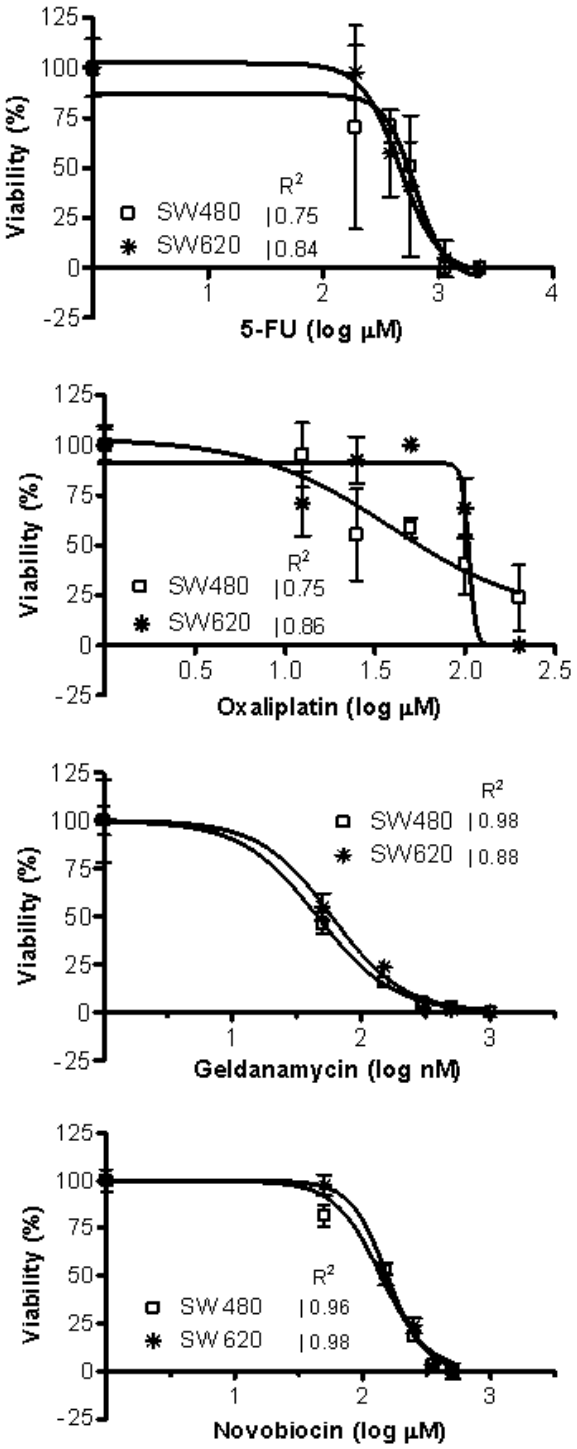

Figure 3.4. Sensitivity of SW480 and SW620 cells to chemotherapeutic agents.

The sensitivity of SW480 (squares) and SW620 (stars) cells to chemotherapeutics used to treat colon cancer, 5-fluorouracil (5-FU) and oxaliplatin, and the Hsp90 inhibitors, geldanamycin and novobiocin. 5-FU: 0, 25, 50, 75, 150, 300 µM. Oxaliplatin: 0, 12.5, 25, 50, 100, 200, µM. Geldanamycin: 0.1, 1, 10, 100, 1000 nM. Novobiocin: 1, 50, 150, 250, 350, 500 µM. Chemotherapeutic effects on viability were assessed by WST-1 assay over 72 H. Each assay represents the mean ± SD of six replicates. The concentration of chemotherapeutic agent to effectively reduce cell viability by 50 % (EC_{50}) for each cell line was calculated from the dose response curve using GraphPad Prism.

Sensitivity of SW480 and SW620 tumourspheres Hsp90 inhibition *in vitro*

We previously demonstrated that SW480 and SW620 cells could both form tumourspheres (TS), with the SW620 showing a significantly greater propensity to form TS than SW480 cells. SW480 and SW620 derived TS were subsequently analysed for sensitivity to anti-cancer therapies. The ability of TS to form from the equivalent number of plated cells in the absence versus presence of inhibitors was tested. TS were grown under anchorage independent conditions with increasing dosage of 5-FU, oxaliplatin, geldanamycin or novobiocin included from the time of seeding. Cell survival, represented as viability, was determined by WST-1 assay in comparison to untreated TS (a reference of 100 % TS viability). The concentration ranges of compounds tested were selected based on the EC_{50} values determined in adherent culture (Figure 3.4). The effect of treatments on TS morphology was assessed by microscopy (Supplementary Figure S1).

SW480 and SW620 TS showed a dose dependent decrease in cellular viability in response to 5-FU and oxaliplatin treatments (Figure 3.5). TS treated with 5-FU appeared less uniformly shaped than the control ("-") TS (see Supplementary Figure S1A). The treatment of TS with 5 µM 5-FU resulted in more than 90 % reduction in viability for SW620 TS and a 60 % reduction in cell viability for SW480 TS. This concentration was substantially lower than the EC_{50} values determined for adherent cells (Figure 3.4; EC_{50}: SW480: 35.13 µM, SW620: 107.4 µM). At concentrations of or above 50 µM 5-FU formation of viable TS was completely prevented in both cell lines. TS treated with oxaliplatin were largely disrupted, with surviving TS displaying a high degree of granularity when compared with the control ("-") TS (see Supplementary Figure S1A). With 12.5 µM oxaliplatin in the SW620 TS, viability was reduced by 90 % and the SW480 TS viability was reduced by 60 % (Figure 3.5). This concentration is between 40 to 50 times lower than the EC_{50} values determined for adherent cells (Figure 3.4; EC_{50}: SW480: 627.1 µM, SW620: 468 µM). Taken together, these findings demonstrated that TS of both cells were more sensitive to both inhibitors than adherent cells, while SW620 TS were more sensitive to 5-FU and oxaliplatin than SW480 TS.

TS cultured in the presence of geldanamycin had an increased granular appearance, with the formation of irregular-shaped spheres at high concentrations (see Supplementary Figure S1B). Unlike the response of the adherent SW620 cells, SW620 TS displayed an enhanced sensitivity to geldanamycin over SW480 TS. The SW620 TS showed more than 90 % reduction in viability with 12.5 nM geldanamycin (compared to the EC_{50} of 59 nM in adherent SW620 cells), while the viability of SW480 TS cells only decreased by approximately 30 % with between 12.5 and 75 nM geldanamycin (compared to the EC_{50} of 45.6 nM in adherent SW480 cells) (Figure 3.5). The co-culture of TS with novobiocin did not produce any visible alteration to TS morphology in the SW480 cell lines, while SW620 TS showed a reduction in

sphere size upon treatment with more than 100 µM novobiocin (see Supplementary Figure S1B). In contrast, the SW480 TS showed a dose-dependent increase in viability in the presence of 5 – 500 µM novobiocin (Figure 3.5). While the SW620 TS showed a similar trend between 5 and 50 µM novobiocin, the viability of SW620 TS was reduced with more than 100 µM, and the greatest reduction in TS viability with novobiocin was seen at 150 µM with ~ 65 % viability. The adherent paired cell lines demonstrated similar effective concentrations for novobiocin in SW480 and SW620 cells (EC_{50}: 139.2 and 155.1 µM, respectively). Comparing viability upon TS co-culture with novobiocin showed enhanced sensitivity of the SW620 TS to novobiocin and also revealed that novobiocin improved the viability of SW480 TS. In order to attempt understand the differential effect of Hsp90 inhibition in SW480 and SW620 TS formation, the effect of geldanamycin and novobiocin on the proportion of TS derived cells bearing the putative CSC-associated $CD44^+/CD24^-$ or $CD44^+/CD133^+$ marker phenotype was assessed. There was no statistically significant difference in the $CD44^+/CD24^-$ or $CD44^+/CD133^+$ populations upon treatment with geldanamycin or novobiocin that would explain the response of the TS to treatment (data not shown).

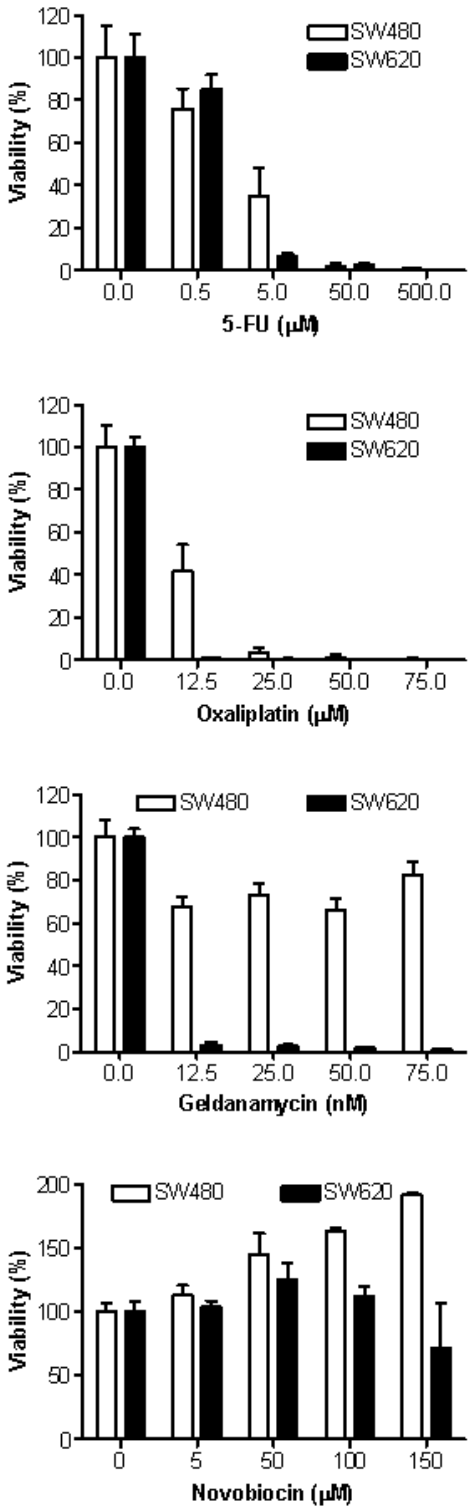

Figure 3.5. Comparison of tumoursphere formation by SW480 and SW620 in the presence of inhibitors.

The growth and development of tumourspheres under anchorage-independent conditions was analysed 7 days after seeding cells in the presence of an increasing dosage of 5-fluorouracil (5-FU), oxaliplatin, geldanamycin and novobiocin treatments. 5-FU: 0, 0.5, 5, 50 and 500 µM. Oxaliplatin: 0, 12.5, 25, 50 and 75 µM. Geldanamycin: 0, 12.5, 25, 50 and 75 nM. Novobiocin: 0, 5, 50, 100 and 150 µM. Results represented the mean ± SD of triplicate biological experiments, each of 3 technical replicates, with 1000 cells were seeded per well under anchorage-independent conditions (96-well plate). Data were analysed using GraphPad Prism software.

Analysis of pre-formed SW480 and SW620 tumoursphere resistance to Hsp90 inhibitors *in vitro*

The effect of inhibitors on the removal of existing tumourspheres was tested. This study addressed the effectiveness of treatments on TS after their formation, thereby assessing TS resistance to treatment. Following 5 days of anchorage independent growth, SW480 and SW620 TS were subjected to a range of concentrations of 5-FU, oxaliplatin, novobiocin and geldanamycin. The effects of different concentrations of inhibitors on TS viability (using the WST-1 assay) and TS morphology (assessed by microscopy) was assessed after 4 days.

Few effects on morphology were observed with up to 50 µM of 5-FU after 4 days of treatment across the paired line TS, with disruption in TS morphology only evident at the highest dosage (500 µM) (see Supplementary Figure S2). The quantitative assessment of TS cellular viability on Day 9 of analysis for each treatment confirmed that 5-FU failed to reduce the viability of established SW480 tumourspheres, and only at 500 µM did SW620 tumourspheres show decreased viability to 5-FU (Figure 3.6). Treating established (5 day old) TS with oxaliplatin showed an increase in smaller aggregates of single cells, presumably caused by the dissociation of cells of the TS. Both SW480 and SW620 TS showed a dose-dependent disruption of TS upon treatment with oxaliplatin (see Supplementary Figure S2). The dose-dependency of the oxaliplatin treatment of established TS was quantified and confirmed by analysis of viability following the WST-1 assay (Figure 3.6). With 75 µM oxaliplatin, the viability of SW480 and SW620 TS was reduced by approximately 25 % and 50 %, respectively, relative to the untreated controls (which was taken as 100 % viability).

The effects of geldanamycin on TS disruption were less pronounced than the effects of 5-FU or oxaliplatin, with few dissociated cells observed even at the highest dosage (see Supplementary Figure S2). Quantitatively, geldanamycin produced a dose-dependent increase in the average viability of TS up to 25 nM of geldanamycin, after which the response plateaued but was still greater than 100 % for both cell lines. Treating 5 day old TS with 75 nM geldanamycin resulted in approximately 125 % viability in both SW480 and SW620 TS, relative to untreated controls (Figure 3.6). Novobiocin treatments of SW480 and SW620 TS showed a dose-dependent increase in the size of TS, an effect which was less distinct in SW620 TS (see Supplementary Figure S2). A closer investigation into the viability of TS indicated that only at the highest tested concentration (150 µM) of novobiocin did the SW620 TS show reduced viability, while SW480 showed a dose-dependent increase in TS viability to approximately 150 % with up to 50 µM novobiocin (Figure 3.6). These data suggeted that once established, both SW480 and SW620 TS are more resistant to anti-cancer therapies.

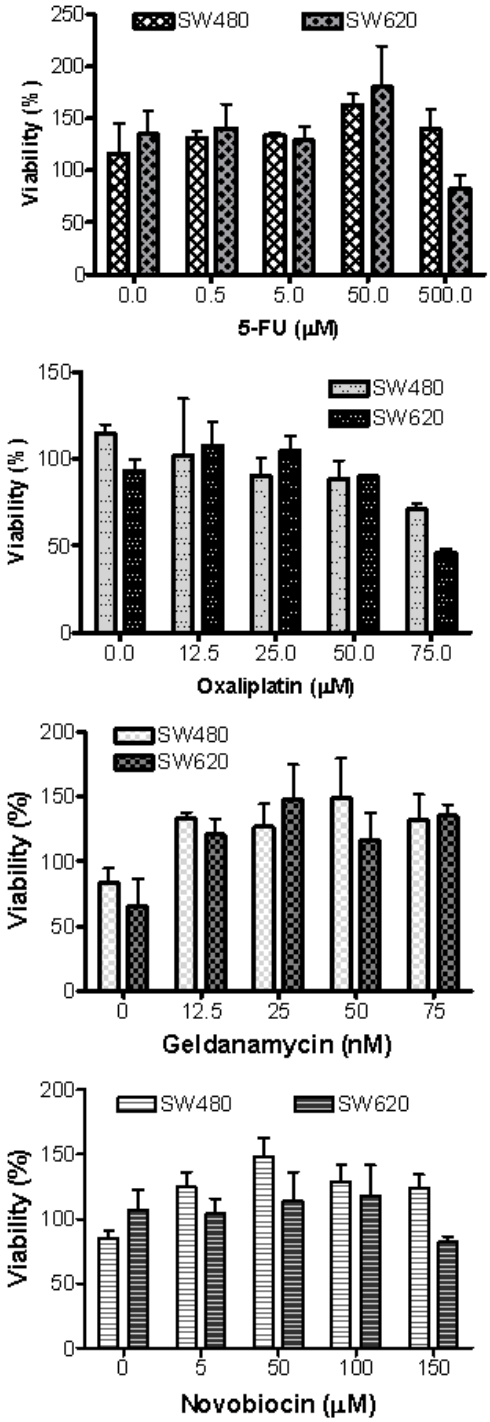

Figure 3.6. Sensitivity of established SW480 and SW620 tumourspheres to inhibitors.

The effects of treating established tumourspheres with 5-FU, oxaliplatin, geldanamycin and novobiocin was analysed by WST-1 assay. Tumourspheres (5 day old) were analysed for changes to cell viability 4 days (Day 9) following treatment. 5-FU: 0, 0.5, 5, 50 and 500 µM. Oxaliplatin: 0, 12.5, 25, 50 and 75 µM. Geldanamycin: 0, 12.5, 25, 50 and 75 nM. Novobiocin: 0, 5, 50, 100 and 150 µM. Cell viability was calculated as a percentage relative to the viability of the untreated cells. Results represent the average (mean ± SD) of triplicate results, each of 3 replicates, with 1000 cells seeded per well. Data were analysed using GraphPad Prism software.

Effects of Hsp90 inhibition on the cell cycle

We next evaluated the effect of Hsp90 inhibition on the cell cycle in adherent cells and TS of the paired cell lines. The cell cycle refers to the series of coordinated events that result in the replication of DNA and the division that cells undergo for the production of daughter progeny (Collins et al., 1997). In normal cells, programmed cell death is a tightly controlled process for the discarding of unwanted or damaged cells. There are four phases to the eukaryotic cell cycle. The first is the gap 0 (G0) phase, where cells resting cells prepare to enter the cell cycle for the purpose of division. At the gap 1 (G1) phase, cells enlarge in preparation for division. From the G1 phase, cells pass through the S phase where DNA is synthesised for replication, and on to the gap 2 (G2) phase where again the cell enlarges to accommodate the replicated DNA. From the G2 phase, cells enter the mitotic phase wherein cells physically divide, producing two daughter cells. Two checkpoints regulate the progression of cells through the cell cycle: the G1/S and the G2/M checkpoints. The checkpoints ensure that no damaged DNA is transferred to the progeny. Quiescent cells, or cells that do not need to divide, are found in the G0 resting phase.

Changes in cell distribution across the phases (G1, S and G2M) of the cell cycle were used to elucidate the possible mechanism of action of geldanamycin and novobiocin. PI staining was utilised to define the DNA content of adherent cells and TS of SW480 and SW620 cell lines treated with 65 nM geldanamycin or 150 µM novobiocin. The results of this study were analysed by means of two-way ANOVA for the detection of statistical significance between the distributions of cells. The proportion of SW480 and SW620 cells in the G1, G2M and S phases of the cell cycle were very similar, indicating that similar numbers of cells in either cell line was actively undergoing DNA replication (Figure 3.7). SW480 TS showed a larger proportion of cells in the G1/G0 phase (represented together as G1) and a smaller proportion of cells in the S-phase than SW620 TS. The SW480 TS also showed increased G1 phase (and corresponding decrease in S phase) when compared to the SW480 cells cultured under adherent conditions. Treating with geldanamycin, SW480 cells and TS showed an increase in the proportion of cells in the G2M phase. The G2M phase increase observed for SW480 cells treated with geldanamycin was accompanied by a reduced S phase. Treating SW480 TS with novobiocin showed a similar distribution across the phases on the cell cycle to the untreated SW480 TS. SW480 cells treated with novobiocin resulted in an increase in the proportion of cells in the G1 phase and concomitant reduction in G2M population, relative to the novobiocin-treated SW480 TS derived cells. Hsp90 inhibition did not significantly alter the proportion of cells in different phases in the cell cycle between SW620 cells and TS. However, both SW620 TS and adherent cells showed an increased in G2M upon geldanamycin, but not upon treatment with novobiocin. These findings supported the unique pharmacological mechanism

of C-terminal Hsp90 inhibition by novobiocin, in comparison to N-terminal inhibition, as demonstrated by trypan blue dye exclusion, luciferase refolding activity and cytotoxicity assays in prostate cancer cells *in vitro* (Eskew *et al*., 2011). The increase of G1 phase and decrease of G2M phase cells in SW480 TS treated with novobiocin, relative to SW480 cells, may be one way to explain the resistance of SW480 cells to novobiocin during TS formation and increase in viability observed when SW480 TS are treated after sphere formation (see Figure 3.5 and 3.6), when compared to the response of the SW620 cells and TS to novobiocin.

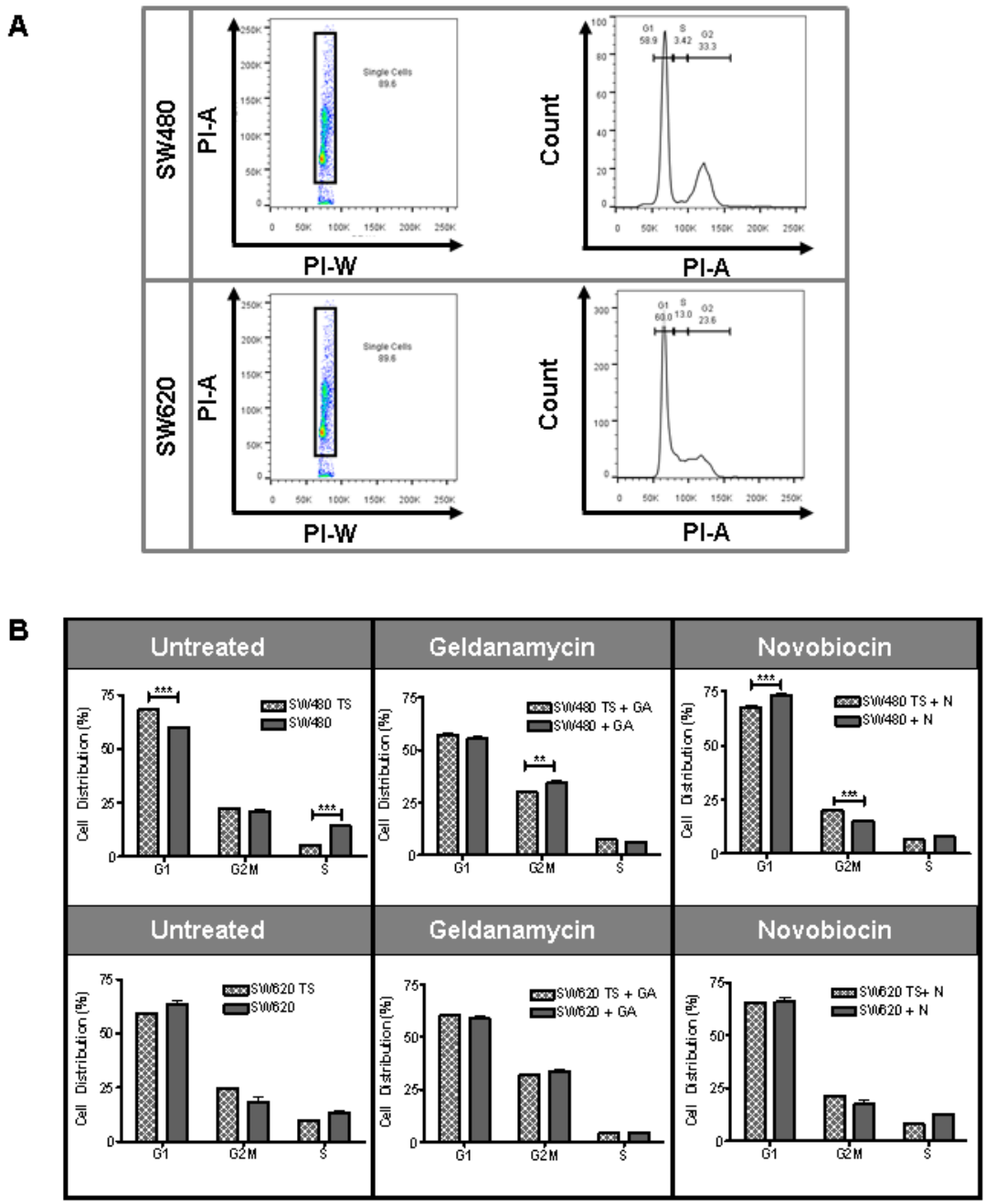

Figure 3.7. Cell cycle analysis of SW480 and SW620 cells and tumourspheres under Hsp90 inhibition.

The cell cycles of SW480 and SW620 cells and TS were analysed for the effects of 48 H of Hsp90 inhibition. A. Gating strategy employed for the discrimination of single cells (dot plot of PI-Area (A) vs PI-Width (W)) and the identification of G1, S and G2M phases of the cell cycle by flow cytometry (histogram of events counted vs PI-A). B. Analysis of propidium iodide staining (50 µg/ml) across the G1 (inclusive of G0), S and G2 (G2M) phases of SW480 and SW620 cells and TS. Untreated (control) cells and TS were compared to cells and TS inhibited with geldanamycin (GA: 65 nM) or novobiocin (N: 150 µM), and differences in the effects of Hsp90 inhibition, compared between cells and TS, were analysed. Triplicate experiments assessed the cell distribution of 5000 events captured by flow cytometric analysis of propidium iodide staining (50 µg/ml) across the G1 (inclusive of G0), S and G2M phases. Data represent mean ± SD for three replicated experiments, analysed by two-way ANOVA with Bonferroni post-tests using GraphPad Prism software (* = P < 0.05; ** = P < 0.01; *** = P < 0.001).

Novobiocin sensitised tumourspheres to oxaliplatin treatment

Our previous studies suggested that pre-formed SW480 and SW620 TS resist treatment with the Hsp90 inhibitor novobiocin (Figure 3.5). Additionally, we observed that novobiocin treatment, in particular, improved the viability of SW480, if introduced upon seeding or after TS formation, and SW620 TS if treatment was introduced after the formation of TS (Figure 3.6). In this study, we investigated whether novobiocin was able to sensitise existing TS to treatment with oxaliplatin. TS from 2000 cells/ml SW480 and SW620 cells were cultured for 5 days under anchorage-independent conditions prior to treatment with 0 – 100 µM oxaliplatin with or without 50 µM novobiocin. The results of this study were analysed after 9 days by WST-1 assay. The untreated (0 µM oxaliplatin) TS were used to establish 100 % viability.

SW480 and SW620 TS treated with 0 – 100 µM oxaliplatin showed a dose dependent decrease in viability of TS up to 100 µM, with noticeable fluctuations (Figure 3.8). Simultaneous treatment of TS with 0 – 100 µM oxaliplatin and 50 µM novobiocin showed an improved concentration-dependent decrease in viability, with reduced fluctuation seen in the viability of SW480 and SW620 TS under simultaneous treatment of novobiocin and oxaliplatin. SW480 and SW620 TS treated with between 45 and 100 µM oxaliplatin and 50 µM novobiocin resulted in diminished cellular viability to approximately 20 %. With 45 µM oxaliplatin, SW480 and SW620 TS treated with novobiocin represented 3-fold and 2-fold increased sensitivity, respectively, in comparison to TS treated with 45 µM oxaliplatin alone. This suggested enhanced sensitivity of TS to oxaliplatin in the presence of novobiocin, despite the fact that novobiocin alone at that concentration did not have a significant toxic effect on established TS.

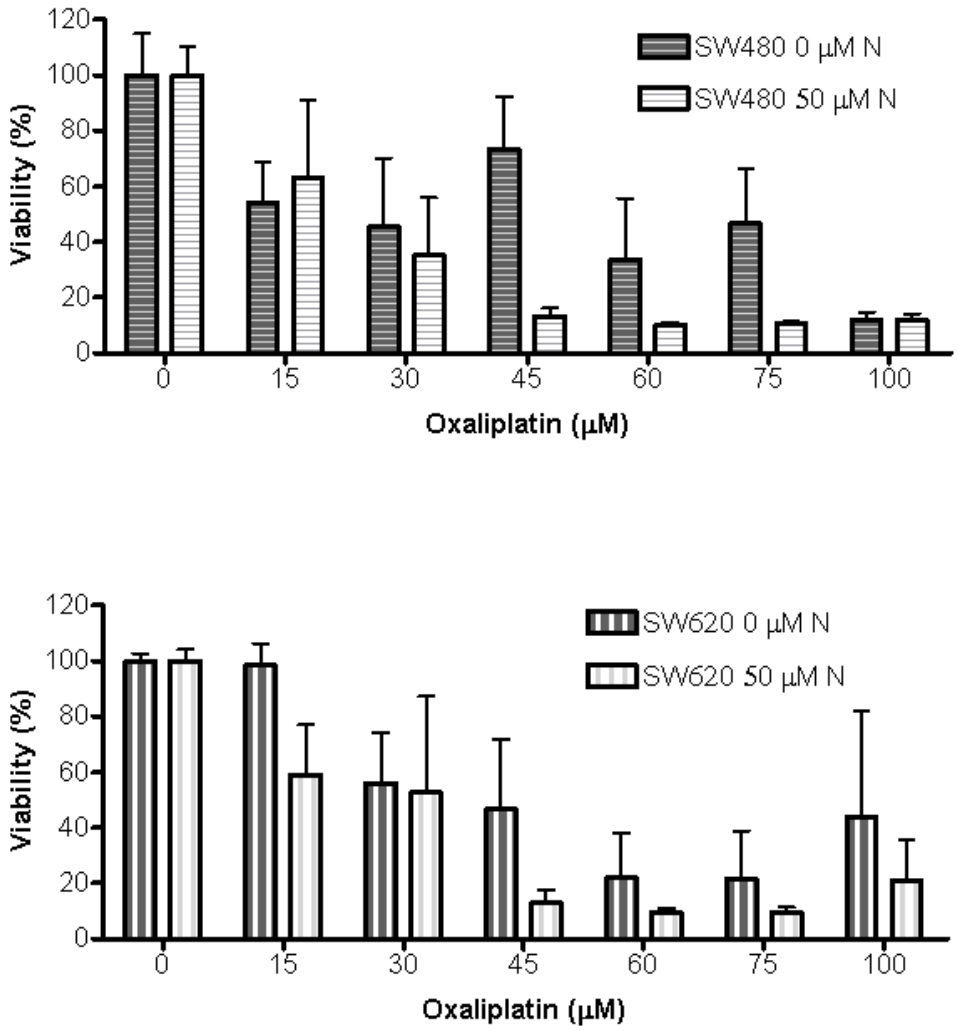

Figure 3.8. Novobiocin sensitised SW480 and SW620 tumourspheres to oxaliplatin.

SW480 and SW620 cells were seeded (2000 cells/ml) under anchorage independent conditions for the culture of tumourspheres prior to the addition of 50 µM novobiocin (N). Cells were then subjected to 0, 15, 30, 45, 50, 75 or 100 µM oxaliplatin prior to WST-1 analysis for viability. Each assay represents the mean ± SD of four replicates. Percentage viability was determined using negative controls as a reference of 100 % cell viability per cell line. Data were analysed using GraphPad Prism software.

Discussion

Comparison of SW480 and SW620 cell lines by the expression of molecular chaperones and co-chaperones

The SW480 and SW620 cell lines showed similar levels and distribution of the major molecular chaperones, Hsp90 and Hsp70. The Hsp90α protein staining showed cytoplasmic and nuclear subcellular localisation both the SW480 and SW620 cells by confocal microscopy (Figure 3.1). Interestingly, heat shock resulted in increased Hsp27 in SW480 cells, but not in SW620 cells, while hypoxic stress conditions increased the expression of Hsp90α in both SW480 and SW620 cell lines (Figure 3.2).

The overexpression of proteins of the Hsp90 complex (Hop, Hsp90 and Hsc70) have been observed in human colon cancer cells (Kubota *et al.,* 2010). Hsp overexpression in response to stress facilitates cell growth due to the cytoprotective and protein folding roles of Hsp (Ciocca and Calderwood, 2005). Hsp90 is a highly abundant cytosolic protein that has also shown some nuclear localisation, despite lacking a nuclear localisation signal (Perdew *et al.,* 1993). To the best of my knowledge this report is the first characterisation of molecular chaperone and co-chaperone expression, distribution and location in the SW480 and SW620 paired colon cancer cells. Further examination of TS from the paired cell lines with additional extracellular Hsp90 and the sensitivity of cells and TS to Hsp90 inhibitors facilitated our investigation into the role of Hsp90 in colon cancer and CSC biology.

Extracellular Hsp90 has no significant effect on tumoursphere formation

The culture of TS in the presence of extracellular Hsp90βresulted in no distinct morphological changes in SW480 and SW620 TS relative to untreated TS. While the SW620 TS demonstrated a slight increase in TS viability, the findings were not statistically significant (Figure 3.3).

Hsp90 is not confined to the intracellular space, but has been found extracellularly (Sidera and Patsavoudi, 2008). The interaction of extracellular Hsp90 with the CD91 cell surface receptor is associated with cancer cell migration under adherent conditions (Basu *et al.,* 2001; Cheng *et al.,* 2008). Interestingly, many groups maintain that Hsp90α is the only Hsp90 isoform that is functional in the extracellular environment, despite the fact that other groups have identified Hsp90β in the extracellular environment (Hunter *et al.,* 2014). Hsp90α has been shown to be involved in cancer cell motility, tumour invasiveness and angiogenesis, all of which were

conducted under adherent conditions (Eustace *et al.,* 2004; Song *et al.,* 2010). Hypoxic stress induces the secretion of Hsp90α in the extracellular space, which was shown to stimulate wound healing (Li *et al.,* 2007). Hsp90α stimulates colorectal cancer cell invasion through interactions with cell surface receptors, further providing support for a role for extracellular Hsp90 in colon cancer (Chen *et al.,* 2010). Hsp90α and Hsp90β have been shown to interact with ECM protein, fibronectin, and regulate the dynamics of the extracellular matrix in breast cancer cells, supporting a role for extracellular Hsp90 in the metastatic progression of cancer (Hunter *et al.,* 2014).

The fact that extracellular Hsp90β treatment of TS failed to induce significant differences to the growth or morphology of SW480 and SW620 TS may suggest that the role of extracellular Hsp90 relies on cells being cultured under adherent conditions and that under anchorage independent conditions. Alternatively, it may be that Hsp90β is not functional in this context and that, similar to other studies, different effects may have been observed had the Hsp90α isoform been used. However, at the time of the study, we only had access to an endotoxin-free preparation of Hsp90β. Because contaminating endotoxin in recombinant proteins can cause changes in cell behaviour, it would not be possible to use bacterially produced Hsp90α for these assays. Therefore, the analysis of the effect of Hsp90α on TS formation will need to be conducted once we have obtained a source of endotoxin-free protein.

Sensitivity of SW480 and SW620 cells and tumourspheres to Hsp90 inhibition

Under adherent conditions, the SW480 and SW620 cells were similarly sensitive to 5-FU and the Hsp90 inhibitors, geldanamycin and novobiocin, while SW480 cell lines were more sensitive to oxaliplatin than the SW620 cell lines. The chemicals 5-FU, oxaliplatin and geldanamycin were able to inhibit or reduce, as in the case of geldanamycin, TS formation in both lines at concentrations below the EC_{50} values determined for adherent lines, but only when cells were treated at seeding (Figure 3.5 and 3.6). In contrast to the other treatments, novobiocin treatment at seeding led to an increase in TS viability, particularly in the SW480 cell line. The effects of geldanamycin and novobiocin were determined not to be due to a change in the proportion of cells expressing the putative CSC phenotype. Equivalent concentrations of the inhibitors were ineffective at removing established TS, although addition of 50 µM of novobiocin was able to increase the sensitivity of pre-formed (established) TS to oxaliplatin.

RNA processing and DNA synthesis *in vivo* are inhibited by the 5-FU antimetabolite to prevent cell proliferation (Waxman and Bruckner, 1982). The administration of 5-FU has been shown to be toxic normal cells as well as certain cancers, preventing the development of 5-FU as a

stand-alone treatment in clinical trials, but providing new therapeutic avenues with adjuvant chemotherapeutics (Han *et al*., 2013). Oxaliplatin is a platinum-based cisplatin analogue. The structure of oxaliplatin is similar to that of cisplatin, except for the presence of oxalate leaving group and the diaminocyclohexane carrier ligand (Alcindor and Beauger, 2011). Oxaliplatin induces DNA damage through the formation of DNA adducts and has demonstrated a greater cytotoxicity than cisplatin (Di Francesco *et al.,* 2002). Previously, it was shown that oxaliplatin maintained activity in cisplatin-resistant and 5-FU-resistant cell lines (Rixe *et al.,* 1996).

More recently, much research focuses on developing CSC-targeting therapy to prevent cancer recurrence and metastasis (Clarke and Fuller, 2006; Dean *et al.,* 2005; Han *et al.,* 2013). We showed that colon cancer TS cultured with 5-FU and oxaliplatin showed dose-dependent sensitivities to treatment, but when administered after TS formation, the TS displayed resistance to oxaliplatin and 5-FU. Using the culture of serum-free spheres from 25 colon cancer cell lines, including the paired cell lines, Collura and colleagues demonstrated that the treatment of the adherent cells with 5-FU enhanced sphere-formation ability of HCT116 cells (Collura *et al*., 2013). This suggested that the CSC-like cells are resistant to the drug when cultured under adherent conditions. This study, however, derived spheres from the serum-free culture medium supplemeted with different additives and growth factors, such as putrescine, BSA and progesterone, and pre-treated the cell lines with the drugs prior to TS formation. This is different to the approaches used in our study, and may explain the differences in response.

While the SW480 and SW620 cell lines were equally sensitive to novobiocin and geldanamycin treatment under adherent conditions, the response of the genetically paired cell lines differed to C- and N-terminal inhibition by novobiocin and geldanamycin during TS formation. The response was dependent on whether the Hsp90 inhibition was initiated during TS formation or after. In both cases, TS formation was inhibited at concentrations below the EC_{50} value determined for the adherent cell lines, However, the SW620 TS consistently showed enhanced sensitivity to Hsp90 inhibition, whereby both geldanamycin and novobiocin inhibited TS formation. In contrast, the formation of SW480 TS was reduced but not prevented by geldanamycin treatment, and novobiocin increased TS formation. Previous studies using tumour-initiating cells from human colon cancer cell lines with KRAS mutation, the effect of PU-H71, a purine-based Hsp90 inhibitor, has demonstrated the ability to reduce sphere formation *in vitro* and restricted tumour growth *in vivo* (Azoitei *et al*., 2012).

The differential sensitivity of SW480 and SW620 TS to Hsp90 inhibition during or after formation may be as a result of different cohorts of prospective client proteins between the paired cell line TS. The identification of upregulated oncogenes, including TERT, MAF, ERBB3 and SAP2 in SW620 cells and not SW480 cells, has suggested that these oncogenes support

survival of the SW620 cell line (Melcher *et al.,* 2000). The TERT gene encodes a telomerase reverse transcriptase, which has been demonstrated to increase in expression during cancer progression (Kolquist *et al.,* 1998). While there are no data on MAF and SAP2, telomerase and ERBB3 are known Hsp90 client proteins. Geldanamycin induces degradation of newly synthesised ERBB3 (Gerbin and Landgraf, 2010) and active Hsp90 is required for the formation of active telomerase complexes (Holt *et al.,* 1999). Hsp90 was also shown to associate with the TERT promotor in human oral cancer cells (Kim *et al.,* 2008). In the context of other oncogenes, both ERBB3 and telomerase have been shown to support anchorage independent growth (Hamad *et al.,* 2002; Wei *et al.,* 2003; Yuan *et al.,* 2002; Wu *et al.,* 2009; Oda *et al.,* 2008). If the SW620 is dependent on these oncogenes for growth under anchorage independent conditions, then this cell line may be more sensitive to Hsp90 inhibition. In addition, a number of proteins involved in cytoskeletal dynamics are upregulated in the SW620 cell line compared to the SW480 cell line (Ghosh *et al.,* 2011). While the SW620 line is not dependent on these proteins for survival, these alterations may explain why the SW480 cell line has a greater sphere forming efficiency and could contribute to the enhanced sensitivity of the SW620 cell line to Hsp90 inhibition, given that Hsp90 chaperones a number of these cytoskeletal proteins. In order to confirm these proposals, it would be necessary to conduct knockdown studies of the respective proteins in the two cell lines and assess the effects on TS formation.

Novobiocin treatment alone led to an increase in TS formation, particularly in the SW480 cell line. These observations are unexpected and in contrast to other studies showing that novobiocin and other C-terminal Hsp90 inibitors were able to block anchorage independent growth of cancer cell lines (Wu *et al.,* 2013; Hieronymus *et al.,* 2006), although both of these studies used the soft agar assay not the TS assay to measure anchorage independent growth. Novobiocin is also known to inibit topoisomerase at concentrations above 100 µM (Osheroff *et al.,* 1983). However, inhibition of topoisomerase using the inhibitor quinacrine has been shown to inhibit anchorage independent growth, not enhance it (Preet *et al.,* 2012). This response may reflect some specific changes in the biology of the SW480 cell line, as this was not observed in the SW620 cell line.

Given that the TS appeared resistant to novobiocin, we next asked whether novobiocin would improve the sensitivity of TS to oxaliplatin by simultaneous treatment with novobiocin. In addition to their use as anti-cancer agents, Hsp90 inhibitiors are also some of the best agents for sensitising cancer cells to adjuvant therapy (Neckers, 2002; McNamara *et al.,* 2012) Treatment with both novobiocin and oxaliplatin, demonstrated improved targeting of putative CSC by increasing the sensitivity of SW480 and SW620 TS to the combination of novobiocin and oxaliplatin (Figure 3.8). Oxaliplatin works primarily by inducing DNA damage, similar to

the effect of radiation. We therefore hypothesise that the sensitisation of cancers by combination of Hsp90 inhibition and DNA-damaging agents, may be due to a similar to the mechanism by which Hsp90 inhibition, for example using 17-AAG induces its radiosensitisation effects (Sauvageot *et al.,* 2008). Alternatively, cisplatin is capable of binding to the C-terminus of Hsp90, close to the binding site of novobiocin (Soti *et al.,* 2002; Marcu *et al.,* 2000). Based on the structural similarity between oxaliplatin and cisplatin, it is tempting to speculate that that oxaliplatin, may also bind Hsp90, producing a synergistic effect that resulted in inhibition of TS growth *in vitro*. Simultaneous targeting with the N terminal Hsp90 inhibitor 17-DMAG and oxaliplatin reduced the invasive characteristics of the SW620 cell line in a mouse animal model (Moser *et al*., 2007). When co-administered with cisplatin, 17-DMAG sensitized the putative CSC to the DNA-damaging agent (Wright *et al*., 2008). Recently, a reduction in size of tumour growth from murine xenografts of HT-29 and HCT-116 was observed when Hsp90 was inhibited by ganetespib in combination with oxaliplatin (Nagaraju *et al.,* 2014).

Using the genetically paired cell lines we demonstrated that the cell lines respond similarly to geldanamycin or novobiocin treatment, under adherent conditions, but respond differently as TS. We observed resistance of preformed TS to 5-FU, oxaliplatin, geldanamycin and novobiocin treatments, but demonstrated TS sensitisation upon co-treatment with oxaliplatin and novobiocin. These studies, however, were limited to the investigation of mechanism of Hsp90 inhibition without distinguishing between targeted Hsp90 isoforms. The function of Hsp90α and Hsp90β differ in cells (Sreedhar *et al*., 2004). The inhibition of Hsp90 with compounds like geldanamycin upregulates the stress response which invariably increases the expression of HSP (Zou *et al*., 1998). Therefore, the development of isoform-specific approaches, such as RNA interference (RNAi) techniques to inhibit Hsp90 and modulate the stress response has begun to receive interest for potential therapeutic benefits and understanding cancer biology (Trepel *et al*., 2010; Azoitei *et al*., 2012).

Chapter 4: Analysis of the effect of Hsp90α knockdown on the Wnt pathway in the SW480 cell line.

Introduction

Downstream of Wnt/β-catenin signaling are genes that regulate cell growth and differentiation, the cell cycle and migration (Harris and Peifer, 2005). Mutations in genes encoding for Wnt pathway proteins APC or β-catenin are responsible for the sporadic development of the majority of colon cancers (Voloshanenko *et al.,* 2013). Wnt proteins are a family of 19 highly conserved secreted glycoproteins that are associated with signaling pathways important for cell proliferation and embryonic development (Cadigan and Nusse, 1997). The Wnt receptors are cell surface transmembrane proteins from the Frizzled family that contain low density lipoprotein receptor proteins (LRP5/6) (Polakis, 2000). The binding of Wnt proteins to the appropriate receptors may stimulate several signaling pathways including, the β-catenin independent non-canonical pathway and the canonical Wnt/β-catenin pathway.

The extracellular stimulation of intracellular signal transduction by Wnt proteins is responsible for the regulation of gene expression within the nucleus through either a canonical or non-canonical Wnt/β-catenin pathway. The canonical pathway governs cell fate determination, and non-canonical pathways, regulate cell movement control and tissue polarity (Katoh and Katoh, 2007). In normal cells, β-catenin is found in a complex with E-cadherin and α-catenin in cell junctions, and plays a role in cell adhesion. Active Wnt signaling results in the stabilisation and nuclear localisation of β-catenin for the activation of T cell factor/ Lymphoid enhancer factor (TCF/LEF) regulated genes involved in oncogenesis, such as c-myc and c-jun in cell proliferation, survivin in apoptosis inhibition and MMP7 in tumour metastasis (Crawford *et al.,* 1999; He *et al.,* 1998; Shtutmen *et al.,* 1999, Zhang *et al.,* 2001). In the absence of Wnt signaling, cytoplasmic β-catenin is targeted for degradation by the components of the "destruction complex", namely, axin, APC, glycogen synthase kinase-3β (GSK-3β), casein kinase 1 (CK1) and protein phosphatase 2A (PP2A) (Price, 2006). The phosphorylation of β-catenin, axin and APC by GSK3β and CK1 increases the affinity of the association between axin and APC with β-catenin and results in the subsequent ubiquitination of β-catenin (Huang and He, 2008; Kimelman and Xu, 2006; Peifer and Polakis, 2000) (see Figure 4.1). Polyubiquitinated β-catenin is processed by the 26S proteasome for degradation.

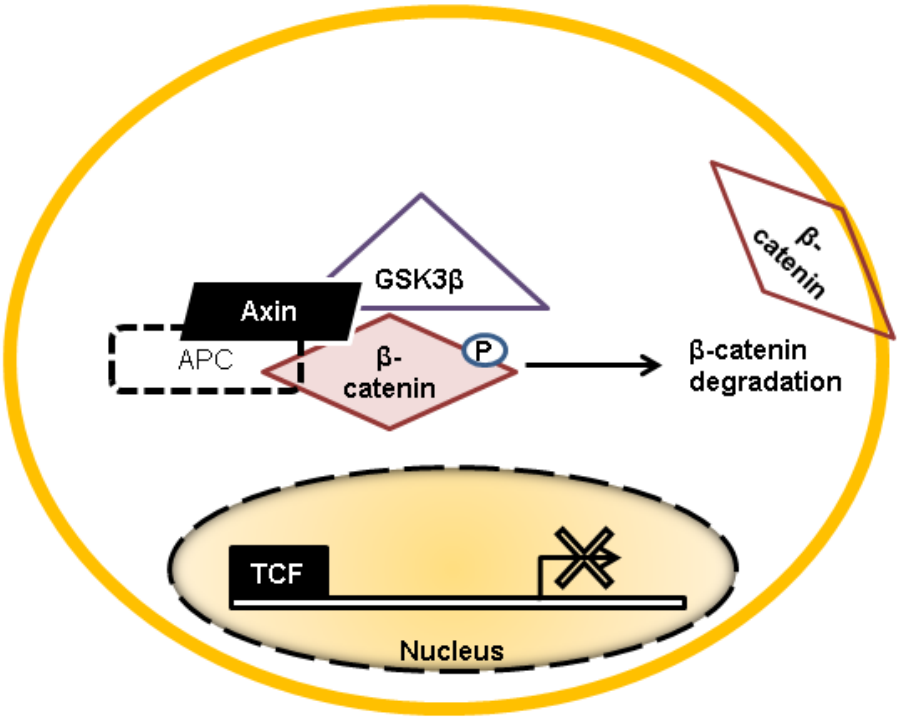

Figure 4.1. The degradation of β-catenin through the ubiquitin pathway in the absence of Wnt signaling.

Schematic diagram of the intracellular degradation of β-catenin by the destruction complex in the absence of Wnt signaling. Proteins of the destruction complex interact to phosphorylate and target β-catenin for destruction in the absence of Wnt signal stimulation. β-catenin is degraded before any activation of the TCF gene. The circular periphery illustrates the cell membrane. Proteins represented: Axin, APC, β-catenin and GSK3β.

Mutations found in the genes encoding for β-catenin, APC, axin or the overexpression of Wnt ligands are associated with the activation of the Wnt/β-catenin pathway within cancer (Brown, 2001, Jin *et al.,* 2003; Morin *et al.,* 1997; Polakis, 2007; Schlosshauer *et al.,* 2000). Mutations in colon cancers typically result in a "Wnt-less" activation of β-catenin signaling (Figure 4.2). Without stimulation from Wnt proteins, cancers demonstrate that β-catenin translocates to the nucleus. The β-catenin is not degraded due to the inactivation of the destruction complex, dependent on the type of colon cancer. In the nucleus, rather, β-catenin acts as an activator of TCF/LEF gene transcription, resulting in the expression of oncogenes (c-myc and c-jun), cell surface glycoprotein CD44 and E-cadherin (reviewed by Schneikert and Behrens, 2007; Zeilstra *et al.,* 2008).

The resultant nuclear localisation of β-catenin following Wnt pathway activation in cancer is associated with EMT through the loss of E-cadherin and increase of mesenchymal markers (Kirchner and Brabletz, 2000; Thiery, 2002). In addition, the loss of cellular adhesion along with increased cellular motility accentuates the importance of EMT during metastasis (Thiery, 2002). The expression of survivin, following the activation of transcription by β-catenin has been suggested to induce a stem-cell phenotype in colorectal cancers (Zhang *et al.,* 2001). Brabletz and colleagues drive a concept of migrating cancer stem cell in light of their influence on tumour progression, through their stem-like nature and their migratory phenotype as link to EMT (Brabletz *et al*., 2005). Cells which acquire a mesenchymal phenotype from the deregulation of Wnt/β-catenin signaling targets of EMT thereby links the relevance of studying oncogenic progression in carcinogenesis and the importance of targeting CSC as a strategic therapy for the prevention of metastases.

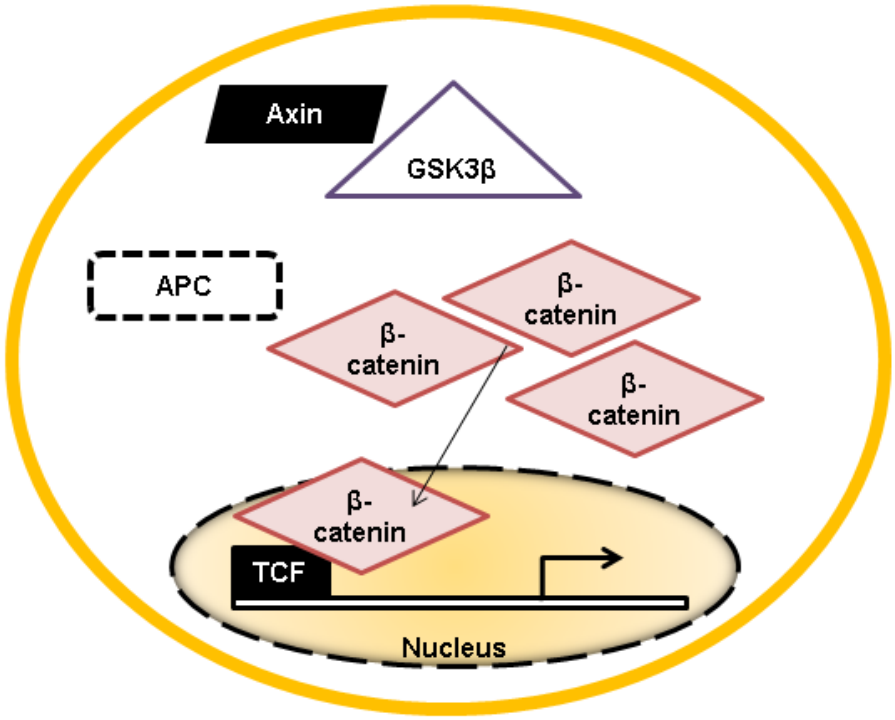

Figure 4.2. Activation of Wnt signaling in cancer.

Illustration of the intracellular relocalisation of β-catenin during a "Wnt-less" stimulation of TCF gene expression. Proteins of the destruction complex fail to interact and target β-catenin for destruction in the absence of Wnt signal stimulation. β-catenin moves into the nucleus where it interacts with and transcriptionally activates TCF gene expression. The circular periphery illustrates the cell membrane. Proteins represented: Axin, APC, β-catenin and GSK3β.

The chaperone functions of Hsp and their over expression in cancers supports the dependency of cancers on signaling proteins regulated by Hsp (Neckers, 2002; Ciocca and Calderwood, 2005). Client proteins of Hsp90 in particular, such as oncoproteins and signaling proteins, have been shown to contribute to the development of malignant transformation of cells (see Table 2, Chapter 1). In breast cancer, Hsp90 has been identified in complex with Wnt pathway proteins GSK3beta/axin1/phosphorylated β-catenin (Cooper *et al.,* 2011). Hsp27 has been shown to interact directly with β-catenin in breast cancer (Fanelli *et al.,* 2008). The co-chaperone DNAJB6, a heat shock protein 40 (Hsp40), has been shown linked to maintaining an epithelial phenotype, which when the long isoform of DNAJB6 is overexpressed is correlated to depleted β-catenin and reversal of metastatic phenotype (Mitra *et al.,* 2010). Deregulated Wnt/β-catenin signaling in cancer has shown to promote the development of tumours, influencing EMT and metastasis (Polarkis, 2012; Komiya and Habas, 2008).

Hsp90 is constitutively expressed by cells as the Hsp90β isoform, encoded by the HSP90AB1 gene (Sreedhar *et al*., 2004). The expression of the Hsp90α isoform, encoded by the HSP90AA1 gene, is thermal (heat) stress induced and estimated to represent approximately 2.8 % of protein in colon cancer cells (Wang *et al.,* 2008). Through interaction with MMP2, extracellular Hsp90α influences tumour invasiveness and angiogenesis (Eustace *et al*., 2004; Song *et al*., 2010). Inhibitors of Hsp90, such as geldanamycin, non-specifically target Hsp90 isoforms and promote the heat stress response by increasing the stability of the HSF1 trimer (Zou *et al*., 1998). As the Hsp90α and Hsp90β isoforms are not functionally redundant, the development of isoform-specific approaches to inhibit Hsp90 has received interest in the scientific community (Trepel *et al*., 2010). Gene silencing has demonstrated that Hsp90β knock out studies were lethal in mice after E9/9.5 of embryonic growth (Voss *et al.,* 2000). Hsp90α mutant mice are viable, although spermatogenesis is disrupted due to meiotic arrest. There is evidence to suggest, as a result of Hsp90α knock out, the dendritic cells of mice presented with defective antigen cross-presentation (Grad *et al.,* 2010; Imai *et al*., 2011).

Following our analysis of Hsp90 inhibition in the SW480 and SW620 cell lines, we sought to develop a more specific approach to study the effects of knockdown of Hsp90α on colon cancer biology, with an emphasis on the Wnt pathway. Using lentivirus for the delivery of short hairpin (sh)RNA specific for HSP90AA1 we sought to analyse the effects of Hsp90α knockdown effects on colon cancer and colon CSC biology. Through an assessment of sensitivity (toxicity), the distribution and localisation of β-catenin and morphology under modulation of the Wnt/β-catenin pathway, the effects of targeting the Wnt/β-catenin pathway were compared in cells under Hsp90α knockdown.

Materials and Methods

Materials

General reagents mentioned were purchased from Sigma-Aldrich (Germany) or Saarchem (Merck, South Africa). Specialised reagents, plasticware and kits purchased were reflected in the appropriate methodology.

Methods

SW480 cell lines were cultured under adherent conditions and anchorage-independently as tumourspheres (TS) as previously mentioned in Chapter 2. Transduced cell lines were maintained with supplementation of complete medium with 2 µg/ml puromycin following cell line selection, optimisation and expansion. To analyse protein expression, SDS-PAGE and Western blotting techniques were performed (see Chapter 2 methodology). Detailed specification of antibodies may be found in Table 3, Table 4 and Table 5.

HEK293FT cell line maintenance

The human embryonic kidney cell line (HEK293FT) was a kind gift from Prof. Sharon Prince (UCT, South Africa), maintained in in Dulbecco's Modified Eagle's Medium (DMEM; Gibco, Invitrogen UK) supplemented with 10 % (v/v) FBS, 100 U/ml PSA, 2 mM L-Glutamine, 0.1 mM non-essential amino acids (NEAA; Sigma-Aldrich, South Africa), 1 mM sodium pyruvate (Sigma-Aldrich) and 500 µg/mL geneticin (G418; Sigma-Aldrich, South Africa), at 37°C, with 5 % CO_2.

Restriction enzyme digestion

The packaging plasmids pMD2.G and psPAX2 were transformed into DH5α *Escherichia coli* cells and *E.coli* Stbl2 cells. All plasmids were purified with endotoxin removal (EndoFree Plasmid Maxi Kit; QIAGEN, cat no.: 12362). Restriction enzyme digestion was used to verify the pMD2.G, psPAX2 and pTRIPZ-HSP90AA1 (pTRIPZ-V3THS) vectors by agarose gel electrophoresis, and the pTRIPZ-HSP90AA1 and pTRIPZ-NTshRNA (control) vectors were submitted for sequence verification (Inqaba Biotechnical Industries). Each DNA restriction was performed according to manufacturer's instructions using commercially available restriction

endonucleases, reagents and buffers from Promega or New England BioLabs (Promega Corporation, USA and NEB Inc., Germany; respectively). Briefly, each restriction sample contained 55 µg plasmid DNA, 1x restriction buffer(s), 5 U restriction enzyme(s), BSA (if required; 10 µg/ml, cat no.: R396D) and distilled water to the volume of 16 µl. For dual enzyme digestion, restriction enzymes and buffers were added simultaneously for double digestion of plasmid DNA. pMD2.G was restricted using NEB2 buffer (B7002S), for *Hind*III (R0104S) and *Not*I (R0189S). psPAX2 was restricted with *Nhe*I (R0131S) and *Sac*II (R0157S) using NEB2. The pTRIPZ-HSP90AA1 (V3THS) vector was restricted with *Spe*I (R1033S) and *Xba*I (R0145S) using NEB4 (B7004S). Restriction samples were incubated at 37°C for 2 H and analysed by agarose gel electrophoresis (AGE).

Agarose gel electrophoresis

Samples were resuspended (1 part to 5 parts) in 6x loading dye (0.1 % (w/v) SDS, 60 mM Tris-HCl [pH 8.0], 60 mM EDTA, 0.125 % Orange G, 0.025 % xylene cyanol and 60 % glycerol; KAPA Biosystems, South Africa). For DNA analysis 0.8 % (w/v) agarose gels were generated using TAE buffer (40 mM Tris-acetate and 1 mM EDTA [pH 7.5]) and heated prior to the addition of 50 µg/ml ethidium bromide. Samples were electrophoresed alongside a 100 – 10000 bp ladder (KK6303; KAPA Biosystems, South Africa) at 100 V for approximately 1 H. Following electrophoresis, visible band fragments were documented and imaged under UV light.

Generation of lentiviral particles in HEK293FT packaging line

Lentiviruses are a subclass of retroviruses that are used for gene delivery in the generation of stable cell lines. The pMD2.G (Addgene plasmid 12259) plasmid encodes for virion structural capsid proteins, the psPAX2 plasmid encodes for gag, pol and rev functional genes (Addgene plasmid 12260), the pTRIPZ vector (Open Biosystems; Thermo-Scientific, USA) encodes the psi, SIN and LTR sequences required for gene transfer in a replication-deficient manner, and doxycycline-inducible plasmids encode for HSP90AA1 shRNA or non-targeting control shRNA; pTRIPZ-HSP90AA1 (V3THS_398910 cat no.: RHS4696) or pTRIPZ-NTshRNA (cat no.: RHS4743), respectively.

HEK293FT cells were seeded in medium without PSA and grown to ~ 80 % confluency in a 6-well plate at 37°C with 5 % CO_2. All components required for virion assembly were combined, including 500 ng shRNA from pTRIPZ-NTshRNA or pTRIPZ-HSP90AA1, 50 ng pMD2.G, 450 ng psPAX2 and 1.5 µl X-tremeGENE HP DNA Transfection Reagent (Roche Applied Science, Germany; Cat no.: 06 366 236 001), made up to 100 µl in OptiMEM and

incubated for 30 minutes at room temperature. This transfection mixture was then added to HEK293FT cells in a drop-wise manner, with gently swirling to ensure amalgamation. The medium was replaced after 18 H of incubation (37°C with 5 % CO_2) with complete medium for the suspension of virus particles following emergence from the transfected HEK293FT cells. Under sterile conditions, the medium from the transfected HEK293FT cells (spent medium) was collected after 24 H by aspiration for the harvesting and collection of lentivirus particles (virions). The harvested medium was passed through a sterile 0.45 µm filter and stored at -80°C until required.

Lentiviral transduction of SW480 cells and selection of knockdown cells

SW480 cells were seeded and grown to ~ 50 % confluency in complete medium. The collected virus particles were equilibrated to room temperature and incubated with 8 µg/ml polybrene (Sigma-Aldrich, Germany) for 5 minutes. The cells were washed with PBS, and replaced with the virus-polybrene mixture for incubation overnight. After washing the transduced cells with PBS, the medium was supplemented with 2 µg/ml puromycin and turboRFP (tRFP) expression induced with 1 µg/ml doxycycline during the development of transduced cell lines, as recommended by the manufacturer's instructions. As the tRFP cells began to multiply, colonies begun to form and grow. Successful pTRIPZ-HSP90AA1 or pTRIPZ-NTshRNA transduced SW480 cells (SW480-HSP90AA1 and SW480-NTshRNA) were selected for by resistance to puromycin and visualised following the expression of the tRFP reporter gene as a result of doxycycline after 3 days by fluorescent microscopy. Regular replacement of culture medium supplemented with puromycin, and cell lifting was conducted for the expansion of transduced cell lines over several weeks.

WST-1 assay for cell cytotoxicity to puromycin

Cells were seeded at 3 x 10^4 cells/ml in 96-well plates at 37°C overnight, prior to treatment with 0 – 5 µg/ml puromycin for 72 H. Untreated cells were used as negative controls. After the addition of 10 µl/well WST-1 proliferation reagent and incubation for 3 H, the absorbance at 440 nm was analysed on the PowereWave spectrophotometer (Bio-Tek Instruments, USA). The concentration at which puromycin effectively reduced cell viability by 50 % (EC_{50}) was calculated in GraphPad Prism software using non-linear regression to determine puromycin cytotoxicity. Results represented the mean ± SD of triplicate assessments.

Generation of polyclonal cell lines by cell sorting

Cells induced with doxycycline (1 µg/ml; 48 H) were washed in PBS and harvested using accutase (Sigma-Aldrich, Germany). The harvested cells were pelleted (500 *x g*, 5 minutes) washed in PBS prior to analysis. Cells were sorted using the FACSAria II (BD Biosciences, Belgium). The blue (488 nm) laser was used to excite the PI fluorochrome and emissions were recorded in the 585/42 filter channel. Using the FACSDiva software, a gate was used to detect the threshold for different levels of fluorescent intensities detected, and used to eliminate cell debris, to facilitate the sorting of high, medium and low turboRFP (tRFP) expressing cells into growth medium for expansion.

Development of monoclonal cell lines

After the successful expansion of polyclonal transduced cell lines over several weeks, SW480-HSP90AA1 and SW480-NTshRNA polyclonal cell lines were subjected to cloning by multiple rounds of colony isolation and serial dilution of cells for the development of stable monoclonal cell lines. Transduced cells were maintained in complete medium supplemented with 2 µg/ml puromycin, for selection. Two monoclonal SW480-HSP90AA1 cell lines, numbered #5 and #7, and two monoclonal SW480-NTshRNA cell lines, numbered #6 and #8 were developed over several months under selective conditions.

Kinetic analysis of effect of doxycycline on Hsp90α knockdown and tRFP expression

The SW480 shRNA-transduced cells were analysed in response to 1 µg/ml doxycycline induction over 96 H. Transduced cells were seeded (3 x 10^3 cells/well) in 96-well plates at 37°C overnight in fresh medium supplemented with 2 µg/ml puromycin and 1 µg/ml doxycycline for 24, 48, 72 and 96 H. Cells were analysed for the expression of tRFP by fluorescent microscopy, flow cytometry, SDS-PAGE and Western blotting. Analysing the effects of knockdown over time and the ability of cells to recover after the removal of doxycycline over 72 H was performed using Western blotting.

Analysis tRFP expression by induction of Hsp90α knockdown using a dosage rage of doxycycline

The expression of tRFP and Hsp90α in SW480 shRNA-transduced cells were analysed in response to increasing concentrations of doxycycline. Transduced cells were seeded (3 x 10^3 cells/well) in 96-well plates at 37°C overnight in fresh medium supplemented with 2 µg/ml puromycin and a range of increasing doxycycline concentrations (0 – 5 µg/ml) for 72 H. Cells

treated with a range of doxycycline concentrations were analysed for the expression of tRFP by fluorescent microscopy and for the knockdown of Hsp90α by SDS-PAGE and Western blotting.

Cell adhesion on tissue culture plastic under Hsp90α knockdown

This protocol was adapted from literature (Wong *et al*., 2007). Cells were washed in PBS and lifted using 1 % (w/v) trypsin solution made up in 0.3 % (w/v) EDTA. Cells were pelleted by centrifugation (1000 *x g*, 2 minutes), stained with trypan blue for the exclusion of dead cells and counted using a haemocytometer. The cells were seeded in a 96-well plate at 2 x 10^4 cells/well in fresh medium and allowed to adhere for 8 H at 37°C. After three washes in PBS, cells were fixed in paraformaldehyde (4 % (w/v) paraformaldehyde in PBS) for 15 minutes with shaking at room temperature. Once the fixative was discarded and the cells washed in distilled water, they were stained in crystal violet (10 % (w/v) crystal violet in 5 % (v/v) ethanol) for 30 minutes and washed three more times in distilled water. Following the aspiration of remaining liquid and brief air-drying of the wells, either images were captured by phase contrast microscopy or the crystal violet retained by the cells was solubilised (0.1 % (w/v) sodium dodecyl sulphate (SDS), 1 % (v/v) Triton X-100) overnight and the absorbance read at 590 nm using a PowerWave spectrophotometer (Bio-Tek Instruments, USA).

Cell adherence on collagen surface under Hsp90α knockdown

Cells were grown at 37°C for 72 H in medium supplemented with 1 µg/ml doxycycline before being washed in PBS and lifted with trypsin (1 % (w/v) trypsin, 0.3 % (w/v) EDTA). Cells were pelleted by centrifugation (1500 *x g*, 2 minutes), stained with trypan blue for the exclusion of dead cells and counted using a haemocytometer. Cells were seeded in a 96-well collagen-coated plate at 1 x 10^4 cells/well in fresh medium and allowed to adhere for 8 H at 37°C. After three washes in PBS, cells were fixed in 4 % (w/v) paraformaldehyde for 15 minutes with shaking at room temperature. Once the cells were washed in distilled water, and stained with crystal violet (10 % (w/v) crystal violet, 5 % (v/v) ethanol) for 30 minutes, they were washed three more times in distilled water before pictures were taken by phase contrast microscopy. After aspirating the remaining liquid and briefly air-drying the wells, the remaining crystal violet was solubilised (0.1 % (w/v) sodium dodecyl sulphate (SDS), 1 % (v/v) Triton X-100) overnight and the absorbance read at 590 nm using a PowerWave spectrophotometer (Bio-Tek Instruments, USA).

Immunoprecipitation assay

Cells were grown to ~ 80 % confluency in T150 culture flasks. The culture medium was replaced with PBS which was discarded for RIPA buffer (50 mM Tris-HCl [pH 7.5], 150 mM NaCl, 0.5 % (v/v) NP-40, 1 mM phenylmethylsulfonyl fluoride, 1 mM EDTA, 1 mM sodium deoxycholate, 1 mM Na_3VO_4, protease inhibitor cocktail) and incubated for 90 minutes at 4°C with shaking. The cell monolayer was disrupted by scraping, and the lysate collected. MagReSyn Protein A beads (25 µl) were washed thrice in TBS-Tween (TBS-T; 50 mM Tris [pH 7.5], 150 mM NaCl, 0.05 % (v/v) Tween-20) prior to 30 minutes of interaction with 1 µg Hsp90α/β antibody or species matched IgG as a control. Beads were again washed three times in TBS-T. Following the removal of debris by centrifugation (800 *x g*, 5 minutes), cleared RIPA lysates were incubated with the antibody-bound beads for 16 H at 4°C. Later, after three more TBS-T washes, the antibody-bound fraction was eluted from the beads under denaturing conditions (in SDS lysis buffer and by incubation for 95°C for 10 minutes). Elutions from lysates interacting either with antibody-bound beads (immunopecipitate) or control beads (non-specific binding) were analysed along with a sample of the cell lysate input by SDS-PAGE and Western blotting for possible *in vitro* interactions.

MTT assay for cell proliferation and cytotoxicity

An MTT (3-[4,5-dimethylthiazol-2-yl]-2,5-diphenyltetrazolium bromide) cell proliferation assay kit was purchased from Roche Applied Sciences (Germany; cat no.: 11 465 007 001). The MTT assay was utilised for determining the effective concentration of quercitin, IQ-1 and SB-216763 for SW480-HSP90AA1 and SW480-NTshRNA transduced cell lines. Cells were seeded at 1 x 10^4 cells/well in 96-well plates at 37°C overnight. Cells were treated with range of concentrations of quercetin, SB-216763 or IQ-1 for 48 H. Untreated or DMSO treated cells were used as negative controls. After the addition of 0.5 mg/ml (10 µl) MTT reagent and incubation for 4 H, formazan crystals were solubilised by the addition of 100 µl solubilisation solution (10 % w/v SDS, 0.01 M HCl). After 16 H of solubilisation, the absorbance at 550 nm was analysed using a PowerWave spectrophotometer (Bio-Tek Instruments, USA). The percentage cell viability (a measurement of cell proliferation indicated by the association of cellular metabolic activity) was established by dividing the absorbance of the sample by that of the untreated control, multiplied by 100. The concentration at which a chemotherapeutic agent effectively reduced or altered cell viability by 50 % (EC_{50}) for each cell line was analysed using non-linear regression using GraphPad Prism.

Results

We initially attempted induce the depletion of Hsp90α and Hsp90β using transient transfection of isoform-specific short interfering (si)RNA. However, these attempts were largely unsuccessful (Supplementary Figure S3A), which we predicted were due to the sensitivity of the SW480 and SW620 cell lines to transfection reagents and poor transfection efficiency (Supplementary Figure S3B). We therefore chose to develop Hsp90 knockdown cell lines, using an inducible shRNA which could be delivered by lentiviral particles to overcome the low transfection efficiency. Since there is evidence suggesting that directly targeting the HSP90AB1 gene (encoding the constitutive Hsp90β isoform) may be results in substantiallydecreased cell viability due to its essential nature (Voss *et al.,* 2000), we elected to use shRNA directed towards the HSP90AA1 gene, which encodes for the Hsp90α protein. The inducible nature of the Hsp90α isoform and its association with migration and invasion further motivated our choise of shRNA (Eustace *et al.,* 2004; Chen *et al.,* 2010). Inducible knockdown of Hsp90α protein was elected for study within the SW480 cell line. We selected the SW480 cell line over the SW620 cell line as it is representative of a pre-metastatic colon cancer. Furthermore, we demonstrated that SW480 cells had a greater migration potential and demonstrated greater sphere formation under anchorage-independent conditions over SW620 cells, features which are considered important in tumour progression.

We developed an shRNA system for the inducible knockdown of Hsp90α using the TRIPZ plasmid encoding shRNA directed towards transcripts from the HSP90AA1 gene in comparison to a non-targeting shRNA (NTshRNA) control, packaged by a lentivirus delivery system. Lentiviruses are capable of transducing both dividing and non-dividing mammalian cells, and contain a self-inactivating sequence to reduce the risk of transcriptional activity from the 3'-long terminal repeat (LTR) sequence. Replication-deficient lentiviruses have since been utilised in the development of stable packaging cell lines, used to minimise potential influence of genetic variations, however their generation is time-consuming (Xu *et al.,* 2001). In the TRIPZ plasmid, the expression of the shRNA is under the control of a promoter containing a tetracycline response element. This makes the expression of the shRNA, as well as a fluorescent marker, turboRFP (tRFP), inducible in the presence of the doxycycline inducer. The pTRIPZ plasmid constructs encoding for non-targeting shRNA (henceforth referred to as NT) and the HSP90AA1 specific shRNA were utilised as the control and test constructs respectively.

Verification of plasmid vectors for generation of lentivirus particles

Prior to the generation of virus particles, the plasmid vectors encoding the DNA required for the assembly of the virions were isolated and contaminating endotoxin removed. The plasmids psPAX2, pMD2.G and either pTRIPZ-V3THS_398910 (encoding HSP90AA1 specific shRNA) or the control pTRIPZ plasmid (encoding a non-targeting shRNA sequence) were utilised for the generation of the lentivirus particles. The plasmids were analysed by restriction endonuclease digestion (Figure 4.3). The psPAX2 vector, encoding *gag, pol* and *rev* genes, was restricted with *Nhe*I and *Sac*II. From the plasmid map and the predicted restriction sites of the *Nhe*I and *Sac*II enzymes, it was anticipated that linearisation by an enzyme cutting once would produce the predicted size of the full vector (10703 bp), and together predicting dual cutting fragment sizes of 4015 and 6688 bp. Individually, the restriction enzymes produced bands greater than 10000 bp and together produced fragments of approximately 6500 bp and 4000 bp, thereby verifying the psPAX2 plasmid by size (Figure 4.3A). The pMD2.G vector, encoding the capsid proteins, was restricted with *Hind*III and *Not*I. Linearisation was predicted to produce the full plasmid size of 5824 bp and dual restriction was predicted to produce two bands (2778 and 2036 bp). Linearisation was successful, resulting in a band of approximately 6000bp, and dual restriction produced two small bands of approximately 3100 and 2900 bp, verifying the size of the pMD2.G plasmid (Figure 4.3B). The pTRIPZ-HSP90AA1 vector was restricted with *Spe*I and *Xba*I. Individually, it was predicted each enzyme would produce one fragment the size of the vector, 13320 bp, and together they would produce two fragments, of 10796 and 2524 bp. The plasmid linearisation produced one band, much greater than the 10000 bp marker, and the dual restriction produced two bands, one slightly higher than 10000 bp and the other of around 2800 bp (Figure 4.3C). Furthermore, the pTRIPZ-V3THS_398910 (pTRIPZ-HSP90AA1) plasmid was sequenced to verify the specificity of the encoded shRNA sequence (5'-TAATATGCAGCTCTTTCCC-3') by alignment (data not shown). The control pTRIPZ plasmid was similarly validated by another member of the laboratory (data not shown).

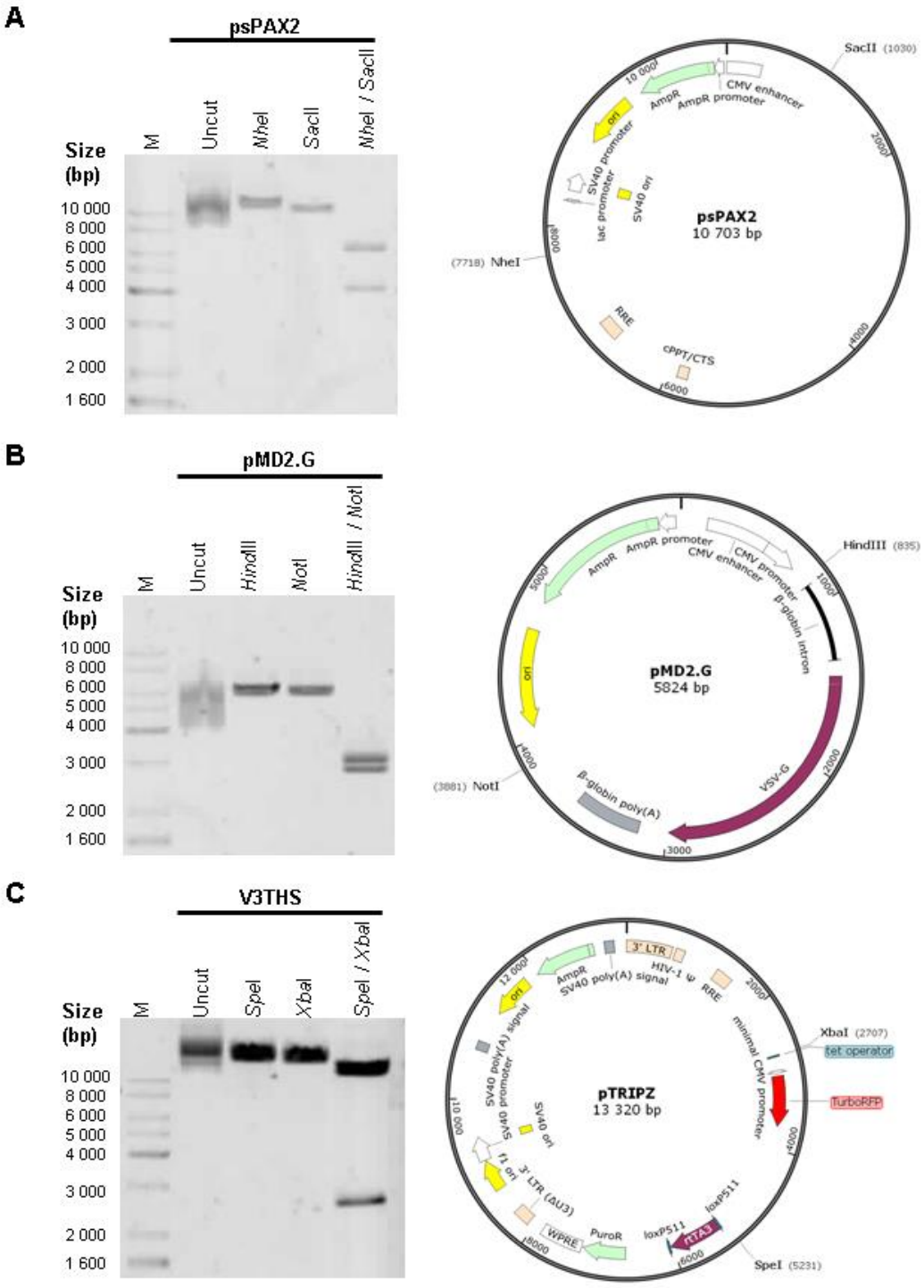

Figure 4.3. Restriction digestion and verification of lentivirus packaging system plasmids.

Plasmid verification by restriction digestion and agarose gel electrophoresis [0.8 % (w/v) AGE in TAE]. A. psPAX2 plasmid restriction digestion and corresponding plasmid map. psPAX2 was restricted with either *Nhe*I, *Sac*II or both *Nhe*I and *Sac*II enzymes. B. pMD2.G plasmid restriction digestion and corresponding plasmid map. pMD2.G was restricted with *Hin*dIII, *Not*I or both *Hin*dIII and *Not*I. C. V3THS (HSP90AA1) plasmid restriction digestion and the pTRIPZ plasmid map, from which the V3THS plasmid was derived. V3THS plasmid was restricted with *Spe*I, *Xba*I or *Spe*I and *Xba*I. Plasmid fragments were stained by 50 µg/ml ethidium bromide and sized using Kapa Universal DNA ladder. Plasmid maps were generated using SnapGene Viewer v 2.5.

Generation of cell lines stably transfected with control and Hsp90α specific shRNA

Plasmids containing coding sequences for structural capsid proteins, functional genes, sequences required for gene transfer and either NT or HSP90AA1 shRNA (pMD2.G, psPAX2, pTRIPZ-NTshRNA or pTRIPZ-HSP90AA1, respectively), were used to transfect early-passage HEK293FT cells. After allowing for sufficient time for protein expression and virion assembly, the spent medium from transfected HEK293FT cells was harvested for the collection of assembled lentivirus particles containing NT and HSP90AA1 shRNA. Collected virus particles were used for the transduction SW480 cells (SW480-NTshRNA and SW480-HSP90AA1) for the development of polyclonal transduced cell lines.

Prior to selection, we investigated the sensitivity of SW480 cells to increasing concentrations of puromycin, to determine the effects of puromycin on cell viability. SW480 cells revealed a dose-dependent decrease in viability with increasing puromycin concentrations, with an EC_{50} of 1.8 µg/ml puromycin (Figure 4.4A). Thereafter, transduced SW480 cells were selected for using 2 µg/ml puromycin. SW480 cells transduced with either the NTshRNA or the Hsp90 specific shRNA were treated for the selection of stable transformants using puromycin. Once colonies of the SW480-NTshRNA and SW480-HSP90AA1 cell lines had begun to emerge, the expression of the tRFP reporter gene, and indirectly the shRNA, was analysed by treatment of cells with 1 µg/ml doxycycline (Figure 4.4B). Many of the emerging colonies were shown to be positive for tRFP (RFP) expression by fluorescent microscopy and confirmed the selection of stably transformed cells in colonies. Interestingly, not all puromycin resistant cells were positive for tRFP, which perhaps suggests silencing of the integrated plasmid DNA due to the position of insertion into the genome. The puromycin resistant colonies were allowed to grow and merge, to establish the polyclonal SW480-NTshRNA and SW480-HSP90AA1 lines, prior to optimisation of the knockdown conditions using doxycycline.

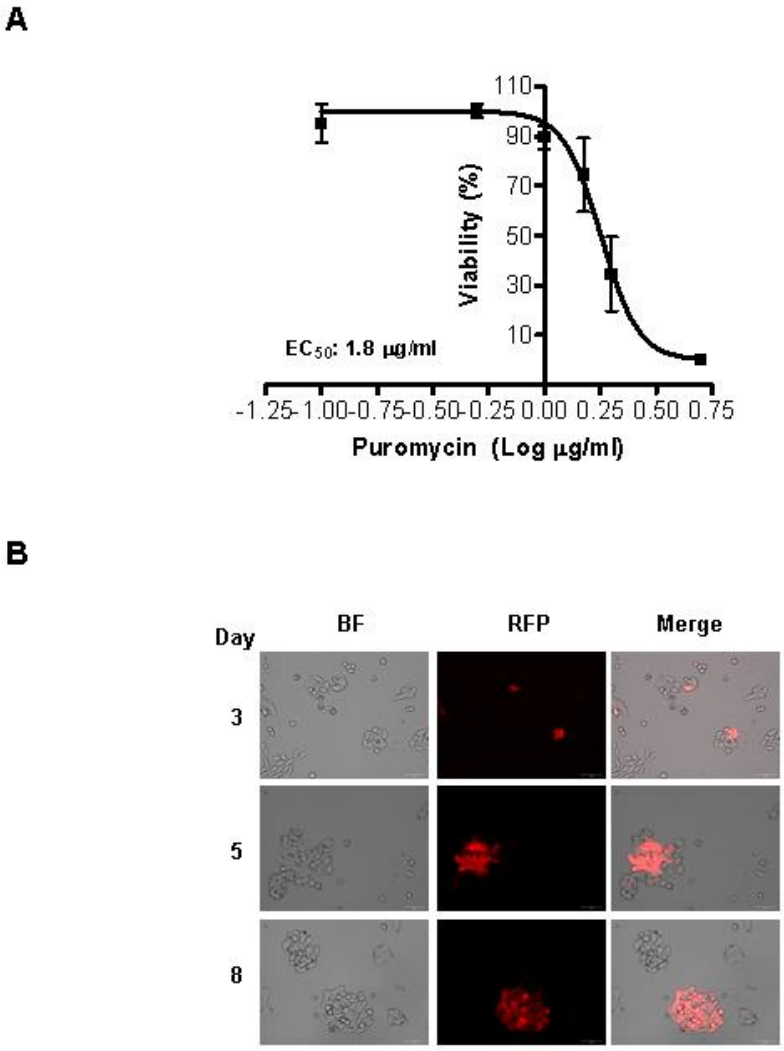

Figure 4.4. Transduction and selection of puromycin resistant SW480 cells

Selection of transduced cells and cell line expansion using puromycin. A. Puromycin kill curve for SW480 cells (0 – 5 µg/ml) analysed by WST-1 assay after 72 H treatment. Each assay represents the mean ± SD of triplicate replicates. The concentration of puromycin to effectively reduce cell viability by 50 % (EC_{50}) was calculated. Percentage viability was determined using negative controls as a reference of 100 % cell viability. B. Example of the procedure used to monitor development of stable cell lines. SW480 cells were transduced with shRNA-containing lentivirus. Day 3 post transduction and addition of 1 µg/ml doxycycline saw the expression of tRFP, Day 5 – 8 illustrate colony expansion *in vitro*. Immunofluorescent microscopy images of cells under brightfield (BF), red fluorescence (RFP) and merged images were taken using Zeiss AxioVert.A1 Fluorescence LED Inverted Microscope with a High Resolution AxioCam MRm Rev 3 (200 x magnification). Data were analysed using ZEN Lite 2012 and GraphPad Prism software.

Following the cell line expansion, stably transduced polyclonal SW480-NTshRNA and SW480-HSP90AA1 cell lines were treated with a range of doxycycline concentrations (0 – 5 µg/ml) and analysed by fluorescent microscopy for the detection of tRFP signal (Figure 4.5A). The tRFP signal substantiated the success of the lentivirus transduction of SW480-NTshRNA and SW480-HSP90AA1 cell lines and confirmed expression of shRNA because the tRFP and shRNA are under the control of the same promoter in the TRIPZ plasmid. There was a dose dependent increase in the tRFP signal intensity in SW480-HSP90AA1 cells and SW480-NTshRNA cells with increasing concentrations of doxycycline. A concentration of 1 µg/ml doxycycline was selected for further treatment.

To investigate the optimum time for the induction of knockdown by 1 µg/ml doxycycline, SW480-NTshRNA and SW480-HSP90AA1 cell lines were analysed over 96 H for Hsp90α by Western blotting (Figure 4.5B). The level of Hsp90α did not fluctuate within SW480-NTshRNA cells. SW480-HSP90AA1 cells exhibited a minor yet time-dependent decrease in Hsp90α compared to the control cell line, with the greatest reductions observed between 72 and 96 H after induction of knockdown. These finding suggested that induction of Hsp90α knockdown in the SW480 transduced cell lines was optimised for at least 72 H of 1 µg/ml doxycycline treatment.

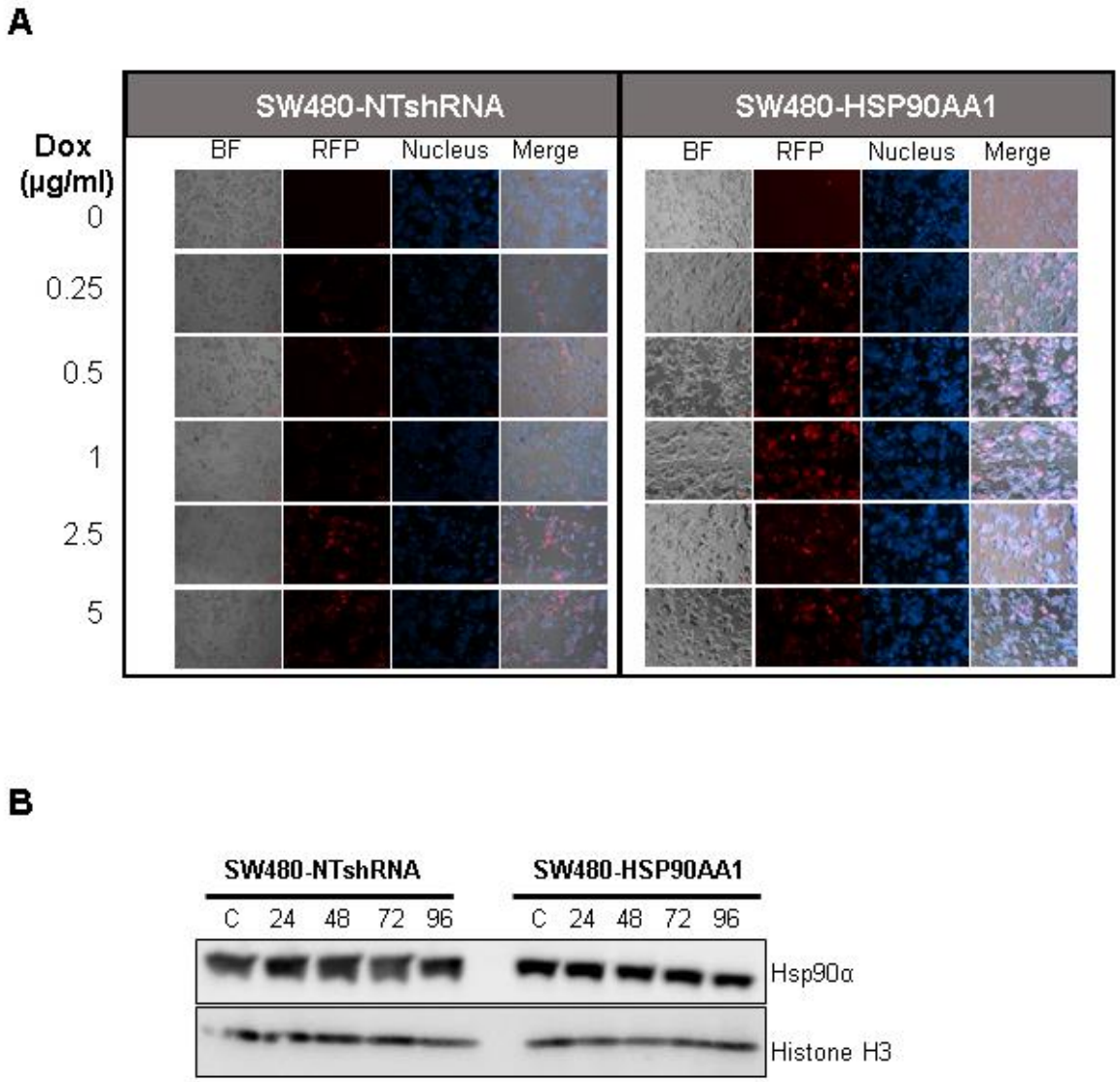

Figure 4.5. Development and optimisation of conditions for Hsp90α knockdown in the polyclonal cell lines.

Polyclonal SW480-NTshRNA and SW480-HSP90AA1 cell lines treated with doxycycline. A. Immunofluorescent microscopy analysis of tRFP expression in response to doxycycline (Dox, 0 – 5 µg/ml) induction. Magnification: 100 x. B. Kinetic analysis (24, 48, 72, 96 H) of levels of Hsp90 α effect of Dox (1 µg/ml) induction against uninduced control ("C") cells by western blot with densitometry. Histone H3 was used as the loading control. Chemiluminescent detection of proteins using antibody-antigen detection using the Chemidoc EQ system (Biorad, UK). Data were analysed using ImageJ software.

Isolation of polyclonal SW480-transduced cell lines based on tRFP expression

To define the level of expression of the control and Hsp90α specific shRNAs by transduced SW480 cells, a flow cytometric approach was taken to analyse the tRFP (RFP) expression in response to doxycycline treatment. Different populations were identified on the basis of the level of tRFP expression (Figure 4.6). Figure 4.6A depicts the histograms showing the different populations identifiable based on the detected tRFP signal in SW480-NTshRNA and SW480-HSP90AA1 cells. Two populations of SW480-NTshRNA cells were identified (labelled uninduced and induced, based of tRFP signal) and three distinct populations of SW480-HSP90AA1 cells were detected (RFP-L, RFP-M and RFP-H, based on the low, medium or high tRFP signal, respectively). Cells from these distinct populations were sorted, based on their RFP signal, by FACS. An analysis of these distinct populations of cells sorted from the SW480-NTshRNA and SW480-HSP90AA1 cell lines was conducted to define the relationship between tRFP signal intensity and level of Hsp90α knockdown achievable using 1 µg/ml doxycycline. The SW480-NTshRNA cell lines were the control to which the sorted populations of SW480-HSP90AA1 cells (RFP-L, RFP-M and RFP-H) were compared.

The level of Hsp90α protein detected in RFP-L, RFP-M and RFP-H SW480-HSP90AA1 cells was analysed by Western blotting. The level of Hsp90α correlated with the level of tRFP, with RFP-L cells representing SW480-HSP90AA1 cells with more Hsp90α, RFP-M cells showing less Hsp90α than RFP-L cells and RFP-H cells showing the lowest amount of Hsp90α, relative to the whole cell population lysates of the original SW480-HSP90AA1 cells and SW480-NTshRNA cells (Figure 4.6B). These findings illustrated that the SW480-HSP90AA1 RFP-H cells were able to achieve approximately 50 % of Hsp90α protein knockdown, relative to the SW480-NTshRNA control cell line with 1 µg/ml doxycycline.

A

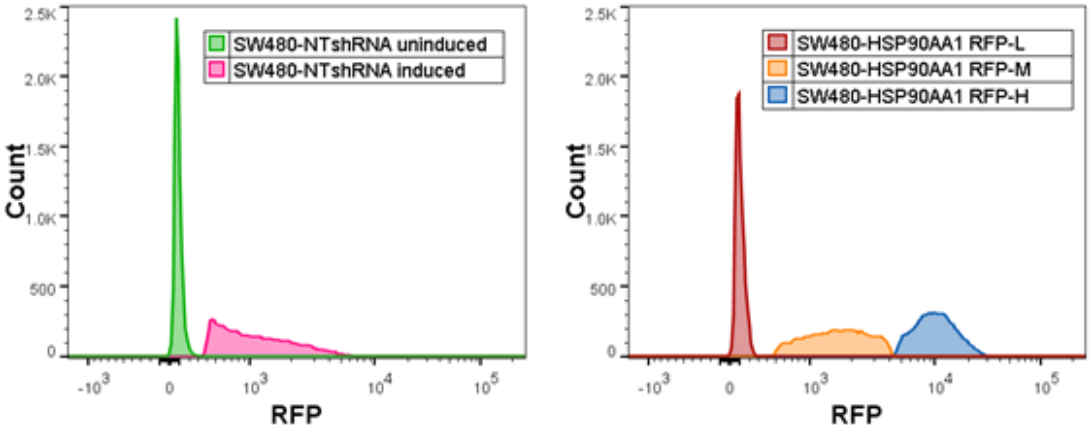

B

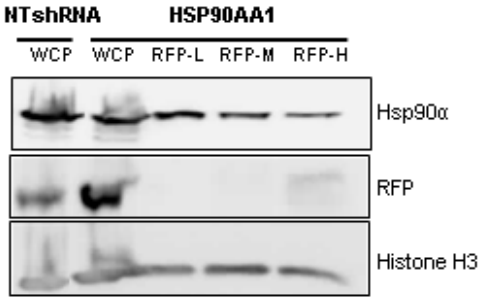

Figure 4.6. Isolation of different polyclonal SW480-transduced cell lines based on tRFP expression Identification of SW480-NTshRNA and SW480-HSP90AA1 cells by differential RFP expression.

A. Histogram of SW480-NTshRNA and SW480-HSP90AA1 cells with 1 µg/ml Dox analysed by flow cytometry for identification of RFP expressing populations. NTshRNA cells were sorted based on induction of tRFP (RFP) expression. HSP90AA1 cells were sorted based on RFP fluorescence intensity into low (L), medium (M) and high (H) expressing populations using FACS Aria II. B. Western blotting of 50 µg of protein lysed from sorted SW480-NTshRNA and SW480-HSP90AA1 polyclonal cell lines and whole cell populations (WCP). Membrane was probed for anti- Hsp90α, tRFP (RFP) and loading control (histone H3). Chemiluminescent detection of proteins using antibody-antigen detection using the Chemidoc EQ system (Biorad, UK). Data were analysed using ImageJ software.

Generation of monoclonal SW480-transduced cell lines

We next sought to derive monoclonal cell lines for SW480-HSP90AA1 and SW480-NTshRNA cell lines from the polyclonal lines. The selection of monoclonal stable cell lines involved the use of cloning and limited dilution techniques prior to the expansion of the cell line from one single clone. This strategy was utilised to minimise any potential differences in Hsp90α expression and provided us with more than one cell line representative for analysis of the effects of Hsp90α targeting. Two monoclonal SW480-HSP90AA1 cell lines (numbered: #5 and #7) and two SW480-NTshRNA cell lines (numbered: #6 and #8) were expanded and later compared to the previously described polyclonal RFP-H expressing SW480-HSP90AA1 and SW480-NTshRNA cell lines.

The conditions for the induction of knockdown were analysed across the monoclonal cell lines. Firstly, the SW480-NTshRNA #6 and #8 and SW480-HSP90AA1 # 5 and #7 monoclonal cell lines were analysed for expression of tRFP (RFP) signal by flow cytometry after treatment with increasing amounts of doxycycline. The effect of treatment with doxycycline on transduced cells was dose-dependent, and substantiated the use of 1 µg/ml doxycycline (as suggested by the manufacturer). Analysis of the monoclonal cell lines treated with 1 µg/ml doxycycline over 96 H revealed that 72 H was sufficient to detect expression of tRFP in both the control and Hsp90α knockdown cell lines by flow cytometry (data not shown). These findings confirmed that the usage of 1 µ/ml doxycycline for 72 H was optimal for the induction of knockdown in the SW480-NTshRNA #6 and #8 and SW480-HSP90AA1 # 5 and #7 monoclonal cell lines.

To show the reduction of Hsp90α expression in cells under the induction of knockdown, the monoclonal cell lines were analysed with and without 48 H of doxycycline treatment. The SW480-HSP90AA1 #5, SW480-HSP90AA1 #7, SW480-NTshRNA #6 and SW480-NTshRNA #8 monoclonal cell lines were investigated for changes in the two cytosolic Hsp90 isoforms under induction of knockdown. Western blot analysis showed no change in the levels of Hsp90α in either SW480-NTshRNA #6 and #8 monoclonal cell lines between the untreated and doxycycline treated cells. The levels of Hsp90α were reduced in doxycycline treated SW480-HSP90AA1 #5 and #7 cell lines, relative to both the untreated SW480-HSP90AA1 #5 and #7 cell lines and the doxycycline treated NTshRNA cell lines (Figure 4.7). These studies confirmed that the reduction in Hsp90α levels was sufficient, in that it was not completely depleted. This level of Hsp90α reduction was deemed sufficient for further functional analysis in an effort to avoid substantial reductions in cell viability. Although Hsp90α was reduced in SW480-HSP90AA1 #5 and #7 cell lines, the levels of Hsp90β did not vary upon induction with doxycycline, suggesting the shRNA HSP90AA1 targeting sequence for Hsp90α did not affect the expression of Hsp90β.

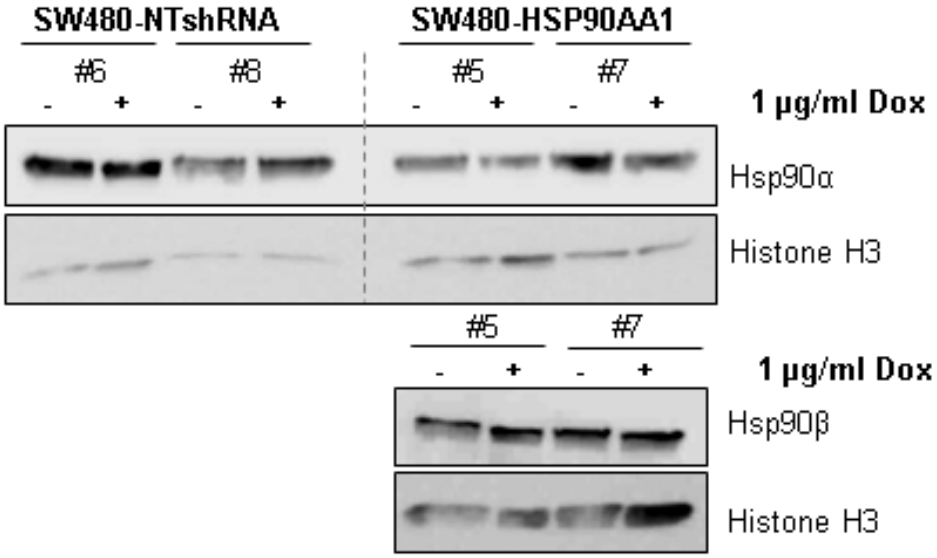

Figure 4.7. Development of monoclonal SW480-HSP90AA1 and SW480-NTshRNA cell lines.

Western blot analysis of Hsp90 levels in the monoclonal cell lines after treatment with 1µg/ml doxycycline (Dox). SW480-NTshRNA #6 and #8 and SW480-HSP90AA1 # 5 and #7 monoclonal cells were treated with Dox for 48 H prior to lysis. Western blotting (50 µg of total protein loaded per lane) using anti- Hsp90α, Hsp90β and loading control (histone H3). Chemiluminescent detection of proteins using antibody-antigen detection using the Chemidoc EQ system (Biorad, UK).

Characterising the stress response in response to Hsp90α knockdown

To determine the effect of stress on colon cancer cells with reduced Hsp90α, the SW480-HSP90AA1 #5, SW480-HSP90AA1 #7, SW480-NTshRNA #6 and SW480-NTshRNA #8 monoclonal cell lines were treated with doxycycline for 72 H prior to being subjected to heat and hypoxic stress (Figure 4.8) and estimation of cell viability by WST-1 assay. The cells were also treated with or without a heat shock of 42°C and then allowed to recover at 37°C for 16 H before cell viability was determined (Figure 4.8A). SW480-NTshRNA cell lines showed a higher absorbance compared to the SW480-HSP90AA1 #5 or #7 cell lines, for both the heat shocked and non-heated shocked treatments. This suggested a lower cell viability in the Hsp90α depleted cells compared to the control cells even in the absence of the heat stress. These data demonstrated a correlation between the level of Hsp90α and viability, with reduced Hsp90α leading to susceptibility reduction in cell survival independently of heat shock.

To investigate the effect of hypoxic conditions, the SW480-NTshRNA #6 and #8 and SW480-HSP90AA1 #5 and #7 monoclonal cell lines were treated with doxycycline (1 µg/ml, 72 H) followed by treatment with $CoCl_2$ (500 µM, 24 H) prior to analysis by WST-1 assay. The results indicated that $CoCl_2$ consistently reduced the absorbance across all of the SW480-NTshRNA and SW480-HSP90AA1 monoclonal cell lines (Figure 4.8B). The hypoxic conditions resulted in a decrease the absorbance of the SW480-HSP90AA1 #5 and #7 cell lines to approximately half of the untreated cells. These same conditions produced statistically significant differences in both SW480-NTshRNA #6 and SW480-NTshRNA #8 cell lines, reducing the absorbance by more than half of the untreated cells, respectively.

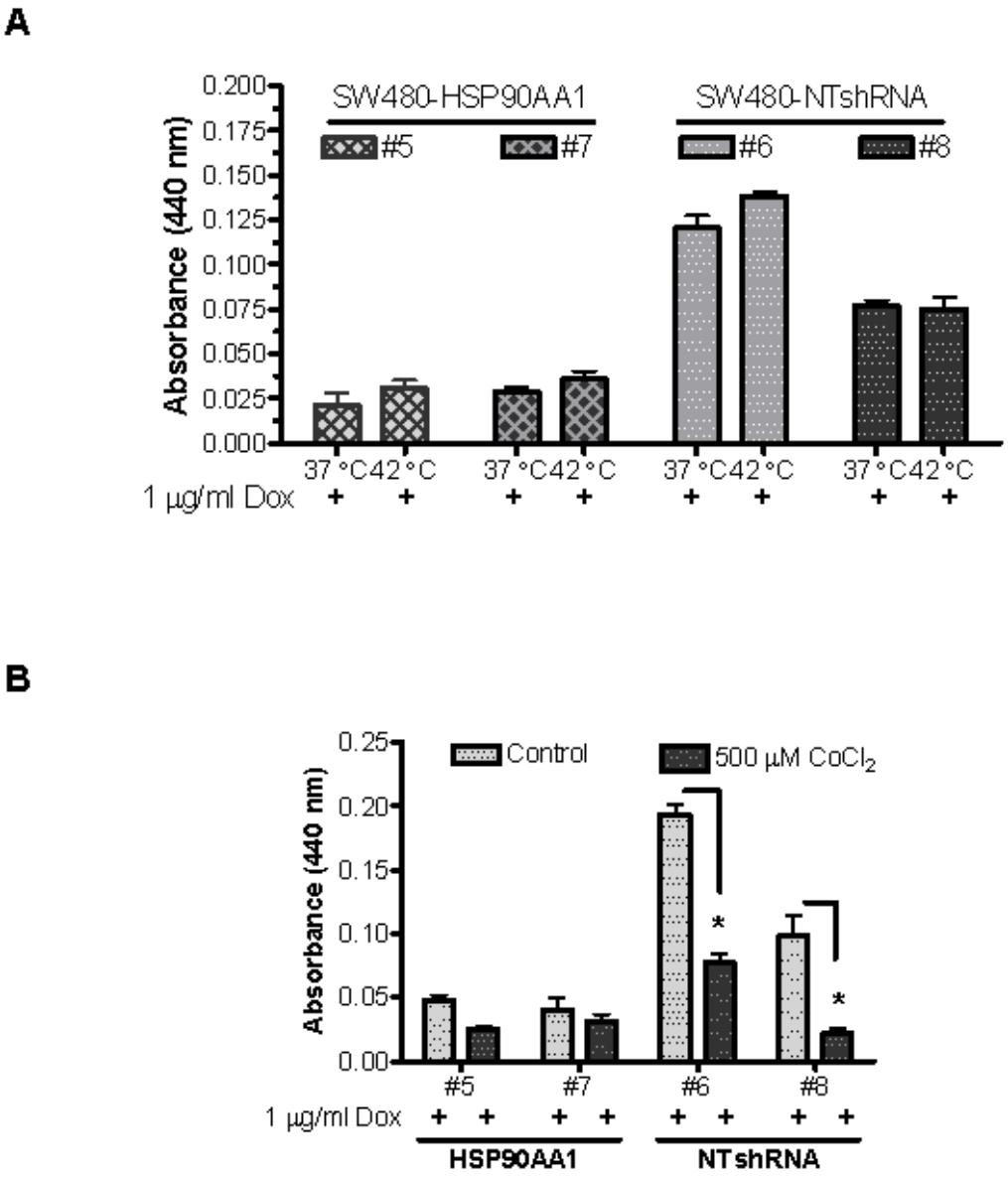

Figure 4.8. Response of monoclonal cell lines to stress during induction of knockdown.

SW480-NTshRNA #6 and #8 and SW480-HSP90AA1 # 5 and #7 monoclonal cell lines under induction of knockdown with 1 µg/ml doxycycline (Dox; 72 H). A. Dox induced monoclonal cell lines were heat-shocked (42 °C for 90 min followed by 16 H recovery at 37°C) and analysed by WST-1 assay. Results represent the mean ± SD of 15 replicates (3000 cells). Heat-shocked cells were compared to non-stressed cells (42°C v 37°C, respectively). B. Dox induced monoclonal cell lines (1 µg/ml; 72 H) were subjected to hypoxic conditions (500 µM $CoCl_2$, 24 H) and analysed by WST-1 assay. Results represent the mean ± SD of 5 replicates (3000 cells). $CoCl_2$ -treated cells were compared to untreated control cells. Data were analysed by two-way ANOVA (* = $p < 0.05$; ** = $p < 0.01$; *** = $p < 0.001$) using GraphPad Prism software.

Effect of Hsp90 depletion on the Wnt pathway and biology

β-catenin and DNAJB6 form a complex with Hsp90 *in vitro*

Wnt/β-catenin signaling is one of the most important signaling pathways in colon cancer (Vermeulen *et al.,* 2010). Our group has previously shown that Hsp90 associates with β-catenin in breast cancer cells by immunoprecipitation (Cooper *et al.,* 2011). To determine whether Hsp90 forms a complex with Wnt pathway proteins in the SW480 and SW620 cell lines, an immunoprecipitation assay was performed. An antibody against total cytosolic Hsp90 (alpha and beta isoforms) was used to capture possible interacting proteins, which were analysed by SDS-PAGE and Western blotting. Figure 4.9 illustrated the isolation of a complex containing Hsp90, β-catenin and the long isoform of the β-catenin-interacting Hsp40 co-chaperone, DNAJB6 (also known as MRJ-L); corresponding to protein bands detected at approximately 90 and 40 kDa, respectively. Hsp90 was detected in the input and within the elution from immunoprecipitation with the Hsp90 antibody (immunoprecipitate), but not in the control immunoprecipitate. β-catenin was detected in the input, in the elution with Hsp90 antibody and in low levels in the control immunoprecipitation. While β-catenin non-specifically bound to the beads used (control), the amount of protein bound was lower than that in the immunoprecipitation. The association between β-catenin and Hsp90 was confirmed by the higher level of β-catenin protein detected in the Hsp90-bound immunoprecipitate for both SW480 and SW620 cell lines. The immunoprecipitation of DNAJB6 further supported the isolation of a β-catenin containing complex with Hsp90. The proportion of DNAJB6 in the SW480 immunoprecipitate was greater than that from the SW620 cells, despite the fact that equivalent levels of Hsp90 and β-catenin were isolated. This demonstrated that Hsp90 interacted with a protein complex containing β-catenin and DNAJB6.

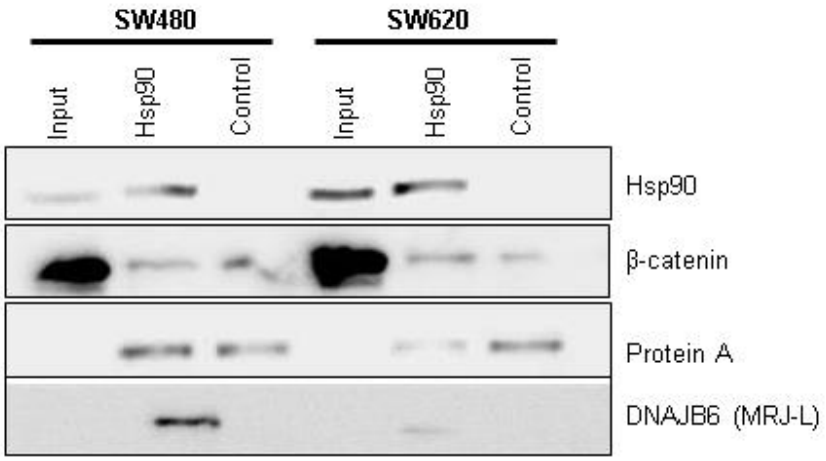

Figure 4.9. β-catenin and DNAJB6 form a complex with Hsp90 *in vitro*.

Western blot analysis of anti-Hsp90 immunoprecipitation from SW480 and SW620 whole cell lysate. Anti-Hsp90 was used for protein capture and associating proteins were eluted to be resolved by SDS-PAGE. Potential interactions were assessed using Hsp90, β-catenin and DNAJB6 antibodies. Input: original lysate sample prior to immunoprecipitation, Hsp90: anti-Hsp90 bound elution immunoprecipitate. Control: immunoprecipitate from bead binding with lysate without antibody. Chemiluminescent detection of proteins using the Chemidoc EQ system (Biorad, UK). Data were analysed using ImageJ software.

Analysis of the effects of Hsp90α knockdown on β-catenin and Hsp27

Our findings provided evidence that supports the association of Hsp90 with a β-catenin containing complex. To further investigate the relationship between Hsp90α and β-catenin, we compared the expression of proteins in the SW480 and SW620 cell lines, anticipating an effect on the proteins of the heat shock response, such as an increase in the expression of Hsp70 and Hsp40 (Lindquist and Craig, 1988; Calderwood, 2005). However, initial investigations into the expression of molecular chaperones and co-chaperones revealed no effect of Hsp90α knockdown on Hsp70, Hsp90β and Hsp40 (data not shown). Comparative assessment of SW480-HSP90AA1 and SW480-NTshRNA cell lines revealed a substantial reduction of Hsp27 as a consequence of Hsp90α knockdown (Figure 4.10). The parent SW480 and SW620 cell lines expressed similar levels of Hsp90α, Hsp27 and β-catenin, relative to the loading control (Figure 4.10A).

We next analysed the effects of Hsp90α knockdown on the expression of β-catenin. The SW480-HSP90AA1 #5, #7, and RFP-H, and the SW480-NTshRNA #6, #8 and RFP-H cells were treated with 1 µg/ml doxycycline for induction of the shRNA. After 24, 48 or 72 H of induction, the cells were lysed for the analysis of Hsp90α, β-catenin and Hsp27 proteins by Western blotting. The kinetic analysis of control SW80-NTshRNA cells (#6, #8 and RFP-H) revealed no change in the expression of Hsp90α, Hsp27 or β-catenin over 72 H of induction (Figure 4.10B). Analysis of the doxycycline shRNA-induced polyclonal SW480-HSP90AA1 RFP-H cell line illustrated that knockdown was achieved within 48 H of treatment, with a concomitant loss of β-catenin and Hsp27 levels. The effect of knockdown in SW480-HSP90AA1 #5 cell line revealed a time-dependent decrease in Hsp90α, Hsp27 and β-catenin with the addition of doxycycline. The kinetic analysis of Hsp90α knockdown in SW480-HSP90AA1 #7 cells revealed that the loss of Hsp90α was less pronounced, and the levels of Hsp27 and β-catenin were similar to the levels of Hsp90α. These data suggested a relationship between the level of β-catenin, Hsp27 and level of Hsp90α knockdown observed.

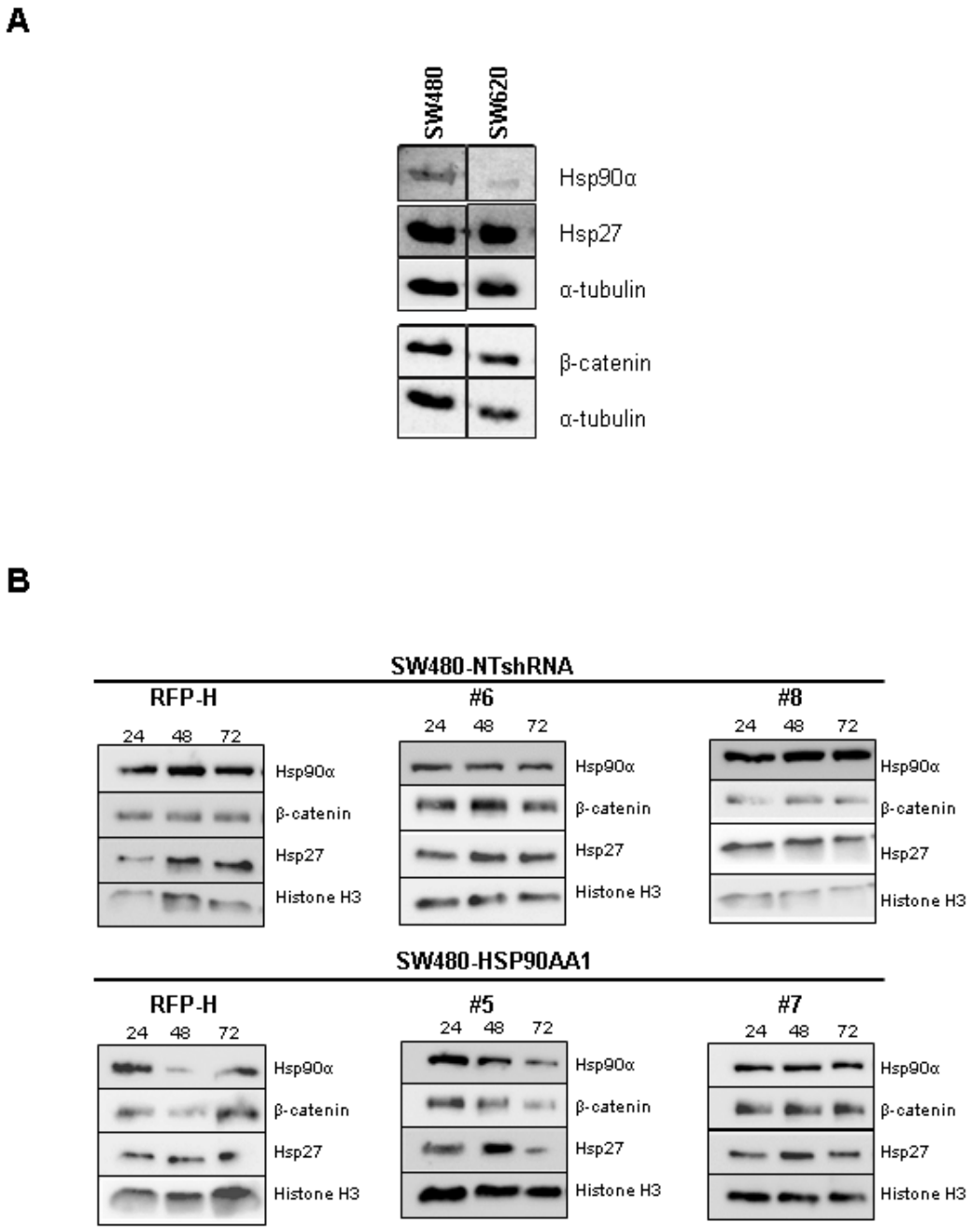

Figure 4.10. Kinetic analysis of changes in β-catenin and Hsp27 with Hsp90α knockdown.

A. Levels of Hsp90α, Hsp27 and β-catenin expression in the parent SW480 and SW620 cell lines. B. Time-dependent analysis of Hsp90α, β-catenin and Hsp27 during doxycycline treatment. SW480-NTshRNA and SW480-HSP90AA1 monoclonal (#6, #8, and #5, #7, respectively) and polyclonal RFP-H cells were treated with 1 µg/ml doxycycline for 24, 48 or 72 H prior to cells harvesting and lysis. Western blots (50 µg of total protein) were probed for anti-Hsp90α, β-catenin, Hsp27 and loading control (histone H3 or α-tubulin). Chemiluminescent detection of proteins using antibody-antigen detection using the Chemidoc EQ system (Biorad, UK). Data were analysed using ImageJ software.

β-catenin and Hsp27 form a complex with Hsp90 *in vitro*.

Hsp27 and β-catenin have been shown to interact in breast cancer cells, using immunoprecipitation and liquid chromatography and tandem mass spectrometry with electrospray ionization, and in breast tissue biopsies, using protein staining (Fanelli *et al.,* 2008). We next sought to confirm an association between Hsp90, Hsp27 and β-catenin following our observations of simultaneous reductions in protein following Hsp90α knockdown (Figure 4.10).

To test the effect of 72 H of Hsp90α knockdown on the formation of a complex with β-catenin, we used an antibody against total Hsp90 (alpha and beta isoforms) to immunoprecipitate the complex from a control and Hsp90α knockdown cell line after 72 H treated with doxycycline. Hsp90α/β was precipitated from both the Hsp90α knockdown line SW480-HSP90AA1 #7 and the control line SW480-NTshRNA #8. Lower levels of Hsp90 were detected in the immunoprecipitate from the SW480-HSP90AA1 #7 cells than the SW480-NTshRNA #8 cells, correlating with reduced Hsp90α in SW480-HSP90AA1 #7 cells (Figure 4.11). However, there was a greater amount of co-precipitating β-catenin in SW480-HSP90AA1 #7 immunoprecipitate, than in the SW480-NTshRNA #8 immunoprecipitate. Relative to the amount of Hsp90 isolated, there was also a greater amount of Hsp27 in the SW480-HSP90AA1 #7 compared to the SW480-NTshRNA #8 immunoprecipitate. These findings demonstrated that reduced Hsp90α increased the formation of an Hsp90/Hsp27/β-catenin complex.

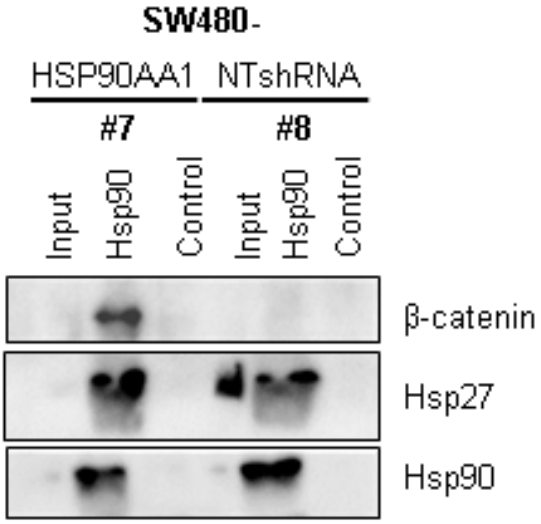

Figure 4.11. Hsp90α knockdown increases the levels of βcatenin and Hsp27 in complex with Hsp90

Immunoprecipitation of Hsp90 containing complexes from SW480-HSP90AA1 #7 and SW480-NTshRNA #8 cell lines. Knockdown was induced in cells with doxycycline for 72 H prior to lysis in RIPA buffer. Hsp90 (total; alpha and beta isoforms; interacting proteins were eluted and resolved by SDS-PAGE and Western blotting. Input: original lysate sample prior to immunoprecipitation, Hsp90: anti-Hsp90 bound elution. Control: elution from bead binding with lysate without antibody Interactions were assessed using Hsp90, β-catenin and Hsp27 antibodies. Chemiluminescent detection of proteins using the Chemidoc EQ system (Biorad, UK). Data were analysed using ImageJ software.

Effect of Hsp90α knockdown on tumoursphere formation

To characterise the effects of Hsp90α knockdown on anchorage independent growth, we compared the formation of tumourspheres by the SW480-HSP90AA1 #5 and SW480-HSP90AA1 #7 to the SW480-NTshRNA #6 and SW480-NTshRNA #8 under knockdown conditions (Figure 4.12). After 7 days of anchorage-independent growth, both the SW480-NTshRNA clones #6 and #8 tumourspheres were characterised by compact irregularly-shaped spheres, of approximately 85 µm in diameter. Interestingly, the Hsp90α knockdown cell lines (SW480-HSP90AA1 #5 and #7) produced spheres that were bigger in dimension (approximately 120 µm) than that of the average SW480-NTshRNA sphere (Figure 4.12A). Quantifying the average number of spheres formed demonstrated that while the SW480-HSP90AA1 #5 and #7 and SW480-NTshRNA #6 and #8 monoclonal cell lines retained their ability to form tumourspheres under doxycycline induction, the average number of spheres formed from 100 cells seeded was reduced by Hsp90α knockdown (Figure 4.12B). These findings demonstrated that reduced levels of Hsp90α correlated with enlarged tumourspheres but a lower sphere-forming ability.

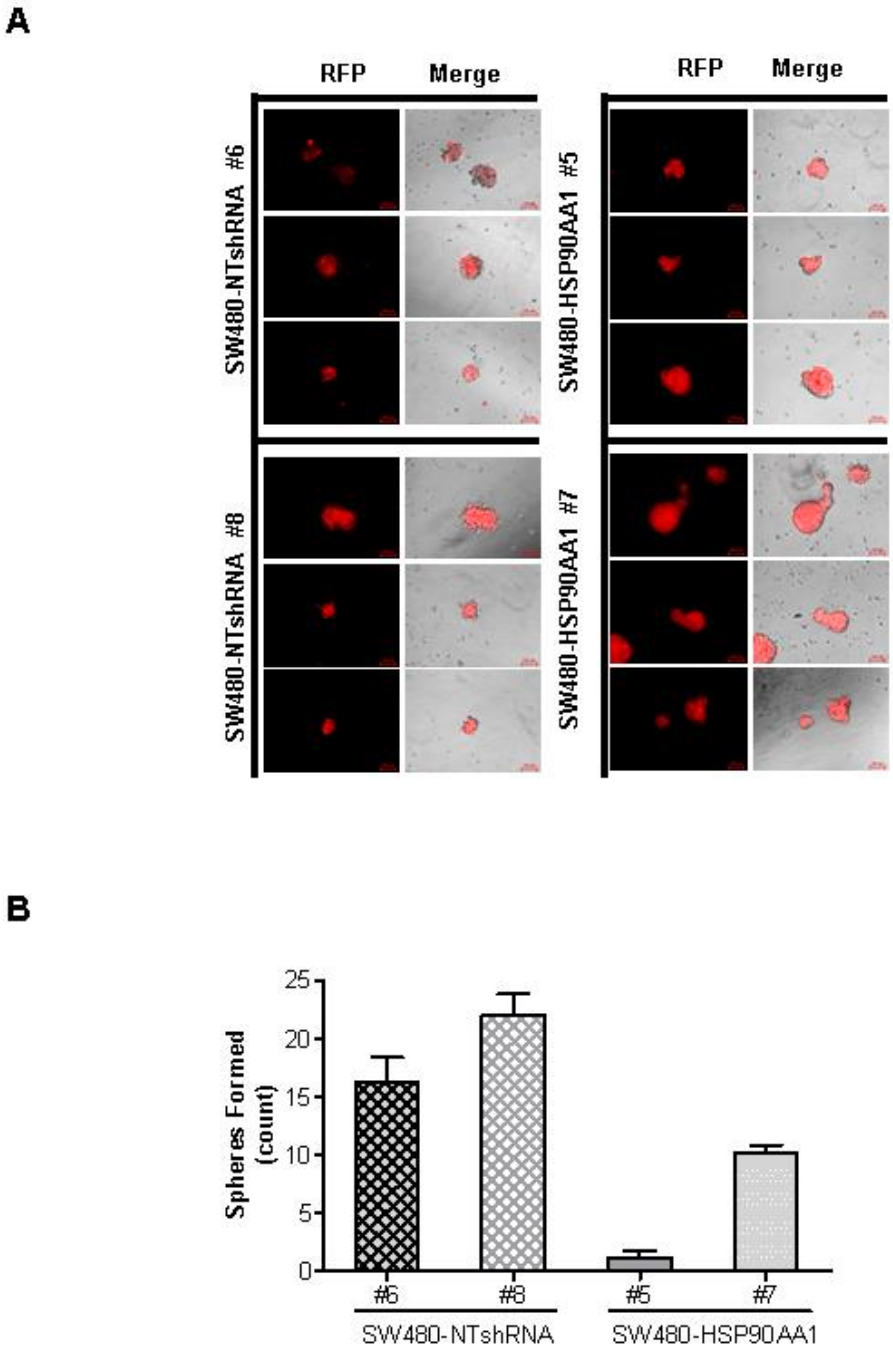

Figure 4.12. Assessment of tumoursphere formation in response to Hsp90α knockdown.

The effects of Hsp90α knockdown induction (1µg/ml doxycycline, Dox) on tumoursphere (TS) formation. A. Immunofluorescent microscopy images of induction by tRFP expression in TS under red fluorescence (RFP) and merged RFP/brightfield. Images of the SW480 (parent) TS, SW480-NTshRNA TS and SW480-HSP90AA1 TS were taken after 9 days of anchorage-independent growth (100 cells seeded). TS were induced with Dox for 72 H (day 5 - 7) prior to the analysis tRFP expression B. Enumeration of spheres formed/100 cells seeded under anchorage-independent conditions after 7 days of growth (mean of triplicate results ± SD). TS were treated with Dox for 72 H (day 5 - 7) prior to analysis. Immunofluorescent microscopy images were taken using Zeiss AxioVert.A1 Fluorescence LED Inverted Microscope with a High Resolution AxioCam MRm Rev 3. Scale bar: 100 µm. Data were analysed using ZEN Lite 2012 software and GraphPad Prism software.

Effect of Hsp90α knockdown on adhesion

The effects of Hsp90α knockdown on the adherence to tissue culture plastic of the SW480-HSP90AA1 #5, SW480-HSP90AA1 #7, SW480-NTshRNA #6 and SW480-NTshRNA #8 monoclonal cell lines was investigated. Crystal violet was used to stain cells after 8 H of adhesion. Enhanced retention of crystal violet by cells is represented in the higher level of absorbance at 590 nm. The retention, indicated by the absorbance, of crystal violet was measured as 1.0 and 1.3 for SW480-NTshRNA #6 and #8, while for SW480-HSP90AA1 #5 and #7 the absorbance of crystal violet was approximately 0.5 for both cell lines (Figure 4.13A). This suggested greater adherence in the monoclonal SW480-NTshRNA #6 and #8 cell lines in comparison to the SW480-HSP90AA1 #5 and #7 cell lines, where Hsp90α was depleted.

We have previously demonstrated that the migratory potential of the SW480 parent line was enhanced by adhesion on a collagen surface (Figure 2.3; Chapter 2). We therefore compared the adhesion of the SW480-HSP90AA1 and SW480-NTshRNA cell lines on a collagen matrix. Similar to the uncoated tissue culture plastic, the SW480-NTshRNA #6 and #8 cell lines adhered more to the collagen matrix compared with the SW480-HSP90AA1 cell lines #5 and #7 cell lines (Figure 4.13B). A closer examination of the morphology of cells allowed to adhere to a collagen coated surface was conducted (Figure 4.13C). Both SW480-NTshRNA cell lines showed epithelial-like cells with pronounced cell extensions (long cell projections) and a high degree of cell spreading. The degree to which the cells could be seen to extend was greater for the SW480-NTshRNA #8 cell line over the SW480-NTshRNA #6 cell line. In comparison to the SW480-NTshRNA cells, the SW480-HSP90AA1 cells showed more compact, less spindle-like morphology, with shorter projections. The quantification of cell spreading (calculated from images as the area covered per the number of individual cells) indicated that NTshRNA cell lines illustrated a higher degree of spreading after 8 H of adhesion on collagen, compared to the Hsp90α depleted cells (Figure 4.13D). Together these data confirmed that Hsp90α knockdown led to decreased cell adhesion and spreading.

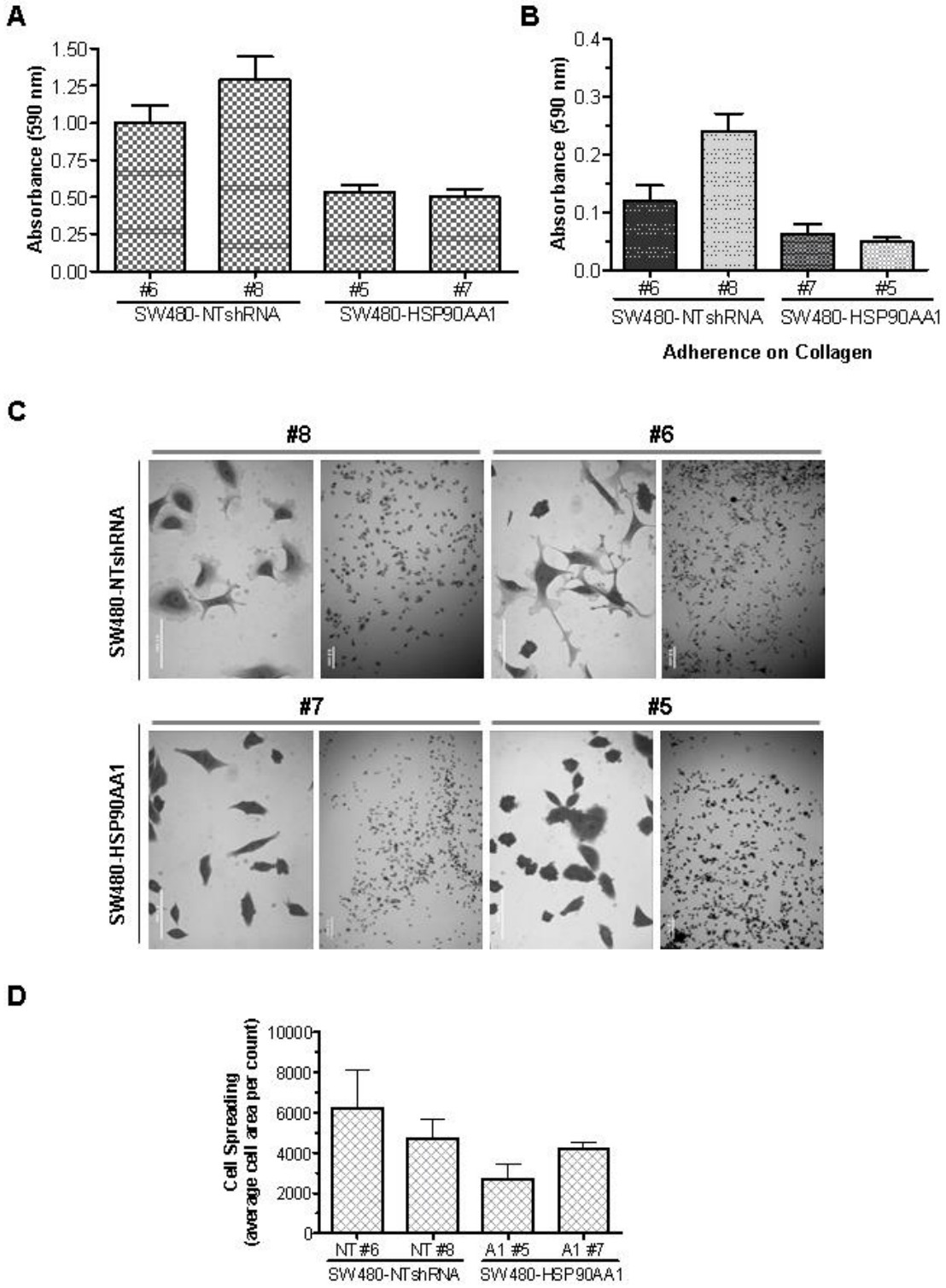

Figure 4.13. Characterisation of the effects of Hsp90α knockdown on cell adhesion (continued over page).

Figure 4.13. Characterisation of the effects of Hsp90α knockdown on cell adhesion.

A. SW480-NTshRNA and SW480-HSP90AA1 monoclonal cells (2 x 10^4 cells) were seeded at 37 °C on tissue culture plastic, in triplicate, 8 H prior to staining of adherent cells with crystal violet (10 % w/v). B. Analysis of triplicate crystal violet-stained monoclonal cell lines from 1 x 10^4 cells following 8 H adhesion on collagen under knockdown conditions (72 H, 1 µg/ml Dox). C. Images of adherence from 1 x 10^4 cells seeded after 8 H on Collagen tissue culture plastic ware under knockdown conditions (72 H, 1 µg/ml Dox). Images are representative of the average of 3 replicates, taken using a phase contrast DSZ5000X microscope and analysed using ImageJ software. Scale bar: 0.1 mm. D. The average area (mm^2) covered per number of cells counted was utilised as a measurement of cell spreading and compared across the SW480-NTshRNA and SW480-HSP90AA1 monoclonal cell lines following adherence on collagen after treatment for 72 H with 1 µg/ml Dox. Crystal violet absorbance was measured at 590 nm using a PowerWave spectrophotometer (Bio-Tek Instruments, USA). Data represent the mean ± SD for triplicate results and analysed with GraphPad Prism software.

Effects of Wnt/β-catenin targeting in colon cancer cell lines with reduced Hsp90α

Targeting the Wnt/β-catenin pathway

To study the effects of Hsp90α depletion on Wnt pathway modulation, we utilised selective modulators of proteins of the Wnt/β-catenin signaling pathway. IQ-1, or (2E)-2-[(E)-(4-acetylphenyl)diazenyl]-2-(3,3-dimethyl-3,4-dihydro-1(2H)-isoquinolinylidene)-acetamide, is a cell permeable inhibitor of PP2A that disrupts the interaction of β-catenin with p300 and leads to the down regulation of c-myc, a major regulator of stem cell self-renewal and differentiation (Miyabayashi *et al*., 2007). SB-216763, or 3-(2,4-dichlorophenyl)-4-(1-methyl-1H-indol-3-yl)-1H-pyrrole-2,5-dione, is a GSK3 (alpha and beta isoform) inhibitor (Grassilli *et al*., 2014). Alterations to mitotic spindles demonstrated through GSK3 inhibition has revealed the functional consequences of deregulated GSK3 in cancers (Wakefield *et al.,* 2003). By preventing the degradation of β-catenin, IQ-1 and SB-216763 treatments should result in the accumulation of β-catenin. Quercetin, or 2-(3,4-dihydroxyphenyl)-3,5,7-trihydroxy-4H-chromen-4-one, is a natural bioflavonoid modulator of Wnt/β-catenin signaling pathway (Takahashi-Yanaga and Kahn 2010; Yao *et al*., 2013). Quercetin also inhibits the binding between heat shock elements to heat shock factor proteins, resulting in a suppression of the heat shock response of Hsp27, Hsp70 and Hsp90 chaperones (Nagai *et al*., 1995; Lin *et al*., 2012).

Sensitivity of polyclonal and monoclonal cells under Hsp90α knockdown to Wnt/β-catenin modulation

Quercetin, IQ-1 and SB-216763 were utilised to modulate β-catenin to establish any differences between sensitivity of cells under knockdown. The SW480-HSP90AA1 (#5, #7 and RFP-H) and SW480-NTshRNA (#6, #8 and RFP-H) cell lines were treated with increasing dosages of quercetin, SB-216763 or IQ-1 after 24 H of knockdown, and analysed after 48 H of treatment by MTT cell assay. An illustration of the mechanism of action of the compound in question is represented in the schematic diagram alongside the results of the viability assay (Figure 4.14). Analysis of the results of the MTT analysis by non-linear regression was used to determine the effective concentration of each compound (the concentration of treatment that correlated to a change in 50 % of the cell population viability). Quercetin treatment induced cell growth in all monoclonal and polyclonal transduced SW480 cell lines (Figure 4.14A). No significant difference was detected between SW480-NTshRNA and SW480-HSP90AA1 cells, with EC_{50} values ranging between 51 – 59 and 49 – 70 µM, respectively (Table 8). The SW480-HSP90AA1 (#5, #7 and RFP-H) and SW480-NTshRNA (#6, #8 and RFP-H) cell lines showed similar sensitivities to IQ-1 and SB-216763 treatment (Figure 4.14 B and C). The SW480-HSP90AA1 knockdown cell line EC_{50} sensitivities to IQ-1 were between 1.45 and 1.5 µM, while SW480-NTshRNA cell lines ranged between 0 (non-toxic; flat regression curve, Figure 14.4B) to 1.75 µM (Table 8). SB-216763 sensitivities observed were also similar between SW480-NTshRNA and SW480-HSP90AA1 cells, reporting EC_{50} ranges of between 1.75 - 1.85 and 1.7 – 2.0 µM, respectively (Table 8). Together, these findings demonstrated that there was no significant difference in the sensitivity of Hsp90α knockdown cells and control cells.

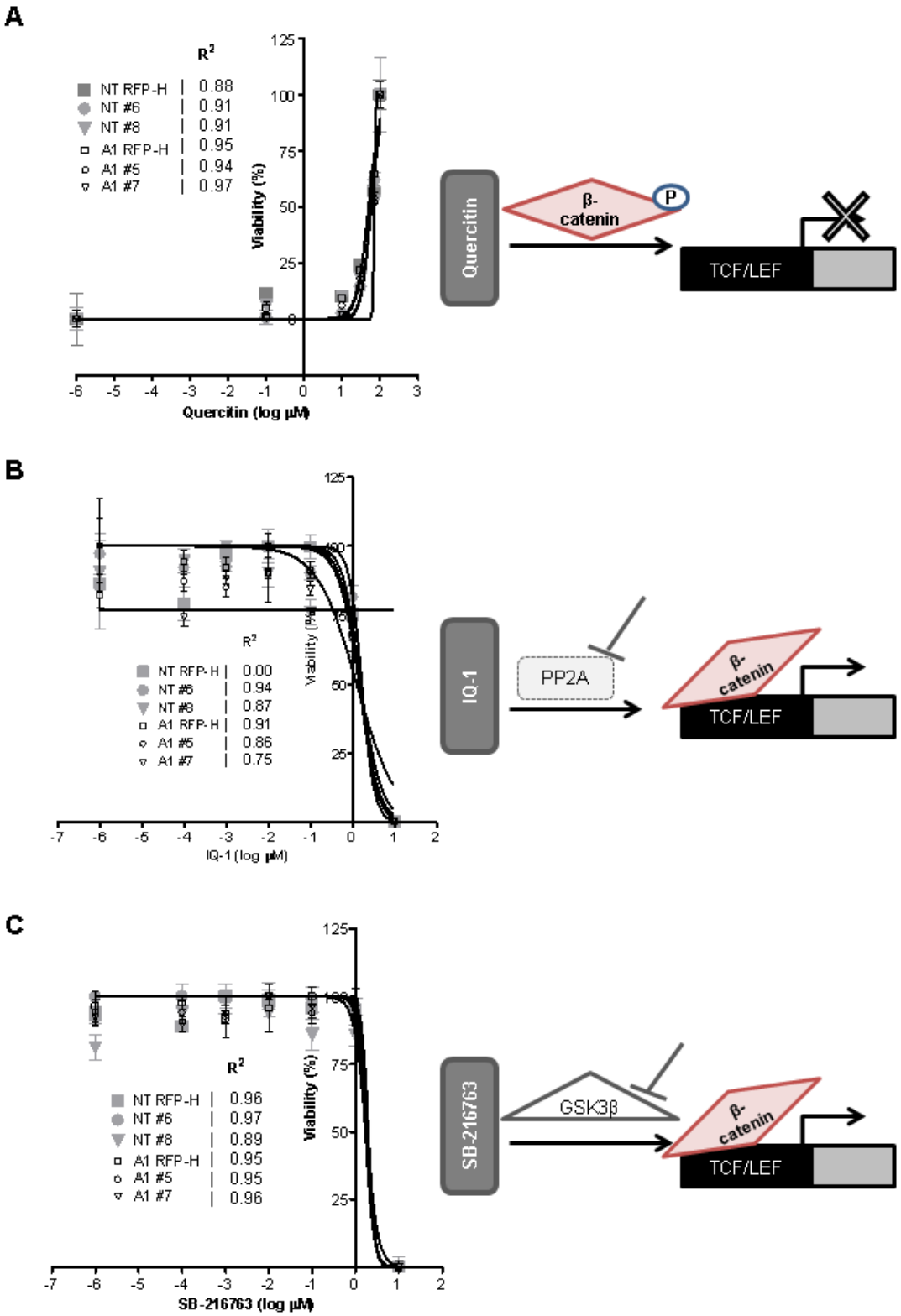

Figure 4.14. Effect of modulators of the Wnt/β-catenin pathway on cell viability (continued over page)

Figure 4.14. Effect of modulators of the Wnt/β-catenin pathway on cell viability

SW480-NTshRNA and SW480-HSP90AA1 cells treated with doxycycline for induction of knockdown (10 000 cells, 72 H 1 µg/ml Dox). After 24 H adherence under knockdown, cells were treated with modulators of the Wnt pathway for 48 H prior to analysis by MTT assay. A. Quercetin (0, 0.1, 10, 30, 70 and 100 µM). B. IQ-1 (0, 0.0001, 0.001, 0.01, 0.1, 1, 10 µM). C. SB-216763 (0, 0.0001, 0.001, 0.01, 0.1, 1, 10 µM). The method of treatment action for the modulation of Wnt/β-catenin pathway is represented alongside each treatment. Quercetin attenuates TCF/LEF transcriptional activity, IQ-1 inhibits PP2A and SB-216763 inhibits GSK. Each assay represents the mean ± SD of three replicates. The concentration of chemotherapeutic agent (µM) to effectively reduce cell viability by 50 % (EC_{50}) for each cell line was calculated. Percentage viability was determined using negative controls as a reference of 100 % cell viability per cell line. Data were analysed by non-linear regression using GraphPad Prism software.

Table 8. Summary of sensitivity of cells with or without Hsp90α knockdown to Wnt/β-catenin modulation

SW480 Cell Line	EC_{50} (µM): Quercetin	IQ-1	SB-216763
NTshRNA (RFP-H)	51.22	Non-toxic (0)	1.813
NTshRNA #6	56.30	1.655	1.835
NTshRNA #8	58.61	1.252	1.753
HSP90AA1 (RFP-H)	49.39	1.496	1.972
HSP90AA1 #5	58.09	1.440	1.766
HSP90AA1 #7	69.88	1.502	1.693

Effects of Wnt/β-catenin modulation on protein expression under Hsp90α knockdown

To demonstrate the effects of Wnt/β-catenin modulation, the levels of β-catenin, Hsp90α and Hsp27 protein expression in the monoclonal knockdown cell lines were analysed by Western blotting (Figure 4.15). The Ponceau S stained membranes have been included as a loading control for total protein on the membrane due to variability in the loading control.

SW480-HSP90AA1 #5 and #7, and the SW480-NTshRNA #6 and #8 cell lines were treated for knockdown (72 H with 1 µg/ml doxycycline) prior to a short 4 H treatment of cells and lysis for analysis of changes to β-catenin, Hsp90α and Hsp27 levels. Quercetin should reduce the proteins of the heat shock response (including Hsp27) and attenuate the transcriptional

activation of the TCF/LEF gene by β-catenin translocation to the nucleus. Quercetin-treated cells showed that β-catenin and Hsp90α protein levels were slightly increased following treatment in both SW480-HSP90AA1 #5 and #7, and the SW480-NTshRNA #6 and #8 cell lines (Figure 4.15A). The Hsp90α knockdown lines showed substantial reductions in Hsp27, a feature which was not rescued by quercetin treatment.

To study the effects of GSK3 and PP2A inhibition, SW480-HSP90AA1 #5 and #7, and the SW480-NTshRNA #6 and #8 cells were treated with SB-216763 and IQ-1, respectively (Figure 4.14 B and C). Treating cells with IQ-1 and SB-216763, should result in an accumulation of β-catenin, due to the inhibition of GSK3 and PP2A preventing the degradation of β-catenin (see Figure 4.14 for illustration). When accounting for minor differences in protein loading, it was concluded that there was no effect on the Hsp90α protein expression following treatment with IQ-1 or SB-216763 in the Hsp90α knockdown or control cell lines. However, the Hsp90α levels were still slightly reduced in the knockdown cells. β-catenin was slightly raised in response to treatment with IQ-1, but this result was consistent, with no difference between the Hsp90α knockdown and control cell lines. No response was detected upon SB-216763 treatment in either of the cell lines, which suggested that 4 H may not have been sufficient to detect a protein response to SB-216763. The Hsp90 knockdown lines revealed a substantial reduction in Hsp27, a feature which was not altered by treatment with either IQ-1 or SB-216763.

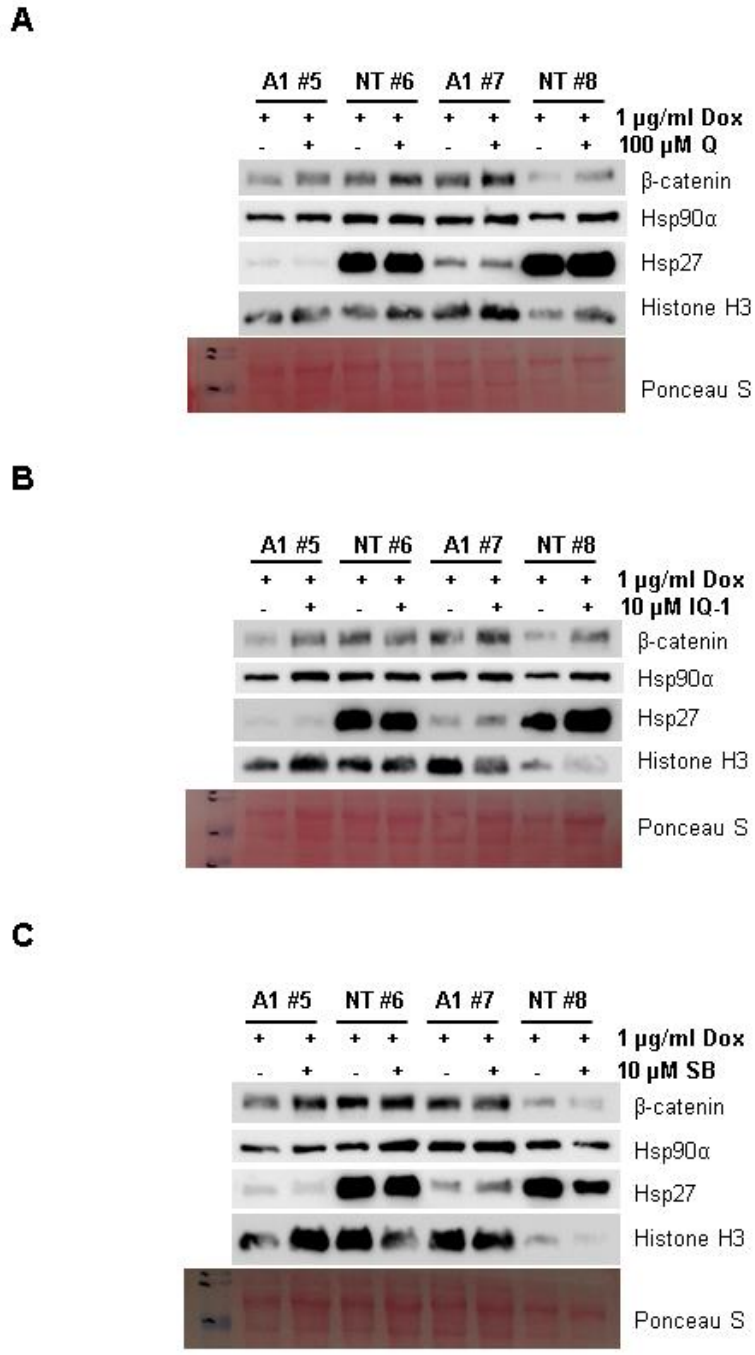

Figure 4.15. Effects of Wnt/β-catenin pathway modulation by Quercetin, IQ-1 and SB-216763.

Western blot analysis with accompanying ponceau S stains of lysed SW480-NTshRNA and SW480-HSP90AA1 monoclonal cell lines under Wnt/β-catenin modulation. Monoclonal cell lines were induced with doxycycline (1 µg/ml) for 72 H prior to treatment. Cell lines: SW480-HSP90AA1 #5 (A1 #5), SW480-NTshRNA #6 (NT #6), SW480-HSP90AA1 #7 (A1 #7) and SW480-NTshRNA #8 (NT #8). A. Treatment with 100 µM Quercetin (Q) for 4 H prior to lysis. B Treatment with 10 µM IQ-1 (PP2A inhibitor) for 4 H prior to lysis. Treatment with 10 µM SB-216763 (SB; GSK3β inhibitor) for 4 H prior to lysis. Western blotting for comparison of treatment (+) on the expression of β-catenin, Hsp90α, Hsp27 and histone H3 proteins, relative to untreated (-) controls. Ponceau S stain demonstrated equivalent loading between cell lines. Chemiluminescent detection of 50 µg protein loaded using the Chemidoc EQ system (Biorad, UK). Images were analysed by ImageJ software.

Both the Hsp90α-targeted and control cell lines responded in a similar manner to modulators of the Wnt pathway with respect to the levels of β-catenin and Hsp90α. These data suggested that the response of modulators of the Wnt pathway was similar between the SW480-HSP90AA1 and SW480-NTshRNA cell lines, irrespective of the amount of Hsp90α protein. We interpret this to mean that the effect of Hsp90α depletion on β-catenin is not via modulation of the Wnt signaling pathway. Further investigation into the activation state of the Wnt/β-catenin pathway of SW480-HSP90AA1 and SW480-NTshRNA cell lines by the subcellular localisation of β-catenin, by confocal microscopy, revealed predominant staining for β-catenin in the cytoplasm and some nuclear staining across all monoclonal cell lines, demonstrating the activity of the Wnt/β-catenin pathway in these cells (data not shown), similar to that which was seen in the parent SW480 cell line (Figure 2.1, Chapter 2). The treatment of the monoclonal cell lines with Wnt/β-catenin pathway modulators revealed no significant change to the distribution or location of β-catenin between the control and the Hsp90α knockdown cell lines upon treatment with quercetin, IQ-1 or SB-216763 (data not shown). This confirmed our previous findings by, where 4 H of Wnt/β-catenin modulation was insufficient to detect a change in protein expression between the control and the Hsp90α knockdown cell lines

Sensitivity of tumourspheres with or without Hsp90α knockdown to Wnt/β-catenin modulation

To explore the effects of Wnt/β-catenin modulation on anchorage independent growth in the presence of Hsp90α knockdown, TS of the monoclonal Hsp90α and control knockdown cell lines were treated with quercetin, IQ-1 and SB-216763. Using 200 µM quercetin, 20 µM IQ-1 or 20 µM SB-216763, the effects on pre-formed TS of the induced SW480-HSP90AA1 (#5, #7 and RFP-H) and SW480-NTshRNA (#6, #8 and RFP-H) cell lines were analysed after 24 H treatment for morphological differences. Treatment with quercetin, IQ-1 and SB-216763 caused the visible dissociation of TS under doxycycline treatment (Figure 4.16). The disruption of TS, indicated by the separation of cells from the outermost region of visible sphere masses, was evident across all monoclonal cell lines upon Wnt/β-catenin modulation.

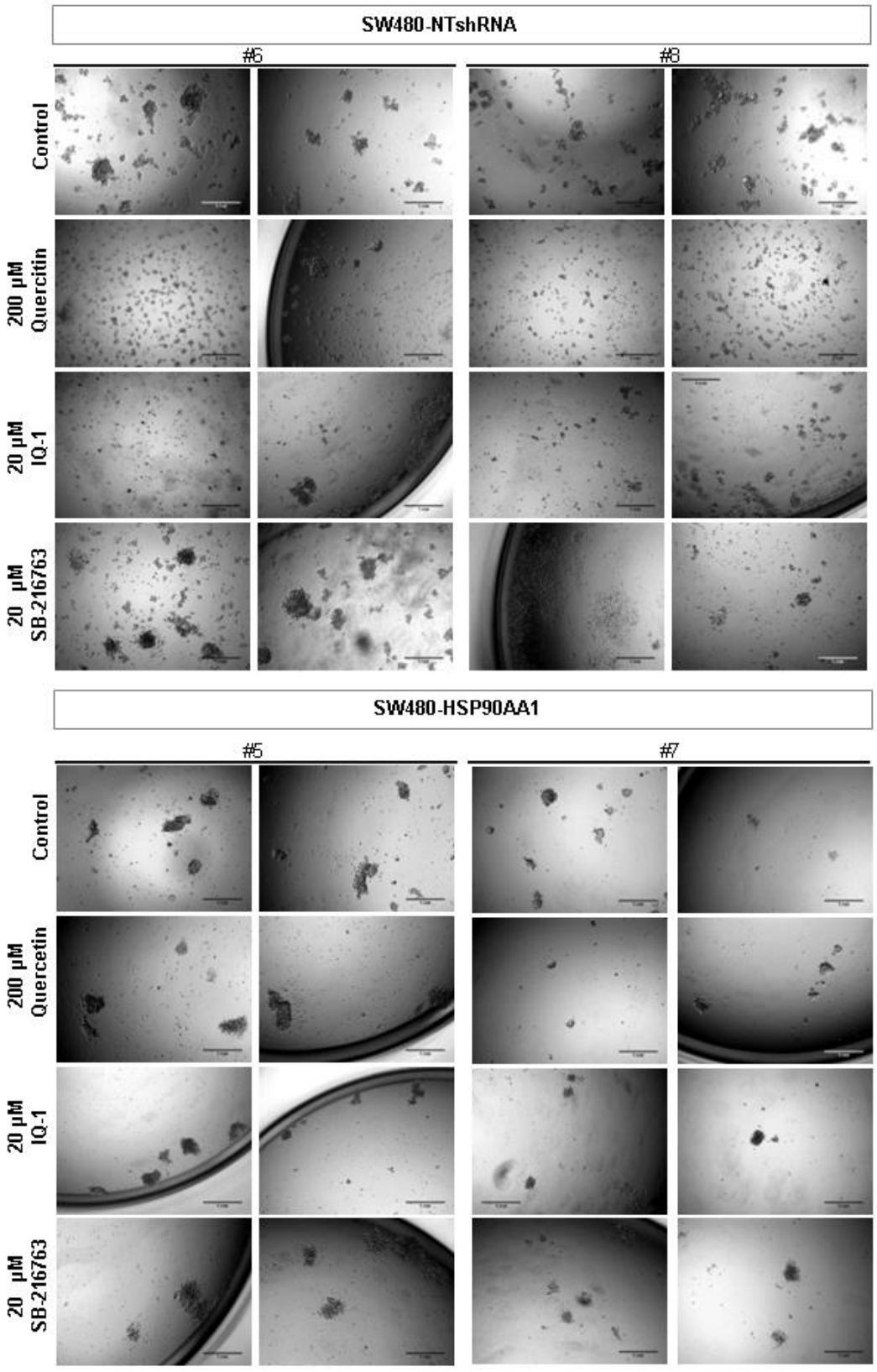

Figure 4.16. Effect of modulators of the Wnt pathway on tumourspheres formation in cell lines with or without HSP90α knockdown (continued over page).

Figure 4.16. Effect of modulators of the Wnt pathway on tumourspheres formation in cell lines with or without HSP90α knockdown.

Morphological changes in tumourspheres (TS) of SW480-HSP90AA1 (#5, #7) and SW480-NTshRNA (#6, #8) cell lines after doxycycline treatment. Treatments for Wnt/β-catenin modulation include: 200 µM quercetin, 20 µM SB-216763 and 20 µM IQ-1 (GSK3 and PP2A inhibitors, respectively). Hsp90α knockdown was induced for 72 H prior to treatment of TS for 24 H with modulators (on day 7 of TS culture). Images, taken on day 8, are duplicate representatives of triplicate experimental analyses. Images were taken using a phase contrast DSZ5000X microscope and analysed using ImageJ software. Scale bar: 1 mm.

Discussion

Development of HSP90AA1 and NTshRNA knockdown-inducible colon cancer cell lines

This chapter described the development of polyclonal and monoclonal SW480 HSP90AA1- or NTshRNA-transduced colon cancer cell lines. The optimisation of induction conditions revealed Hsp90α knockdown in SW480 transduced cell lines required at least 72 H of 1 µg/ml doxycycline, achieving the maximum reduction in the expression of Hsp90α in comparison to the control cell lines. The complete depletion of Hsp90α was not achieved within 72 H of 1 µg/ml doxycycline for any of the monoclonal or polyclonal cell lines generated, and the level of Hsp90β remained consistent in both cell lines (Figure 4.7). This report is the first documented use of HSP90AA1 targeting by shRNA for analysis of Hsp90α reduction in colon cancer cell lines and Wnt/β-catenin signaling. Current Hsp90 inhibitors are not designed to specifically target individual isoforms of Hsp90, and recent studies have focussed on isoform specific inhibition, for example through lentiviral delivery of Hsp90AA1-targeted shRNA in KRAS wild type and mutant lung cancer cells (NCI-H520 and A549, respectively) *in vitro* (Azoitei *et al.,* 2012). Several inhibitors of Hsp90 have demonstrated some potential in phase I and II clinical trials (Kim *et al*., 2009; Socinski *et al*., 2013), although translational relevance has yet to be established using RNAi as a therapy. The generation of stable-transduced cell lines is a slow and laborious process, which is a limitation of the development of shRNA-transduced cell lines and demonstrated one benefit of the use of siRNA. However, we showed that SW480 colon cancer cells exhibited low transfection efficiencies and high sensitivity to transfection reagents, releaved the advantages of lentiviral delivery for gene targeting (Koponen *et al.,* 2003).

Cellular response to stress is deregulated under Hsp90α knockdown

To characterise the SW480-HSP90AA1 and SW480-NTshRNA cell lines, we characterised their response under shRNA knockdown to thermal (heat) and hypoxia (chemically-induced by $CoCl_2$ treatment) stress. Cells with reduced Hsp90α showed reduced viability at both 37°C and after a heat shock at 42°C compared to the control cells, but did demonstrate a slightly increased ability to survive hypoxic conditions. Stressful events, such as heat shock and oxygen stress, usually drive the increased expression HSP genes though the interaction of HSF1 with heat shock elements (HSE) (Georgopolis and Welch, 1993). The increased expression of Hsp, including Hsp90α, Hsp70 and Hsp27, facilitates cell survival during stressful conditions (Zou *et al.,* 1988; Calderwood *et al*., 2006). The stressful environment of tumours, such as nutrient and oxygen stress, is often compensated by the upregulation of Hsp90 in cancers (Maloney and Workman, 2002; Whitesell and Lindquist, 2005).

The Hsp90α knockdown cells showed a minor reduction of Hsp90α expression correlating to reduced β-catenin and substantial decreases in Hsp27 protein in comparison to the control cells (Figure 4.10). To the best of our knowledge, this is the first observation of a reduction in Hsp27 upon Hsp90α depletion. The dramatic loss of Hsp27 led us to investigate any potential sequence similarity between our shRNA against Hsp90α and the Hsp27 mRNA sequence. We performed a BLAST and ClustalW2 alignments of the HSP90AA1 and HSPB1 genes. The lack of sequence identity between the two genes suggested that it was unlikely that the response of Hsp27 to Hsp90α knockdown was due to the HSP90AA1 shRNA directly targeting the Hsp27 mRNA (data not shown). Hsp27 is a member of the small HSP family and is often upregulated in cancer and involved in cytoprotection of cells during stress (Parcellier *et al.,* 2005). Both Hsp90α and Hsp27 are inducible with stress and regulate protein folding, but their mechanisms and activities differ (Powers and Workman, 2007; Saibil, 2013). The loss of Hsp27, together with Hsp90α, may partially explain the response of the Hsp90α depleted cells to heat shock, although it does not explain why the cells demonstrate an increased resistance to hypoxia (Rogalla *et al.,* 1999). Hsp27 demonstrates cytoprotective roles by interacting with other stress proteins to promote cell survival and prevent the aggregation of denatured peptides in response to stress. The expression of Hsp27 has been implicated in resistance to chemotherapeutics from in lung CSC (Hsu *et al.,* 2011). Examination of the p38MAPK-MAPKAPK2-Hsp27 pathway has demonstrated that Hsp27 facillitates the survival of hypoxia and serum depletion by colorectal (HT-29) tumour-initiating cells (Lin *et al.,* 2012). Hsp27 overexpression is correlated with poor patient prognosis at least in part due to the Hsp27-facilitated evasion of apoptosis in malignant cells (Vidyasagar *et al*., 2012). Targeting Hsp27

and Hsp90 by inhibition has demonstrated synergistic cytotoxic effects in breast CSC (Lee *et al.,* 2012). Additionally, the combination of Hsp27 targeting using RNAi and Hsp90 targeting by 17-AAG has revealed distinct advantages as a therapy through synergistic anti-proliferative potential (Belkacemi and Hebb, 2014). Further investigation into the relationship between Hsp90α and Hsp27, Hsp70 and HSF1, is required to fully interpret the role of Hsp90α knockdown in the deregulation of the stress response.

Hsp90α knockdown alters adhesion and tumoursphere formation through changes in Hsp27 and β-catenin.

As a consequence of the reduction in levels of Hsp90α, we demonstrated a reduced ability of cells to adhere, even in the presence of the ECM protein, collagen. While collagen improved the migration potential of the parent SW480 cell line during would healing (Figure 2.3), collagen failed to improve adhesion in both Hsp90α knockdown monoclonal cell lines Furthermore, the Hsp90α knockdown cell lines showed a reduced ability to adhere and spread compared to the control cell lines (Figure 4.13). In addition, in response to Hsp90 knockdown, the SW480-HSP90AA1 TS showed a reduced ability to form spheres although the TS that did form were larger in size in comparison to the control cells (Figure 4.12). These observations are partially supported by previous studies that showed that treating colon cancer cell line derived TS with PU-H71 (0.5 μM; 48 H), an N terminal purine inhibitor of both isoforms of Hsp90, reduced the viability and size of spheres formed (Azoitei *et al.,* 2012).

It is tempting to speculate that the reduction in adhesion of cell with Hsp90α depletion also explains the increased TS size observed when Hsp90α depleted cells were cultured under anchorage independent conditions. We focussed our analysis on the Wnt/β-catenin pathway due to its well described role in colon cancer biology (Schneikert, and Behrens, 2007; Voloshanenko et al., 2013). Using iTRAQ, β-catenin was identified as a major indicator of metastatic potential, with lower levels detected in the SW620 cell line than the SW480 cell line (Ghosh *et al.,* 2011). Previous reports from our group demonstrate a role for Hsp90 in Wnt/β-catenin signaling through the discovery of a complex of Hsp90 with GSK3β, axin1 and phosphorylated β-catenin in breast cancer cells *in vitro* (Cooper *et al.,* 2011). Here we demonstrate that Hsp90 and β-catenin can be isolated in a common complex from both the SW480 and SW620 cell lines (Figure 4.9). The SW480 complex was enriched in DNAJB6, compared to the SW620 complex. DNAJB6 is a type II Hsp40 co-chaperone which when upregulated facilitates the degradation of β-catenin by disrupting Wnt/β-catenin signaling and thereby reduces the expression of as tumourigenic or “pro-invasive” proteins and markers of the metastatic phenotype (Mitra *et al*., 2008; Mitra *et al*., 2010). The phosphorylation of

GSK3β, member of the destruction complex in the Wnt pathway responsible for β-catenin degradation, at the Serine 9 amino acid position by PP2A was shown to be dependent on the interaction of DNAJB6 and HSPA8 (Hsp70 chaperone) in melanoma (Mitra *et al.,* 2012). In addition, we demonstrated that when Hsp90α is depleted, a complex containing Hsp90, β-catenin and Hsp27 could be isolated (Figure 4.11). Fanelli and colleagues have previously demonstrated that Hsp27 and β-catenin interact *in vitro,* although, they failed to detect an association between Hsp90 and β-catenin. In their examination of interacting proteins, showed by immunoprecipitation, a non-specific protein band of ~ 83 kDa (Fanelli *et al.,* 2008). We speculate that this protein may have represented Hsp90, based on size. They also indicated a preferential association of β-catenin with Hsp27, indicating that 70 % of total β-catenin associated with Hsp27, while 40 % of Hsp27 was found in association with β-catenin (Fanelli *et al.,* 2008). Taken together, these data support a role for Hsp90 and Hsp27 in the Wnt complex in the SW480 cell lines. The presence of Hsp90 in Wnt complexes may be to stabilise β-catenin, which would explain the reduction in β-catenin levels when Hsp90α levels were reduced. Alternatively, given the interaction between Hsp27 and β-catenin, it is possible that the reductions in β-catenin are as a result of the substantial loss of Hsp27 in Hsp90α depleted cells.

Targeting Hsp90 in cancer has demonstrated that Hsp90 inhibition consequentially disrupts several signaling pathways due to the association of Hsp90 with more than 300 client proteins (Richter and Buchner, 2001; Neckers, 2002). Inhibition of Hsp90 is therefore likely to exert its effects via multiple mechanisms. We speculate that the loss of adhesion and spreading and the increased size of TS formation are related to changes in levels of Hsp27 and β-catenin in SW480 cells when Hsp90α is reduced. The β-catenin protein has been proposed to exist in two distinct pools, one pool in association with cadherins at the cell junctions, while the other functions as a transcription factor in the nucleus (Harris and Peifer, 2005). β-catenin regulates cell adhesion via its interaction with cadherins and EMT and Wnt/β-catenin signaling by regulating the transcription of genes that influence cell proliferation and migration (Crawford *et al.,* 1999; Zhang *et al.,* 2001). Gottardi and Gumbiner (2004) described a model where cells may control the function of β-catenin depending of the form of β-catenin present. The interaction of β-catenin with α-catenin, cadherin and TCF, determines whether these functions are independent of one another (separate pools of β-catenin) or coordinated simultaneously (in competition) (Gottardi and Gumbiner, 2004). The deregulation of Wnt/β-catenin pathway signals that culminate in activation of TCF/LEF containing promoters, responsible for the maintenance of stem cells through self-renewal, has shown to have oncogenic consequences (Many and Brown, 2014).

The reduction of Hsp90α in the SW480-HSP90AA1 cell lines did not sensitise cells to Wnt /β-catenin signaling modulators quercetin, SB-216763 or IQ-1 (see Table 8) in comparison to the control cell lines when treated under either adherent or anchorage independent conditions. We also observed similar responses to quercetin, SB-216763 and IQ-1 in the level of β-catenin, Hsp90α or Hsp27 protein between the control cell lines and the Hsp90α knockdown cell lines (Figure 4.15). Taken together, these data suggested that reduction of Hsp90α did not affect signalling via the Wnt pathway. This may be due to the fact that the Wnt pathway is constitutively active in the SW480 cell line. Evidence links APC and β-catenin mutations, which dominate almost 90 % of colorectal cancers, with insensitivity to changes in β-catenin levels upon inhibition of GSK3β (Yuan *et al.,* 1999). Mutations found in the genes encoding for β-catenin, APC, axin or the overexpression of Wnt ligands are associated with the activation of the Wnt/β-catenin pathway within cancers (Polakis, 2000). The SW480 cell line represents an activated Wnt pathway, where β-catenin can translocate to the nucleus due to the deletion of the 1338 amino acid residue in the APC gene, a member of the destruction complex (Brocardo *et al.,* 2005; Yang *et al*., 2006). We interpreted these data to mean that depletion of Hsp90α was not affecting the transcriptional activity of β-catenin, but was perhaps rather affecting the pool of β-catenin involved in cell adhesion (Mitra *et al*., 2010).

The pool of β-catenin associated with cell adhesion is invoved in protein-protein interactions at the adherens junctions (Gottardi and Gumbiner, (2004). We have shown that β-catenin is in a complex with Hsp90 in these cells. The reduction in cell adhesion may be directly due to the loss of β-catenin from adhesions in response to the depletion of Hsp90α. However, given the interaction between Hsp27 and β-catenin and the substantial reductions in Hsp27 observed in Hsp90α knockdown cells, it is possible that the loss of Hsp27 in response to Hsp90α depletion indirectly results in the reduction in β-catenin. Given that a substantial portion of β-catenin is predicted to be in complex with Hsp27, and Hsp27 interacts with the cytoskeleton which is associated with adherens junctions (Pichon *et al.,* 2004), it is possible that β-catenin adhesion complexes include Hsp27. Hsp27 regulates cell adhesion processes via multiple mechanisms, including a direct interaction with the actin cytoskeleton, signalling pathways and focal adhesions (Lee *et al*., 2008; Doshi *et al*., 2009). Therefore, the effects of Hsp90α on cell adhesion are likely to be mediated by depletion of Hsp27, which may also influence β-catenin levels. Indeed, direct depletion of Hsp27 in SW480 cells has been shown to reduce cell migration via regulation of the actin cytoskeleton (Doshi *et al*., 2009).

We still need to confirm that Hsp90α depletion changes the subcellular localisation of β-catenin and does not change the transcriptional activity of β-catenin. The subcellular localisation, as well as co-localisation studies with Hsp27, will be performed using confocal microscopy, while the transcriptional activity can be assessed using a reporter gene assay for

the TCF/LEF transcription factor. However, due to the low transfection efficiency of the SW480 cell line, this would require generation of lentiviral delivery systems. Alternatively, we have subsequently developed a HEK293T cell line stably transfected with the shRNA against Hsp90α (Supplemenatry Figure S4). We plan to use this model system, which is easily transfectable, to study whether Hsp90α depletion reduces β-catenin transcriptional activity. This model has a further benefit in that the Wnt pathway is not constitutively active in these cell lines. In addition, to confirm whether Hsp27 is responsible for the changes observed with Hsp90α depletion, it would be necessary to repeat the experiments using cell lines in which Hsp27 was depleted by shRNA.

Chapter 5: Conclusions and Future Work

Concluding Remarks

We compared the paired SW480 and SW620 cell lines for distinguishable biological characteristics. From our analysis of morphology, growth phenotype, protein levels and distribution we demonstrated that the paired cell lines represented an interesting model by which to study colon cancer progression *in vitro*. Similar proportions of putative CSC were discovered between the paired lines based on the analysis of the side population (Hoechst 33342 efflux by ABCG2), expression of aldehyde dehydrogenase, while variable expression of $CD44^{+}/CD133^{+}$ was detected. Our investigations revealed SW480 cells possess a greater sphere-formation ability and migration potential over SW620 cells.

Comparison of the paired cell lines revealed similar levels of Hsp90 expression and distribution between the SW480 and SW620 cells. Investigations into the role of Hsp90 in colon cancer biology revealed that extracellular Hsp90 failed to significantly influence the viability and morphology of TS. In adherent culture, SW480 and SW620 cells were similarly sensitive to geldanamycin and novobiocin. However, Hsp90 inhibition by novobiocin in SW480 TS enhanced TS formation. We observed that treating cells with 5-FU or oxaliplatin prior to their establishment of TS correlated with TS sensitivity to the treatments, while established TS resisted anti-cancer treatment. Simultaneous oxaliplatin and novobiocin treatment was able to increase the sensitivity of established TS to treatment.

To define the specific isoform-dependent role of Hsp90 in the progression of colon cancers we considered two mechanisms of RNAi to facilitate protein knockdown. While we failed to observe isoform-specific Hsp90α and Hsp90β knockdown using siRNA, we successfully developed an RNA interference approach to reducing Hsp90α in colon cancer cells using inducible shRNA-targeting cell lines for Hsp90α knockdown. Hsp90α reduction corresponded with a reduction in cell adhesion and reduction in the ability of SW480-HSP90AA1 cells to form spheres *in vitro,* and with a deregulation of the stress response. We hypothesise that this resulted from changes in β-catenin and Hsp27, both of which are involved in cell adhesion formation.

Hsp90α knockdown corresponded to reduced Hsp27 and β-catenin protein levels and a more prominent Hsp90/β-catenin association in complex with Hsp27. Initially, we considered that Hsp27 was involved in the Wnt pathway through β-catenin. If we accept that β-catenin associates with Hsp27 (Fanelli *et al.,* 2008), we can speculate that based on the reduction of protein, changes to cell adherence, morphology and TS formation observed, the knockdown of Hsp90α did not influence β-catenin signaling through modulation of the Wnt/β-catenin pathway, but through its association with Hsp27. We suggest that the deregulation of Hsp27

following Hsp90α knockdown influences the association of Hsp27 with β-catenin, and subsequently influences the role of β-catenin in cell adhesion and EMT. In support of this, we found no difference in the treatment effects between Hsp90α knockdown and control cells after modulation of the Wnt/β-catenin pathway through inhibition by IQ-1, SB-216763 or quercitin. In the p38MAPK-MAPKAPK2-Hsp27 pathway, Hsp27 has been associated with the survival of colorectal tumour-initiating (CSC) under hypoxic and serum-depleted conditions (Vidyasagar *et al*., 2012; Lin *et al.,* 2012). The reduction of Hsp27 subsequent to Hsp90α knockdown was thereby implicated in the reduced sphere-formation of these cells due the cytoprotective roles of Hsp27.

The upregulation of Hsp90 in cancers and interaction with cell surface receptors, such as MMP2 and CD91, is associated with the growth, survival and spread of cancerous cells (Ciocca and Calderwood, 2005; Eustace et al., 2004; Cheng et al., 2008). Hsp90 is a validated drug target in cancer therapy due to the importance of Hsp90 in cell motility and invasion, features necessary for the metastatic spread of cancer. While cell-impermeable Hsp90 agonists have seen success in vitro, blocking tumour cell motility and invasion (Tsutsumi et al., 2008; Snigireva et al., 2014), specific targets for Hsp90 by isoform (Hsp90α, Hsp90β, TRAP1 or Grp94) have yet to be developed. This is the first to demonstrate the use of shRNA for the reduction of Hsp90α by knockdown in colon cancer cells in vitro.

The use of genetically paired colon cancer cell lines facilitated a study of the role of Hsp90 in cancer and CSC biology in relation to the cellular changes associated with the development of a metastatic phenotype. Hsp90α knockdown corresponded to reduced Hsp27 and β-catenin, supporting a role for Hsp90 and Hsp27 in the Wnt complex of colon cancer cells. Reduced cell adhesion and a lack of influence on Wnt/β-catenin signaling by Hsp90α knockdown suggested that the influence of Hsp90α knockdown on the reduction of β-catenin was not at the transcriptional level as anticipated, but rather from the pool of β-catenin association with cell adhesion, mediated by a simultaneous depletion of Hsp27.

The findings of this report support a role for Hsp90 in colon cancer biology and propose the use of isoform-specific targeting of Hsp90α for the controlled reduction of protein *in vitro*. The impact of this research, as it pertains to the management and treatment of patients, would greatly be improved by the translation of this research from model cell lines with limited application *in vitro* to pre-clinical animal models (*in vitro*) prior to the consideration of targeting of Hsp90α in the clinical setting.

Recommendations for Future Work

To address the relevance of using putative CSC from cell lines to model tumour progression, a greater importance of alternative markers for identifying CSC should be addressed. To improve the impact of these research findings additional cell line pairs representative of genetically matched pre-metastatic and metastatic colon cancers should be considered, either from commercially available resources (if available) or primary colon cancer specimens.

We used wound healing as a measure of cell migration potential and utilised *in vitro* techniques, such as serum-free anchorage-independent sphere culture, to address the tumourigenicity of a cancer cell lines. However to investigate the true tumourigenic and invasive potential of cells further investigation is required. Xenotransplanted cells *in vivo* (using animal models) demonstrate tumourigenicity by metastatic potential through cell invasion, migration and tumour initiation (Wong *et al.,* 2007; Chen *et al.,* 2012). Some consideration should be given to the use of *in vivo* experimentation to further demonstrate the pre-clinical relevance of our investigation into the effects of Hsp90 targeting on colon cancer progression (Hsu *et al.,* 2013).

Cell lines derived from single progenies of the SW480 cell line have demonstrated different invasive and metastatic potential of colon cancers (Li *et al*., 2010). In addition to our analysis of Hsp90α knockdown in colon cancer SW480 cells, we initiated investigation to demonstrate the effects of Hsp90α targeting in non-neoplastic immortalised HEK293FT cells. As a proof-of-concept, due to the ease of transfection, HEK293FT polyclonal NT and HSP90AA1 shRNA knockdown cell lines were transduced and expanded *in vitro*. The HEK293FT-HSP90AA1 and HEK293FT-NTshRNA polyclonal cell lines demonstrated successful Hsp90α knockdown after 72 H of 1 µg/ml doxycycline (see Supplementary Figure S4).

Using these HEK293FT-HSP90AA1 and HEK293FT-NTshRNA polyclonal cell lines we hope to demonstrate the same response in Hsp27 and β-catenin reduction upon Hsp90α knockdown. Further investigation using the HEK293FT-HSP90AA1 and HEK293FT-NTshRNA cell lines may better define the relationship between Hsp90α, Hsp27 and β-catenin in an Hsp90α knockdown model without influence of the Wnt pathway activation by APC truncation, such as was demonstrated by the colon cancer NT and HSP90AA1 shRNA knockdown cell lines (Brocardo *et al.,* 2005; Yang *et al.,* 2006).

Using Hsp90α knockdown models, we may begin to speculate on whether Hsp90 preferentially influences the adhesive or transcriptional roles of β-catenin, although our data suggest the former. To account for potential off-target effects that may explain the relationship between Hsp90α, Hsp27 and β-catenin, a series of different sequences of shRNA specific to

Hsp90α could be studied to demonstrate a similar response. The impact of this research may benefit from investigation of whether Hsp90 isoform-specificity may influence the association of Hsp27 with β-catenin, by *in vitro* immunoprecipitation assays. Furthermore, surface plasmon resonance may elucidate on the binding affinities between the Hsp90, Hsp27 and β-catenin proteins.

Chapter 6: References

Reference List

Abdullah, L.N. and Chow, E.K.-H. (2013). Mechanisms of chemoresistance in cancer stem cells. Clinical and translational medicine. 2 (1), 3.

Adams, R.L. and Przyborski, S.A. (2012). Developing a novel 3D migration model to study colon cancer cell invasion. European Cells and Materials. 23, 92.

Albane`se, V., Yam, A.Y., Baughman, J., Parnot, C. and Frydman, J. (2006). Systems analyses reveal two chaperone networks with distinct functions in eukaryotic cells. Cell. 124, 75 – 88.

Alcindor, T. and Beauger, N. (2011). Oxaliplatin: a review in the era of molecularly targeted therapy. Current Oncology. 18 (1). (http://www.current-oncology.com/index.php/oncology/article/view/708/600).

Al-Hajj, M., Wicha, M.S., Benito-Hernandez, A., Morrison, S.J. and Clarke, M.F. (2003). Prospective identification of tumorigenic breast cancer cells. PNAS. 100 (7), 3983 – 3988.

Allikmets, R., Gerrard, B., Hutchinson, A. and Dean, M. (1996). Characterization of the human ABC superfamily: isolation and mapping of 21 new genes using the expressed sequence tags database. Hum. Mol. Genet. 5, 1649 – 1655.

American Cancer Society. Cancer Facts & Figures (2015). American Cancer Society Inc., Atlanta.

Anderson, E.C., Hessman, C., Levin, T., Monroe, M. and Wong, M. (2011). The role of colorectal cancer stem cells in metastatic disease and therapeutic response. 3 (1), 319 – 339.

Aplin, A.E., Howe, A.K. and Juliano, R.L. (1999). Cell adhesion molecules, signal transduction and cell growth. Current Opinion in Cell Biology. 11, 737 – 744.

Atlasi, Y., Mowla, S.J., Ziaee, S.A.M. and Bahrami, A.-R. (2007). OCT-4, an embryonic stem cell marker, is highly expressed in bladder cancer. International journal of cancer. 120, 1598 – 1602.

Azoitei, N., Hoffmann, C., Ellegast, J, Ball, C., Obermayer, K. *et al.* (2012). Targeting of KRAS mutant tumors by Hsp90 inhibitors involves degradation of STK33. Journal of Experimental Medicine. 209 (4), 679 – 711.

Bagatell, R. and Whitesell, L. (2004). Altered Hsp90 function in cancer: a unique therapeutic opportunity. Mol Cancer Ther. 3, 1021 – 1030.

Bao, S., Ouyang, G., Bai, X., Huang, Z., Ma, C. *et al.* (2004). Periostin potentially promotes metastatic growth of colon cancer by augmenting cell survival via the Akt/PKB pathway. Cancer Cell. 5, 329 – 339.

Barker, N. and Clevers, H. (2006). Mining the wnt pathway for cancer therapeutics. Nature Rev. 5, 997 – 1014.

Bartsch, J.E., Starren, E.D. and Appert, H.E. (2003). Adhesion and migration of extracellular matrix stimulated breast cancer. J. Surg. Res. 110, 287 – 294.

Basso, A.D., Solit, D.B., Chiosis, G., Giri, B., Tsichlis, P. *et al.* (2002). Akt forms an intracellular complex with heat shock protein 90 (Hsp90) and Cdc37 and is destabilized by inhibitors of Hsp90 function. J. Biol. Chem. 277, 39858 – 39866.

Basu, S., Binder, R.J., Ramalingam, T. and Srivastava, P.K. (2001). CD91 is a common receptor for heat shock proteins gp96, hsp90, hsp70, and calreticulin. Immunity. 14, 303 – 313.

Beck, B. and Blanpain, C. (2013). Unravelling cancer stem cell potential. Nature reviews. Cancer. 13 (10), 727 – 738.

Beck, R., Verrax, J., Gonze, T., Zappone, M., Pedrosa, R.C. *et al.* (2009). Hsp90 cleavage by an oxidative stress leads to its client proteins degradation and cancer cell death. Biochem. Pharmacol. 77, 375 – 383.

Becker, B., Multhoff, G., Farkas, B., Wild, P.J., Landthaler, M. *et al.* (2004). Induction of Hsp90 protein expression in malignant melanoma metastases. Exp. Dermatol. 13, 27 – 32.

Behrens, J. (1999). Cadherins and catenins: role in signal transduction and tumor progression. Cancer Metastasis Rev.18, 15 – 30.

Beliakoff, J., Paine-Murrieta, G., Taylor, C.W., Lykkesfeldt, A.E. and Whitesell, L. (2003). Hormonerefractory breast cancer remains sensitive to the antitumor activity of heat shock protein 90 inhibitors. Clin. Cancer Res. 9, 4961 – 4971.

Belkacemi, L. and Hebb, M.O. (2014). HSP27 Knockdown Produces Synergistic Induction of Apoptosis by HSP90 and Kinase Inhibitors in Glioblastoma Multiforme. Anticancer Research. 34, 4915 – 4927.

Bisson, I. and Prowse, D.M. (2009). WNT signaling regulates self-renewal and differentiation of prostate cancer cells with stem cell characteristics. Cell research. 19 (6), 683 – 697.

Bjerkner, M. and Cheng, H. (1999). Clonal analysis of mouse intestinal epithelial progenitors. Gastroenterology. 116, 7 – 14.

Blagosklonny, M.V. (2002). Hsp-90-associated oncoproteins: Multiple targets of geldanamycin and its analogs. Leukaemia. 16, 455 – 462.

Bonnet, D. and Dick, J. (1997). Human acute myeloid leukemia is organized as a hierarchy that originates form a primitive hematopoietic cell. Nat. Med. 3, 730 – 737.

Boman, B.M., Wicha, M., Fields, J.Z. and Runquist, O.A. (2007). Symmetric division in cancer stem cells: A key mechanism in tumor growth that should be targeted in future therapeutic approaches. Clin. Pharmacol. Ther. 81, 892 – 898.

Boman, B.M. and Wicha, M. (2008). Cancer stem cells: A step toward the cure. Journal of Clinical Oncology. 26, 2795 – 2799.

Bonnet D. and Dick J.E. (1997). Human acute myeloid leukemia is organized as a hierarchy that originates from a primitive hematopoietic cell. Nature Medicine. 3, 730 – 737.

Botchkina, I.L., Rowehl, R., Rivadenira, D., Karpeh, M., Crawfore, H. *et al*. (2009). Phenotypic subpopulations of metastatic colon cancer stem cells: genomic analysis. Cancer genomics & proteomics. 6 (1), 19 – 29.

Brabletz, T., Jung, A., Spaderna, S., Hlubek, F. and Kirchner, T. (2005). Opinion: migrating cancer stem cells - an integrated concept of malignant tumour progression. Nature reviews Cancer. 5 (9),744 – 749.

Bradley, E., Bieberich, E., Mivechi, N., Tangpisuthipongsa, D. and Wang, G. (2012). Regulation of Embryonic Stem Cell Pluripotency by Heat Shock Protein 90. Stem Cells. 30 (8), 1624 – 1633.

Brakebusch, C. and Fassler, R. (2003). The integrin–actin connection, an eternal love affair. Embo J. 22, 2324 – 2333.

Brehme, M. Voisine, C., Rolland, T., Wachi, S., Soper, J. *et al.* (2014). A Chaperome Subnetwork Safeguards Proteostasis in Aging and Neurodegenerative Disease. Cell Reports. 9 (3),1135 – 1150.

Brocardo, M., Näthke, I.S. and Henderson, B.R. (2005). Redefining the subcellular location and transport of APC: new insights using a panel of antibodies. EMBO Rep. 6 (2), 184 – 190.

Brown, (2001). Wnt signaling in breast cancer: have we come full circle? Breast Cancer Res. 3, 351 – 355.

Brown, M.D., Gilmore, P.E., Hart, C.A., Samuel, J.D., Ramani, V.A. *et al.* (2007). Characterization of benign and malignant prostate epithelial Hoechst 33342 side populations. Prostate, 67, 1384 – 1396.

Buchner, J. (1999). Hsp90 & Co. – a holding for folding. Trends Biochem. Sci. 24, 136 – 142.

Buick, R.N. and Pollak, M.N. (1984). Perspectives on clonogenic tumor cells, stem cells, and oncogenes. Cancer Research. 44 (11), 4909 – 4918.

Burlison, J. A., Avila, C., Vielhauer, G., Lubbers, D. J., Holzbeierlein, J and Blagg, B. S. (2008). Development of novobiocin analogues that manifest antiproliferative activity against several cancer cell lines. The Journal of Organic Chemistry. 73, 2130 – 21.

Cadigan, K.M. and Nusse, R. (1997). Wnt signalling: a common theme in animal development. Genes Dev. 11, 3286 – 3305.

Calderwood, S. (2005). Regulatory interfaces between the stress protein response and other gene expression programs in the cell. Methods. 35, 139 – 148.

Calderwood, S., Khaleque, M.A., Sawyer, D.B., and Ciocca, D.R. (2006). Heat shock proteins in cancer: chaperones of tumorigenesis. Trends Biochem. Sci. 31, 164 – 172.

Calvet, C.Y., André, F.M. and Mir, L.. (2014). The culture of cancer cell lines as tumorspheres does not systematically result in cancer stem cell enrichment. PloS one. 9 (2), p.e89644.

Cao, L. Zhou, Y., Zhai, B., Liao, J., Xu, W. *et al.* (2011). Sphere-forming cell subpopulations with cancer stem cell properties in human hepatoma cell lines. BMC gastroenterology. 11 (1), 71.

Carpentino, J.E., Hynes, M.J., Appleman, H., Tong, Z., Steindler, D. *et al.* (2009). Aldehyde dehydrogenase-expressing colon stem cells contribute to tumorigenesis in the transition from colitis to cancer. Cancer Research. 69 (23), 8208 – 8215.

Chambers, A.F., Groom, A.C. and MacDonald, I.C. (2002). Metastasis: dissemination and growth of cancer cells in metastatic sites. National Review Cancer. 2, 563 – 572.

Chen, H., Paradies, N.E., Fedor-Chaiken, M. and Brackenbury, R. (1997). E-cadherin mediates adhesion and suppresses cell motility via distinct mechanisms. Journal of Cell Science. 110, 345 – 356.

Chen, J.S., Hsu, Y.M., Chen, C.C., Chen, L.L., Lee, C.C. and Huang, T.S. (2010). Secreted heat shock protein 90α induces colorectal cancer cell invasion through CD91/LRP-1 and NF-kappaB-mediated integrin αV expression. J. Biol. Chem. 285, 25458 – 25466.

Chen, L.L., Blumm, N., Christakis, N.A., Barabasi, A.L. and Deisboeck, T.S. (2009). Cancer metastasis networks and the prediction of progression patterns. British Journal of Cancer. 101, 749 – 758.

Chen, S.F., Nieh, S., Jao, S.W., Liu, C.L., Wu, C.H. *et al.* (2012). Quercetin Suppresses Drug-Resistant Spheres via the p38 MAPK-Hsp27 Apoptotic Pathway in Oral Cancer Cells. PLoS one. 7(11).

Cheng, C.F., Fan, J., Fedesco, M., Guan, S., Li, Y. *et al*. (2008). Transforming growth factor alpha (TGFα) stimulated secretion of HSP90alpha: using the receptor LRP-1/CD91 to promote human skin cell migration against TGFβ-rich environment during wound healing. Mol. Cell. Biol. 28, 3344 – 3358.

Chiosis, G. Timaul, M.N., Lucas, B., Munster, P.N., Zheng, F.F. *et al.* (2001). A small molecule designed to bind to the adenine nucleotide pocket of Hsp90 causes Her2 degradation and the growth arrest and differentiation of breast cancer cells. Chem. Biol. 8, 289 – 299.

Chow, A.Y. (2010). Cell Cycle Control by Oncogenes and Tumor Suppressors: Driving the Transformation of Normal Cells into Cancerous Cells. Nature Education. 3 (9), 7.

Christofori, G. (2003) Changing neighbours, changing behaviour: cell adhesion molecule-mediated signalling during tumour progression. EMBO J.22, 2318 – 23.

Ciocca, D.R. and Calderwood, S.K. (2005). Heat shock proteins incancer: Diagnostic, prognostic, predictive, and treatment implications. Cell Stress Chaperones. 10, 86 – 103.

Clarke, M.F., Dick, J.E., Dirks, P.B., Eaves, C.J., Jamieson, C.H.M., Jones, D.L., Visvader, J., Weissman, I.L. and Wahl, G.M. (2006). Cancer stem cells – Perspectives on current status and future directions: AACR workshop on cancer stem cells. Cancer Research. 66, 9339 – 9344.

Clarke, M.F. and Fuller, M. (2006). Stem cells and cancer: Two faces of eve. Cell. 124, 1111 – 1115.

Cohnheim, J. (1867). Ueber entzundung und eiterung. Path Anat Physiol Klin Med. 40, 1 – 79.

Collins, A.T., Berry, P.A., Hyde, C., Stower M.J. and Maitland, N.J. (2005). Prospective identification of tumourigenic prostate cancer stem cells. Cancer Res. 65 (23), 10946 - 10951.

Collins, A.T., Habib, F.K., Maitland, N.J. and Neal, D.E. (2001) Identification and isolation of human prostate epithelial stem cells based on alpha (2) beta (1)-integrin expression. J Cell Sci. 114, 3865 – 3872.

Collins, K., Jacks, T. and Pavletich, N.P. (1997). The cell cycle and cancer. PNAS. 94, 2776–2778.

Collins, T.S., Lee, L.F. and Ting, J.P. (2000). Paclitaxel upregulates interleukin-8 synthesis in human lung carcinoma through a NFκB and AP-1 -dependent mechanism. Cancer Immunol Immunother. 49, 79 – 84.

Collura, A., Marisa, L. Trojan, D., Buhard, O., Lagrange, A. *et al.* (2013). Extensive characterization of sphere models established from colorectal cancer cell lines. Cellular and Molecular Life Sciences. 70, 729 – 742.

Connell, P., Ballinger, C.A., Jiang, J., Wu, Y., Thompson, L.J. *et al.* (2001). The co-chaperone CHIP regulates protein triage decisions mediated by heat-shock proteins. Nature Cell Biology. 3, 93 – 96.

Cooper, L. C., Prinsloo, E., Edkins, A.L. and Blatch, G.L. (2011) Hsp90alpha/beta associates with the GSK3beta/axin1/phospho- beta-catenin complex in the human MCF-7 epithelial breast cancer model. Biochem Biophys Res Commun. 413, 550 – 554.

Crawford, H.C., Fingleton, B.M., Rudolph-Owen, L.A., Goss, K.J., Rubinfeld, B. *et al.* (1999). The metalloproteinase matrilysin is a target of β-catenin transactivation in intestinal tumours. Oncogene. 18, 2883 – 2891.

Crocker, A.K. and Allan, A.L. (2008). Cancer stem cells: Implications for the progression and treatment of metastatic disease. J. Cell. Mol. Med. 12, 374 – 390.

Dalerba, P., Dylla, S.J., Park, I.K., Liu, R., Wang, X. *et al*. (2007). Phenotypic characterization of human colorectal cancer stem cells. PNAS. 104, 10258 – 10163.

Daniel, S., Bradley, G., Longshaw, V.M., Soti, C., Csermely, P. *et al.* (2008). Nuclear translocation of the phosphoprotein Hop (Hsp70/Hsp90 organising protein) occurs under heat shock, and its proposed nuclear localization signal is involved in Hsp90 binding. Biochim. Biophys. Acta. 1783, 1003 – 1014.

Danjo, Y. and Gipson, I.K. (1998). Actin 'purse string' filaments are anchored by E-cadherin-mediated adherens junctions at the leading edge of the epithelial wound, providing coordinated cell movement. J. Cell Sci. 111, 3323 – 3332.

Dean, M., Fojo, T. and Bates, S. (2005). Tumour stem cells and drug resistance. Nature Reviews Cancer. 5, 275 – 284.

Debatin, K.M. and Krammer, P.H. (2004). Death receptors in chemotherapy and cancer. Oncogene. 23, 2950 – 2966.

de la Mare, J.A., Sterrenberg, J.N., Sukhthankar, M., Chiwakata, M., Beukes, D. *et al.* (2013). Assessment of potential anti-cancer stem cell activity of marine algal compounds using an *in vitro* mammosphere assay. Cancer cell international. 13 (1), 39.

Dezwaan, D.C. and Freeman, B.C. (2008). HSP90: the Rosetta stone for cellular protein dynamics? Cell Cycle. 7, 1006 – 1012.

DiCara, D., Rapisarda, C., Sutcliffe, J.L, Violette, S.M., Weinreb, P.H. *et al*. (2007). Structure-function analysis pf RGD-helix motifs in alpha v beta 6 integrin ligands. Journal of Biological Chemistry. 282, 9657 – 9665.

Dick, J.E. (2008). Stem cell concepts renew cancer research. Blood. 112, 4793 – 4807.

Dick, J.E. (2009). Looking ahead in cancer stem cell research. Nat Biotechnol. 27, 44 – 46.

Di Francesco, A., Ruggiero, A. and Riccardi, R. (2002). Cellular and molecular aspects for drugs of the future: oxaliplatin. Cell Mol. Life Sci. 59, 1914 – 27.

Dontu, G., Abdallah, W.M., Foley, J.M., Jackson, K.W., Clarke, M.F. *et al*. (2003). *In vitro* propagation and transcriptional profiling of human mammary stem/progenitor cells. Genes and Development. 17, 1253 – 1270.

Dontu, G., Al-Hajj, M., Abdallah, W.M., Clarke, M.F. and Wicha, M.S. (2003). Stem cells in normal breast development and breast cancer. Cell Proliferation. 36 (1), 59–72.

Dontu, G., El-Ashry, D. and Wicha, MS. (2004). Breast cancer, stem/progenitor cells and the estrogen receptor. Trends Endocrinol. Metab. 15, 193 – 197.

Doshi, B.M., Hightower, L.E. and Lee, J. (2009). The role of Hsp27 and actin in the regulation of movement in human cancer cells responding to heat shock. Cell Stress and Chaperones. 14, 445 – 457.

Dou, J., Pan, M., Wen, P., Li, Y., Tang, Q. *et al*. (2007). Isolation and identification of cancer stem-like cells from murine melanoma cell lines. Cellular and Molecular Immunology. 4, 467 – 472.

Duranton, B., Holl, V., Schneider, Y, Carnesecchi, S., Gossé, F. *et al*. (2003). Polyamine metabolism in primary human colon adenocarcinoma cells (SW480) and their lymph node metastatic derivatives (SW620). Amino Acids. 24, 63 – 72.

Eckert, L.B., Repasky, G.A., Ulku, A.S., McFall, A., Zhou, H. *et al*. (2004). Involvement of Ras Activation in Human Breast Cancer Cell Signaling, Invasion, and Anoikis. Cancer Research. 64, 4585 – 4592.

Egorin, M.J., Sentz, D.L., Zuhowski, E.G., Dobson, J.M., Schulte, T.W. *et al*. (1999). PC3 human prostate xenograft retention of, and oncoprotein modulation by 17(allylamino)-17demothoxygeldanamycin (17AAG) *in vivo.* Proc. Am. Assoc. Cancer Res. 40, 3409.

Eramo, A., Lotti, F., Sette, G., Pilozzi, E., Biffoni, M. *et al.* (2008). Identification and expansion of the tumorigenic lung cancer stem cell population. Cell Death Differ. 15, 504 – 514.

Eskew, J.D., Sadikot, T., Morales, P., Duren, A., Dunwiddie, I. *et al.* (2011). Development and characterization of a novel C-terminal inhibitor of Hsp90 in androgen dependent and independent prostate cancer cells. BMC Cancer. 11 (1), 468.

Eustace, B.K., Sakurai, T., Stewart, J.K., Yimlamai, D., Unger, C., *et al.* (2004). Functional proteomic screens reveal an essential extracellular role for hsp90 α in cancer cell invasiveness. Nature Cell Biol. 6, 507 – 514.

Fan, C.Y., Lee, S. and Cyr, D.M. (2003). Mechanisms for regulation of Hsp70 function by Hsp40. Cell Stress & Chaperones. 8, 309 – 316.

Fanelli, M.A., Montt-Guevara, M., Diblasi, A.M., Gago, F.E., Tello, O. *et al.* (2008). P-cadherin and beta-catenin are useful prognostic markers in breast cancer patients; beta-catenin interacts with heat shock protein Hsp27. Cell stress & chaperones. 13, 207 – 220.

Fang, D.D., Kim, Y, Lee, C., Aggarwal, S. McKinnon, K. *et al*. (2010). Expansion of CD133(+) colon cancer cultures retaining stem cell properties to enable cancer stem cell target discovery. British journal of cancer. 102 (8), 1265 – 1275.

Fidler, I.J. (2003). The pathogenesis of cancer metastasis: the 'seed and soil' hypothesis revisited. Nature Review Cancer. 3, 453 – 458.

Fillmore, C.M. and Kuperwasser, C. (2008). Human breast cancer cell lines contain stem cell-like cells that self-renew, give rise to phenotypically diverse progeny and survive chemotherapy. Breast Cancer Res. 10, R25 (doi: 10.1186/bcr1982).

Fink, A.L. (2004). Chaperone-mediated protein folding. Physiol. Rev. 79, 425 – 449.

Fitzgerald, T.L., Rangan, S., Dobbs, L., Starr, S. and Sigounas, G. (2014). The impact of Aldehyde dehydrogenase 1 expression on prognosis for metastatic colon cancer. Journal of Surgical Research. 192 (1), 82 – 89.

Flaherty, K., DeLuca-Flaherty, C and McKay, D. (1990). Three-dimensional structure of the ATPase fragment of a 70K heat-shock cognate protein. Nature. 346, 623 - 628.

Fleming, W.H., Alpern, E.J., Uchida, N., Ikuta, K. and Weissman, I.L. (1993). Steel factor influences the distribution and activity of murine hematopoietic stem cells *in vivo*. PNAS USA. 90, 3760 – 3764.

Freedman, V.H. and Shin, S. (1974). Cellular tumorigenicity in nude mice: correlation with cell growth in semisolid medium. Cell. 3, 355 – 359.

Frisch, S.M. and Francis, H. (1994). Disruption of epithelial cell-matrix interaction induces apoptosis. Journal of Cell Biology. 124, 619 – 626.

Futschik, M., Jeffs, A., Pattison, S., Kasabov, N., Sullivan, M. *et al*. (2002). Gene expression profiling of metastatic and non metastatic colorectal cancer cell lines. Genome Lett. 1, 26 – 34.

Gava, L.M. and Ramos, C.H.I. (2009). Human 90 kDa Heat Shock Protein Hsp90 as a Target for Cancer Therapeutics. 3, 330–341

Georgopolis, C. and Welch, W.J. (1993) Role of the major heat shock proteins as molecular chaperones. Annu. Rev. Cell Biol. 9, 601 – 634.

Gerbin, C.S. and Landgraf, R. (2010). Geldanamycin selectively targets the nascent form of ERBB3 for degradation. Cell Stress & Chaperones. 15, 529 – 544.

Ghosh, D., Yu, H., Tan, X.F., Lim, T.K., Zubaidah, R.M. *et al*. (2011). Identification of key players for colorectal cancer metastasis by iTRAQ quantitative proteomics profiling of isogenic SW480 and SW620 cell lines. Journal of Proteome Research. 10, 4373 – 4387.

Giacchetti S, Perpoint B, Zidani R, Le Bail, N., Faggiuolo, R., *et al*. (2000). Phase III multicenter randomized trial of oxaliplatin added to chronomodulated fluorouracil-leucovorin as first-line treatment of metastatic colorectal cancer. J. Clin. Oncol. 18, 136 – 147.

Golebiewska, A., Brons, N., Bjerkvig, R and Niclou, S. (2011). Critical appraisal of the side population assay in stem cell and cancer stem cell research. Cell Stem Cell. 8 (2), 136 – 47.

Goodsell, D.S. (1999). The molecular perspective: p53 tumor suppressor. The Oncologist. 4, 138 – 139.

Goodell, M.A., Brose, K., Paradis, G., Conner, A.S. and Mulligan, R.C. (1996). Isolation and functional properties of murine hematopoietic stem cells that are replicating in vivo. J. Exp. Med. 183, 1797 – 1806.

Gottardi, C.J. and Gumbiner, B.M. (2004). Distinct molecular forms of beta-catenin are targeted to adhesive or transcriptional complexes. J Cell Biol. 167(2), 339 – 49.

Grad, I., Cederroth, C. R., Walicki, J., Grey, C., Barluenga, S., Winssinger, N., De Massy, B., Nef, S. and Picard, D. (2010). The molecular chaperone Hsp90α is required for meiotic progression of spermatocytes beyond pachytene in the mouse. PLoS ONE 5, e15770.

Grady, W.M. (2006). Genomic instability and colorectal cancer. Current Colorectal Cancer Reports. 2, 66 – 71.

Grassilli, E., Ianzano, L., Bonomo, S., Missaglia, C., Cerrito, M. *et al.* (2014). GSK3A Is Redundant with GSK3B in Modulating Drug Resistance and Chemotherapy-Induced Necroptosis. PloS one. 9 (7), e100947.

Greene, H.S.N., 1951. A Conception of Tumor Autonomy Based on Transplantation Studies : A Review. Cancer Research. 11, 899 – 903.

Guo, W. and Giancotti, F.G. (2004). Integrin signalling during tumour progression. Nature Reviews Molecular Cell Biology. 5, 816 – 826.

Gupta, G.P. and Massague, J. (2006). Cancer metastasis: building a framework. Cell. 127, 679 – 695.

Hamad, N.M., Banik, S.S.R. and Counter, C.M. (2002). Mutational analysis defines a minimum level of telomerase activity required for tumourigenic growth of human cells. Oncogene. 21, 7121 – 7125.

Han, L., Shi, S., Gong, T., Zhang, Z. and Sun, X. (2013). Cancer stem cells: therapeutic implications and perspectives in cancer therapy. Acta Pharmaceutica Sinica B. 3 (2), 65 – 75.

Han, M.-E, Oh, S. (2013). Gastric stem cells and gastric cancer stem cells. Anatomy & Cell Biology. 46 (1), 8 – 18.

Hanahan, D. and Weinberg, R.A. (2000). The Hallmarks of Cancer. Cell Press. 100, 57 – 70.

Hanahan, D. and Weinberg, R.A. (2011). Hallmarks of cancer: The next generation. Cell 144 (5), 646 – 674.

Haraguchi, N., Utsunomiya, T., Inoue, H., Tanaka, F., Mimori, K. *et al.* (2006). Characterisation of a side population of cancer cells from human gastrointestinal system. Stem Cells. 24, 506 – 513.

Harris, T.J.C. and Peifer, M. (2005). Decisions, decisions: β-catenin chooses between adhesion and transcription. Trends in Cell Biology. 15, 234 – 237.

Hay, E.D. and Zuk, A. (1995) Transformations between epithelium and mesenchyme: normal, pathological, and experimentally induced. Am. J. Kidney Dis. 26, 678 – 690.

He, T.C., Sparks, A.B., Rago, C., Hermeking, H., Zawel, L. *et al.* (1998). Identification of c-MYC as a target of the APC pathway. Science. 281, 1509 – 1512.

Hendrick, J.P., Langer, T., Davis, T.A., Hartl, F.U., and Wiedmann, M. (1993). Control of folding and membrane translocation by binding of the chaperone DnaJ to nascent polypeptides. PNAS USA. 90, 10216 – 10220.

Hermann, P.C., Huber, S.L., Herrler, T., Aicher, A., Ellwart, J.W. *et al.* (2007). Distinct populations of cancer stem cells determine tumor growth and metastatic activity in human pancreatic cancer. Cell Stem Cell. 1, 313 – 323.

Hewitt, R.E., McMarlin, A., Wersto, R., Martin, P., Tsoskas, M. *et al.* (2000). Validation of a model of colon cancer progression. The Journal of Pathology. 192 (4), 446 – 454.

Hieronymus, H., Lamb, J., Ross, K.N., Peng, X.P., Clement, C. *et al.* (2006). Gene expression signature-based chemical genomic prediction identifies a novel class of HSP90 pathway modulators. Cancer Cell. 10, 321 – 330.

Ho, M.M., Ng, A.V., Lam, S. and Hung, J.Y. (2007). Side population in human lung cancer cell lines and tumors is enriched with stem-like cancer cell. Cancer Research. 67, 4827 – 4833.

Hollingshead, M., Alley, M., Burger, A.M., Borgel, S., Pacula-Cox, C. *et al.* (2005) *In vivo* antitumor efficacy of 17-DMAG (17-dimethylaminoethylamino-17-demethoxygeldanamycin hydrochloride), a water-soluble geldanamycin derivative. Cancer Chemotherapy and Pharmacology. 56, 115 – 125.

Holt, S.E., Aisner, D.L., Baur, J., Tesmer, V.M., Dy, M., Ouellette, M. *et al.* (1999). Functional requirement of p23 and Hsp90 in telomerase complexes. Genes Devel. 13, 817 – 824.

Hood, J.D. and Cheresh, D.A. (2002). Role of integrins in cell invasion and migration. Nature Reviews Cancer. 2, 91 – 100.

Horst, D., Scheel, S.K., Liebmann, S., Neumann, J., Maatz, S. *et al.* (2009). The cancer stem cell marker CD133 has high prognostic impact but unknown functional relevance for the metastasis of human colon cancer. Journal of Pathology. 219, 427 – 434.

Hostein, I., Robertson, D., DiStefano, F., Workman, P. and Clarke, P.A. (2001). Inhibition of signal transduction by the Hsp90 inhibitor 17-allylamino-17-demethoxygeldanamycin results in cytostasis and apoptosis. Cancer Research. 61, 4003 – 4009.

Hsu, C.S., Tung, C.Y. and Lin, C.H. (2013). Response to stress in early tumor colonization modulates switching of CD133-positive and CD133-negative subpopulations in a human metastatic colon cancer cell line, SW620. PloS one. 8 (4), e61133.

Hsu, H.S., Lin, J.H., Huang, W.C., Hsu, T.W., Su, K. *et al.* (2011). Chemoresistance of lung cancer stem like cells depends on activation of Hsp27. Cancer. 117, 1516 – 1528.

Huang, E.H., Hynes, M.J., Zhang, T., Ginestier, C., Dontu, G. *et al.* (2009). Aldehyde dehydrogenase 1 is a marker for normal and malignant human colonic stem cells (SC) and tracks SC overpopulation during colon tumorigenesis. Cancer Res. 69, 3382 – 3389.

Huang, H. and He, X. (2008). Wnt/β-catenin signaling: new (and old) players and new insights. Curr. Opin. Cell Biol. 20, 119 – 125.

Huang, S.D., Yuan, Y., Tang, H., Liu, X.H., Fu, C.G. *et al.* (2013). Tumor cells positive and negative for the common cancer stem cell markers are capable of initiating tumor growth and generating both progenies. PloS one. 8 (1), e54579.

Hughes, L., Malone, C., Chumsri, S., Burger, A. and McDonnell, S. (2008). Characterisation of breast cancer cell lines and establishment of a novel isogenic subclone to study migration, invasion and tumourigenicity. Clinical & experimental metastasis. 25 (5), 549 – 557.

Hunter, M.C., O'Hagan, K.L., Kenyon, A., Dhanani, K.C.H., Prinsloo, E. *et al.* (2014). Hsp90 Binds Directly to Fibronectin (FN) and Inhibition Reduces the Extracellular Fibronectin Matrix in Breast Cancer Cells. PLoS one. 9(1). e86842.

Huntly, B.J.P. and Gilliland, D.G. (2005). Leukemia stem cells and the evolution of cancer-stem-cell research. Nat Rev Cancer. 5, 311 – 321.

Hynes, R.O. (2002). Integrins: Bidirectional, allosteric signalling machines. Cell. 110, 673 – 687.

Illmensee, K. And Mintz, B. (1976). Totipotency and normal differentiation of single teratocarcinoma cells cloned by injection into blastocysts. PNAS USA. 73, 549 – 553.

Imai, T., Kato, Y., Kajiwara, C., Mizukami, S., Ishige, I. *et al.* (2011). Heat shock protein 90 (HSP90) contributes to cytosolic translocation of extracellular antigen for cross-presentation by dendritic cells. PNAS USA. 108, 16363 – 16368.

Isaacs, J.S., Jung, Y., Mimnaugh, E.G., Martinez, A., Cuttitta, F. *et al.* (2002). Hsp90 regulates a von Hippel Lindau-independent hypoxia-inducible factor-1 α-degradative pathway. J. Biol. Chem. 277, 29936 – 29944.

Jemal, A., Siegel, R., Xu, J. and Ward, E. (2010). Cancer statistics. CA Cancer J. Clin. 60, 277 – 300.

Jemal, A., Siegel, R., Ward, E., Murray, T., Xu, J., Smigal, C. and Thun, M.J. (2006). Cancer statistics. A Cancer Journal for Clinicians. 56, 106 – 130.

Jin, L.H., Shao, Q.J., Luo, W., Ye, Z.Y. and Li, S.C. (2003). Detection of point mutations of the *Axin1* gene in colorectal cancers. Int. J. Cancer. 107, 696 – 699.

Kamal, A., Thao, L., Sensintaffar, J., Zhang, L., Boehm, M.F. *et al.* (2003). A high-affinity conformation of Hsp90 confers tumour selectivity on Hsp90 inhibitors. Nature. 425, 407 – 410.

Kang, Y. and Massague, J. (2004). Epithelial–mesenchymal transitions: twist in develop- ment and metastasis. Cell.118, 277 – 9.

Karzai, A.W., and MaMacken, R. (1996). A bipartite signaling mechanism involved in DnaJ-mediated activation of the Escherichia coli DnaK protein J. Biol. Chem. 271, 11236 – 11246.

Katoah, M. (2006). Bioinformatics for cancer management in the post-genome era. Technol. Cancer Res. Treat. 5, 169 – 176.

Katoh, M. and Katoh, M. (2007). Wnt signalling pathway and stem cell signalling network. Clin. Cancer Res. 13, 4042 – 4045.

Katoh, M., Koninkx, J. and Schumacher, U. (2000). Heat shock protein expression in human tumours grown in severe combined immunodeficient mice. Cancer letters. 161, 113 – 120.

Kaufmann, S.H.E. (1990). Heat-shock proteins and the immune response. Immunol. Today. 11, 129 – 207.

Kelly, W.L. (1999). Molecular chaperones: how J domains turn on Hsp70s. Current Biology, 9, 305 – 308.

Kim, R.H., Kim, R., Chen, W., Hu, S., Shin, K.H. *et al.* (2008). Association of hsp90 to the hTERT promoter is necessary for hTERT expression in human oral cancer cells. Carcinogenesis. 29, 2425 – 2431.

Kim, Y.S., Alarcon, S.V., Lee, S., Lee, M.J., Giaccone, G. *et al.* (2009). Update on Hsp90 inhibitors in clinical trial. Curr. Top. Med. Chem. 9, 1479 – 1492.

Kimelman, D. and Xu, W. (2006). B-catenin destruction complex: insights and questions from a structural persepective. Oncogene. 25, 7482 – 7491.

Kirchner, T. and Brabletz, T. (2000). Patterning and nuclear β-catenin expression in the colonic adenoma-carcinoma sequence. Analogies with embryonic gastrulation. Am. J. Pathol. 157, 1113 – 1121.

Klein, C.A. (2008). Cancer the metastasis cascade. Nature. 321, 1785 – 1787.

Klco, J.M., Spencer, D., Miller, C., Griffith, M., Lamprecht, T. *et al*. (2014). Functional heterogeneity of genetically defined subclones in acute myeloid leukemia. Cancer cell. 25 (3), 379 – 392.

Klonisch, T., Wiechec, E., Hombach-Klonisch, S., Ande, S.R., Wesselborg, S. *et al.* (2008). Cancer stem cell markers in common cancers – therapeutic implications. Trends in Molecular Medicine. 14, 450 – 460.

Kolquist, K.A., Ellisen, L.W., Counter, C.M., Meyerson, M *et al.* (1998). Expression of TERT in early premalignant lesions and a subset of cells in normal tissues. Nature Genet. 19, 182 – 186.

Komiya, Y. and Habas, R. (2008). Wnt signal transduction pathways. Organogenesis. 4(2), 68 - 75.

Koponen, J.K., Kankkonen, H., Kannasto, J., Wirth, T., Hillen, W. *et al.* (2003). Doxycycline-regulated lentiviral vector system with a novel reverse transactivator rtTA2 S -M2 shows a tight control of gene expression in vitro and *in vivo*. , 459 – 466.

Koshiba, T., Hosotani, R., Miyamoto, Y., Ida, J., Tsuji, S. *et al.* (2000). Expression of stromal cell-derived factor 1 and CXCR4 ligand receptor system in pancreatic cancer: A possible role for tumor progression. Clin. Cancer Res. 6, 3530 – 3535.

Kotiligam, D., Lazat, A.J., Pollock, R.E. and Lev, D. (2008). Desmoid tumour: a disease opportune for molecular insights. Histol. Histopathol. 23, 117 – 126.

Kregel, K.C. (2001). Molecular Biology of Thermoregulation Invited Review: Heat shock proteins: modifying factors in physiological stress responses and acquired thermotolerance. J. Appl. Physiol. 92, 2177 – 2186.

Kreso, A. and Dick, J.E. (2014). Evolution of the Cancer Stem Cell Model. Cell Stem Cell. 14 (3), 275 – 291.

Kreso, A. and O'Brien, C.A. (2008). Colon Cancer Stem Cells. Current Protocols in Stem Cell Biology. Wiley Interscience. John Wiley & Sons, Inc. (doi: 10.1002/9780470151808.sc0301s7).

Kubota, H., Yamamoto, S., Itoh, E., Abe, Y., Nakamura, A. *et al*. (2010). Increased expression of co-chaperone HOP with HSP90 and HSC70 and complex formation in human colonic carcinoma. Cell Stress Chaperones 15, 1003 – 1011.

Kumar, V., Fausto, N. and Abbas, A. (2005). Robbins and Cotran Pathological Basis of Disease. Seventh ed. Elsevier Inc., Philadelphia, PA.

Laemmli, U.K (1970). Cleavage of structural proteins during the assembly of the head of bacteriophage T4. Nature. 227, 680 – 685.

Lagerstedt Robinson K., Liu, T., Vandrovcova, J., Halvarsson, B., Clendenning, M. *et al*. (2007). Lynch syndrome (hereditary nonpolyposis colorectal cancer) diagnostics. J. Natl. Cancer Inst. 99, 291 – 299.

Laird, D.J, von Andrian, U.H. and Wagers, A.J. (2008). Stem cell trafficking in tissue development, growth and disease. Cell. 132, 612 – 630.

Lajkó, E., Polgár, L., Láng, O., Lengyel, J., Kóhidai, L. *et al*. (2012). Basic cell physiological activities (cell adhesion, chemotaxis and proliferation) induced by selegiline and its derivatives in Mono Mac 6 human monocytes. Journal of Neural Transmission. 119 (5), 545 – 556.

Langan, R.C., Mullinax, J., Raiji, M., Upham, T. Summers, T. *et al*. (2013). Colorectal cancer biomarkers and the potential role of cancer stem cells. Journal of Cancer. 4 (3), 241 – 250.

Lapidot, T., Sirard, C., Vormoor, J., Murdoch, B., Hoang, T. *et al*. (1994). A cell initiating human acute myeloid leukaemia after transplantation into SCID mice. Nature. 367, 645 – 648.

Lawson, J.C., Blatch, G.L. and Edkins, A.L. (2009). Cancer stem cells in breast cancer and metastasis. Breast Cancer Research and Treatment. 118 (2), 241 - 254.

Lee, C.H., Hong, H.M., Chang, Y.Y. and Chang, W.W. (2012). Inhibition of heat-shock protein (Hsp) 27 potentiates the suppressive effect of Hsp90 inhibitors in targeting breast cancer stem-like cells. Biochimie. 94, 1382 – 1389.

Lee, J.W., Kwak, H.J., Lee, J.J., Kim, Y.N., Lee, J.W. *et al*. (2008). HSP27 regulates cell adhesion and invasion via modulation of focal adhesion kinase and MMP-2 expression. European Journal of Cell Biology. 87, 377 – 387.

Leibovitz, A., Stinson, J.C., McCombs, W.B., McCoy, C.E., Mazur, K.C. *et al*. (1976). Classification of human colorectal adenocarcinomas cell lines. Cancer Research. 36, 4562 – 4569.

Le Roy, C. And Wrana, J.L. (2005). Clathein- and non-clatherin mediated endocytic regulation of cell signalling. Nature Reviews Molecular Cell Biology. 6, 112 – 126.

Levesque, J.P., Hendy, J., Takamatsu, Y., Simmons, P.J., and Bendall, L.J. (2003). Disruption of the CXCR4/CXCL12 chemotactic interaction during hematopoietic stem cell mobilization induced by GCSF or cyclophosphamide. J. Clin. Invest. 111, 187 – 196.

Li, G., Liu, C., Yuan, J., Xiao, X., Tang, N. *et al.* (2010). CD133(+) single cell-derived progenies of colorectal cancer cell line SW480 with different invasive and metastatic potential. Clinical & Experimental Metastasis. 27 (7), 517 – 527.

Li, J., Soroka, J. and Buchner, J. (2012). The Hsp90 chaperone machinery: Conformational dynamics and regulation by co-chaperones. BBA Molecular Cell Research. 1823 (3), 624 – 635.

Li, W., Li, Y., Guan, S., Fan, J., Cheng, C.F. *et al.* (2007). Extracellular heat shock protein-90α: linking hypoxia to skin cell motility and wound healing. EMBO J. 26, 1221 – 1233.

Lin, S.P., Lee, Y.T., Wang, J.Y., Miller, S.A. Chiou, S.H. *et al.* (2012). Survival of cancer stem cells under hypoxia and serum depletion via decrease in PP2A activity and activation of p38-MAPKAPK2-Hsp27. PloS one. 7 (11), e49605.

Lindquist, S. and Craig, E.A. (1988). The heat shock proteins. Annu. Rev. Genet. 22, 631 – 637.

Liu, G., Yuan, X., Zeng, Z., Tunici, P. Ng, H. *et al*. (2006). Analysis of gene expression and chemoresistance of CD133+ cancer stem cells in gioblastoma. Mol. Cancer. 5, 67.

Liu, S., Dontu, G., Mantle, I.D., Patel, S., Ahn, N. *et al*. (2006). Hedgehog signaling and BMi-1 regulate self-renewal of normal and malignant human mammary stem cells. Cancer Research. 66, 6063 – 6071.

Liu, S., Dontu, G. and Wicha, M.S. (2005). Mammary stem cells, self-renewal pathways and carcinogenesis. Breast Cancer Research. 7, 86 – 95.

Liu, S., Cong, Y., Wang, D., Sun, Y., Deng, L. *et al.* (2014). Breast Cancer Stem Cells Transition between Epithelial and Mesenchymal States Reflective of their Normal Counterparts. Stem Cell Reports. 2 (1), 78 - 91.

Longley, D.B. and Johnston, P.G. (2005). Molecular mechanisms of drug resistance. The Journal of Pathology. 205 (2), 275 – 292.

Longshaw, V.M., Baxter, M., Prewitz, M. and Blatch, G.L. (2009). Knockdown of the co-chaperone Hop promotes extranuclear accumulation of Stat3 in mouse embryonic stem cells. The European Journal of Cell Biology. 88, 153 – 166.

López, J., Poitevin, A., Mendoza-Martinez, V., Pérez-Plasencia, C. and García-Carrancá, A. (2012). Cancer-initiating cells derived from established cervical cell lines exhibit stem-cell markers and increased radioresistance. BMC Cancer. 12 (1), 48.

Lu, X., Wang, X., Zhuo, W., Jia, L., Jiang, Y. *et al*. (2014). The regulatory mechanism of a client kinase controlling its own release from Hsp90 chaperone machinery through phosphorylation. The Biochemical Journal. 457 (1), 171 – 183.

Mak, I.W., Evaniew, N. and Ghert, M. (2014). Lost in translation: animal models and clinical trials in cancer treatment. American Journal of Translational Research. 6 (2), 114 – 118.

Maloney, A. and Workman, P. (2002). HSP90 as a new therapeutic target for cancer therapy the story unfolds. Expert. Opin. Biol. Ther. 2, 3 – 24.

Mani, S.A., Yang, J., Brooks, M., Schwaninger, G., Zhou, A. *et al*. (2007). Mesenchymal Forkhead 1 (FOXC2) plays a key role in metastasis and is associated with aggressive basal-like breast cancers. PNAS USA. 104, 10069 – 10074.

Månsson, C., Kakkar, V., Monsellier, E., Sourigues, Y., Härmark, J. et al. (2014). DNAJB6 is a peptide-binding chaperone which can suppress amyloid fibrillation of polyglutamine peptides at substoichiometric molar ratios. Cell Stress & Chaperones. 19 (2), 227 – 239.

Many, A.M. and Brown, A.M.C. (2014). Both canonical and non-canonical Wnt signaling independently promote stem cell growth in mammospheres. PloS one. 9 (7), e101800.

Marchesi, F. Monti, P., Leonne, B.E., Zerbi, A., Vecchi, A. *et al*. (2004). Increased survival, proliferation, and migration in metastatic human pancreatic tumor cells expressing functional CXCR4. Cancer Research. 64, 8420 – 8427.

Marcu, M.G., Chadli, A., Bouhouche, I., Catelli, M. and Neckers, L.M. (2000). The heat shock protein 90 antagonist novobiocin interacts with a previously unrecognized ATP-binding domain in the carboxyl terminus of the chaperone. Journal of Biological Chemistry. 275, 37181 – 37186.

Marcu, M.G., Schulte, T.W. and Neckers, L. (2000). Novobiocin and related coumarins and depletion of heat shock protein 90-dependent signaling proteins. Journal of the National Cancer Institute. 92(3), 242 – 248.

Martin, J., and Hartl, F. U. (1997). Chaperone-assisted protein folding. Curr. Opin. Struct. Biol. 7, 41–52 9.

Martin, S.S. and Leder, P. (2001). Human MCF 10A mammary epithelial cells undergo apoptosis following actin depolymerisation that is independent of attachment and rescued by Bcl-2. Mol. Cel. Biol. 21, 6529 – 6536.

Martin, S.S. and Vuori, K. (2004). Regulation of Bcl-2 proteins during anoikis and amorphosis. Biochim. Biophys. Acta. 1692, 145 – 157.

Matthews, S.B., Vielhauer, G.A., Manthe, C.A., Chaguturu, V.K., Szabla, K. *et al*. (2010). Characterization of a novel novobiocin analogue as a putative C-terminal inhibitor of heat shock protein 90 in prostate cancer cells. Prostate. 1, 27 – 36.

McCulloch, J.E. and Till, J.E. (2005). Perspectives on the properties of stem cells. Nature Medicine. 11, 1026 – 1028.

Mehlen, P. and Puisieux, A. (2006). Metastasis: A question of life or death. Nature Reviews Cancer. 6, 449 – 458.

Melcher, R., Steinlein, C., Feichtinger, W., Müller, C.R., Menzel, T. *et al*. (2000). Spectral karyotyping of the human colon cancer cell lines SW480 and SW620. Cytogenetics Cell Genetics. 88, 145 - 152.

Menezes, M.E. (2014). The Wnt / β -catenin Signaling Pathway in Epithelial Mesenchymal Transition. Journal of Postdoctoral Research. 2 (7), 1 – 12.

Mitra, A., Menezes, M.E., Pannell, L.K., Honkanen, R.E., Shevde, L.A. and Samat, R.S. (2012). DNAJB6 chaperones PP2A mediated dephosphorylation of GSK3β to downregulate β-catenin transcription target, osteopontin. Oncogene. 11 (41), 4472 – 4483.

Mitra, A., Menezes, M.E., Shevde, L.A. and Samat, R.S. (2010). DNAJB6 induces degradation of beta-catenin and causes partial reversal of mesenchymal phenotype. The Journal of biological chemistry. 285 (32), 24686 – 24694.

Mitra, A., Fillmore, R., Metge, B., Rajesh, M., Xi, Y. *et al.* (2008). Large isoform of MRJ (DNAJB6) reduces malignant activity of breast cancer. Breast cancer research: BCR. 10 (2), R22.

Miyabayashi, T., Teo, J.L., Yamamoto, M., McMillan, M., Nguywn, C. *et al*. (2007). Wnt/beta-catenin/CBP signaling maintains long-term murine embryonic stem cell pluripotency. PNAS. 104, 5668 – 5673.

Molofsky, A.V., Pardal, R. And Morrison, S.J. (2004). Diverse mechanisms regulate stem cell self-renewal. Curr. Opin. Cell. Biol. 16, 700 - 707.

Moreno-Bueno, G., Portillo, F., and Cano, A. (2008). Transcriptional regulation of cell polarity in EMT and cancer. Oncogene. 27, 6958 - 6969.

Morin, P.J. Sparks, A.B., Kornek, V., Barker, N., Clevers, H. *et al*. (1997). Activation of β-catenin-Tcf signaling in colon cancer by mutations in β-catenin or APC. Science. 275, 1787 – 1790.

Morita, R., Nishizawa, S., Torigoe, T., Takahashi, A., Tamura, Y. *et al.* (2014). Heat shock protein DNAJB8 is a novel target for immunotherapy of colon cancer-initiating cells. Cancer science. (doi: 10.1111/cas. 12362)

Morrow, D., Cullen, J.P., Liu, W., Guha, S., Sweeney, C. *et al*. (2009). Sonic hedgehog induces Notch target gene expression in vascular smooth muscle cells via VEGF-A. Arterioscler. Thromb. Vasc. Biol. 29, 1112 – 1118.

Moser, C., Lang, S., Kainz, S., Gaumann, A., Fichtner-Feigl, S. *et al*. (2007). Blocking heat shock protein-90 inhibits the invasive properties and hepatic growth of human colon cancer cells and improves the efficacy of oxaliplatin in p53-deficient colon cancer tumors *in vivo*. Molecular cancer therapeutics. 6 (11), 2868 – 2878.

Munshi, H.G. and Stack, M.S. (2006). Reciprocal between adhesion receptor signalling and MMP regulation. Cancer and Metastasis Reviews. 25, 45 – 56.

Munster, P.N., Marchion, D.C., Basso, A.D. and Rosen, N. (2002). Degradation of HER2 by ansamycins induces growth arrest and apoptosis in cells with HER2 overexpression via a HER3, phosphatidylinositol 3'-kinase-AKT-dependent pathway. Cancer Res. 62, 3132 – 3137.

Nagai, N., Nakai, A. and Nagata, K. (1995). Quercetin Suppresses Heat Shock Response by Down-Regulation of HSF1. Biochemical and Biophysical Research Communications. 208 (3), 1099 – 1105.

Nagaraju, G.P., Alese, O.B., Landry, J., Diaz, R. and El-rayes, B.F. (2014). HSP90 inhibition downregulates thymidylate synthase and sensitizes colorectal cancer cell lines to the effect of 5FU-based chemotherapy. Oncotarget. 5 (20), 9980 – 9991.

Naor, D., Nedvetzki, S., Golan, I., Melnik, L. and Faitelson, Y. (2007). CD44 in cancer. Crit Rev Clin Lab Sci. 39, 527 – 579.

Naylor, M.J., Li, N., Cheung, J., Lowe, E.T., Lambert, E. *et al*. (2005). Ablation of beta1 integrin in mammary epithelium reveals a key role for integrin in glandular morphogenesis and differentiation. Journal of Cell Biology. 171, 717 – 728.

Neckers, L. (2002). Hsp90 inhibitors as novel cancer chemotherapeutic agents. Trends in molecular medicine. 8 (4), 55 – 61.

Nikolopoulos, S.N., Blaikie, P., Yoshioka, T., Guo, W. and Giancotti, F.G. (2004). Integrin beta4 signalling promotes tumor angiogenesis. Cancer Cell. 6, 471 – 483.

Nowell, P.C. (1976). The clonal evolution of tumour cell populations. Science. 194, 23 – 28.

O'Brien, C.A., Pollett, A., Gallinger, S. and Dick, J.E. (2007). A human colon cancer cell capable of initiating tumor growth in immunodeficient mice. Nature, 445, 106 – 110.

Oda, K., Okada J., Timmerman, L., Rodriguez-Viciana, P., Stokoe, D. *et al*. (2008). PIK3CA cooperates with other phosphatidylinositol 3′-kinase pathway mutations to effect oncogenic transformation. Cancer Research. 68(19), 8127 – 8136.

Ohtsuka, K. and Hata, M. (2000). Mammalian HSP40/DNAJ homologs: cloning of novel cDNAs and a proposal for their classification and nomenclature. Cell Stress & Chaperones. 5, 98 – 112.

Osheroff, N., Shelton, E.R. and Brutlag, D.L. (1983). DNA topoisomerase II from Drosophila melanogaster. Relaxation of supercoiled DNA. The Journal of Biological Chemistry. 258(15), 9536 – 9543.

Oshima, H., Rochat, A., Kedzia, C., Kobayashi, K. and Barrandon, Y. (2001). Morphogenesis and renewal of hair follicles from adult multipotent stem cells. Cell. 104, 233–245.

Ouhtit, A., Elnageed, Z.Y.A., Abdraboh, M.E., Lioe, T.F. and Raj, M.H.G. (2007). *In vivo* evidence for the role of CD44s in promoting breast cancer metastasis. The American Journal of Pathology. 171, 2033 – 2039.

Overall, C.M. and Lopez-Otin, C. (2002). Strategies for MMP inhibition in cancer: innovations for the post-trial era. Nat. Rev. Cancer. 2, 657 – 672.

Panaretou, B., Prodromou, C., Roe, S.M., O'Brien, R., Ladbury, J.E. *et al*. (1998). ATP binding and hydrolysis are essential to the function of the Hsp90 molecular chaperone in vivo. EMBO J. 17, 4829 – 4836.

Parcellier, A., Schmitt, E., Brunet, M., Hammann, A., Solary, E. *et al*. (2005). Small Heat Shock Proteins Hsp27 and AlphaBeta-Crystallin: Cytoprotective and Oncogenic Functions. Antioxidants & Redox Signaling. 7(3), 404 – 413.

Parsons, B.L. (2008). Many different tumor types have polyclonal tumor origin: evidence and implications. Mutation Research. 659 (3), 232 – 247.

Patel, K., Piagentini, M., Rascher, A., Tian, Z.Q. Buchanan, G.O. *et al*. (2004). Engineered biosynthesis of geldanamycin analogs for Hsp90 inhibition. Chemistry & Biology. 11, 1625 – 1633.

Patrawala, L., Calhoun, T., Schneider-Broussard, R., Li, H., Bhatia, B. *et al*. (2006). Highly purified $CD44^+$ prostate cancer cells from xenograft human tumors are enriched in tumourigenic and metastatic progenitor cells. Oncogene. 25, 1696 – 1708.

Pearl, L. H and Prodromou, C. (2006). Structure and mechanism of the Hsp90 molecular chaperone machinery. Annual Review of Biochemistry. 75, 271 – 294.

Peifer, M. and Polakis, P. (2000). Wnt signaling in oncogenesis and embryogenesis – a look outside the nucleus. Science. 287, 1606 – 1609.

Perdew, G.H., Hord, N., Hollenback, C.E. and Welsh, M.J. (1993). Localization and characterization of the 86- and 84-kDa heat shock proteins in Hepa 1c1c7 cells. Exp. Cell Res. 209, 350 – 356.

Petit, P.X. (2002). Flow cytometric analysis of Rhodamine 123 fluorescence during modulation of the membrane potential in plant mitochondria. Plant Physiology. 98, 279 – 286.

Pichon, S., Bryckaert, M. and Berrou, E. (2004). Control of actin dynamics by p38 MAP kinase - Hsp27 distribution in the lamellipodium of smooth muscle cells. Journal of Cell Science. 117, 2569 – 2577.

Polakis, P. (2000). Wnt signalling and cancer. Genes Dev. 14, 45 – 51.

Polakis, P. (2007). The many ways of Wnt in cancer. Curr. Opin. Genet. Dev. 17, 45 – 51.

Polakis, P. (2012). Wnt signaling in cancer. Cold Spring Harb. Perspect Biol., 2012. 4(5).

Ponta, H., Wainwright, D. and Herrlich, P. (1998). The CD44 protein family. Int. J. Biochem. Cell Biol. 30, 299 – 305.

Ponti, D., Costa, A., Zaffaroni, N., Pierotti, G., Petrangolini, G. *et al*. (2005). Isolation and in vitro propagation of tumorigenic breast cancer cells with stem/progenitor cell properties. Cancer Research. 65, 5506 – 5511.

Powers, M.V. and Workman, P. (2006). Targeting of multiple signalling pathways by heat shock protein 90 molecular chaperone inhibitors. Endocrine-Related Cancer. 13, S125 – S135.

Powers, M.V. and Workman, P. (2007). Inhibitors of the heat-shock response: biology and pharmacology. FEBS Lett. 581, 3758- 3769.

Pratt, W.B., Galigniana, M.D., Harrell, J.M. and De Franco, D.B. (2004). Role of hsp90 and the hsp90-binding immunophilins in signal protein movement. Cell. Signal. 16, 857 – 872.

Pratt, W.B. and Toft, D.O. (2003). Regulation of signalling protein function and trafficking by the hsp90/hsp70-based chaperone machinery. Exp. Biol. Med. 228, 111 – 133.

Preet, R., Mohapatra, P., Mohanty, S., Sahu, S.K., Choudhuri, T. *et al*. (2012). Quinacrine has anticancer activity in breast cancer cells through inhibition of topoisomerase activity. International Journal of Cancer. 130, 1660 – 70.

Price, M.A. (2006). CK1, there's more than one: casein kinase family 1 members in Wnt and Hedgehog signaling. Genes Dev. 20, 399 – 410.

Prinsloo, E., Setati, M.M., Longshaw, V.M. and Blatch, G.L. (2009). Chaperoning stem cells: a role for heat shock proteins in the modulation of stem cell self-renewal and differentiation? BioEssays. 31, 370 – 377.

Prodromou, C., Panaretou, B., Chohan, S., Siligardi, G., O'Brien, R. *et al*. (2000). The ATPase cycle of Hsp90 drives a molecular 'clamp' via transient dimerization of the N-terminal domains. EMBO J. 19, 4384 – 4392.

Prodromou, C., Roe, S.M., O'Brien, R., Ladbury, J.E., Piper, P.W. *et al*. (1997). Identification and structural characterization of the ATP/ADP-binding site in the Hsp90 molecular chaperone. Cell. 90, 65 – 75.

Proia, D.A., Foley, K.P., Korbut, T., Sang, J., Smith, D. *et al*. (2011). Multifaceted intervention by the Hsp90 inhibitor ganetespib (STA-9090) in cancer cells with activated JAK/STAT signaling. PLoS one. 6, e18552.

Qiang, L., Yang, Y., Ma, Y.J., Chen, F.H., Ahang, L.B. *et al*. (2009). Isolation and characterisation of cancer stem like cells in human glioblastoma cell lines. Blood. 91, 2272.

Ramsay, A.G., Marshall, J.F. and Hart, I.R. (2007). Integrin trafficking and its role in cancer metastasis. Cancer Metastasis. 26, 567 – 578.

Reddig, P.J. and Juliano, R.L. (2005). Clinging to life: Cell to matrix adhesion and cell survival. Cancer and Metastasis Reviews. 24, 425 – 439.

Reya, T. and Clevers, H. (2005). Wnt signaling in stem cells and cancer. Nature. 434, 843 – 850.

Reya T., Duncan, A.W., Ailles, L., Domen, J., Scherer, D.C. *et al*. (2003). A role for Wnt signalling in self-renewal of haematopoietic stem cells. Nature. 423, 409 – 414.

Reya, T., Morrison, S.J., Clarcke, M.F. and Weissman, I.L. (2001). Stem cells, cancer, and cancer stem cells. Nature. 414, 105 – 111.

Ricci-Vitiani, L., Fabrizi, E., Palio, E. and De Maria, R. (2009). Colon cancer stem cells. J. Mol. Med. 87, 1097 – 1104.

Ricci-Vitiani, L., Lombardi, D., Pilozzi, E., Biffoni, M., Todaro, M. *et al*. (2007). Identification and expansion of human colon-cancer-initiating cells. Nature. 445 (4), 111 – 115.

Richardson G.D., Robson C.N., Lang S.H., Neal, D.E., Maitland, N.J. *et al*. (2004). CD133, a novel marker for human prostatic epithelial stem cells. J Cell Sci. 117, 3539 – 3545.

Richter, K. and Buchner, J. (2001). Hsp90: Chaperone signal transduction. J. Cell Physiol. 188, 281 – 290.

Ritossa, F. (1962). A new puffing pattern induced by temperature shock and DNP in drosophila. Experientia. 18(12), 571 – 573.

Rixe, O., Ortuzar, W., Alvarez, M., Parker, R., Reed, E. *et al*. (1996). Oxaliplatin, tetraplatin, cisplatin and carboplatin: spectrum of activity in drug-resistant cell lines and in cell lines of the National Cancer Institute's Anticancer Drug Screen panel. Biochem. Pharmacol. 52(12),1855 – 1865.

Rogalla, T., Ehrnsperger, M., Preville, X., Kotlyarov, A., Lutsch G., *et al*. (1999). Regulation of Hsp27 Oligomerization, Chaperone Function, and Protective Activity against Oxidative Stress / Tumor Necrosis Factor α by Phosphorylation. The Journal of biological chemistry. 274 (27), 18947 – 18956.

Saigusa, S., Tanaka, K., Toiyama, Y., Yokoe, T., Okugawa, Y. *et al*. (2009). Correlation of CD133, OCT4 and SOX2 in rectal cancer and their association with distant recurrence after chemoradiotherapy. Ann. Surg. Oncol. 16, 3488 – 3498.

Saibil, H. (2013). Chaperone machines for protein folding, unfolding and disaggregation. Nat. Rev. Mol. Cell Biol. 14, 630 – 642.

Sauvageot, C.M., Weatherbee, J.L., Kesari, S., Winters, S.E., Barnes, J. *et al.* (2008). Efficacy of the HSP90 inhibitor 17-AAG in human glioma cell lines and tumorigenic glioma stem cells. Neuro. Oncol. 11(2), 109 – 121.

Schulte, T.W., Blagosklonny, M.V., Romanova, L., Mushinski, J.F., Monia, B.P. *et al*. (1996). Destabilization of Raf-1 by geldanamycin leads to disruption of the RAF1-MEK-mitogen-activated protein kinase signalling pathway. Mol. Cell. Biol. 16, 5839 – 5845.

Schneikert, J. and Behrens, J. (2007). The canonical Wnt signalling pathway and its APC partner in colon cancer development. Gut. 56 (3), 417 – 425.

Seaberg, R.M. and Van Der Kooy, D. (2003). Stem and progenitor cells: the premature desertion of rigorous definitions. Trends Neurosci. 26, 125 – 131.

Sell, S. (1993). Cellular origin of cancer: dedifferentiation or stem cell maturation arrest? Environmental Health Perspectives. 101, 15 – 26.

Sell, S. (2004). Stem cell origin of cancer and differentiation therapy. Critical Reviews in Oncology Hematology. 51, 1 – 28.

Setati, M.M., Prinsloo, E., Longshaw, V.M., Murray, P.A., Edgar, D.H. *et al*. (2010). Leukemia inhibitory factor promotes Hsp90 association with STAT3 in mouse embryonic stem cells. IUBMB life. 62 (1), 61 – 6.

Shackleton, M., Vaillant, F., Simpson, K.J., Stingl, J., Smyth, G.K. *et al*. (2006). Generation of a functional mammary gland from a single stem cell. Nature. 439, 84 – 88.

Shackleton, M., Quintana, E., Fearon, E.R. and Morrison, S.J. (2009). Heterogeneity in cancer: cancer stem cells versus clonal evolution. Cell. 138, 822 – 829.

Sherman, M.Y., Gabai, V., O'Callagham, C. and Yaglom, J.T. (2007). Molecular chaperones regulate p53 and suppress senescence programs. FEBS Lett. 581, 3711 – 3715.

Shi, Q., Abbruzzese, J.L., Huang, S., Fidler, I.J., Xiong, Q. *et al*. (1999). Constitutive and inducible interleukin 8 expression by hypoxia and acidosis renders human pancreatic cancer cells more tumorigneic and metastatic. Clin. Cancer Res. 5, 3711 – 3721.

Shmelkov, S.V., Butler, J.M., Hooper, A.T., Hormigo, A., Kushner, J. *et al.* (2008). CD133 expression is not restricted to stem cells, and both CD133+ and CD133- metastatic colon cancer cells initiate tumors. J. Clin. Invest. 118 (6), 2111 – 2120.

Shtutman, M., Zhurinsky, J., Simcha, I., Albanese, C., D'Amico, M. *et al*. (1999). The cyclin D1 gene is a target of the β-catenin/LEF-1 pathway. PNAS USA. 96, 5522 – 5527.

Sidera, K. and Patsavoudi, E. (2008). Extracellular HSP90: conquering the cell surface. Cell Cycle. 7, 1564 – 1568.

Singh, S.K., Clarke, I.D., Terasaki, M., Bonn, V.E., Hawkins, C. *et al*. (2003). Identification of a cancer stem cell in human brain tumors. Cancer Research. 63, 5821 – 5828.

Singh, S.K., Hawkins, C., Clarke, I.D., Squire, J.A., Bayani, J. *et al*. (2004). Identification of human brain tumor initiating cells. Nature. 432, 396 – 401.

Snigireva, A.V., Vrublevskaya, V.V., Skarga, Y.Y., Evdokimovskaya, Y.V. and Morenkov, O.S. (2014). Effect of Heat Shock Protein 90 (Hsp90) on Migration and Invasion of Human Cancer Cells *in Vitro*. Bull. Exp. Biol. Med. 157(4), 476 - 478.

Socinski, M., Goldman, J., El-Hariry, I., Koczywas, M., Vukovic, V. *et al.* (2013). A multicenter phase II study of ganetespib monotherapy in patients with genotypically defined advanced non-small cell lung cancer. Clinical Cancer Research. 19 (11), 3068 – 3077.

Song, X., Wang, X., Zhuo, W., Shi, H., Feng, D. *et al.* (2010). The regulatory mechanism of extracellular Hsp90{alpha} on matrix metalloproteinase-2 processing and tumor angiogenesis. J. Biol. Chem. 285 (51), 40039 – 40049.

Soti, C. and Csermely, P. (2002). Chaperones come of age. Cell Stress Chaperones. 7, 186 – 190.

Soti, C. and Csermely, P. (2003). Aging and molecular chaperones. Exp. Gerontol. 38, 1037 – 1040.

Soti, C., Racz, A. and Csermely, P. (2002). A nucleotide-dependent molecular switch controls ATP binding at the C- terminal domain of Hsp90: N-terminal nucleotide binding unmasks a C- terminal binding pocket. J. Biol. Chem. 277, 7066 – 7075.

Sreedhar, S.A., Kalmar, E., Csermely, P. and Shen, Y.F. (2004). Hsp90 isoforms: functions, expression and clinical importance. FEBS Letters. 562, 11 – 15.

Stepanova, L., Leng, X., Parker, S.B. and Harper, J.W. (1996). Mammalian p50Cdc37 is a protein kinasetargeting subunit of Hsp90 that binds and stabilizes Cdk4. Genes Devel. 10, 1491 – 1502.

Stewart, S.L., Wike, J.M., Kato, I., Lewis, D.R. and Michaud, F. (2006). A population-based study of colorectal cancer histology in the United States, 1993 – 2001. Cancer. 107, 1128 – 1141.

Streuli, C.H. and Gilmore, A.P. (1999). Adhesion-mediated signalling in the regulation of mammary epithelial cell survival. J. Mammary Gland Biol. 4, 183 – 191.

Stingl, J., Eirew, P., Ricketson, I., Shackleton, M., Vaillant, F. *et al.* (2006). Purification and unique properties of mammary epithelial stem cells. Nature. 439, 993 – 997.

Supko, J.G., Hickman, R.L., Grever, M.R. and Malspeis, L. (1995). Preclinical pharmacologic evaluation of geldanamycin as an antitumor agent. Cancer Chemotherapy and Pharmacology. 36, 305 – 315.

Sussman, R.T., Ricci, M.S. and Hart, L.S. (2007). Chemotherapy-Resistant Side-Population of Colon Cancer Cells has a Higher Sensitivity to TRAIL than Non-SP, a Higher Expression of C-Myc and TRAIL Receptor DR4. Cancer Biol. Ther. 6 (9), 1490 – 1495.

Sylvester, K.G. and Longmaker, M.Y. (2004). Stem cells: Review and update. Archives Surgery. 139, 93 – 99.

Takahashi-Yanaga, F. and Kahn, M. (2010). Targeting Wnt signaling: can we safely eradicate cancer stem cells? Clinical Cancer Research. 16 (12), 3153 – 3162.

Tariq, M., Nussbaumer, U., Chen, Y., Beisel, C. and Paro, R. (2009). Trithorax requires Hsp90 for maintenance of active chromatin at sites of gene expression. PNAS USA. 106, 1157 – 1162.

Thiery, J.P. (2002). Epithelial-mesenchymal transitions in tumour progression. Nature Rev. Cancer. 2, 442 – 454.

Thiery, J.P., Acloque, H., Huang, R.Y. and Nieto, M.A. (2009). Epithelial-mesenchymal transitions in development and disease. Cell. 139, 871 – 890.

Tissières, A., Mitchell, H.K. and Tracy, U.M. (1974). Protein synthesis in salivary glands of Drosophila melanogaster: relation to chromosome puffs. Journal of Molecular Biology. 84, 389 – 398.

Todaro, M., Alea, M.P., Di Stefano, A.B., Cammareri, P., Vermeulen, L. *et al.* (2007). Colon cancer stem cells dictate tumor growth and resist cell death by production of interleukin-4. Cell Stem Cell. 1, 389 – 402.

Towbin, H., Staehelin, T. and Gordon, J. (1979). Electrophoresis transfer of proteins from polyacrylamide gels to nitrocellulose sheets: procedure and some applications. PNAS. 76, 4350 – 4354.

Trepel, J., Mollapour, M., Giaccone, G. and Neckers, L. (2010). Targeting the dynamic HSP90 complex in cancer. Nature Rev. 10, 537 – 549.

Tsutsumi, S., Scroggins B, Koga F, Lee MJ, Trepel J. *et al.* (2008). A small molecule cell-impermeant Hsp90 antagonist inhibits tumor cell motility and invasion. Oncogene. 27, 2478 – 2487.

Tucker, G.C. (2006). Integrins: Molecular targets in cancer therapy. Current Oncology Reports. 80, 96 – 103.

Uchida, D., Begum, N.M., Tomizuka, Y., Bando, T., Almofti, A. *et al.* (2004). Acquisition of lymph node, but not distant metastatic potentials, by the overexpression of CXCR4 in human oral squamous cell carcinoma. Lab Invest. 84, 1538 – 1546.

Vacca, A., Ria, R., Presta, M., Ribatti, D., Iurlaro, M., *et al.* (2001). Alpha(v)beta3 integrin engagement modulates cell adhesion, proliferation, and protease secretion in human lymphoid tumor cells. Exp. Hematol. 29, 993 – 1003.

Vasen, H.F.A, Mölsein, G., Alonso, A., Bernstein, I., Bertario, L. *et al*. (2007). Guidelines for the clinical management of Lynch syndrome (hereditary non-polyposis cancer). J. Med. Genet. 44, 353 – 362.

Vassiloploulos, A., Wang, R.H., Petrovas, C., Ambrozak, D., Koup, R. *et al.* (2008). Identification and characterization of cancer initiating cells from BRCA-1 related mammary tumors using markers for normal mammary stem cells. Int. J. Biol. Sci. 4, 133 – 142.

Venter, J.C., Adams, M.D., Myers, E.W., Li, P.W., Mural, R.J. *et al.* (2001). The sequence of the human genome. Science. 291, 1304–1351.

Vermeulen, L., de Sousa, E.M.F., van der Heijden, M., Cameron, K., de Jong, J.H. *et al*. (2010). Wnt activity defines colon cancer stem cells and is regulated by the microenvironment. Nat. Cell Biol. 12, 468 – 476.

Vermeulen, L., Todaro, M., de Sousa Mello, F., Sprick, M.R., Kemper, K. *et al*. (2009). Single-cell cloning of colon cancer stem cells reveals a multi-lineage differentiation capacity. PNAS. 105(36), 13427 – 13432.

Virchow, R. (1855). Die multiloculäre, ulcerirende Echinokokkengeschwulst der Leber. Verhandlungen der Physicalisch-Medicinischen Gesellschaft. Archiv fuer pathologische Anatomie und Physiologie und fuer klinische Medizin, 8, 23.

Vidyasagar, A., Wilson, N.A. and Djamali, A. (2012). Heat shock protein 27 (HSP27): biomarker of disease and therapeutic target . Fibrogenesis & Tissue Repair. 5 (7).

Voloshanenko, E., Erdmann, G., Dubash, T.D., Augustin, I. *et al.* (2013). Wnt secretion is required to maintain high levels of Wnt activity in colon cancer cells. Nature Communications. 4, 2610 (doi: 10.1038/ncomms3610).

Voss, A.K., Thomas, T. and Gruss, P. (2000). Mice lacking HSP90β fail to develop a placental labyrinth. Development. 127, 1 – 11.

Wakefield, J.G., Stephens, D.J. and Tavare, J.M. (2003). A role for glycogen synthase kinase-3 in mitotic spindle dynamics and chromosome alignment. J. Cell Sci.116, 637 – 46.

Wang, L., Xie, C., Greggio, E., Parisiadou, L., Shim, H*. et al.* (2008). The chaperone activity of heat shock protein 90 is critical for maintaining the stability of leucine-rich repeat kinase 2. J. Neurosci. 28, 3384 – 3391.

Waugh, D.J.J. and Wilson, C. (2008). The interleukin-8 pathway in cancer. Clinical Cancer Research. 14 (21), 6735 – 6741.

Waxman, S. and Bruckner, H. (1982). The enhancement of 5-fluorouracil antimetabolic activity by leucovorin, menadione and alpha- tocopherol. Eur. J. Cancer Clin. Oncol. 18, 685 – 692.

Wegele, H., Wandinger, S. K., Schmid, A. B., Reinstein, J. and Buchner, J. (2006). Substrate transfer from the chaperone Hsp70 to Hsp90. J. Mol. Biol. 356, 802 – 811.

Wehrli, W. (1977). Ansamycins. Chemistry, biosynthesis and biological activity. Top Curr. Chem. 72, 21 – 49.

Wei, W., Jobling, W.A., Chen, W., Hahn, W.C. and Sedivy, J.M. (2003). Abolition of Cyclin-Dependent Kinase Inhibitor p16 Ink4a and Growth in Telomerase-Immortalized Human Fibroblasts. 23(8), 2859 – 2870.

Weigeit, B., Peterse, J.L. and van‘t Veer, L. (2005). Breast cancer metastasis: Markers and models. Nature Review Cancer. 5, 591 – 602.

Whitesell, L. and Lindquist, S.L. (2005). HSP90 and the chaperoning of cancer. Nature Reviews. Cancer. 5, 761 – 772.

Wicha, M.S., Liu, S. and Dontu, G. (2006). Cancer stem cells: An old idea – A paradigm shift. Cancer Research. 66, 1883 – 1890.

Wigmore, S.J., Fearon, K.C., Sangster, K., Maingay, J.P., Garden, O.J. *et al.* (2002). Cytokine regulation of constitutive production of interleukin-8 and -6 by human pancreatic cancer cell lines and serum cytokine concentrations in patients with pancreatic cancer. Int. J. Oncol. 21, 881 – 886.

Wong, R.P.C., Ng, P., Dedhar, S. and Li, G. (2007). The role of integrin-linked kinase in melanoma cell migration, invasion, and tumor growth. Molecular Cancer Therapeutics. 6 (6), 1692 – 1700.

Wright, N.A. (2000). Epithelial stem cell repertoire in the gut: clues to the origin of cell lineages, proliferative units and cancer. Int. J. Exp. Pathol. 81, 117 – 143.

Wright, M.H., Calcagno, A.M., Salcido, C.D., Carlson, M.D., Ambudkar, S.V. *et al.* (2008). BRCA1 breast tumors contain distinct $CD44^{+}/CD24^{-}$ and $CD133^{+}$ cells with cancer stem cell characteristics. Breast Cancer Res. 10, R10.

Wu, D., Zhang, R., Zhao, R., Chen, G., Cai, Y. *et al.* (2013). A Novel Function of Novobiocin: Disrupting the Interaction of HIF 1α and p300/CBP through Direct Binding to the HIF1α C-Terminal Activation Domain. PLoS one. 8(5), 1 – 10.

Wu, H., Zhu, S. and Mo, Y.-Y. (2009). Suppression of cell growth and invasion by miR-205 in breast cancer. Cell Research. 19, 439 – 448.

Wu, X., Gan, B., Yoo, Y. And Guan, J.L. (2005). FAK-mediated src phosphorylation of endophilin A2 inhibits endocytosis of MT1-MMP and promotes ECM degradation. Developmental Cell. 9, 185 – 196.

Xu, K., Ma, H., McCown, T.J., Verma, I.M. and Kafri, T. (2001). Generation of a stable cell line producing high-titer self- inactivating lentiviral vectors. Mol. Ther. 3, 97-104.

Yamazaki, D., Kurisu, S. and Takenawa, T. (2005). Regulation of cancer cell motility through actin reorganization. Cancer Sci. 96, 379 – 386.

Yang, J. and Weinberg, R.A. (2008). Epithelial–mesenchymal transition: at the crossroads of development and tumor metastasis. Developmental Cell. 14, 818 – 29.

Yang, J., Zhang, W., Evans, P., Chen, X., He, X. *et al.* (2006). Adenomatous polyposis coli (APC) differentially regulates beta-catenin phosphorylation and ubiquitination in colon cancer cells. The Journal of biological chemistry, 281(26), pp.17751 – 17757.

Yao, C.J., Lai, G.M., Yeh, C.T., Lai, M.T., Shih, P.H. *et al.* (2013). Honokiol Eliminates Human Oral Cancer Stem-Like Cells Accompanied with Suppression of Wnt/ β -Catenin Signaling and Apoptosis Induction. Evidence-based complementary and alternative medicine. 146136. (doi: 10.1155/2013/146136)

Yoshida, A., Rzhetsky, A., Hsu, L.C. and Chang, C. (1998). Human aldehyde dehydrogenase gene family. Eur. J. Biochem. 251, 549 – 557.

Yuan, H., Mao, J., Li, L. and Wu, D. (1999). Suppression of glycogen synthase kinase activity is not sufficient for leukemia enhancer factor-1 activation. J. Biol. Chem. 274 (30), 419 – 423.

Yuan, H., Veldman, T., Rundell, K. and Schlegel, R. (2002). Simian virus 40 small tumor antigen activates AKT and telomerase and induces anchorage-independent growth of human epithelial cells. Journal of virology. 76(21), 10685 – 10691.

Zeilstra, J., Joosten, S.P.J., Dokter, M., Verwiel, E., Spaargaren, M. and Pals, S.T. (2008). Deletion of the WNT target and cancer stem cell marker CD44 in Apc(Min/+) mice attenuates intestinal tumorigenesis. Cancer Research. 68 (10), 3655 – 3661.

Zhang, H. and Burrows, F. (2004). Targeting multiple signal transduction pathways through inhibition of Hsp90. Journal of Molecular Medicine. 82 (8), 488 – 499.

Zhang, T., Otevrel. T., Gao, Z., Ehrlich, S.M., Fields, J.Z. and Bowman, B.M. (2001). Evidence that APC regulates *survivin* expression, a possible mechanism contribution to the stem cell origin of colon cancer. Cancer Research. 61, 8664 – 8667.

Zhao, R. and Houry, W.A. (2008). Hsp90: a chaperone for protein folding and gene regulation. Biochem. Cell Biol. 83, 703 – 710.

Zhou, S., Schuetz, J.D., Bunting, K.D., Sampath, A.M.J., Morris, J.J. *et al.* (2001). The ABC transporter Bcrp1/ABCG2 is expressed in a wide variety of stem cells and is a molecular determinant of the side-population phenotype. Nature Medicine. 7, 1028 – 1034.

Zhou, J., Wang, C.Y., Liu, T., Wu, B., Zhou, F. *et al.* (2008). Persistence of side population cells with high drug efflux capacity in pancreatic cancer. World J. Gastroenterol. 14, 925 – 930.

Zhu, X.T., Zhao, X., Burkholder, W.F., Gragerov, A., Ogata, C.M. *et al.* (1996). Structural analysis of substrate binding by the molecular chaperone DnaK. Science. 272, 1606 – 1614.

Zlotnik, A. and Yoshie, O. (2000). Chemokines: A new classification system and their role in immunity. Immunity. 12, 121 – 127.

Zou, J., Guo, Y., Guettouche, T., Smith, D.F. and Voellmy, R. (1998). Repression of heat shock transcription factor HSF1 activation by HSP90 (HSP90 complex) that forms a stress-sensitive complex with HSF1. Cell. 94, 471 – 480.

Chapter 7: Supplementary Information

Supplementary Methodology

Mammalian cell transfection of siRNA

For isoform-specific targeting of Hsp90 (alpha and beta, independently) transient transfections with siRNA targeting Hsp90α (M-005186-02), Hsp90β (M-005187-02) or a non-targetting siRNA (D-001206-13-05) were analysed in SW480 and SW620 cells. Cells were grown to between 70 and 80 % confluence in 24-well plates under serum-free conditions. To transfect cells, each well was treated with 1 µl Lipofectamine® 2000 Transfection Reagent and 125 nM siRNA, diluted in OptiMEM (Gibco, Invitrogen, UK)as indicated by the manufacturer's instructions (www.lifetechnologies.com/support). Cells were incubated for 24 H at 37°C prior to medium replacement. After 24 H the cells were lysed and the effects of transient transfection of siRNA were compared to that of mock-transfected cells by SDS-PAGE and Western blotting.

Supplementary Results

A

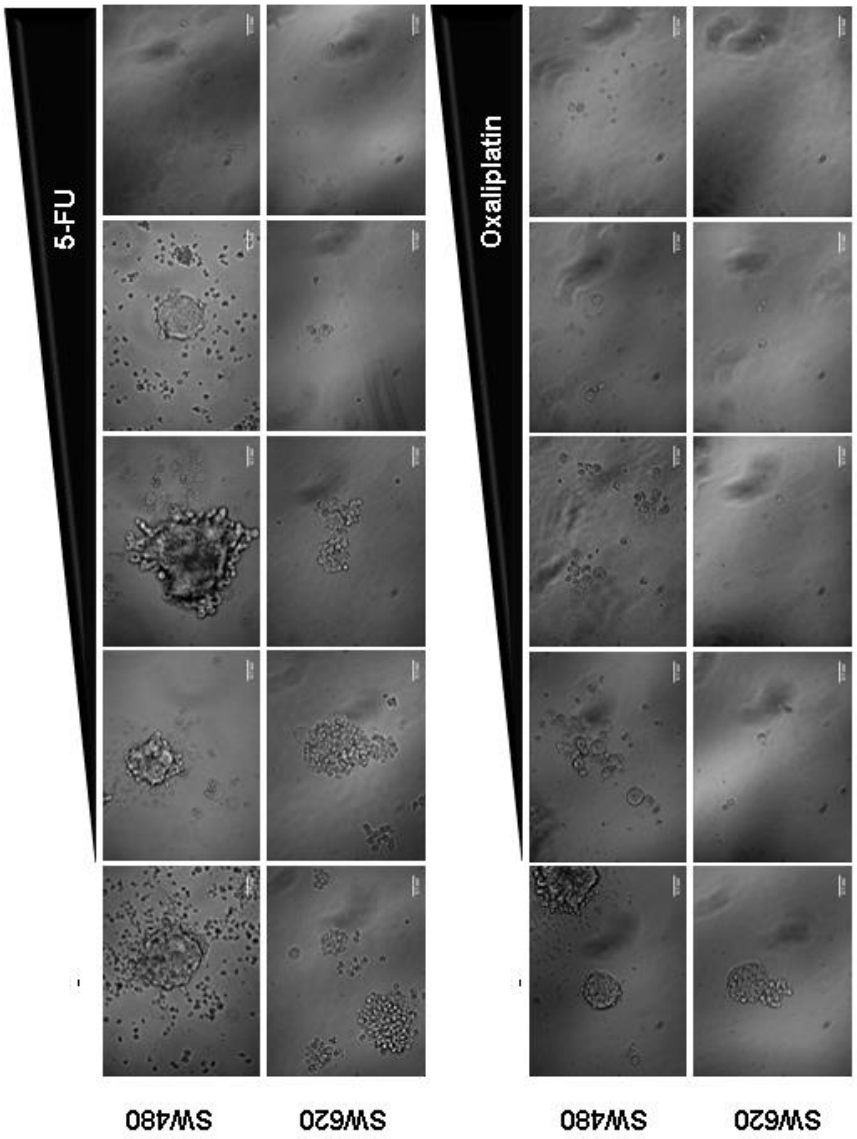

Figure S1. Chemosensitivity of cells to Hsp90 inhibition during tumoursphere formation and growth (continues over page).

B

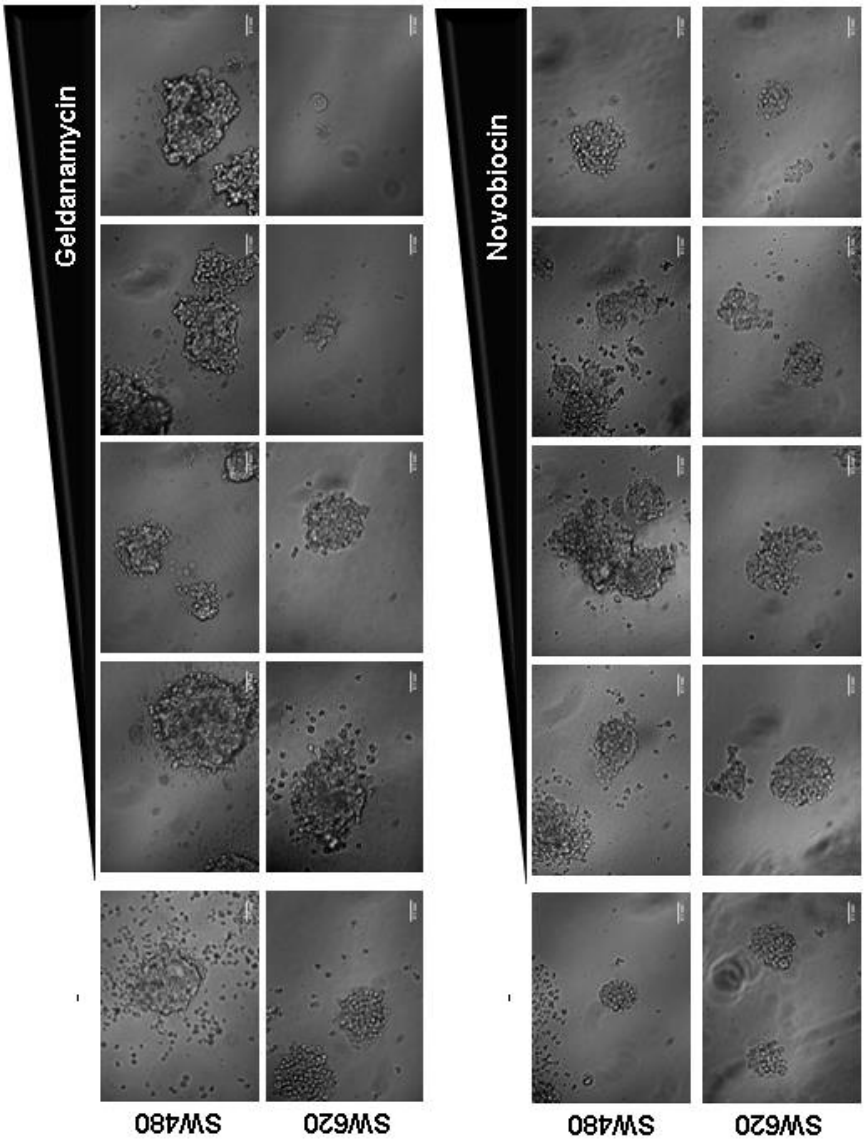

Figure S1. Chemosensitivity of cells to Hsp90 inhibition during tumoursphere formation and growth.

The growth and development of tumourspheres under anchorage-independent conditions was analysed 7 days after seeding cells and treating with a range of 5-fluorouracil (5-FU), oxaliplatin, geldanamycin or novobiocin concentrations (treatment and TS growth co-culture). Cellular chemotherapeutic sensitivity was analysed though the calculated percentage viability in comparison to negative (untreated) control cell samples. A. Cells treated with 5-fluorouracil (5-FU) at 0, 0.5, 5, 50 and 500 µM or with oxaliplatin at 0, 12.5, 25, 50, 75 µM. B. Cells treated with geldanamycin at 0, 12.5, 25, 50, 75 nM or with novobiocin at 0, 5, 50, 100, 150 µM. Results represented illustrate the average of triplicate results, each of 3 replicates, with 1000 cells seeded per well under anchorage-independent conditions. Images were analysed using ImageJ software. Scale bars: 0.1 mm.

A

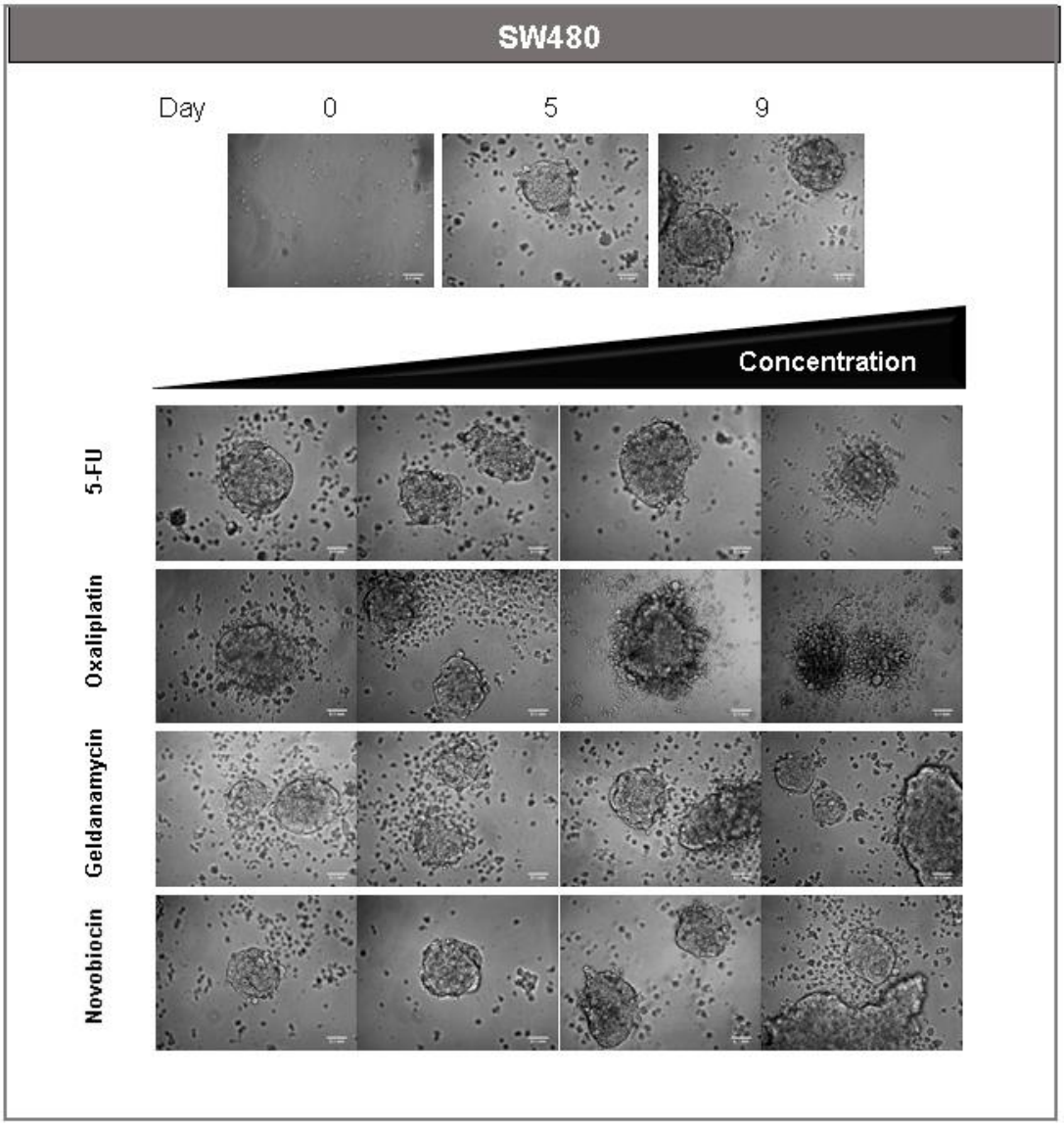

Figure S2. Effect of chemotherapeutic agents and Hsp90 inhibitors on size and morphology of established tumourspheres (continues over page).

B

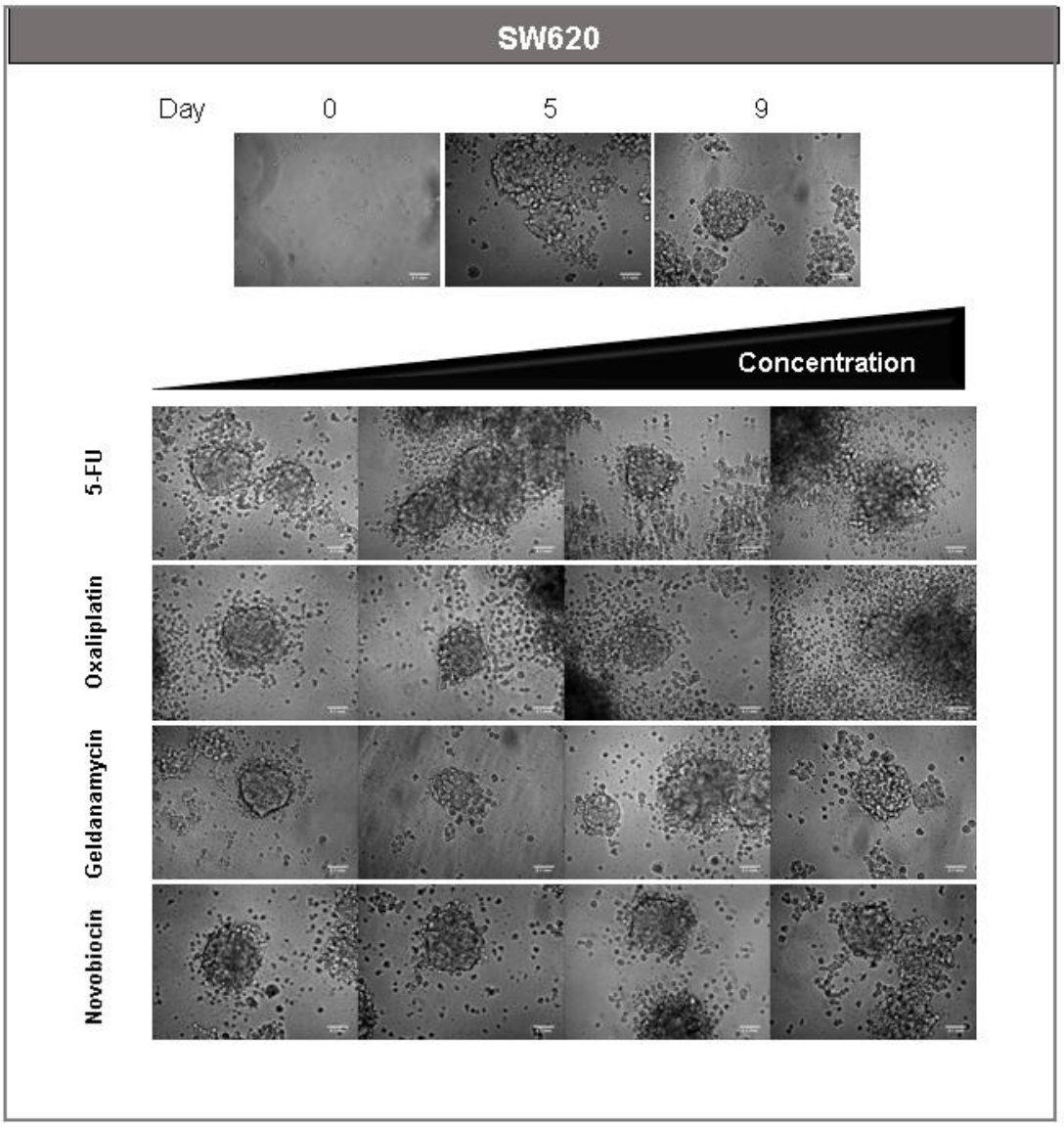

Figure S2. Effect of chemotherapeutic agents and Hsp90 inhibitors on size and morphology of established tumourspheres.

Analysis of the size and morphology of SW480 (A) and SW620 (B) tumourspheres under anchorage-independent conditions. From single-cells (Day 0), tumourspheres were grown for 5 days, treated with the respective concentration of chemotherapeutic agent and analysed 4 days later (Day 9). Tumourspheres treatments: 5-FU (0, 0.5, 5, 50 and 500 µM), oxaliplatin (0, 12.5, 25, 50 and 75 µM), geldanamycin (0, 12.5, 25, 50 and 75 nM) and novobiocin (0, 5, 50, 100 and 150 µM). Results represent the average of triplicate results, each of 3 replicates, with 1000 cells seeded per well. Images were analysed using ImageJ software. Scale bars represent 100 µm.

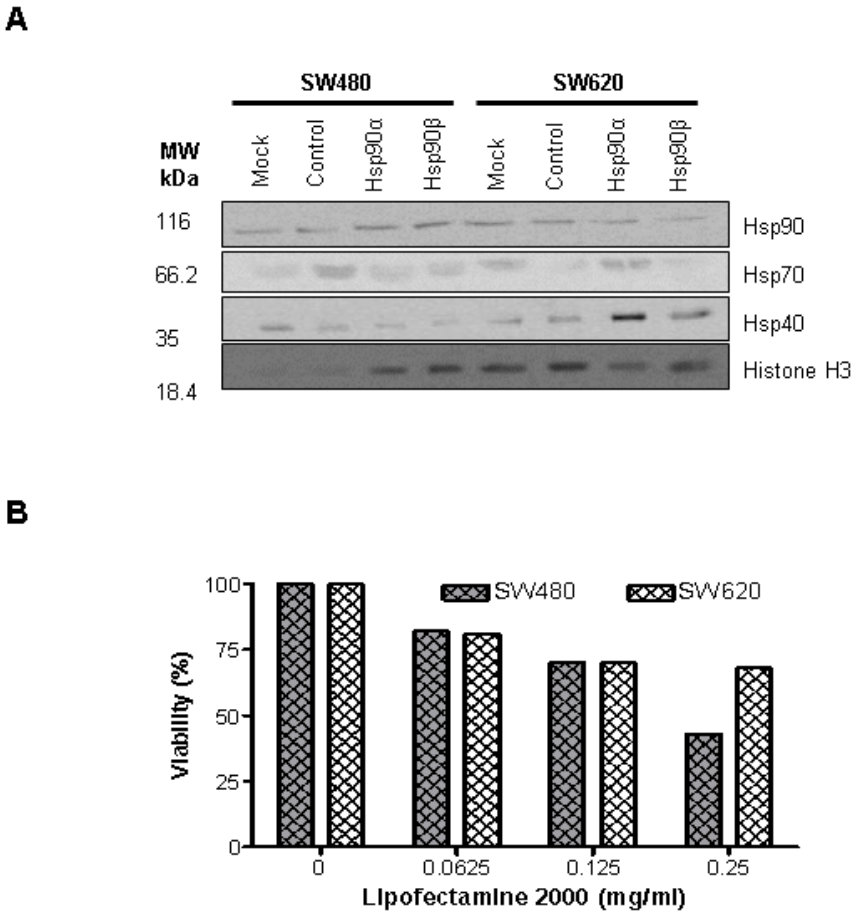

Figure S3. Targeting Hsp90 by isoform using siRNA.

SW480 and SW620 cells were transfected with 125 nM siRNA directed towards Hsp90α and Hsp90β for analysis of transient knockdown. A. Western blot and corresponding densitometric analysis (50 µg protein per lane) demonstrate the effects of Hsp90α or Hsp90β knockdown on Hsp90 (both isoforms), Hsp70 and Hsp40 (histone H3 loading control). Mock: Lipofectamine control. Hsp90α: HSP90AA1 siRNA. Hsp90β: HSP90AB1 siRNA. B. Demonstration of the sensitivity of SW480 and SW620 to the Lipofectamine® 2000 Transfection Reagent by WST-1 assay. Cell viability was calculated as a percentage relative to the viability of the untreated cells. Results represent the average of triplicate results, each of 3 replicates. Data were analysed using GraphPad Prism software.

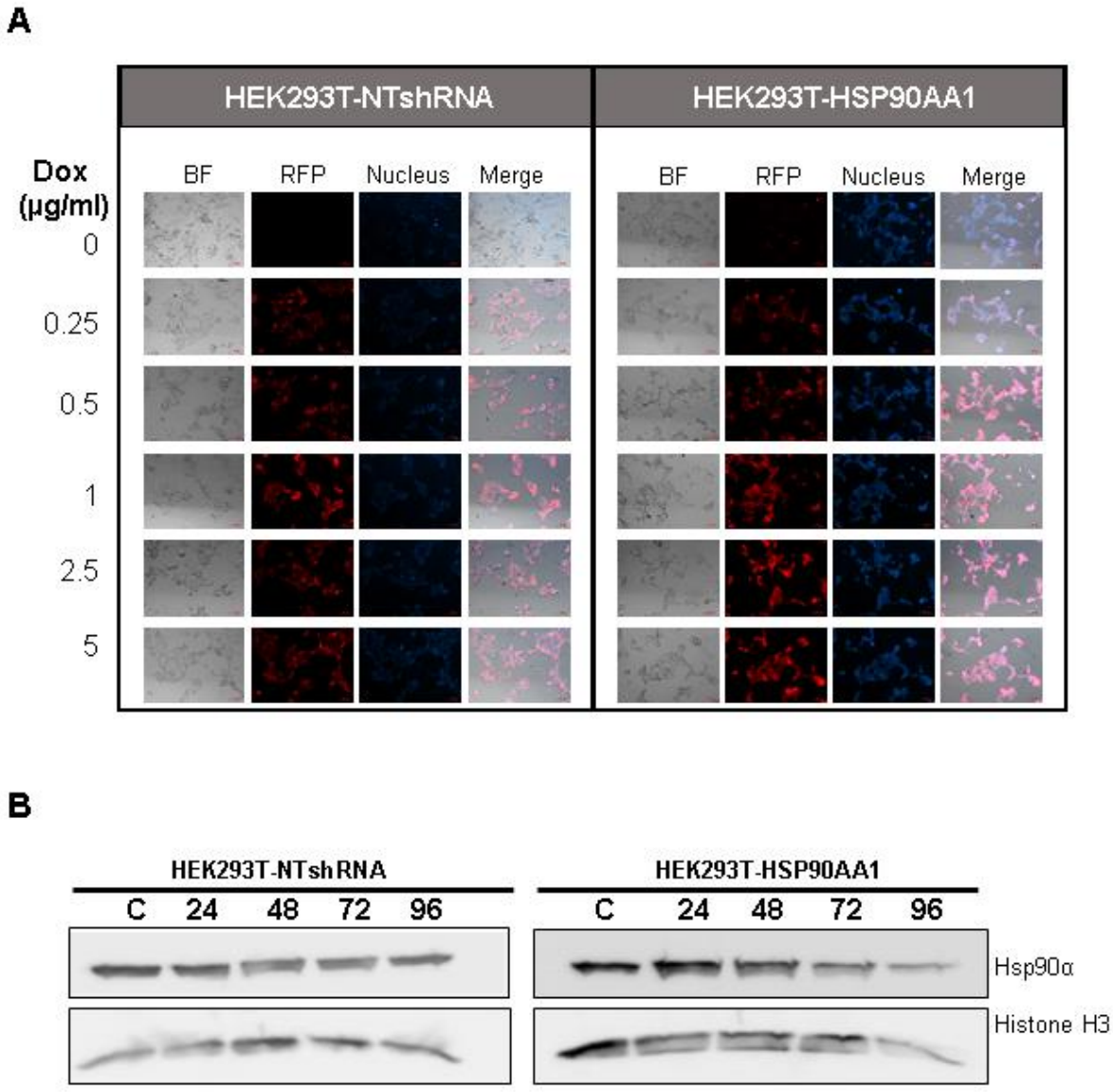

Figure S4. Characterisation of inducible knockdown in HEK293FT polyclonal cell lines.

Induction of lentivirus-transduced HEK293T cells containing non-targeting (NT) shRNA or HSP90AA1 shRNA. A. Immunofluorescent microscopy analysis of turboRFP expression indicative doxycycline (Dox, 0 – 5 µg/ml) induction. Images were taken using Zeiss AxioVert.A1 Fluorescence LED Inverted Microscope with a High Resolution AxioCam MRm Rev 3 and analysed using ZEN Lite software. B. Western blots and densitometry for 50 µg of protein lysed from HEK293T-NTshRNA and HEK293T-HSP90AA1 polyclonal cell lines under kinetic analysis (24, 48, 72, 96 H) of polyclonal cell lines under Dox (1 µg/ml) induction. Membrane was probed for anti- Hsp90α and loading control (histone H3). Chemiluminescent detection of proteins using antibody-antigen detection using the Chemidoc EQ system (Biorad, UK). Data were analysed using ImageJ software.

Generation of non-neoplastic immortalised cell lines for Hsp90α knockdown

HEK293FT-NTshRNA and HEK293FT-HSP90AA1 cell lines were examined after doxycycline treatment following the expansion of the polyclonal cell lines to demonstrate the success of lentivirus transduction (see Supplementary Figure S4). Using fluorescent microscopy, we observed the direct effects of doxycycline, in a dose-dependent manner, on the development of a red (RFP) signal as a direct consequence of the co-expression of a turboRFP reporter gene, which is regulated by the same promoter regulating the shRNA sequences (Supplementary Figure S4A). Fluorescent intensities observed for HEK293FT-NTshRNA and HEK293FT-HSP90AA1 indicated that 1 µg/ml doxycycline was optimal for the observation of tRFP signal, with little change in intensity at concentrations greater than 1 µg/ml doxycycline. The application of 1 µg/ml doxycycline to HEK293FT-NTshRNA and HEK293FT-HSP90AA1 cell lines over 96 H verified that Hsp90α was not affected in HEK293FT-NTshRNA cells, but showed a time-dependent decrease in Hsp90α in HEK293FT-HSP90AA1 cells relative to the HEK293FT control and HEK293FT-NTshRNA cell lines (Supplementary Figure S4B). HEK293FT-HSP90AA1 showed that 72 H was sufficient to achieve Hsp90α protein knockdown.